

FEDERAL UNIVERSITY OF SÃO CARLOS
CENTER FOR EXACT SCIENCES AND TECHNOLOGY
CHEMICAL ENGINEERING DEPARTMENT
GRADUATE PROGRAM IN CHEMICAL ENGINEERING

DOCTORAL THESIS

Cellulose nanomaterials isolated via enzymatic and
mechanical routes for application in hydrogels

PAULA SQUINCA DE CARVALHO

São Carlos, SP
November, 2021

UNIVERSIDADE FEDERAL DE SÃO CARLOS'
CENTRO DE CIÊNCIAS EXATAS E DE TECNOLOGIA
DEPARTAMENTO DE ENGENHARIA QUÍMICA
PROGRAMA DE PÓS-GRADUAÇÃO EM ENGENHARIA QUÍMICA

TESE DE DOUTORADO

Nanomateriais celulósicos isolados via rotas enzimática e mecânica para aplicação em hidrogéis

Paula Squinca de Carvalho

Tese de doutorado apresentada ao Programa de Pós-Graduação em Engenharia Química da Universidade Federal de São Carlos, para obtenção do título de doutora em Engenharia Química, área de concentração em Pesquisa e Desenvolvimento de Processos Químicos.

Orientadora: Dra. Cristiane Sanchez Farinas

Coorientador: Dr. Alberto Colli Badino Junior

São Carlos, SP
Novembro, 2021

FEDERAL UNIVERSITY OF SÃO CARLOS
CENTER FOR EXACT SCIENCES AND TECHNOLOGY
CHEMICAL ENGINEERING DEPARTMENT
GRADUATE PROGRAM IN CHEMICAL ENGINEERING

DOCTORAL THESIS

Cellulose nanomaterials isolated via enzymatic and mechanical routes for application in hydrogels

Paula Squinca de Carvalho

Thesis presented as part requirements to obtain PhD degree in Chemical Engineering, concentration area: Research and Development of Chemical Processes.

Supervisor: Dr. Cristiane Sanchez Farinas

Co-supervisor: Dr. Alberto Colli Badino Junior

São Carlos, SP
Novembro, 2021



UNIVERSIDADE FEDERAL DE SÃO CARLOS

Centro de Ciências Exatas e de Tecnologia
Programa de Pós-Graduação em Engenharia Química

Folha de Aprovação

Defesa de Tese de Doutorado da candidata Paula Squinca de Carvalho, realizada em 10/11/2021.

Comissão Julgadora:

Profa. Dra. Cristiane Sanchez Farinas (EMBRAPA)

Prof. Dr. Alberto Colli Badino Junior (UFSCar)

Prof. Dr. Stanley Endrigo Bilatto Rodrigues (EMBRAPA)

Profa. Dra. Renata Maria Rosas Garcia Almeida (UFAL)

Prof. Dr. Luiz Henrique Capparelli Mattoso (EMBRAPA)



O presente trabalho foi realizado com apoio da Coordenação de Aperfeiçoamento de Pessoal de Nível Superior - Brasil (CAPES) - Código de Financiamento 001.

O Relatório de Defesa assinado pelos membros da Comissão Julgadora encontra-se arquivado junto ao Programa de Pós-Graduação em Engenharia Química.

To my parents,

Rita

and

Paulo in *memoriam* 


Because when you stop and look around,
life is pretty amazing ♡

ACKNOWLEDGEMENTS

I would like to acknowledge the financial support received from National Council for Scientific and Technological Development (CNPq), Grant no. 168232/2017-0, Coordination for the Improvement of Higher Education Personnel (CAPES), Grant no. no. 88887.465611/2019-00, and São Paulo Research Foundation (FAPESP).

This work and the PhD journey were only possible due to wonderful people that I met and had by my side along the way.

I would like to express my gratitude to my principal supervisor Dr. Cristiane Sanchez Farinas for guidance, patience, support and for giving me freedom to follow my own ideas. Her constructive ideas, advices and organized work approach provided during the PhD have immensely helped me and inspired me in many ways. Likewise, I am grateful to my co-supervisor, Dr. Alberto Colli Badino Junior, for his support, knowledge, work ethics and fruitful suggestions during the doctoral journey have also significantly contributed to my development as a researcher. It has been a pleasure to work together.

I would like to offer my special thanks to Dr. Luiz Henrique Capparelli Mattoso who believed in me and dedicated his time to help me to seek a dream of doing research abroad even though I was not one of his supervised students. His kindness, humbleness and passion about science are inspirational.

I would like to extend my gratitude to Dr. Antonio José Gonçalves Cruz for his solicitude and help every time I needed it. I am thankful to all the professors at the Department of Chemical Engineering, who has taught me so much since my undergraduate period and employees at Embrapa Instrumentation, especially the laboratory technicians, for their support and assistance.

I also express my sincere gratitude to my colleagues at both institutions Department of Chemical engineering and Embrapa Instrumentation. To name a few: Marina del Bianco, Thamara Coutinho, Camila Favaro, Agnes Mafra, Caroline Lopes, Taíse Martins, Gustavo Batista, Alan Taschin, Cássia Santana, Juliana Alves. I am deeply thankful to Dr. Stanley for his patience, sharing ideas, performing some characterization experiments and encouraging me to pursue my final PhD goals even though I was facing challenges in different aspects of my life.

My sincere gratefulness and admiration are given to Dr. Kristiina Oksman for giving me the opportunity to join her research group during interuniversity exchange

doctorate period in Sweden and to introduce me to hydrogels, such a fascinating material. I am very thankful that she also supported me to stay longer than initially planned in Sweden to conclude the project there.

Special thanks to Dr. Linn Berglund for sharing her knowledge and passion about science, for making time to discuss ideas and experiments even though she was very busy. She helped me beyond the laboratory/research work and I am deeply grateful for it.

Apart from developing a research study and improving my professional skills, the opportunity to do the exchange doctorate in Sweden allowed me to learn a little about Nordic culture, expand my horizons, make new friends and collect good memories. I am thankful to amazing people that I met there who helped me in different ways. Especially Marcus Jansson for his patience, kindness, help and friendship. He contributed to make my stay in Sweden more enjoyable and unforgettable.

Lastly, I would like to thank my family. First, I would like to thank to my parents, for standing by my side in different circumstances and cheering for my decisions. I am very grateful to my “second parents”, Wânia and José, who also helped every time that I needed. I am thankful to my kind and loved grandmother for also cheering and praying things do well. I am thankful to my sister by choice and love, Fernanda, for helping me whenever I needed.

RESUMO

A produção integrada de diferentes bioprodutos tem sido considerada essencial para tornar as biorrefinarias economicamente viáveis, com destaque para os nanomateriais de celulose (NCs) dadas suas propriedades atrativas e amplo espectro de aplicações. É crescente o interesse no uso de enzimas para isolar nanomateriais de celulose devido à sua seletividade e especificidade, além das brandas condições operacionais. Contudo, as preparações enzimáticas comerciais disponíveis atualmente ainda não estão otimizadas para este fim. Outra estratégia vantajosa do ponto de vista econômico e ambiental é a exploração de resíduos agroindustriais como matérias-primas para obtenção desses nanomateriais. Neste trabalho, nanomateriais de celulose foram isolados por meio de rotas enzimáticas e mecânicas e usados na fabricação de hidrogéis. Enzimas foram produzidas por *Aspergillus niger* sob fermentação em estado sólido e utilizadas para obtenção de NCs através de hidrólise enzimática seguida de sonicação utilizando polpa de celulose de eucalipto como substrato modelo. A condição de maior rendimento foi determinada através de planejamento composto central rotacional e resultou em nanocristais de celulose com elevado índice de cristalinidade e boa estabilidade térmica. Resíduo de gengibre foi utilizado como matéria-prima para a obtenção de nanofibrilas de celulose (NFCs) por tratamento mecânico e aplicadas na preparação de hidrogéis obtidos por filtração à vácuo. Os hidrogéis apresentaram transparência, biocompatibilidade, ajustável capacidade de absorção de líquidos, boa flexibilidade e estabilidade mecânica em condições úmidas além de propriedades antimicrobianas, mostrando-se promissores para aplicações como curativos. Na parte final da tese, NCs produzidos utilizando enzimas comerciais e não comerciais foram incorporados a hidrogéis preparados por *solvent casting* utilizando gelatina, ácido tânico como reticulador e óleo essencial de gengibre para aumentar as propriedades antimicrobianas. Os hidrogéis apresentaram atividade antibacteriana inibindo o crescimento de *Staphylococcus aureus* e de *Escherichia coli* e os NCs obtidos com enzimas não comerciais ofereceram melhor contribuição para a integridade estrutural. Tais resultados oferecem uma prova de conceito de que nanomateriais de celulose podem ser eficientemente obtidos utilizando de enzimas não comerciais e aplicados na fabricação de hidrogel. Já para a estabelecida rota mecânica, foi demonstrado que hidrogéis obtidos exclusivamente a partir de nanofibras de gengibre apresentaram propriedades importantes que possibilitam sua aplicação como curativos.

Palavras-chave: Desenvolvimento sustentável. Hidrólise enzimática. Enzimas não comerciais. Gengibre. Hidrogéis.

ABSTRACT

The integrated production of different bioproducts has been considered essential to make biorefineries economically viable. Among the bioproducts, cellulose nanomaterials (CNs) have attracted significant attention due to their attractive properties and wide spectrum of applications. The use of enzymes to isolate cellulose nanomaterials have gained growing interests mainly associated with the milder operational conditions and the selectivity and specificity of these biocatalysts. However, the available commercial enzymatic preparations are not optimized for this purpose yet. Besides, exploiting agro-industrial residues as feedstock to nanomaterials production is another advantageous strategy from environmental and economic point of views. Within this context, cellulose nanomaterials were isolated through enzymatic and mechanical routes for applications in manufacture of hydrogels. Enzymes were produced by *Aspergillus niger* under solid-state fermentation and applied to obtain the CNs via enzymatic hydrolysis followed by sonication using eucalyptus cellulose pulp as a model feedstock. The condition that resulted in the highest yield of cellulose nanocrystals isolation was determined through central composite rotational design and the nanomaterials presented high crystallinity index and good thermal stability. The ginger residue was used as feedstock to obtain cellulose nanofibrils (CNFs) by mechanical treatment and applied to prepare hydrogels through vacuum-assisted filtration. The hydrogels presented transparency, biocompatibility, tunable liquid absorption, flexibility combined with good mechanical stability in moist conditions, and antimicrobial performance showing to be promising materials for wound dressing applications. In the final part of the thesis, cellulose nanomaterials produced with commercial and non-commercial enzymes were incorporated into gelatin-based hydrogels which were prepared by solvent casting using tannic acid as crosslinker and ginger essential oil to increase the antimicrobial properties. The hydrogels inhibited the growth of *Staphylococcus aureus* and *Escherichia coli* and the cellulose nanomaterials obtained with non-commercial enzymes better contributed to their structural integrity. These results provided a proof of concept that cellulose nanomaterials can be efficiently obtained using non-commercial enzymes and applied in hydrogel manufacture. Meanwhile, for an already established route, hydrogels totally based on nanofibrils extracted from ginger showed important properties to be used as wound dressing.

Keywords: Sustainable development. Enzymatic hydrolysis. Non-commercial enzymes. Ginger. Hydrogels.

LIST OF FIGURES

Figure 2.1. Design of systematic mapping steps used in the present work to describe the state of knowledge of the cellulose nanomaterials whose production process included the use of enzyme.	37
Figure 2.2. Search string used to collect articles for the systematic mapping.....	39
Figure 2.3. Number of articles after each selection step.	41
Figure 2.4. Schematic image of a homogenizers and a microfluidizer. Adapted from (NECHYPORCHUK; BELGACEM; BRAS, 2016) with permission provided by Elsevier and Copyright Clearance Center.....	45
Figure 2.5. Annual distribution of articles obtained after the second screening step.....	47
Figure 2.6. Hierarchical structure from hardwood to cellulose chains at different scales. Adapted from Chen and Hu (2018) with permission provided by American Chemical Society and Copyright Clearance Center. Macrofibrils, microfibrils, and elementary fibrils schemes were adapted from Jiang <i>et al.</i> (2018) with permission provided John Wiley and Sons and Copyright Clearance Center.	49
Figure 2.7. Proportion of the main feedstocks used in the enzymatic hydrolysis obtained from the screened articles.	51
Figure 2.8. Overall scheme of the enzymatic hydrolysis of cellulose involving synergistic interaction of the major cellulases (endoglucanase, cellobiohydrolases and β -glucosidase). Adapted from Andlar (2018).	53
Figure 2.9. Proportion of the main a) commercial and b) non-commercial enzymes used in evaluated articles.	55
Figure 2.10. Evaluation of the approaches, strategies and reaction conditions of the cellulose nanomaterials production process reported in the selected articles. A) Percentage occurrence of the selected terms. B) Network analysis of the terms.	57
Figure 2.11. Evaluation of the applications of cellulose nanomaterials reported by the selected articles. A) Percentage occurrence of the selected terms. B) Network analysis of the terms.	59
Figure 3.1. Glucose concentration and cellulose conversion (inset) obtained from enzymatic hydrolysis of cellulose pulp pretreated using different ball milling times (13, 45, 77, and 90 min).	73
Figure 3.2. FTIR spectra of cellulose nanomaterials obtained using hydrolysis for a) 48 h and b) 96 h, under the different experimental conditions of the CCRD (Table 3.1).	74

Figure 3.3. SEM images of a) the original cellulose pulp; b) the cellulose pulp after disintegration in the knife mill; and the cellulose pulp after ball milling for c) 13 min, d) 45 min, e) 77 min, and f) 90 min.	78
Figure 3.4. FE-SEM images and digital photos of the nanocelluloses obtained from a) run 5, b) run 6, c) run 7 and d) run 8.	79
Figure 3.5. TEM images of the cellulose nanocrystals obtained using 96 h of enzymatic hydrolysis and the conditions of run 6.	80
Figure 3.6. TGA curves for the original cellulose pulp and the cellulose nanocrystals obtained in runs 6 (96 h enzymatic hydrolysis) and 12 (control condition without enzymes).	81
Figure 3.7. FE-SEM images of the nanocelluloses obtained from a) run 1, c) run 2, e) run 3, g) run 4, i) run 5, k) run 6, m) run 7, o) run 8, q) run 9 using 48 h of hydrolysis and from b) run 1, d) run 2, f) run 3, h) run 4, j) run 5, l) run 6, n) run 7, p) run 8 and r) run 9 using 96 h of hydrolysis. FE-SEM images of suspensions obtained from s) run 12 and t) run 13 (without enzymes).	86
Figure 4.1. OM images of a1) ginger raw material before and b1) after alkali treatment step. OM images of homogenized nanofiber suspension c1) after only TEMPO treatment (T-GNF) and d1) after alkali and TEMPO treatment (AT 4%-GNF) (Scale bar: 200 μm). SEM images of dried ginger fibers a2) non-alkali treated and b2) after alkali treatment (Scale bar: 50 μm). AFM images of dried nanofiber suspensions c2) T-GNF and d2) AT 4%-GNF (Scale bar: 400 nm).	101
Figure 4.2. Liquid absorption of the hydrogels (40 g/m^2) in a1) water and b1) BSA solution. Liquid absorption of hydrogels curves expanded for the first hour in a2) water and b2) BSA solution.	102
Figure 4.3. a) Water absorption as a function of time for T-GNF hydrogels at different grammages. b) Photographs of the T-GNF hydrogels at different grammages after the equilibrium swelling degree was reached.	105
Figure 4.4. SEM images of ginger nanofiber hydrogels of 120 g/m^2 showing the swelling mechanism due to the water absorption. a1) T-GNF and b1) AT 4%-GNF at 800% of swelling degree; a2) T-GNF and b2) AT 4%-GNF at equilibrium swelling degree. Scale bar, inset: 100 μm	106
Figure 4.5. Mechanical properties and hydrogel appearance a) representative compressive stress-strain curves and b) the compressive modulus of the GNF hydrogels at 40 g/m^2 determined in wet conditions c) representative tensile stress-strain curves and d) tensile	

properties of the GNF hydrogels at 40 g/m ² determined in wet conditions e) photographs of the T-GNF and AT 4%-GNF hydrogels and f) application of the T-GNF hydrogel on a forearm.....	108
Figure 4.6. Images from microbiological assays against <i>S. aureus</i> and <i>E. coli</i> for T-GNF and AT 4%-GNF hydrogels before and after functionalization with ginger essential oil (GEO). Method sketches of (i) drop inoculation of hydrogels (upper rows: A-H), and (i') subsequent contact-dependent transfer of microbes to fresh agar (lower rows: A'-H'). (A-D) <i>S. aureus</i> infected hydrogels, (A'-D') contact transfer of <i>S. aureus</i> ; (E-H) <i>E. coli</i> infected hydrogels, (E'-H') contact transfer of <i>E. coli</i> . Panel (ii) shows summary of antimicrobial results. *zone of inhibition assay is shown in Supporting Information section. Dashed lines approximate area of hydrogel beneath bacterial colony; scale bars show 1 mm.....	110
Figure 4.7. Effects of T-GNF and AT 4%-GNF hydrogels on: fibroblast a1) proliferation and a2) migration; keratinocytes b1) proliferation and b2) migration. n=4.....	112
Figure 4.8. AFM height images and size distribution of the T-GNF and AT 4% - GNF, respectively.....	115
Figure 4.9. Liquid absorption of the hydrogels (40 g/m ²) in PBS solution. a2) Expanded curves (first hour) of the liquid absorption of hydrogels in PBS solution.....	115
Figure 4.10. Water retention capacity of T-GNF and AT 4%-GNF hydrogels (40 g/m ²).	116
Figure 4.11. Photographs of the T-GNF hydrogels at 40 g/m ² after reaching the equilibrium state.	117
Figure 4.12. The representative compressive stress–strain curves enlarged at 30% strain.	117
Figure 4.13. Overview images from microbiological assay for inhibition zones. Top row: i/1) <i>S. aureus</i> and bottom row ii/2) <i>E. coli</i> . A) T-GNF, B) AT 4%-GNF, C) T-GNF after functionalized with ginger essential oil (GEO), D) AT 4%-GNF with GEO. Red arrowheads indicate potential zone of inhibition. Dashed lines approximate hydrogel perimeters. Magnification 12.5x. (Scale bar: 1 mm).....	118
Figure 4.14. Investigation of cell attachment to the T-GNF hydrogel. A) acquired stitch at 10x magnification under UV-excitation along paraffin sectioned T-GNF hydrogel (~7 μm thick) with DAPI-labeled cells – inset: enlargement showing example of nuclei on the hydrogel surface (green arrowheads). B) Cells (keratinocytes shown) were labeled with DAPI and ALEXA546-conjugated Phalloidin. C) duplicate samples of fibroblasts	

and keratinocytes on T-GNF were quantified. Arrowheads indicate DAPI-stained nuclei.	119
Figure 4.15. Images from scratch assay showing migration of fibroblasts at different time points. Scale bar corresponds to $\sim 100\mu\text{m}$	119
Figure 4.16. Images from scratch assay showing migration of keratinocytes at different time points. Scale bar corresponds to $\sim 50\mu\text{m}$	120
Figure 5.1. Schematic illustration showing the preparation process of the hydrogels.	127
Figure 5.2. Glucose concentration and cellulose conversion (inset) obtained from enzymatic hydrolysis using commercial and non-commercial enzymes. Glucose concentration and cellulose conversion values derived from the reactions using non-commercial enzymes were obtained from Squinca <i>et al.</i> (2020) with permission provided by American Chemical Society and Copyright Clearance Center.	131
Figure 5.3. AFM images of cellulose nanomaterials produced using commercial enzymes.	132
Figure 5.4. Water absorption of hydrogels prepared with different gelatin concentrations	134
Figure 5.5. Water absorption of gelatin-based hydrogels with tannic acid and ginger essential oil.	135
Figure 5.6. Water absorption of gelatin-based hydrogels with adding of cellulose nanomaterials prepared with a) commercial and b) non-commercial enzymes.	136
Figure 5.7. Photographs of the hydrogels prepared in this work showing their appearance after submersion in water for 4 hours. All samples were cut in dry state and with dimensions of 0.8×2.4 cm indicated by red dashed rectangles.	137
Figure 5.8. Images from antimicrobial assays with the gelatin-based hydrogels discs against (a–g) <i>S. aureus</i> and (h–n) <i>E. coli</i> . Insets show the growth inhibition area observed around samples.	138

LIST OF TABLES

Table 2.1. Databases used in the systematic mapping along with their search strategy and number of articles obtained in each one.	40
Table 3.1. Design of experiment matrix.	68
Table 3.2. Nanocellulose characterization results: yield (Y), zeta potential, (ZP) and crystallinity index (CrI).	75
Table 3.3. Estimated effects and p-values of the variables ball milling pretreatment time ($t_{\text{ball milling}}$) and sonication time ($t_{\text{sonication}}$), considering the response variables nanocellulose yield, zeta potential, and crystallinity index.	76
Table 3.4. Thermal properties of the pulp and the cellulose nanocrystals produced by enzymatic hydrolysis.	82
Table 4.1. Total yield and weight after each step of the ginger nanofibers production process.	100
Table 4.2. Hydrogel integrity in BSA solution.	116
Table 4.3. Hydrogel integrity in PBS solution.	116
Table 4.4. Mechanical properties of the hydrogels.	118
Table 5.1 Total Protein concentration and specific enzymatic activities of non-commercial and commercial enzymes.	130
Table 5.2. Yield, crystallinity index, thermal properties, zeta potential of the CNs produced by non-commercial and commercial enzymes.	132

LIST OF ABBREVIATIONS

ANOVA	Analysis of variance
BMR	Ball to material weight ratio
BSA	Bovine serum albumin
CCRD	Central composite rotatable design
CFU	Colony forming unit
CMC	Microcrystalline cellulose
CMF	Cellulose microfibril
CN	Cellulose nanomaterials
CNC	Cellulose nanocrystal
CNF	Cellulose nanofibrils
CrI	Crystallinity index
DMA	Dynamic mechanical analysis
FE-SEM	Field emission scanning electron microscopy
FTIR	Fourier transform infrared spectroscopy
GEO	Ginger essential oil
GNF	Ginger nanofiber
ISSO	International Organization for Standardization
IU	International unit
MHA	Muller-Hinton agar
MHB	Muller-Hinton Broth medium
nm	Nanometer
OM	Optical microscopy
PBS	Phosphate buffered saline
rpm	Revolutions per minute
SD	Standard deviation
SDGs	Sustainable development goals
SEM	Scanning electron microscopy
SM	Systematic mapping
TA	Tannic acid
TEMPO	2,2,6,6-tetramethylpiperidine-1-oxyl
TEM	Transmission electron microscopy
TGA	Thermal properties by thermogravimetric analysis
XRD	X-ray diffraction
ZP	Zeta potential

LIST OF SYMBOLS

C_c	Cellulose conversion
C_T	Number of viable cells at the analyzed timepoint
C_{T0}	Number of viable cells at the starting timepoint
g	Gram
h	Hours
I_{002}	Intensity of the crystalline peak
I_{am}	Intensity of the amorphous peak
kV	Kilovolt
L	Liter
mg	Miligram
m_g^0	Initial glucose mass
m_g^t	Glucose mass at time t
min	Minutes
mL	Milliliter
mm	Milimeter
m_p^0	Initial pulp mass
m_s^f	Mass after drying
m_s^i	Mass before drying
nm	Nanometer
R	Ratio of the total volume used in the hydrolysis reaction and volume of the sample
s	Seconds
T_{max}	Maximum degradation temperature
T_{onset}	Initial thermal degradation temperature
v/v	Volume per volume
W	Watt
w/v	Weight per volume
w/w	Initial pulp mass
w_d	Dried weight of sample
w_{es}	Weight at the equilibrium state
w_r	Weight retained after the sample was left to dry
w_t	Weight at time t
wt %	Weight percent
w_w	Wet weight
Y_c	The percentage of cellulose in the pulp
Λ	Wavelength
μmol	Micromol
mm	Micrometer

PUBLICATIONS

SQUINCA, P.; BILATTO, S.; BADINO, A. C.; FARINAS, C. F. Nanocellulose Production in Future Biorefineries: An Integrated Approach Using Tailor-Made Enzymes. **ACS Sustainable Chemistry and Engineering**, v. 8, n. 5, p. 2277–2286, 2020.

SQUINCA, P.; BERGLUND, L., HANNA, K.; RAKAR, J.; JUNKER, J.; KHALAF, H.; FARINAS, C. S.; OKSMAN, K.. Multifunctional Ginger Nanofiber Hydrogels with Tunable Absorption: The Potential for Advanced Wound Dressing Applications. **Biomacromolecules**, v. 22, n. 8, p. 3202–3215, 2021.

CONTRIBUTION NOT INCLUDED IN THE THESIS

FREITAS, J. V.; BILATTO, S.; SQUINCA, P.; PINTO, A.S. S.; BRONDI, M. G.; BONDANCIA, J. K.; BASTISTA, G. B.; KLAIC, R.; FARINAS, C. S. Sugarcane biorefineries: potential opportunities towards shifting from wastes to products. **Industrial Crops and Products**, v. 172, p. 114057, 2021.

SUMMARY

Chapter 1 Introduction	25
1.1 <i>Context and motivation</i>	25
1.2 <i>Purpose of the study</i>	30
1.3 <i>Thesis overview</i>	30
Chapter 2 Systematic map	32
2.1 <i>Abstract</i>	32
2.2 <i>Introduction</i>	33
2.3 <i>Methodology</i>	36
Stage 2: Searching for evidence	37
Stage 3: Screening evidence	40
Stage 4: Coding.....	41
Stage 5: Describing the findings	42
2.4 <i>Results and discussion</i>	42
2.4.1 Nanocellulose overview	42
2.4.2 The use of enzymatic hydrolysis in the cellulose nanomaterials production.....	46
2.4.3 Sources for nanocellulose production	48
2.4.4 Enzymes used in the nanocellulose production.....	52
2.4.5 Trends and main applications of nanocelluloses whose production process includes an enzymatic hydrolysis step	56
2.5 <i>Limitations of the work</i>	60
2.6 <i>Final remarks</i>	60
Chapter 3 Production of non-commercial enzymes and their application to isolate cellulose nanomaterials	63
3.1 <i>Abstract</i>	64
3.2 <i>Introduction</i>	64
3.3 <i>Experimental section</i>	66

3.3.1 Material.....	66
3.3.2 Microorganism.....	66
3.3.3 Solid state fermentation.....	67
3.3.4 Ball milling pretreatment.....	67
3.3.5 Central composite design	67
3.3.6 Extraction of nanocellulose	68
3.3.7 Cellulose conversion	68
3.3.8 Characterization.....	69
3.3.9 Analytical methods.....	71
<i>3.4 Results and discussion</i>	<i>71</i>
3.4.1 Nanocellulose production by enzymatic hydrolysis.....	71
3.4.2 Chemical composition.....	74
3.4.3 Yield, zeta potential and crystallinity	75
3.4.4 Morphological analysis.....	77
3.4.5 Thermal properties	81
<i>3.5 Conclusions</i>	<i>83</i>
<i>3.6 Supplementary data</i>	<i>84</i>
Chapter 4 Use of ginger residue as feedstock to isolate cellulose nanofibers.....	87
<i>4.1 Abstract.....</i>	<i>88</i>
<i>4.2 Introduction</i>	<i>88</i>
<i>4.3 Experimental section</i>	<i>91</i>
4.3.1 Materials.....	91
4.3.2 Alkali treatment.....	91
4.3.3 Bleaching procedure.....	91
4.3.4 Chemical composition.....	91
4.3.5 Yield determination.....	92
4.3.6 Optical microscopy.....	92
4.3.7 Ginger nanofiber production.....	92
4.3.8 Preparation of ginger nanofiber-based hydrogels.....	93
4.3.9 Scanning electron microscopy.....	94
4.3.10 Atomic force microscopy.....	94

4.3.11 Liquid absorption measurement	94
4.3.12 Hydrogel integrity measurement.....	94
4.3.13 Water retention capacity	95
4.3.14 Mechanical testing	95
4.3.15 Antibacterial activity study.....	96
4.3.16 Cytocompatibility study.....	96
<i>4.4 Results and discussion</i>	<i>99</i>
4.4.1 Production and characterization of ginger nanofibers	99
4.4.2 Liquid absorption capacity of ginger nanofiber hydrogels.....	102
4.4.3 Mechanical properties.....	107
4.4.4 Hydrogels antibacterial effects.....	109
4.4.5 <i>In vitro</i> cytocompatibility study	111
4.4.6 Conclusions.....	114
<i>4.5 Supplementary data</i>	<i>115</i>
Chapter 5 Comparison of cellulose nanomaterials produced with commercial and non-commercial enzymes and their application in gelatin-based hydrogels.....	121
<i>5.1 Abstract.....</i>	<i>122</i>
<i>5.2 Introduction</i>	<i>122</i>
<i>5.3 Materials and Methods.....</i>	<i>125</i>
5.3.1 Materials.....	125
5.3.2 Cellulose nanocrystals isolation.....	126
5.3.3 Cellulose conversion	126
5.3.4 Hydrogel preparation	126
5.3.5 Cellulose nanomaterials characterization	127
5.3.6 Hydrogels characterization	128
5.3.7 Analytical methods.....	129
<i>5.4 Results and discussions</i>	<i>130</i>
5.4.1 Enzymatic hydrolysis using non-commercial and commercial enzymes.....	130
5.4.2 Main properties of cellulose nanomaterials produced by non-commercial and commercial enzymes	132
5.4.3 Preparation and characterization of hydrogels.....	134

<i>5.5 Antimicrobial activity tests</i>	137
<i>5.6 Conclusions</i>	140
Chapter 6 Conclusions and future works	141
REFERENCES	144
APPENDIX A	175
APPENDIX B	231

Chapter 1

Introduction

1.1 Context and motivation

The climate change together with the unsustainable consumption of natural resources beyond rates at which these resources can reproduce, regrow and regenerate have been exposing humanity to major systemic risks. One of the most prominent responses to this is the Sustainable Development Goals (SDGs) created by the United Nations (UN) in September 2015 (HEIMANN, 2019; WANG *et al.*, 2014). The SDGs are an integral part of the 2030 Agenda, which is a global action plan to seek sustainability in all UN members that adopted this formal declaration. The Agenda has 169 targets guided by the 17 goals covering almost all aspects for sustainable global development in economic, environmental and social dimensions, such as reduction of poverty, combat climate change and its impacts ensuring sustainable consumption and production patterns (DLOUHÁ; POSPÍŠILOVÁ, 2018; UNITED NATIONS, 2016).

The transition from a fossil-based to a bio-based economy is a necessary change to meet most of the sustainable development goals. Bioeconomy is generally understood as an economy in which the basic building blocks for materials, chemicals and energy are derived from renewable biological resources (MCCORMICK; KAUTTO, 2013). Lignocellulosic biomass has the potential to replace a significant fraction of the fossil raw materials, as it can be used as a renewable carbon source to obtain a wide variety of products and fuels (FIORENTINO; RIPA; ULGIATI, 2017). The development of biorefineries is crucial for the sustainable and integral processing of biomass, enabling the production of biofuels, energy and co-products as an approach analogous to conventional oil refineries (FITZPATRICK *et al.*, 2010; FREITAS *et al.*, 2021). Despite great promises, bio-based fuels and products are still unable to compete at a commercial scale and low price with their petrochemical counterparts (CHANDEL *et al.*, 2020; ROSALES-CALDERON; ARANTES, 2019). One strategy to improve the cost-

competitiveness of the biorefinery is to increase the revenue by producing high-value-added co-products.

Among the co-products, cellulose nanomaterial, also known as nanocellulose, has been receiving important attention owing to their outstanding properties derived from cellulose, such as hydrophilicity, biodegradability, biocompatibility, good mechanical properties making it suitable for applications in composites and polymeric materials, packaging, biomedicine, electronics, among others (BRINCHI *et al.*, 2013; HABIBI; LUCIA; ROJAS, 2010; LIN; DUFRESNE, 2014; PASQUINI *et al.*, 2010; RHIM; PARK; HA, 2013).

Cellulose nanomaterials present at least one dimension in the nanoscale (<100 nm). Considering this definition, nanocellulose can be broadly classified into cellulose nanocrystals (CNCs) and cellulose nanofibrils (CNFs) (ISO, 2017). Cellulose nanocrystals are characterized by their needle-like shape and high crystallinity resulted from the complete removal of the amorphous phase of cellulose mostly by using acid hydrolysis with sulfuric acid (VANDERFLEET; CRANSTON, 2021). Cellulose nanofibrils are elongated and flexible materials formed by alternating regions of amorphous and crystalline cellulose chains (KLEMM *et al.*, 2011). CNFs obtained by the top-down approach are most commonly isolated by mechanical methods through fibrillation. The main used techniques include high-pressure homogenization (using homogenizers and microfluidizers), milling (using the ultra-fine Supermasscolloider mill, for example, or crusher by ultra-fine friction), refinement and ultrasonication (ISOGAI, 2013; NECHYPORCHUK; BELGACEM; BRAS, 2016). As the mechanical disintegration requires high energy consumption (SPENCE *et al.*, 2011; TEJADO *et al.*, 2012), chemical and/or enzymatic treatments are usually combined with mechanical treatments to assist the cellulose fibrillation and reduce the energy demand (NECHYPORCHUK; BELGACEM; BRAS, 2016).

The chemical treatments can introduce surface ionic groups through carboxymethylation reactions (SIRÓ, 2010), oxidation (SAITO *et al.*, 2007) and sulfonation (LIIMATAINEN *et al.*, 2013) to promote interfibrillar repulsion which in turns, facilitate the isolation of CNFs by mechanical processes. Among these reactions, TEMPO-mediated catalytic oxidation (N-oxyl-2,2,6,6-tetramethylpiperidine) is one of the most used auxiliary methods for CNFs extraction (ISOGAI; BERGSTRÖM, 2018). The other strategy that has been used to reduce the energy needed during the mechanical processes involves the use of different types of enzymes (FRITZ *et al.*, 2015). Enzyme-

mediated approaches have attracted much attention mainly due to their environmentally friendly aspect, high selectivity and milder reaction conditions. Besides being used as an auxiliary treatment for mechanical methods, enzymatic hydrolysis has been also evaluated as the main step for cellulose nanomaterials isolation.

In the context of biorefinery, Zhu *et al.* (2011) first reported on the opportunity of producing nanocellulose along with biofuels. The residual material from enzymatic hydrolysis of bleached Kraft eucalyptus pulp using commercial enzymes (Novozyme 476 and Genencor Multifect B) was subjected to mechanical treatment in a microfluidizer for the production of cellulose nanofibrils. Afterwards, other studies also demonstrated the technical feasibility of integrating cellulosic ethanol production and nanocellulose isolation from residual materials of the enzymatic step using sonication (SONG *et al.*, 2014; TSUKAMOTO; DURÁN; TASIC, 2013). More recently, the possibility of producing cellulose nanomaterials using only enzymatic treatment was also demonstrated. Bondancia *et al.* (2017) evaluated the isolation of nanocellulose by enzymatic hydrolysis using commercial enzymes from eucalyptus pulp whereas de Aguiar *et al.* (2020) used sugarcane bagasse and straw as feedstocks.

From the economic point of view, it has been reported that the inclusion of nanocellulose production in the integrated biorefinery scenario could result in a greater financial return and, therefore, contribute to its economic viability (DE ASSIS *et al.*, 2017; LEISTRITZ *et al.*, 2006; LUO; VAN DER VOET; HUPPES, 2010; SONG *et al.*, 2014). It is important to mention that the composition of most commercial enzymatic preparation was optimized for the complete hydrolysis of lignocellulosic materials resulting in high conversions of cellulose into soluble monosaccharides. Thus, there is still a need to develop more specific enzymatic cocktails to favor the production of nanocelluloses.

Besides, it has been reported that on-site production of enzymes is a promising strategy to minimize their costs mainly due to the reduction in the formulation and transport expenses as the purification and logistics step are simplified (JOHNSON, 2016; LIU; ZHANG; BAO, 2016; RANA *et al.*, 2014; SØRENSEN *et al.*, 2011). In the biorefinery context, it is also possible to use the lignocellulosic biomass already available at the location as a carbon source and inducer for enzyme-producing microorganisms (MERINO; CHERRY, 2007). Studies have shown that secreted enzymes are better adapted to act on the substrate that was used for the growth of the microorganism and synthesis of the enzyme itself (CUNHA *et al.*, 2017; VAN DEN BRINK *et al.*, 2014). In

addition to the economic advantage, the use of biomass could lead the production of more specific enzymes for the nanocellulose production.

Among the possible applications of nanocelluloses, their use as reinforcing agents of polymeric composites or building blocks of hydrogels has attracted significant research interest (FRANCE *et al.*, 2017). Nanocellulose-based hydrogels have been considered promising materials for biomedical applications, such as tissue engineering, wound healing materials and drug delivery systems, as they have good mechanical properties, high-water content, porosity, in addition to their apparent biological inertness due to the low or absence of toxicity, biocompatibility and biodegradability. Other applications, such as adsorption material (ZHOU *et al.*, 2014), absorbent (MA; HSIAO; CHU, 2012; MOHAMMED *et al.*, 2015, 2016; YUE *et al.*, 2016) and energy storage (GAO, Xiaoyuan *et al.*, 2015) have been also reported.

Nanocellulose-based hydrogel networks can be prepared by physical methods including freezing and thawing technique, ultrasonic treatment, casting and vacuum-filtration to enable the network formation by physical interactions (noncovalent bonds) such as chain entanglements, van der Waals forces, ionic interactions, hydrogen bonding and crystallite associations (CHANG; ZHANG, 2011; FU *et al.*, 2019; HOFFMAN, 2012; OKSMAN *et al.*, 2016). In general, CNCs are more used as fillers in hydrogel nanocomposites. Due to their limited ability to “entangle” CNCs alone tend to be ill-suited as single-component gels. On the other hand, CNFs possess increased flexibility and propensity for entanglement which enable the hydrogel formation (FRANCE *et al.*, 2017). Besides, hydrogels can be covalently crosslinked using different chemical crosslinking agents, such as epichlorohydrin (WANG *et al.*, 2014), glutaraldehyde (OOI; AHMAD; AMIN, 2016), polyethylene glycol diacrylate (YANG; FANG; TAN, 2006), citric acid (KIM *et al.*, 2017), 1,3-diaminopropane (PASQUI *et al.*, 2014) among others. Important to mention that the use of some crosslinkers may result in a material with some level of toxicity due to the presence of amounts of unreacted crosslinkers and also by-products generated during the synthesis reaction (DIMIDA *et al.*, 2015; ZHANG, Wu *et al.*, 2016). Thus, the use of naturally occurring crosslinkers with low toxicity and higher biocompatibility has garnered much interest, especially for medical applications.

Among the possible biomedical applications of hydrogels, several studies have evaluated their use as a wound dressing, since these materials can absorb a considerable amount of aqueous liquid which is important to prevent the accumulation of exudates while offering a moist environment that favors healing. In addition, they can cool the

wound which contributes to reducing pain (FU *et al.*, 2019; ISHIHARA *et al.*, 2002; XIANG; SHEN; HONG, 2020). Hydrogels also do not cause irritation or adhesion as cells do not readily attach to highly hydrophilic surfaces (CALÓ; KHUTORYANSKIY, 2015; MADAGHIELE *et al.*, 2014). Another desirable feature of wound dressings is to prevent the wound from bacterial infections. Nanocellulose-based hydrogels with antibacterial properties can be prepared by adding antibiotics, combining with nanomaterials (such as, silver and gold nanoparticles), polymers with antibacterial activity and using nanocelluloses which were modified to have functional groups with antimicrobial properties (aldehyde and quaternary ammonium groups) introduced through surface modification (LI *et al.*, 2018). Due to concerns about the increased resistance of bacterial strains to drugs, the development of hydrogels that have intrinsic antibacterial activities, without the addition of antibiotics, is a more promising strategy for obtaining these advanced dressings. Although several multifunctional dressings have been developed, there is no single dressing capable of meeting the requirements of all types of wounds and in the different stages of the healing process (ABDELRAHMAN; NEWTON, 2011).

Zingiber officinale Roscoe, commonly known as ginger, is a perennial herbaceous plant belonging to the Zingiberaceae family, which also includes cardamom and turmeric (GHASEMZADEH; JAAFAR; RAHMAT, 2016). Zingiberaceae plants have received much attention since they produce several compounds that are useful in food as spices and herbs, seasoning agents and for medicinal purposes due to their antimicrobial and antioxidant agents. In ancient times, ginger was highly valued for its medicinal properties and played a significant role in primary healthcare in India and China (GHASEMZADEH; JAAFAR; RAHMAT, 2016; NICOLL; HENEIN, 2009; SEMWAL *et al.*, 2015; SIVASOTHY *et al.*, 2011). Ginger has been fractionated into at least 14 bioactive compounds, including gingerols, zingiberene and shogaols. The chemical composition and proportion of each individual component depend on the area of origin, commercial processor and sample condition (fresh, dried, or processed) (BENZIE; WACHTEL-GALOR, 2011). Moreover, the ginger essential oil mainly composed of geranial, α -zingiberene, (E,E)- α -farnesene, neral and α -curcumene has also been reported to have significant antimicrobial, antifungal and antioxidant activities (EL-BAROTY *et al.*, 2010; SINGH *et al.*, 2008). Although the pharmacological properties have been confirmed by *in vivo* and/or *in vitro* experiments (SANG *et al.*, 2020) only few studies have focused on using ginger and its essential oil in the preparation of films and

hydrogels (ABRAL *et al.*, 2020a; JACOB *et al.*, 2018, 2019a). Thus, the development of hydrogels based in cellulose nanomaterials using ginger as feedstock for wound healing applications still needs to be further explored.

1.2 Purpose of the study

The purpose of this study was to investigate sustainable strategies to produce cellulose nanomaterials using the enzymatic and mechanical treatments for application in the manufacture of hydrogels. To achieve this, fungal enzymes were produced and applied to isolate cellulose nanomaterials from eucalyptus pulp and the mechanical treatment was applied to isolate cellulose nanofibers from ginger residues. The specific objectives can be summarized as follows:

- Describe the state-of-the-art of cellulose nanomaterials whose production process includes the use of enzymes and identify trends and research gaps in the literature by conducting a systematic mapping process;
- Evaluate the potential use of fungal enzymes to extract cellulose nanomaterials from eucalyptus pulp and optimize their production conditions;
- Investigate the use of ginger residue as a raw material source to isolate cellulose nanofibers by high-pressure homogenization and subsequent assembly into hydrogels for wound dressing applications;
- Isolate cellulose nanomaterials from eucalyptus pulp following the conditions optimized previously and evaluate the application of cellulose nanomaterials produced by both, non-commercial and commercial enzymes, in the manufacture of gelatin-based hydrogels prepared with tannic acid and ginger essential oil.

1.3 Thesis overview

This thesis is structured in five chapters. Chapter 1 briefly provides the main concepts regarding cellulose nanomaterials and their production by enzymatic hydrolysis. Additionally, the state-of-the-art of cellulose nanomaterials whose production process includes the use of enzymes along with the trends and research gaps in the literature were identified and described by following the guidelines of systematic mapping methodology.

Chapter 2 reports on the production of non-commercial enzymes and their application to isolate cellulose nanomaterials. This also presents an optimization of the

production process conditions by using a central composite rotational design as a statistical tool, as well, the characterization of nanocellulose materials including morphological analysis by field emission scanning electron microscopy (FE-SEM), thermal properties by thermogravimetric analysis (TGA), surface charge by zeta potential measurements (ZP), crystallinity characterization and chemical composition by X-ray diffraction (XRD), Fourier transform infrared spectroscopy (FTIR), respectively.

Chapter 3 reports on the use of ginger residue as a feedstock to isolate cellulose nanofibers through mechanical route followed by their application to prepare self-assembled hydrogel for wound dressing purposes. The characterization of the hydrogels with regards to their liquid absorption capacity, morphological structures, mechanical, antimicrobial, and cytocompatibility properties are also presented in this chapter. The results of this chapter were obtained during the interuniversity exchange doctorate period supervised by Prof. Kristiina Oksman, at the Department of Engineering Sciences and Mathematics of the Luleå University of Technology (Sweden).

Chapter 4 presents a comparison between cellulose nanomaterials produced using non-commercial (fungal) and commercial enzymes with regards to the production yield and their crystallinity index, surface charge and thermal properties. This chapter also provides initial results about the application of these nanomaterials in the preparation of gelatin-based hydrogels using tannic acid as cross-linking agent and ginger essential oil as a component to improve the antimicrobial activity. The hydrogels were characterized regarding their water absorption capacity and antimicrobial properties as well as a proof of concept of practical uses of CNs produced using non-commercial enzymes.

Finally, chapter 5 summarizes the main results obtained in this work and presents some suggestions for future studies. It should be mentioned that “cellulose nanomaterial” and “nanocellulose” were used as synonyms throughout this thesis.

Chapter 2

Systematic map

2.1 Abstract

Driven towards sustainable development, there is an increasing interest in enzyme-mediated treatments to isolate cellulose nanomaterials due to their green and environment friendly aspects. In this study, the principles of systematic mapping were used to describe the state-of-the-art of the cellulose nanomaterials whose production process included the use of enzymes and identify trends and gaps in the literature. The systematic map follows rigorous, objective and transparent processes to capture evidences (e.g. primary, secondary, theoretical, economic studies) relevant to a particular topic which can be used to develop a greater understanding of concepts, identify trends and knowledge gaps and clusters. The publications were searched during the period from 2000 to 2021 based on a search string made up of 65 terms being 55 “cellulose nanomaterial” synonyms and 8 “Enzymatic hydrolysis” synonyms. Results evidenced a significant increase in the annual number of publications related to nanocellulose production using enzymes during the last decade, especially during the last eight years (2013–2021). With regards to the enzymatic hydrolysis conditions, the most used feedstocks were derived from hardwood, softwood, and residues, mainly from agro-industries, such as sugarcane straw and bagasse, corn cob, oat husks, lemongrass leaves, oil palm empty fruit bunch, rice straw, among others. Cellulases preparation and endoglucanases heterologous expressed were the mostly evaluated commercial and non-commercial enzymes, respectively. Importantly, this systematic mapping showed that there is no enzymatic preparation commercially available and specially designed for nanocellulose production. Considering the applications, the co-occurrences among the terms related to them demonstrated that the nanocelluloses have been more often used for films preparation and as reinforcement agents. Besides the findings derived from the

systematic mapping, this chapter also briefly summarizes the main concepts related to the cellulose nanomaterials produced by the top-down approach and enzymatic hydrolysis.

2.2 Introduction

The development and use of renewable and sustainable materials have become increasingly important as an alternative solution to the ever-depleting non-renewable sources, global climate change, environmental issues and energy crisis. Cellulose is the most widespread biopolymer on Earth and has the potential to replace fossil feedstocks as a carbon source (for producing commodities, specialty chemicals, and high value-added products)(FIORENTINO; RIPA; ULGIATI, 2017). Moreover, applying suitable mechanical and/or biochemical treatments, it is possible to produce nanomaterials, which are known as nanocellulose or cellulose nanomaterials. These nanomaterials present at least one dimension in the nanometer scale (1–100 nm) and can be isolated from any naturally occurring sources of cellulose, thus opening doors to cellulose-based materials with novel functions and application in several fields (ABITBOL *et al.*, 2016; DUFRESNE, 2019; THAKUR *et al.*, 2021). Nanocelluloses combine important cellulose properties, such as stiffness, high strength, hydrophilicity and wide chemical-modification capacity with specific features of nanoscale materials, which are mainly derived from the large specific surface area (KLEMM *et al.*, 2011).

In addition to their excellent mechanical properties and good biocompatibility, cellulose nanomaterials have low coefficient of thermal expansion, low density and interesting optical properties (MOON *et al.*, 2011; PHANTHONG *et al.*, 2018). Due to these remarkable properties, there is an increasing interest for applications of nanocellulose in composites (DUFRESNE, 2018; LIU *et al.*, 2010; SONI; SCHILLING; MAHMOUD, 2016), packaging (LEITE *et al.*, 2021; LI; MASCHERONI; PIERGIOVANNI, 2015; SUN *et al.*, 2015), coatings (AULIN; GÄLLSTEDT; LINDSTRÖM, 2010; KABOORANI *et al.*, 2016), medical applications (KLEMM *et al.*, 2020; LIU *et al.*, 2021; OWOYOKUN *et al.*, 2020; PANDEY, 2021; SQUINCA *et al.*, 2021; WEI *et al.*, 2021), cosmetics (MOON; SCHUENEMAN; SIMONSEN, 2016) electronic devices (HSIEH *et al.*, 2013; HUANG *et al.*, 2013; WANG *et al.*, 2015; YUEN *et al.*, 2017), sensors (TEODORO *et al.*, 2021), among several other uses (DUFRESNE, 2019; NORRRAHIM *et al.*, 2021; SHATKIN *et al.*, 2014; THOMAS *et al.*, 2018).

Several terminologies have been used in the literature to define nanocellulose or cellulose nanomaterial, generating ambiguities and misunderstandings. According to the

International organization for standardization (ISO), cellulose nanomaterials comprise materials constituted predominantly of cellulose with any external dimension or having an internal structure in the nanoscale. Materials mostly composed of cellulose with surface structure in the nanoscale are also considered cellulose nanomaterials according to ISO (2017). Within this definition, cellulose nanocrystals (CNCs) and cellulose nanofibrils (CNFs) both fit.

Cellulose nanocrystals needle like structures characterized by their high crystallinity, have cross-section ranging from 3 to 50 nm, length from 100 nm to several micrometers and aspect ratio between 5 and 50 (ISO, 2017). Although acid hydrolysis (mainly HCl or H₂SO₄) is the most common method used for CNCs production, there is a growing interest in the enzymatic hydrolysis since it has advantages, such as not requiring corrosion-resistant equipment, being carried out in milder operating conditions, being more ecologically attractive and minimizing the formation of undesirable by-products due to the greater specificity of biocatalysts (RIBEIRO *et al.*, 2019).

Cellulose nanofibrils are elongated structures formed by alternating regions of amorphous and crystalline cellulose chains with cross-section ranging from 3 to 100 nm and lengths up to 100 μ m. The terms nanofibrillated cellulose, nanofibrillar cellulose, microfibrillated cellulose, microfibrillar cellulose, cellulose microfibril, cellulose nanofiber and cellulose nanofibre have been used to describe cellulose nanofibrils typically produced by mechanical treatment of plant materials and often combined with chemical or enzymatic pre-treatment steps (ISO, 2017). Besides cellulose nanofibrils isolated from plant cellulose sources via a top-down approach, this category also includes bacterial nanocellulose (BNC), also known as bacterial cellulose, which is obtained through a bottom-up approach being synthesized extracellularly by bacteria from the fermentation of glucose or other carbohydrate feedstocks. The diameter of BNC ranges between 20 and 100 nm arranged in different types of nanofiber network (KLEMM *et al.*, 2011).

Commonly, CNFs are produced by mechanical processes including high-pressure homogenization, ultrafine grinding and ultrasonication (NECHYPORCHUK; BELGACEM; BRAS, 2016). In order to reduce the energy consumption and enhance the fibrillation degree of the mechanical disintegration, pretreatments, such as TEMPO-mediated oxidation, enzymatic hydrolysis and carboxymethylation have been widely used (JONASSON *et al.*, 2020; JONOBI *et al.*, 2015; NECHYPORCHUK; BELGACEM; BRAS, 2016).

Enzymatic hydrolysis reduces the energy needed during mechanical processes as enzymes improve accessibility, hydration and swelling of cellulose (FRITZ *et al.*, 2015). Besides, studies have shown increases in the size uniformity of the CNFs and enhancement of their yield when enzymes were associated with mechanical treatments (WANG *et al.*, 2016; ZHANG *et al.*, 2020). Furthermore, it has been reported enzymatic hydrolysis could be used to produce CNCs with different morphologies (TONG *et al.*, 2020) and increase the yield of CNC when combined with acid hydrolysis (TANG *et al.*, 2015). Thus, the use of enzymes could contribute to improve the economic feasibility of large-scale production of the cellulose nanomaterials (RAMOS *et al.*, 2020).

Nanocellulose market foresees huge potential in the future and forecasts indicate that the market size is estimated to reach USD 418.2 million by 2026, at a compound annual growth rate (CAGR) of approximately 21.4% from 2020 to 2026 according to the report published by Global Market Insights Inc. (2020). Furthermore, the industrial interest in the nanocellulose field increasing is also shown by the astonishing increase in nanocellulose patents since 2010, especially from 2015 to 2017, which suggests increasing tendency may not stop in the upcoming years (CHARREAU; CAVALLO; FORESTI, 2020).

The growing demand for sustainable products, mainly in packaging, food & beverage industries, together with the search for properties of the current nanocellulose-based materials improvements and new applications development are driving forces for research in academia and industry (MARKETS AND MARKETS, 2020).

Several review articles have been published regarding the production of nanocelluloses, their properties and applications (DHALI *et al.*, 2021; DUFRESNE, 2019; KARGARZADEH *et al.*, 2018; KARGARZADEH; MARIANO; *et al.*, 2017; KLEMM *et al.*, 2020; KUMAR *et al.*, 2021; MOKHENA; JOHN, 2020; MOOHAN *et al.*, 2020; NANDI; GUHA, 2018; NORRRAHIM *et al.*, 2021; PARK *et al.*, 2019; SHOJAEIARANI; BAJWA; SHIRZADIFAR, 2019; THAKUR *et al.*, 2021; THOMAS *et al.*, 2018; TRACHE *et al.*, 2020). However, few of them are specifically focused on the enzymatic route to isolate cellulose nanomaterials and their applications (AFRIN; KARIM, 2017; ARANTES *et al.*, 2020; MICHELIN *et al.*, 2020; RAMOS *et al.*, 2020; RIBEIRO *et al.*, 2019). Moreover, there are rigorous evidence review methodologies, such as systematic reviews (SRs) and systematic maps (SMs), which were first developed in the healthcare field to support evidence-based decision making by collating, appraising, synthesizing and reconciling a large amount of primary studies (HIGGINS *et*

al., 2019). SRs are seen as a “gold standard” of evidence synthesis in healthcare (HIGGINS *et al.* 2011) and their use has been continuously expanding into other disciplines, including social welfare, education, crime and justice (SHLONSKY *et al.*, 2011), software engineering (KITCHENHAM *et al.*, 2009; PETERSEN; VAKKALANKA; KUZNIARZ, 2015), conservation and environmental management (PULLIN; STEWART, 2006; ROMANELLI *et al.*, 2021; WOODCOCK; PULLIN; KAISER, 2014), enzymatic synthesis of sugar esters (GONÇALVES *et al.*, 2021) and food/feed safety assessment (AUTHORITY, 2010).

The systematic mapping follows the same rigorous, objective and transparent processes as do systematic reviews to collect evidence that is relevant to a particular topic, but they do not attempt to answer a specific question. Systematic mapping is particularly valuable for broad, multi-faceted questions relating to a topic of interest often used to catalogue evidence, describe the state of knowledge and identify knowledge gaps, unknown trends and research clusters (JAMES; RANDALL; HADDAWAY, 2016). Despite the unquestionable quality of the review articles already published in the literature, none of them followed rigorous methods to conduct the search and evaluate the primary studies related to nanocellulose, mainly, isolated from enzymatic hydrolysis.

Thus, the purpose of this systematic map is to describe the state of knowledge of the cellulose nanomaterials whose production process included the use of enzymes and identify the trends and gaps in the literature. Additionally, the applications of these nanomaterials that have been most studied were identified and reported. This work is focused on top-down strategies and therefore excludes bacterial nanocellulose. This systematic mapping was performed as an attempt to identify the most used substrates and enzymes in the isolation of nanocellulose using enzymatic hydrolysis and the main applications of these nanomaterials based on carefully identifying and analyzing studies from the literature. It is believed that this work could help to identify recent advances, main gaps and assist researchers to conduct future studies on this topic.

2.3 Methodology

The systematic map was conducted in sequential stages which were described by (JAMES; RANDALL; HADDAWAY, 2016) and presented in Figure 2.1. The first stages (1-3) were undertaken following Collaboration for Environmental Evidence (CEE) Systematic Review Guidelines (PETROKOFISKY, 2018).

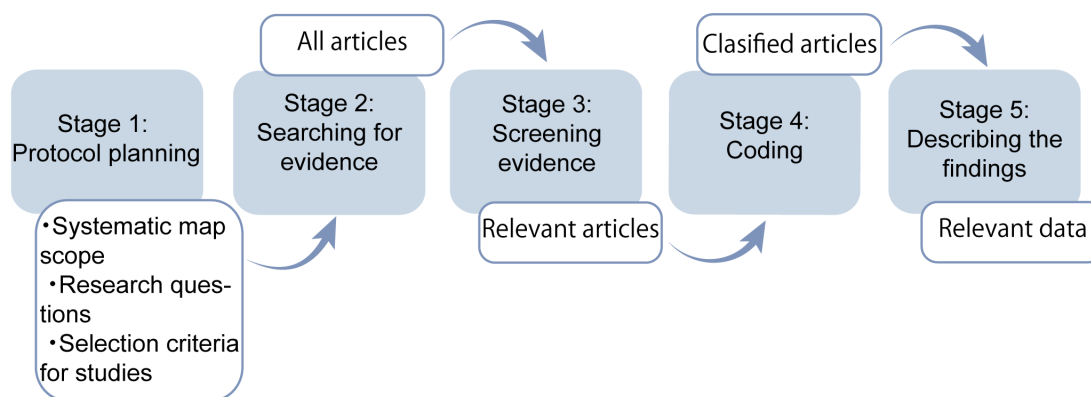


Figure 2.1. Design of systematic mapping steps used in the present work to describe the state of knowledge of the cellulose nanomaterials whose production process included the use of enzyme.

Stage 1: Setting the scope, research questions and inclusion criteria for studies

Since SM collates, describes and catalogues available studies relating to a topic of interest instead of answering a specific question as does a systematic review (BATES; CLAPTON; COREN, 2007), the research questions (RQ) can be more open-framed than those used in systematic reviews (JAMES; RANDALL; HADDAWAY, 2016). Additionally, the research questions are important elements of the research project and formulated to reflect the main and secondary goals of the study. In this study, the following research questions were used:

RQ1: Which are the main purposes for using enzymatic hydrolysis in cellulose nanomaterials production?

RQ2: What type of applications nanocellulose produced by processes which include enzymatic hydrolysis have been commonly used for?

Stage 2: Searching for evidence

Search strings were formulated following a five-step guidelines: 1) definition of the major keys considering the research questions and keywords of the area; 2) identification of alternative words, synonyms or related terms to major keywords; 3) verification if the major keywords are found in relevant articles of the research of interest; 4) association the synonyms, alternative words or terms related to the main keywords with the Boolean “OR”; and 5) relation the major terms with Boolean “AND”(KITCHENHAM; BUDGEN; BRERETON, 2011; KITCHENHAM;

BRERETON; BUDGEN, 2010; WOHLIN *et al.*, 2012).

Figure 2.2 shows the major keywords, “cellulose nanomaterials” and “enzymatic hydrolysis”, their synonyms and related words based on the literature (CHARREAU; CAVALLO; FORESTI, 2020; DUFRESNE, 2019; JONOBI *et al.*, 2015; KARGARZADEH *et al.*, 2018; KARGARZADEH; MARIANO; *et al.*, 2017; MARIANO; EL KISSI; DUFRESNE, 2014; PENNELLS *et al.*, 2020; PHANTHONG *et al.*, 2018; SHOJAEIARANI; BAJWA; SHIRZADIFAR, 2019; TRACHE *et al.*, 2020). It is important to highlight that this work is limited to cellulose nanomaterials derived from plants and through top-down strategies and, therefore, bacterial cellulose is not included.

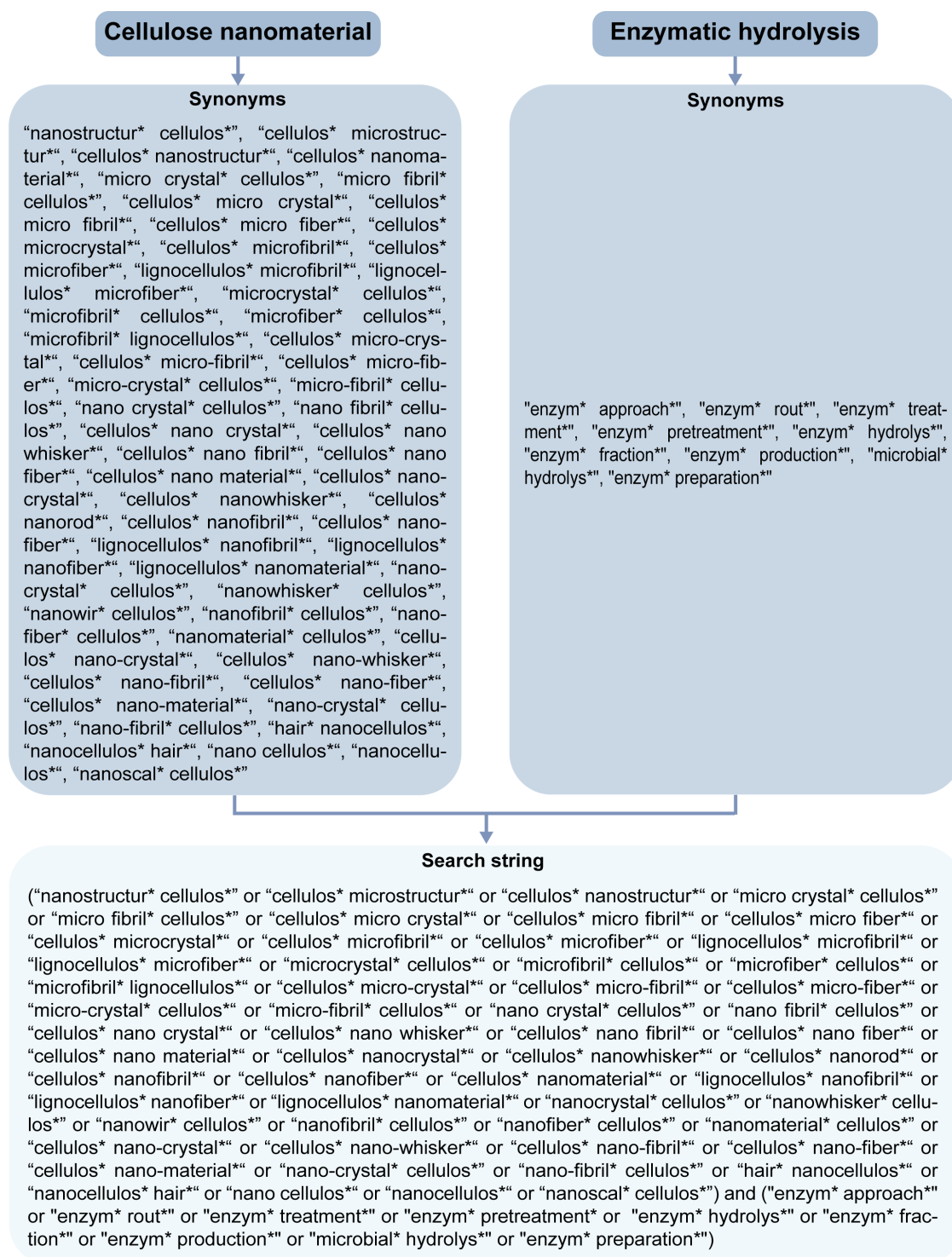


Figure 2.2. Search string used to collect articles for the systematic mapping.

Web of Science, Scopus and Engineering Village were used to search for relevant literature and data. The search string from Figure 2.2 was modified according to the database. Table 2.1 presents the search strategy and the number of articles obtained from each database.

Table 2.1. Databases used in the systematic mapping along with their search strategy and number of articles obtained in each one.

Database	Search Strategy	Search Results
Web of Science	Basic search: ALL FIELDS (Core collection: SCI-E, ESCI)	834
Scopus	Basic search: TITLE-ABS-KEYWORDS	746
Engineering Village	Basic search: ALL FIELDS	1123

Stage 3: Screening evidence

The studies were selected in three steps: preliminary selection, primary selection and final selection. Initially, searches were performed on the selected databases in April of 2021 and they were restricted to articles published between 2000 and 2021. The results from each database were combined in a single Mendeley library file in order to create a database containing the preliminary selection of this systematic map. Then, the duplicates were removed using an automatic function in Mendeley. After that, the selection of relevant studies associated with research questions were conducted by analyzing the titles and abstracts (primary selection) and full reading (final selection) with regards the following inclusion (IC) and exclusion criteria (EC):

IC1: The article was published online within the period of time 2000 (January) to 2021 (March);

IC2: The article is a primary study about (i.e. review articles, conference abstracts were not considered in this systematic mapping);

IC3: The study is related to nanocellulose isolated by enzymatic route;

EC1: The study is not written in English;

EC2: The study is not accessible in full-text;

EC3: The study is a duplicate of other study;

EC4: Data regarding the properties and characteristics of nanocellulose are not well presented.

EC5: The study was published in a journal whose impact factor is lower than 1.5.

The number of included and/or excluded articles at each step is shown in Figure 2.3.

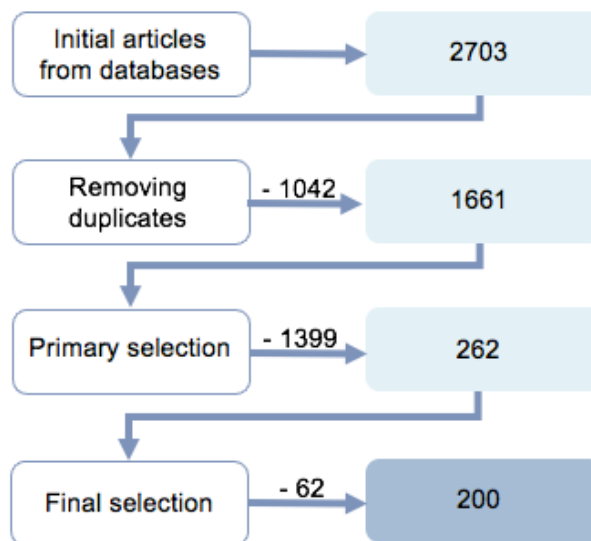


Figure 2.3. Number of articles after each selection step.

The lists of excluded and included in the final selection are presented in appendix A (Table A.1 and Table A.2).

Stage 4: Coding

Coding is the process of assigning categories to each study for a suite of variables that describe the study setting and design (BATES; CLAPTON; COREN, 2007). Usually, it combines metadata and generic (e.g. author, title, year of publication, publication type, data source type, data type) with topic-specific elements (e.g. intervention/s, population/s, length of study, sampling strategy) describing the study setting (JAMES; RANDALL; HADDAWAY, 2016). Thus, the relevant studies which met inclusion criteria were coding with regards their metadata and in accordance with the research questions established previously, as follows:

Article metadata: Publication year, author(s), the title of the article, abstract (if available from bibliographic database or article), source and DOI.

Processing conditions used for the production of nanocellulose by enzymatic hydrolysis: Substrate, production process steps, hydrolysis condition (solids content, type of enzyme, enzyme concentration, duration, temperature, pH and rotation speed).

Main purposes of the article and the reasons for choosing to use enzymes in the nanocellulose production process.

Application of cellulose nanomaterials.

Stage 5: Describing the findings

The calculations were performed using MS Excel (v. 2016) while OriginPro software (version 8.5) was used to make the graphs. Terms were assigned to articles to provide a “fingerprint” of each article in order to answer the research questions and to explore the hot topics of cellulose nanomaterials production using enzymes with the assistance of network maps drawn by VOSviewer software (version 1.16.15). It was used the text mining functions to construct and visualize the co-occurrences of these “terms” and then identify trends across the included literature. VOSviewer is a software tool expressly designed for the analysis of bibliometric data (GONÇALVES *et al.*, 2019; VAN ECK; WALTMAN, 2010).

2.4 Results and discussion

This section briefly presents the main concepts related to nanocellulose and enzymatic hydrolysis followed by the quantitative results obtained from the analysis of the 200 articles selected according to the methodology presented above.

2.4.1 Nanocellulose overview

The continuous expansion of nanocellulose market is due to their broad applicability and differentiated properties. The first pilot-scale plant for the production of nanocellulose was inaugurated in 2011 by Innventia in Sweden (INNVENTIA, 2011). Currently, CNCs are produced industrially by ten organizations, i. e., Alberta-Pacific Forest Industries Inc. (Canada), Anomera Inc. (Canada), Blue Goose Refineries (Canada), Cellulforce Inc. (Canada), Cellulose Lab (Canada), GranBio (USA), FPInnovations (Canada), InnoTech Alberta (Canada), Melodea Ltd. (Israel), USDA Forest Products Laboratory (USA) at the pilot, demonstration or semi-industrial scales (VANDERFLEET; CRANSTON, 2021). Meanwhile, CNFs have been produced by Nippon Paper Industries (Japan), Rise Innventia (Sweden), American Process Inc. (US), UPM-Kymmene Oyj (Finland), Cellucomp (United Kingdom), Oji Paper (Japan), VTT

(Finland), and Sappi (Netherlands), Sugino Machine (Japan), Seiko PMC (Japan), Tianjin Haojia Cellulose Co. Ltd. (China), Dai-ichi Kyogo (Japan), the production capacities ranging from 560 kg to 1 tonne per year (dry basis) (MILLER, 2017).

As previously mentioned, the forecast for the global nanocellulose market is projected to increase to US\$ 418.2 million by 2026 according to a report of Global Market Insights Inc. (2020). Another study from Markets and Markets reported that nanocellulose may reach US\$ 783 million in 2025 at a CAGR of approximately 21.3% (MARKETS AND MARKETS, 2020). Although the NC market size projections may differ depending on the consulting company that evaluated the global market and the end-use product cost is difficult to estimate due to the confidentiality of the financial-related aspects of commercial companies, the NC market is undeniably increasing and will further expand as its production process becomes cheaper (DHALI *et al.*, 2021).

2.4.1.1 Cellulose nanocrystals isolation

Several methods have been reported for CNCs isolation, namely, acid hydrolysis, enzymatic hydrolysis, mechanical refining, ionic liquid treatment, subcritical water hydrolysis, oxidation method and combined processes (TRACHE *et al.*, 2017). However, acid hydrolysis is the most commonly used technique including at an industrial scale (VANDERFLEET; CRANSTON, 2021).

In general, the preparation of CNCs from plant-based materials comprises the following steps: mechanical size reduction, purification by bleaching or alkali and bleaching treatments, controlled chemical or biochemical treatment, mainly, by acid hydrolysis for removing the inter-fibril regions and amorphous parts and releasing CNCs (KARGARZADEH *et al.*, 2018). It should be noted that the purification step may not be required depending on the biomass source. Amorphous regions are prone to hydrolytic action because of the reduced steric hindrance and kinetic factors, while the ordered domains remain preserved due to their higher resistance to the hydrolysis process. At the end of the hydrolysis, cycles of washing/rinsing steps followed by dialysis against deionized water are needed to eliminate residual acid and neutralize salts. Further post-treatments such as mechanical treatment, for instance, sonication and ultrasound, and surface modification can also be applied (TRACHE *et al.*, 2020).

Besides of the feedstock source, the properties of CNCs (morphology, aspect ratio, density, mechanical features, thermal stability, dimensional dispersity and crystallinity) are affected by temperature and reaction time, type and concentration of

acid, as well as the fiber to the acid ratio (AL-DULAIMI; WANROSLI, 2017; BONDESON; MATHEW; OKSMAN, 2006; DUFRESNE, 2017). Sulfuric and hydrochloric acids are more frequently employed to extract CNCs, but other acids, such as citric acid, hydrobromic acid, hydrochloric acid, phosphoric acid, acetic acid, maleic acid, oxalic acid, malonic acid, among others have also been evaluated (BIAN *et al.*, 2017; BONDANCIA *et al.*, 2020; CAMARERO ESPINOSA *et al.*, 2013; CHEN *et al.*, 2016; MOON *et al.*, 2011; SPINELLA *et al.*, 2016; WANG *et al.*, 2017; YU *et al.*, 2019).

When hydrolysis is carried out with sulfuric acid, a fraction of hydroxyl groups on the surface of cellulose fibril is esterified. The sulfuric acid hydrolysis generates a high stable colloidal suspension owing to the high negative surface charge, but the presence of sulfate esters at the cellulose surface decreases its thermal stability (TRACHE *et al.*, 2020). The limited thermal stability certainly restricts the processing of CNCs based nanocomposites at high temperatures (CAMARERO ESPINOSA *et al.*, 2013). In contrast, when hydrolysis is carried out with hydrochloric acid, the CNCs present low-density surface charges with limited dispersibility and tend to aggregate in an aqueous solution (KLEMM *et al.*, 2011; VASCONCELOS *et al.*, 2017). One strategy to overcome this drawback is through functionalization of these nanomaterials (TRACHE *et al.*, 2017).

2.4.1.2 Cellulose nanofibrils extraction

Unlike the cellulose nanocrystals, nanofibrils are long, elongated and flexible materials composed of more or less individualized cellulose microfibrils which alternate crystalline and amorphous domains (GARCÍA *et al.*, 2016). The lateral dimensions of CNFs range from 3 nm, representing individualized elementary fibrils to several nanometers, corresponding to single microfibrils and their bundles (NECHYPORCHUK; BELGACEM; BRAS, 2016). In comparison with CNCs, CNFs have longer length with high aspect ratio and high surface area with abundant hydroxyl groups that facilitates their access for surface modification (LAVOINE *et al.*, 2012; PHANTHONG *et al.*, 2018).

Commonly, nanofibrils are produced by mechanical disintegration using homogenization (homogenizers and microfluidizers) and grinding. In general these techniques cause transverse cleavage along the longitudinal axis of the cellulose microfibrillar structure, resulting in the extraction of long cellulose fibrils by applying high shear forces (MOON *et al.*, 2011). Other techniques less conventional to isolate CNFs are enzymatic hydrolysis, extrusion, blending, ultrasonication, cryocrushing, refining (as a principal mechanical process), steam explosion, ball milling and aqueous

counter collision (NECHYPORCHUK; BELGACEM; BRAS, 2016).

Regarding the high-pressure homogenization (Figure 2.4a), cellulose fibrillation is achieved by forcing the cellulose slurry to pass through a very narrow channel or orifice using a piston, under high-pressure of 50–2,000MPa. The reduction of cellulose fibers size is owing to the high pressure drop and shear forces, the turbulent flow and the collision of the particles against each other. Moreover, the extent of the cellulose fibrillation is mainly determined by the number of homogenization cycles and the applied pressure (KALIA *et al.*, 2014). Unlike the homogenizer, which operates at constant pressure, the microfluidizer (Figure 2.4b) performs at a constant shear rate. The cellulose slurry is pumped in a thin chamber with a specific geometry (Z- or Y-shape) with an orifice width of 100–400 μm where it accelerates to high velocities. High forces and impact of the suspension against the channel walls are achieved resulting in the fibrillation of cellulose. Typically, the process is repeated several times and chambers with different sizes are used to improve the fibrillation degree (KARGARZADEH *et al.*, 2017).

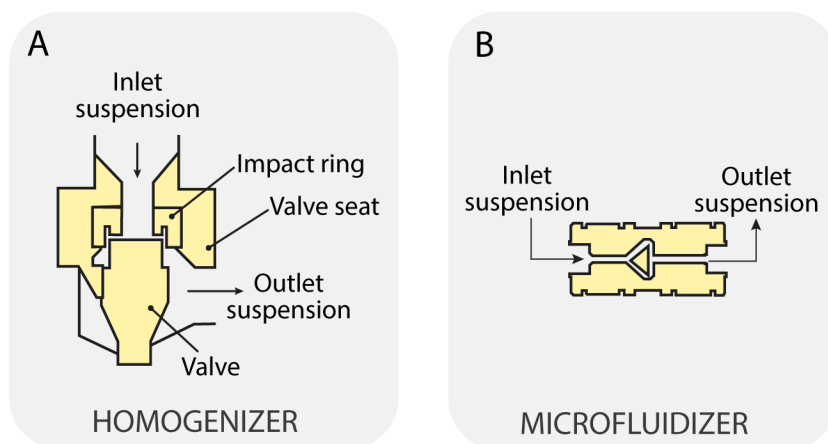


Figure 2.4. Schematic image of a homogenizers and a microfluidizer. Adapted from (NECHYPORCHUK; BELGACEM; BRAS, 2016) with permission provided by Elsevier and Copyright Clearance Center.

Another mechanical treatment to obtain nanosized fibrils is grinding and the Supermasscolloider grinders (Masuko Sangyo Co. Ltd., Japan) are mostly used for such technique. During this process, the cellulose slurry is passed between static and rotating grinding stones (disks) which applies shearing stress to the fibers (NECHYPORCHUK; BELGACEM; BRAS, 2016). The cell wall is delaminated and the nanofibrils are

individualized due to the shearing forces generated between the discs. The fibrillation extent depends on the number of passes through the grinder, the morphology of the disk channels as well as the distance between the disks (KARGARZADEH *et al.*, 2017).

2.4.2 The use of enzymatic hydrolysis in the cellulose nanomaterials production

As mentioned before, acid hydrolysis procedures are broadly used to produce CNCs. However, some drawbacks of this process include aspects related to the safety in material handling, large water usage, equipment corrosion and generation of a huge amount of toxic waste. On the other hand, CNCs production by the enzymatic route is a greener and promising alternative offering advanced selectivity, milder operating conditions in comparison to the chemical processes and acceptable yields (RIBEIRO *et al.*, 2019).

Considering the CNFs, mechanical processes are mostly used for industrial production and their major disadvantage is the high energy consumption. Mechanical treatments are usually combined with chemical treatments, such as 2,2,6,6-tetramethylpiperidine-1-oxyl mediated oxidation (TEMPO) and enzymatic treatments to facilitate cellulose fibrillation and reduce energy demand. Since TEMPO is an expensive reagent and its efficient recovery still needs to be improved (DELGADO AGUILAR *et al.*, 2015; ESPINOSA *et al.*, 2016; KUUTTI *et al.*, 2016), the use of enzymes has been considered a promising eco-friendly alternative step to be used in the production of nanomaterials.

The interest in obtaining cellulose nanomaterials via enzymatic hydrolysis has increased mainly because, unlike the acid hydrolysis and chemical treatment, it does not generate toxic residues, it is carried out under milder conditions of temperature and pressure and the high specificity of the enzymes for the substrate. However, the high cost of these biocatalysts is still considered a major challenge that needs to be overcome. Thus, taking into account the several advantages, particularly related to process sustainability, the development of enzymes at a competitive production cost is relevant to improving the economic viability of nanocellulose production by enzymatic hydrolysis (ARANTES *et al.*, 2020; MICHELIN *et al.*, 2020). Furthermore, relatively lower yields and longer reaction times have been reported and suggested as reflections of the still early stage of process development and need to be addressed as well (ROSALES-CALDERON; PERIRA; ARANTES, 2021).

A total of 2703 articles related to the production of nanocellulose using enzymes

in their production process were retrieved and processed following the methodology described previously. The screening process resulted in an evidence map of 200 primary studies (Figure 2.3). Figure 2.5 illustrates the annual number of primary studies related to the cellulose nanomaterials whose production process included the use of enzymes that were found on surveys performed between 2000 and 2021, screened and selected in this systematic map.

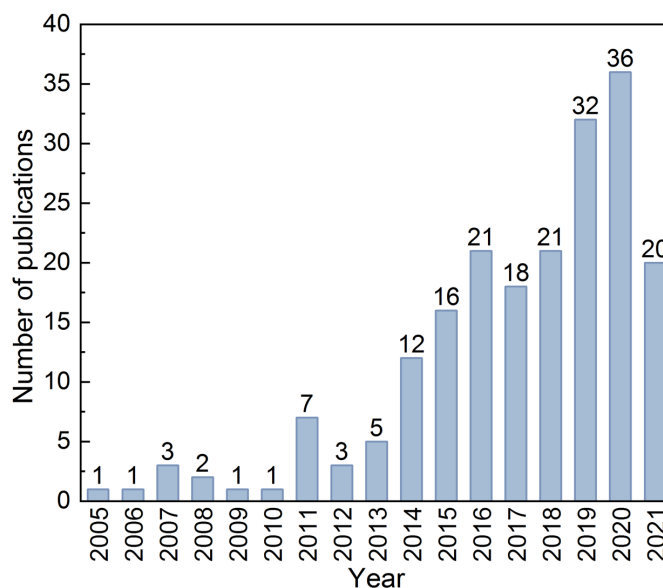


Figure 2.5. Annual distribution of articles obtained after the second screening step.

Considering the time period chosen to conduct this systematic map, the production of cellulose nanomaterials using enzymes was firstly reported by Hayashia, Kondo and Ishihara (2005) when they were investigating the selective enzymatic hydrolysis of microcrystalline cellulose using a fraction rich in cellobiohydrolase which was obtained from commercial cellulases. In 2006, Janardhnan and Sain (2006) demonstrated that the yield of microfibrillated cellulose obtained by mechanical refining could be enhanced by treating kraft pulp with a fungus isolated from Dutch Elm trees infected with Dutch elm disease. In the next year, Henriksson *et al.* (2007) and Paäkko *et al.* (2007) evaluated the application of endoglucanase (Novozym 476) to improve the efficacy of mechanical treatment of cellulose in the microfibrillated cellulose preparation while Agblevor, Ibrahim and El-Zawawy (2007) explored the use of commercial cellulases to produce microcrystalline cellulose from cotton gin waste and corn cob. The following studies have evaluated the use of both monocomponent enzymes and enzymatic complexes together with mechanical and/or chemical treatments as an auxiliary method for different

purposes, such as reduction of the energy consumption (mechanical refinement), decreasing of the acid concentration, improvement of nanomaterial properties (thermal stability, yield, size, morphology). Enzymatic treatment has also been used as the main step of the process for obtaining nanomaterials. Furthermore, enzymatic hydrolysis provides a promising route to integrate the production of nanocellulose and biofuels from lignocellulosic materials in a biorefinery concept as reported by Bondancia *et al.* (2017) and Squinca *et al.* (2020).

From Figure 2.5 it can be observed the growth in the number of publications was not prominent from 2000 to 2012. However, a significant increase can be observed in 2013 and 2021. These results are in agreement with Charreau, Cavallo and Foresti (2020) who reported an astonishing increase in the number of patents referring to cellulose nanomaterials, including cellulose nanofibrils and nanocrystals, from 2010 to 2017 with especially high annual increments since 2015. The continuous increase in the number of studies and patent documents published every year highlights the growing interest among the scientific community and industrials in the field of cellulosic nanomaterials. The tendency observed in Figure 2.5 indicates that this subject is in the early development stages and holds great potential not only for research and development of novel and more efficient production methods but else innovative applications during the following years.

2.4.3 Sources for nanocellulose production

Cellulose can be derived from several sources, such as hardwood (Eucalyptus, Maple, Birch, Aspen, Oak, Elm), softwood (Hemlock, Yew, Pine, Juniper, Cedar), agricultural and forest residues (sugarcane bagasse and straw, garlic straw residues, Mulberry fiber, Mengkuang leaves), municipal waste (organic and paper waste), animal (*Chordata*, Tunicates, *Styela clava*, *Halocynthia roretzi* Drasche), fungi, bacteria (*Acetobacter*, *Azotobacter*, *Aerobacter*, *Sarcina*, *Gluconacetobacter*, *Salmonella*, *Agrobacterium*, *Rhizobium*, *Alkaligenes*, *Pseudomonas*, *Rhodobacter*) and Algae (*Cladophora*, *Cytoseria myrica*, *Posidonia oceanica*) (TRACHE *et al.*, 2020). Vascular plants are the major industrial source of cellulose and their cell wall structure and composition vary between different plant species, different tissues and cells (LAVANYA *et al.*, 2011; SIRÓ; PLACKETT, 2010). Figure 2.6 presents the hierarchical structure from hardwood to cellulose chains.

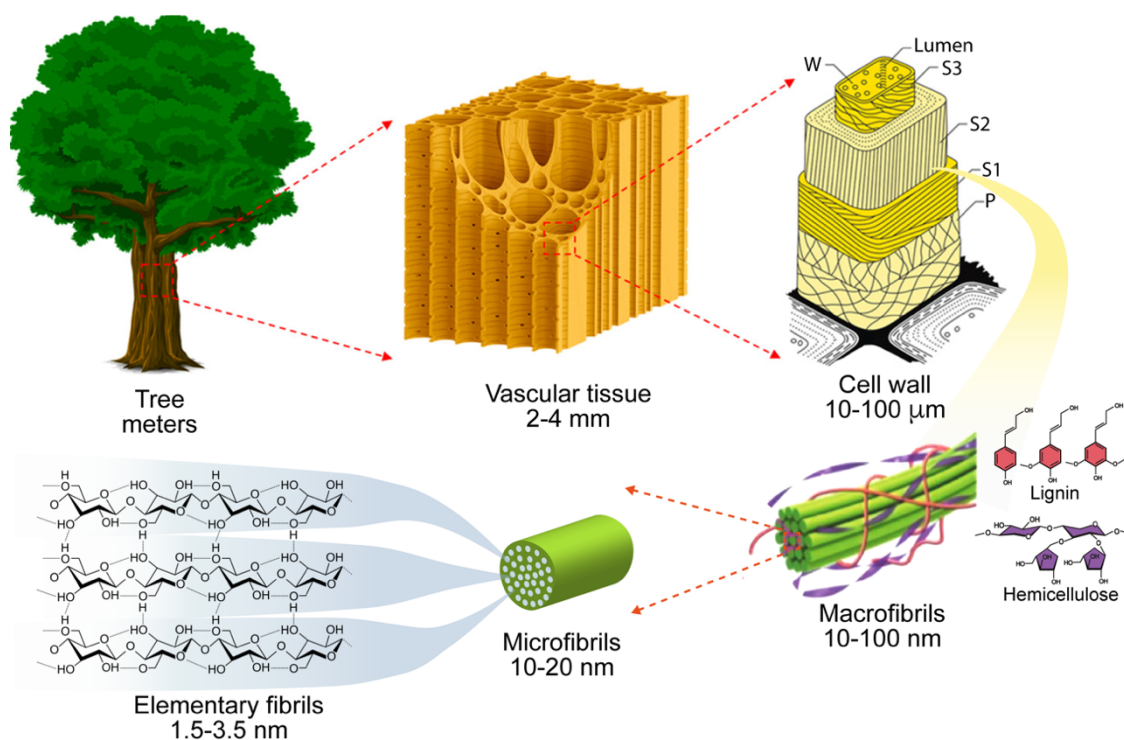


Figure 2.6. Hierarchical structure from hardwood to cellulose chains at different scales. Adapted from Chen and Hu (2018) with permission provided by American Chemical Society and Copyright Clearance Center. Macrofibrils, microfibrils, and elementary fibrils schemes were adapted from Jiang *et al.* (2018) with permission provided John Wiley and Sons and Copyright Clearance Center.

Generally, cellulose (20–50% on a dry weight basis), hemicellulose (15–35%), and lignin (10–30%) are the primary constituents of cell walls, whereas proteins (3–10%), lipids (1–5%), soluble sugars (1–10%) and minerals (5–10%) are minor components (PAULY; KEEGSTRA, 2008). Typically, the plant cell (Figure 2.6) is organized into the middle lamella, the primary and secondary (outer, middle and inner layers) walls and the warty layer. The primary wall is formed mainly by cellulose, hemicellulose and pectin, and the cellulose microfibrils are crosswise located. The secondary wall has more cellulose than the primary wall, hemicellulose and lignin, but lacks pectin. The microfibrils of cellulose are parallel aligned and densely packed in the secondary wall (KLEMM *et al.*, 1998; SJOSTROM, 1993).

Cellulose is a linear homopolysaccharide formed by β -D-glucopyranose (anhydroglucose) monomers linked by β -(1,4) glycosidic bonds. The repeat unit, cellobiose, is a dimer of D-glucose (HABIBI; LUCIA; ROJAS, 2010). Due to the

abundance of several hydroxyl groups of the cellulose chains, hydrogen bonds are formed between OH groups conveniently positioned within the same cellulose molecule (intramolecular) and between adjacent cellulose chains (intermolecular). Intramolecular hydrogen bonds are responsible for the linear configuration of the cellulose chain (LAVOINE *et al.*, 2012). During cellulose biosynthesis, intermolecular hydrogen bonds together with van der Waals forces between neighboring molecules promote the parallel stacking of multiple cellulose chains generating elementary fibrils, which in turn aggregate into microfibrils (10–20 nm in diameter and several micrometers in length) being further assembled into cellulose fibers (DONALDSON, 2007; MOON *et al.*, 2011). The number of cellulose chains in the elementary fibril is also a matter of discussion, since most of the previous works have proposed a 36-chain model (BROWN JR, 1996; CHEBLI *et al.*, 2012), but recently a 24-chain model has been suggested (FERNANDES *et al.*, 2011). Within these elementary fibrils there are regions in which the cellulose chains are arranged in a highly ordered structure (crystalline) and others that are more disordered (amorphous) (JIANG *et al.*, 2018; MOON *et al.*, 2011).

Cellulose can be found in different polymorphs, i.e., cellulose I, II, III_I, III_{II}, IV_I, and IV_{II} which can be transformed from one to another by using thermal or chemical treatments (O'SULLIVAN, 1997). Cellulose I, native cellulose, is the form found in nature, and it occurs in two allomorphs, alfa and beta, and the latter is the most abundant crystalline polymorph found in higher plants which has a two-chain monoclinic unit cell (NISHIYAMA; LANGAN; CHANZY, 2002). The degree of polymerization of cellulose varies, depending on its source, for instance, 10,000 in native wood; 20,000 in cotton; 44,000 in Valonia, extraction and/or purification methods (NECHYPORCHUK; BELGACEM; BRAS, 2016).

Hemicellulose is a diverse group of short-chain branched, usually characterized as heteropolysaccharide, and extractible by alkaline solutions (RAGAUSKAS *et al.*, 2006; SCHELLER; ULVSKOV, 2010). It has a backbone composed of 1, 4-linked β -D-hexosyl residues and may contain pentoses (β -D-xylose, α -L arabinose), hexoses (β -D-mannose, β -D-glucose, α -D-galactose) and/or uronic acids (α -D-glucuronic, α -D-4-O-methylgalacturonic and α -D-galacturonic acids). Other sugars, such as α -L-rhamnose and α -L-fucose, may also be present in small amounts and the hydroxyls of sugars may be partially replaced by acetyl groups (GÍRIO *et al.*, 2010). Its composition also depends on the origin of the material. Softwoods have high proportions of mannose and a higher number of galactose units, while hardwoods have a high amount of xylose (FENGEL;

WEGENER, 1989). Hemicellulose has a lower degree of polymerization than native cellulose (~40 to 200) and contributes to cell wall strengthening through their interaction with cellulose and, in some plant species, with lignin as well (SCHELLER; ULVSKOV, 2010).

Lignin is a three-dimensional cross-linked complex compound (XU *et al.*, 2020). The chemical structure of lignin is quite complex and its composition and content are influenced by different plant species and by the environment. In general, lignin consists of phenylpropane units, derived from the oxidative polymerization of three precursor aromatic alcohols (monolignols): p-coumaryl, coniferyl and synaplic alcohols. Monolignols are differentiated from each other by the substitutions they have on the aromatic ring. The phenolic substructures originated from these monolignols are called: p-hydroxyphenyl (from p-coumarlic alcohol), guaiacyl (from coniferyl alcohol) and syringyl units (from synapyl alcohol) (LAURICHESSE; AVÉROUS, 2014). Lignin is vital for the strength and stiffness of cells, resistance to microbial attack and it also has an important role in nutrients and water transportation (VOELKER *et al.*, 2011).

Figure 2.7 summarizes the feedstocks that were used in the evaluated studies focused on nanocellulose production which includes an enzymatic hydrolysis step. A list of the different feedstocks used in the selected articles and their occurrences can be found in the appendix A (Table A.3).

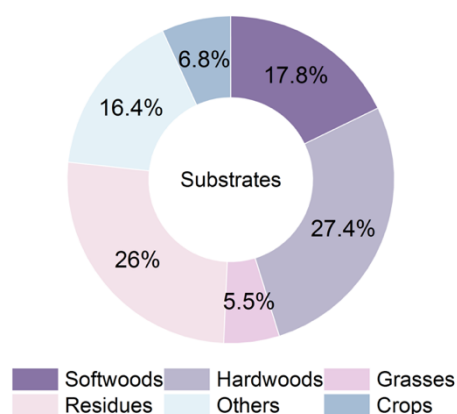


Figure 2.7. Proportion of the main feedstocks used in the enzymatic hydrolysis obtained from the screened articles.

The majority of feedstocks used for the NCs production were derived from

hardwood (28%) and softwood (18%), both mainly composed by bleached Kraft pulp and Northern bleached hardwood Kraft pulp (Appendix A - Table A.3). The main species of hardwood mentioned in the selected articles were Eucalyptus, Acacia, Poplar while those of softwoods were Pine, Spruce, and Pinus (Appendix A - Table A.3). These results were already expected since the pulp and paper industry is the most significant supplier of cellulose for cellulose nanomaterials production providing delignified and bleached pulps (KLEMM *et al.*, 2018). Moreover, bleached pulp wastes from this industry can be more easily converted into NC which contributes to decreasing the consumption of chemicals, energy and overall costs. Interestingly, a quarter of the evaluated studies used feedstocks were residues, mainly from agro-industries, such as sugarcane straw and bagasse, corn cob, oat husks, lemongrass leaves, oil palm empty fruit bunch, rice straw, among others (Appendix A - Table A.3). The use of residues in environmentally friendly processes to produce renewable materials, e. g., cellulose nanomaterials is aligned with the goals of Agenda 2030 for sustainable development. In addition to the minimization of residues, this strategy can provide higher economic profits owing to the industrial value chain increase (DI GRUTTOLA; BORELLO, 2021).

2.4.4 Enzymes used in the nanocellulose production

Initially, the use of enzymes associated with the production of nanocellulose was more often investigated as an assistant step of mechanical treatments. However, enzymatic hydrolysis has been also evaluated as the main step in the process of nanocellulose isolation. Regardless the role in the overall process, carbohydrate-active enzymes, especially cellulases, are the biocatalyst most used in the top-down strategy to obtain nanocellulose from lignocellulosic materials.

Cellulases basically belong to a wider enzyme class, i. e., glycoside hydrolases, that cleave the β -1,4-glucosidic bonds (PANDEY; KUILA; TULI, 2021). Cellulases are produced by a broad range of microorganisms including fungi and bacteria and those belong to the former are the most used for industrial applications (PAYNE *et al.*, 2015). The synergistic action of these enzymes is essential in the hydrolysis of lignocellulose. Besides, studies have demonstrated that copper-dependent lytic polysaccharide monooxygenases (LPMOs), which are oxidative enzymes which oxidatively cleave the cellulose chain thereby potentiating the activity of hydrolytic enzymes (ANDLAR *et al.*, 2018; LI *et al.*, 2021).

Figure 2.8 shows the major classes of cellulases, endo-1,4- β -d-glycanases (EG,

EC 3.2.1.4), cellobiohydrolases (exo-1,4- β -d-glucanases, CBH, EC 3.2.1.91) and β -glycosidases (1, 4- β -d-glycosidases, BG, EC 3.2.1.21), involved in hydrolyzing cellulose microfibrils in the cell wall of plant-based materials.

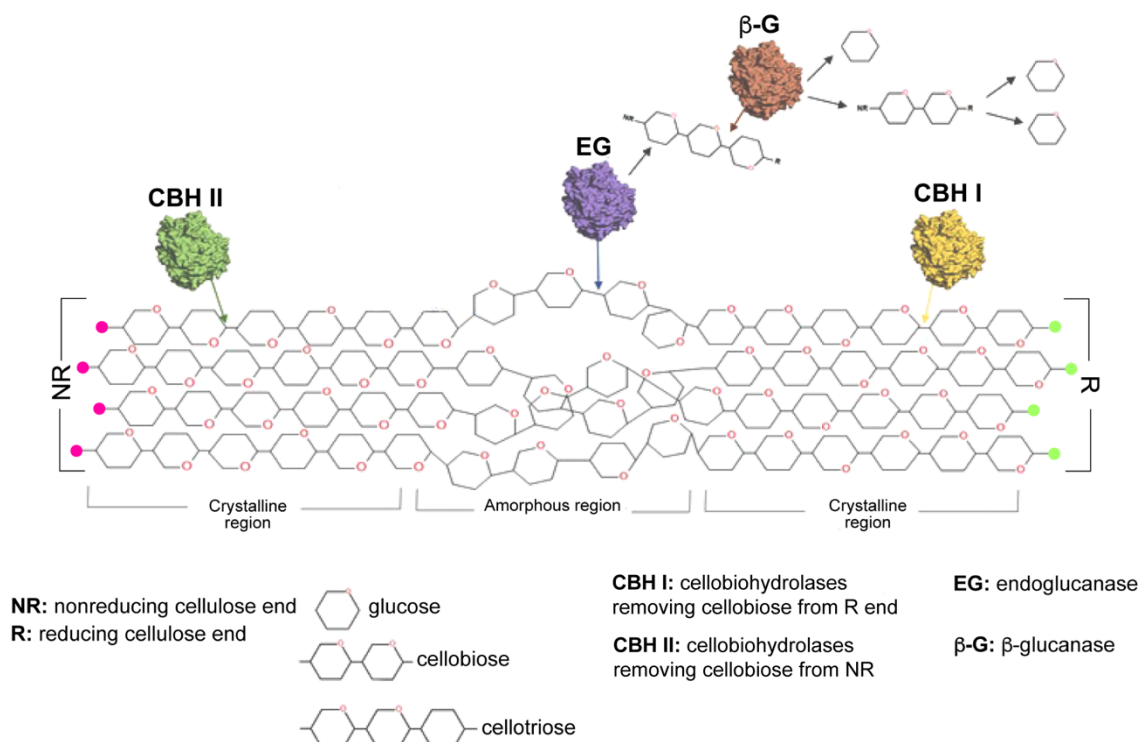


Figure 2.8. Overall scheme of the enzymatic hydrolysis of cellulose involving synergistic interaction of the major cellulases (endoglucanase, cellobiohydrolases and β -glucosidase). Adapted from Andlar (2018).

EGs hydrolyze the beta-1,4 glycosidic bonds mainly of the amorphous regions of cellulose microfibrils, producing oligosaccharides of lower molar mass (cellodextrins), cellobiose and releasing reducing and nonreducing chain ends. Due to its high specificity for acting at the disordered areas of cellulose, EGs were shown to slightly increase the crystallinity of cellulose materials (MANSFIELD; MEDER, 2003). EG action has also an effect on the decrease of degree of polymerization of cellulose (CAO; TAN, 2002). The CBH I acts on the reducing end of the chain while the CBH II attacks the non-reducing end of cellulose polysaccharide chains producing either glucose or cellobiose (a dimer of glucose) as major products. These enzymes can also act on microcrystalline cellulose (LYND *et al.*, 2002). In general, cellobiohydrolases are processive enzymes, i. e., they remain bound to the cellulose until a minimum chain length is reached. The β -

glycosidases act on cellobiose and cellodextrins producing glucose (KUMAR; MURTHY, 2013).

Besides cellulases, xylanases have been also largely applied to nanocellulose production as the lignocellulose materials have some content of hemicellulose. In addition, xylanases may also act synergistically with cellulases improving fibers' swelling and porosity, enhancing the accessibility of cellulases to cellulose (BAJAJ; MAHAJAN, 2019; SONG, HUI-TING *et al.*, 2016).

Among several enzymes involved in the depolymerization of the hemicellulose heterogeneous structure, endo-xylanases (EXs)(EC 3.2.1.8) and exo-b-xylosidase (EC 3.2.1.37) are the most used in the nanocellulose isolation. Endo-1,4- β -xylanases (1,4- β -D-xylan xylanohydrolase; EC 3.2.1.8) do not act randomly on the xylan backbone. These enzymes cleave selected glycosidic bonds depending on chain length, the degree of branching and the presence of substituents. Exo-b-xylosidase (EC 3.2.1.37) liberate xylose from the non-reducing end from the xylo-oligosaccharides (POLIZELI *et al.*, 2005).

Lytic polysaccharide monooxygenases is another class of enzymes that have been evaluated to assist NC production. LPMOs act on cellulose chains by oxidative cleavage of glycosidic bonds, generating oxidized chain ends in different positions, which increases the substrate susceptible to the action of cellulases (VILLARES *et al.*, 2017). Studies have reported the use of LPMO in synergy with cellulases and/or xylanases to facilitate the deconstruction of cellulose fibers for producing CNF (HU *et al.*, 2018; MOREAU *et al.*, 2019; VALENZUELA *et al.*, 2019).

To evaluate the enzymes commonly used in the enzymatic hydrolysis for nanocellulose, the biocatalysts were divided into two main categories: (i) commercial enzymes, and (ii) non-commercial enzymes. It should be mentioned that the non-commercial category includes enzymes from non-commercial proprietary research formulations of private companies, heterologous expression in either prokaryote or eukaryote host systems and microbiological production. The percentages of different commercial and non-commercial enzymes used in the enzymatic hydrolysis for cellulose nanomaterials production are displayed in Figures 2.9a and 2.9b, respectively. A list of the different commercial (Table A.4) and non-commercial (Table A.5) enzymes used in the selected articles and their occurrences can be found in the appendix A.

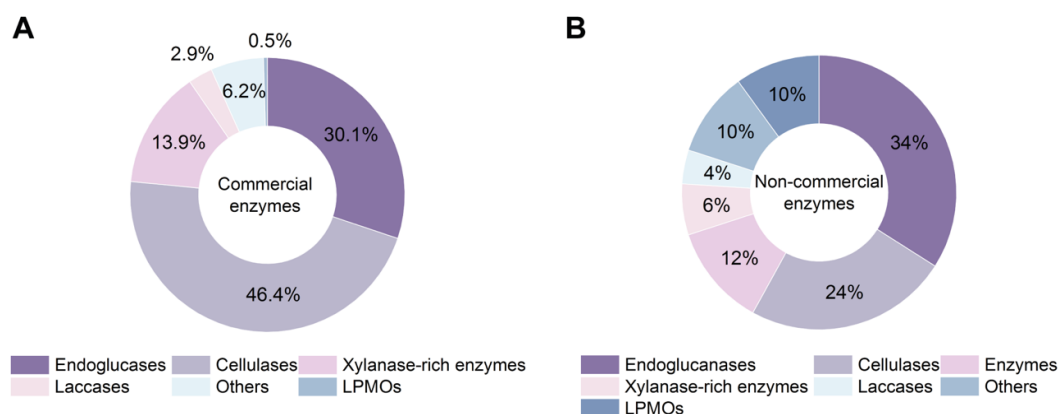


Figure 2.9. Proportion of the main a) commercial and b) non-commercial enzymes used in evaluated articles.

The majority of the selected studies (81.5%) used commercial enzymes while less than a fifth (15.5%) of the articles reported the usage of non-commercial enzymes, and an even smaller number evaluated both (3.0%). Considering the use of commercial products, cellulases preparations, for instance, Celluclast® 1.5 L, Cellic CTec2, CellicCTec3, Cellulase 50013, Cellulases from *Trichoderma reesei* ATCC 26921 among others (Appendix A - Table A.4) are the most used enzymes in the selected studies, at 46%. Monocomponent endoglucanase and endoglucanase rich enzymes, such as Fibercare® R, Novozym 476, Endoglucanase EcoPulp RÒ, Quimizime B among others (Appendix A - Table A.4) were used in 30% of the articles, followed by xylanases (Cellic HTec2, Cellic Htec, Multifect, Pulpzyme HC among others) in 14%.

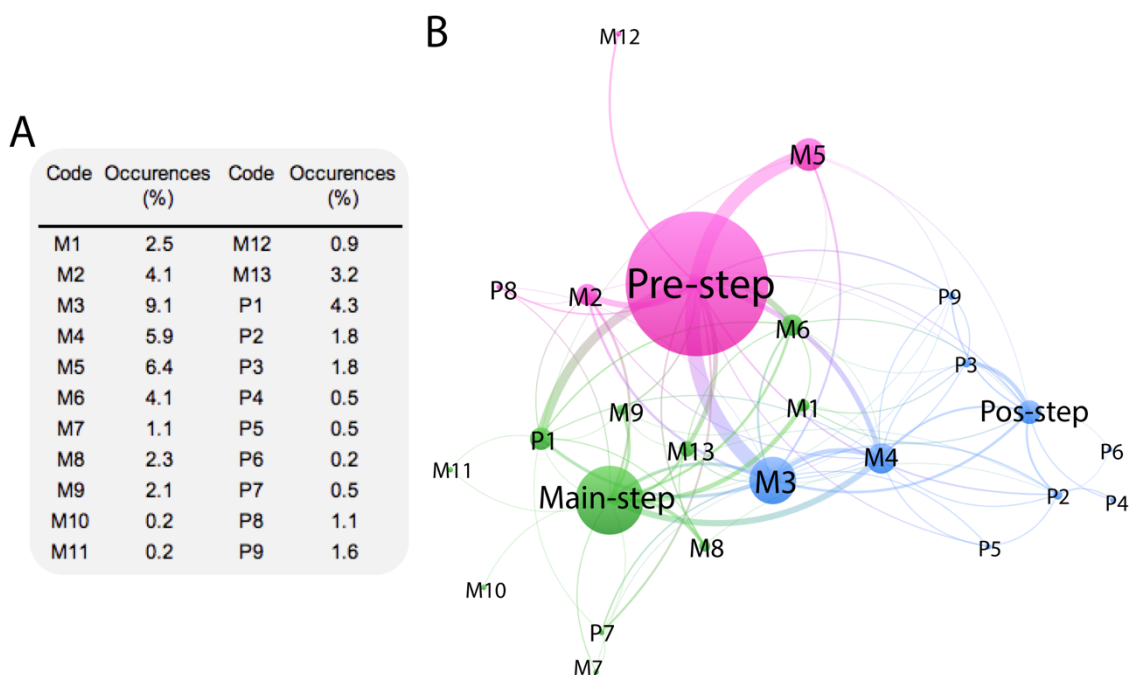
Although endoglucanases have been claimed to be more suitable for nanocellulose isolation due to their selectivity for the amorphous regions, cellulases preparations were the most used commercial enzymes. A possible reason for this is related to the lack of a commercial enzymatic preparation specially designed to cellulose nanomaterials production. Thus, researchers have to use the cellulose-active enzymes available in the market which were developed for other purposes, such as complete hydrolysis of cellulose into soluble sugars (ARANTES *et al.*, 2020). Moreover, a few studies evaluated the synergism between commercial LPMOs and cellulases and the application of laccase in TEMPO-mediated oxidation systems (ARACRI; BARNETO; VIDAL, 2012; JAUŠOVEC; VOGRINČIČ; KOKOL, 2015; JIANG *et al.*, 2020, 2021; LIU *et al.*, 2019; VALLS *et al.*, 2019).

In contrast, endoglucanases, mainly produced by heterologous expression (82.3% of the endoglucanases), were the most used non-commercial enzymes in the selected articles. This is likely due to the possibility of producing and using different recombinant endoglucanases to compare their hydrolytic activities and effects on the cellulose nanomaterials properties, which in turn, provides a b (WANG *et al.*, 2016). On the other hand, microbiological production of enzymes may offer an alternative option to the use of commercial enzymes when it comes to the nanocellulose isolation itself. It has been reported that the produced enzymatic extracts are better adapted for acting on the substrate the fungus was grown on (VAN DEN BRINK *et al.*, 2014). This could facilitate the production of more specific enzymes according to the substrate used for the NC production. The occurrence percentage of non-commercial enzymes reported in the selected articles can be found in Table A.5 of appendix A. As mentioned before, the use of enzymes in the cellulose nanomaterials process is at the early stages of development. Since no commercial enzymatic preparation has been fully developed for nanocellulose isolation, efforts are still required not only to produce enzymes with higher specificity and efficiency but also to reduce the costs of them (YANG *et al.*, 2020).

2.4.5 Trends and main applications of nanocelluloses whose production process includes an enzymatic hydrolysis step

In an attempt to answer the questions initially proposed through a qualitative and semi-quantitative way, text mining tools were used. Network maps and frequency of the co-occurrence of assigned terms enabled the clarification of the state of the art and research hot-spots in the field of using enzymes for cellulose nanomaterials production. Term co-occurrence is one of the most used analytical methods for bibliometric purposes. When the terms/keywords appear in one document, they are recorded as one co-occurrence. The more co-occurrences, the closer the relationships between the two words and the stronger the correlations (GAO; HUANG; ZHANG, 2019).

During the screening step, terms were assigned to articles to provide a “fingerprint” of each article. These terms were chosen based on the research questions, and the most observed trends and highlights of the selected articles. Figure 2.10 displays the terms and their occurrences related to the approaches, strategies and reaction conditions of the cellulose nanomaterials production process reported in the selected articles along with the network map of them.



LEGEND: Pret-Step: Enzymatic hydrolysis was used as a pretreatment step; **Main-Step:** Enzymatic hydrolysis was used as the main step; **Pos-Step:** Enzymatic hydrolysis was used as a posttreatment step. Comparison of different (**M1**) methods, (**M2**) enzymes, (**M3**) enzyme concentrations, (**M4**) reaction times, (**M5**) pretreatments, (**M6**) feedstocks and (**M7**) feedstock concentrations to isolate CNs. The conditions of reaction were optimized (**M8**) without and (**M9**) with design of experiments. (**M10**) CNs were isolated using immobilized enzymes. (**M11**) CNs were produced by twin-screw extrusion with in situ enzymatic hydrolysis. (**M12**) A life cycle assessment was performed. (**M13**) CNs were produced within the biorefinery context. Enzymatic hydrolysis was used (**P1**) to facilitate cellulose nanofibrillation, (**P2**) to control the CNs size, (**P3**) to functionalize CNs, (**P4**) to increase the crystallinity of CNs, (**P5**) to increase the homogeneity of CNs, (**P6**) to improve the CNs yield and (**P7**) for artificial CNs synthesis. Evaluation of the enzymatic hydrolysis effects on (**P8**) the thermal stability of cellulose nanomaterials and (**P9**) the rheological behavior of CNs suspension.

Figure 2.10. Evaluation of the approaches, strategies and reaction conditions of the cellulose nanomaterials production process reported in the selected articles. A) Percentage occurrence of the selected terms. B) Network analysis of the terms.

From Figure 2.10a it can be observed that the pretreatment step had the highest number of occurrences, followed by the main and posttreatment steps. Indeed, approximately 61.1% of the articles used enzymes in the pretreatment, while 28.8% used in the main step, 9.1% used in the posttreatment, and a small percentage evaluated the use of enzymes in both, pretreatment and posttreatment. The use of enzymatic hydrolysis mostly as an auxiliary treatment was already expected since the conventional methods for producing cellulose nanofibrils and nanocrystals are still mechanical and chemical, respectively (NECHYPORCHUK; BELGACEM; BRAS, 2016)

The strongest interactions occurred between pretreatment (Pre-step) and the terms represented by M2, M3, M4, and M5 (Figure 2.10b). These associations suggest a tendency in articles that used enzymatic hydrolysis as a pre-treatment also performed a

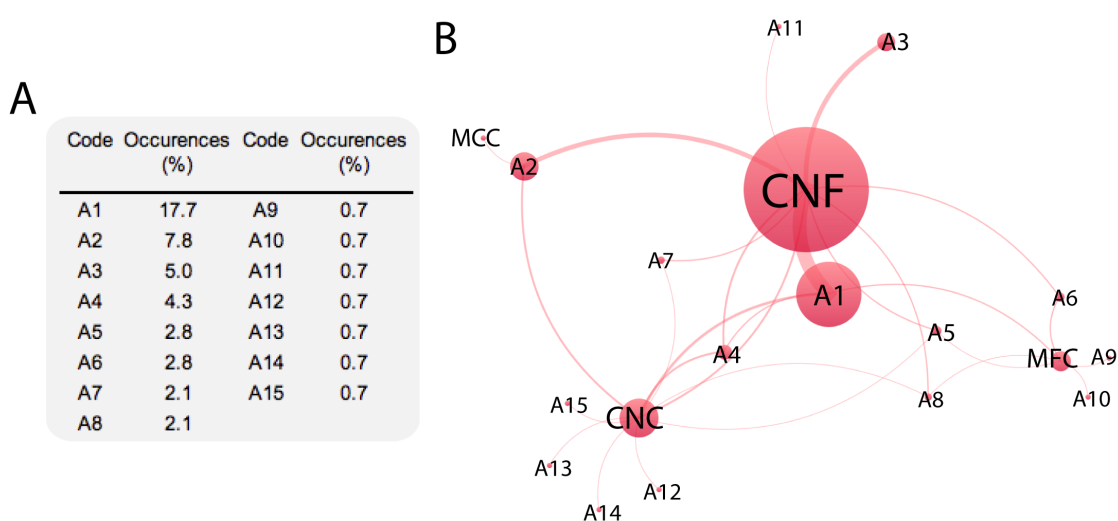
comparative analysis with other different pre-treatments and/or different reaction times, enzymes, feedstocks and their concentrations. Although the effects of different process variables on the cellulose nanomaterials properties were broadly evaluated (~67.7% of the articles), less than 5% of the studies precisely optimized the reactional conditions by using experimental design methodologies.

The articles which used the enzymatic hydrolysis as the main step also compared different reaction conditions on the properties of the produced nanomaterials as can be observed by the strong interactions between Main-Step and M3, M4 and M9. The production of cellulose nanomaterials within the biorefinery context was evaluated by about 7.6% of the total articles being that the use of enzymes as a pre-treatment (~4.5% of publications) was more recurrent than as a main step (~2.5%). Furthermore, life cycle assessments were only reported in articles (~2.0% of publications) that assessed enzymatic hydrolysis as a pretreatment step. On the other hand, unusual and innovative approaches, such as, the use of immobilized enzymes (one publication), twin-screw extrusion with in situ enzymatic hydrolysis (one publication) and artificial synthesis of cellulose nanomaterials (two publications) were only evaluated by articles that investigated enzymatic hydrolysis as the main step of the production process.

Enzymatic hydrolysis has been mostly used for facilitating the cellulose nanofibrillation (~9.6% of publications), as it has been more traditionally reported in the literature (BANVILLET *et al.*, 2021; BIAN *et al.*, 2016; CEBREIROS *et al.*, 2021; HENRIKSSON *et al.*, 2007; LIU *et al.*, 2019; LONG *et al.*, 2017; PERIĆ; PUTZ; PAULIK, 2020; ROSSI *et al.*, 2021; VALENZUELA *et al.*, 2019; VALLS *et al.*, 2019). Additionally, enzymes have also been used to control the size (~5.1% of publications) (CHEN; FAN; *et al.*, 2017; JANG *et al.*, 2020; LIU *et al.*, 2020), increase the crystallinity (~1.0% of publications) (JANG *et al.*, 2020; LAADILA *et al.*, 2020) and homogeneity (~1.0% of publications) (CHEN *et al.*, 2017). Another important advantage of using enzymes is related to the production of cellulose nanomaterials with superior thermal properties which can further expand their range of applications (TAO *et al.*, 2019). Finally, the functionalization nanocellulose through surface modifications of the hydroxyl groups on the cellulose is other important application of enzymes, for instance, the use of laccase in a TEMPO-mediated oxidation of cellulose nanomaterials (JAUŠOVEC; VOGRINČIČ; KOKOL, 2015; JIANG *et al.*, 2020, 2021; LIU *et al.*, 2019).

Figure 2.11 presents the terms related to the application of nanocellulose along

with their network map.



LEGEND: **A1:** Films preparation **A2:** Reinforcement agent in nanocomposites; **A3:** Reinforcement agent in paper-sheets; **A4:** Nanocomposites preparation; **A5:** Reinforcement agent in films; **A6:** Reinforcement agent in hand-sheets; **A7:** Aerogels preparation; **A8:** Nanofiller in nanocomposites; **A9:** Reinforcement agent in foams; **A10:** Coating agent; **A11:** Foams preparation; **A12:** Nanofiller in hydrogels; **A13:** Metal ion removal; **A14:** Oxygen barrier agent; **A15:** Pickering emulsions preparation.

Figure 2.11. Evaluation of the applications of cellulose nanomaterials reported by the selected articles. A) Percentage occurrence of the selected terms. B) Network analysis of the terms.

Among the cellulose nanomaterials applications identified in this systematic map, CNF was the most used nanocellulose type being explored by 66.7% of the articles compared to CNC (~20.8%), MFC (~11.1%) and MCC (~1.4%). The most common applications investigated by the articles include: preparation of films (17.7% of occurrences), reinforcement agent in nanocomposites (7.8% of occurrences), reinforcement agent in paper-sheets (5.0% of occurrences) and preparation of nanocomposites (4.3% of occurrences).

Cellulose nanofibers have been mostly used in the preparation of films as it can be observed in Figure 2.11b by the strongest interaction between CNF and A1 and the highest co-occurrences number being studied by 21 articles. In other words, 44.7% of the articles that evaluated the application of CNF focused on preparing films with them. CNFs have been also considerably used as a reinforcement agent in paper-sheets (7 articles) and in nanocomposites (7 articles). Other less used CNFs applications include

reinforcement agents in films (5 articles), in hand-sheets (2 articles), nano filler in nanocomposites (2 articles), preparation of aerogels (2 articles) and foams (1 article).

Cellulose nanocrystals CNCs were evaluated to prepare films (4 publications), nanocomposite (3 publications), and Pickering emulsions (1 publication). They were also used as nanofiller of hydrogels (1 article), oxygen barrier agent (1 article) and for metal on removal (1 article). It should be noted that the films preparation had the highest number of co-occurrences in both cases (CNFs and CNCs). However, cellulose nanofibrils are preferably used for the preparation of self-assembled films. This is because CNFs have higher aspect ratio, increased flexibility and propensity for entanglement which facilitate their own lend themselves more readily to network formation than do CNCs (FRANCE *et al.*, 2017). MFCs were mainly used for hand-sheets reinforcement and film preparation while MCC was applied as reinforcement agent in nanocomposite.

Although there is a plethora of different nanocelulose applications, just above a third (34.8%) of the selected articles evaluated the application of these nanomaterials and none of them performed any study focused on the practical application of nanocellulose produced in the biorefinery context. This gap motivates future works more aimed to the application of the cellulose nanomaterials whose production process included the use of enzymes.

2.5 Limitations of the work

Reliable evidence reviews are required to have comprehensive search strategies as one of the main principles of their approaches, through which they may capture as much of the relevant scientific information for the synthesis as possible (ABDULLA *et al.*, 2016). In this work, the publications were retrieved in the period from 2000 to 2021 and using a search string made up of 65 terms being 55 “cellulose nanomaterial” synonyms and 8 “enzymatic hydrolysis” synonyms. Therefore, it is acknowledged that eventually any articles related to this theme could not have been found, taking into account the existence of a plethora of terms to describe the different types of nanocellulose. However, this study provides an important contribution to the cellulose nanomaterials field by following the principles of a more rigorous review methodology which was recently introduced to the chemical engineering field.

2.6 Final remarks

Principles of systematic mapping were used to address the cellulose nanomaterials

whose production process includes the use of enzymes over the last twenty years to summarize the state-of-the-art and identify research opportunities in this subject area. This work was committed to systematically reviewing, developing and promoting the evidence base for increasing the current knowledge on this topic. The following contributions can be highlighted:

- Results evidenced a significant increase in the annual number of publications related to the nanocellulose produced using enzymes during this decade, and especially during 2013–2021. It is aligned with the growing search for environmentally friendly and biodegradable materials and industrial interest in this field enabled the setting-up of the first facilities for nanocelluloses production in commercial quantities;

- Although the feedstocks derived from hardwood have been the most used by the publications, a large number of studies evaluated different residues as substrates for cellulose nanomaterials production. The interest in the use of either plant-derived cellulose or residues enables the possibility of extracting nanocellulose from a wide variety and abundance of sources of cellulose, which in turns, guarantee the low cost and renewability of the feedstocks;

- Cellulases preparation were the commercial enzymes more evaluated by the articles related to the nanocelluloses production while endoglucanases heterologous expressed were mostly used by the works that used non-commercial enzymes. Many efforts have been made to produce enzymes with high specificity and at competitive costs. However, there is no enzymatic preparation commercially available and specially designed for nanocellulose production. This gap motivates research and development on enzymes better suitable to produce cellulose nanomaterials;

- The co-occurrence analysis of terms assigned to the articles showed that most of the papers evaluated different pretreatments and reaction conditions, varying the reaction duration, types of substrates and enzyme and their concentrations. However, few studies optimize the reactional conditions by using experimental design tools;

- The co-occurrences among the terms related to the applications demonstrated that the nanocelluloses have been mostly evaluated for films preparation by the selected articles in this systematic map. It was also shown that the application of cellulose nanomaterials whose production process involves enzymes was not frequently investigated. Moreover, it was identified a gap related to the lack of studies that evaluated the application of cellulose nanomaterials which were produced in the biorefinery

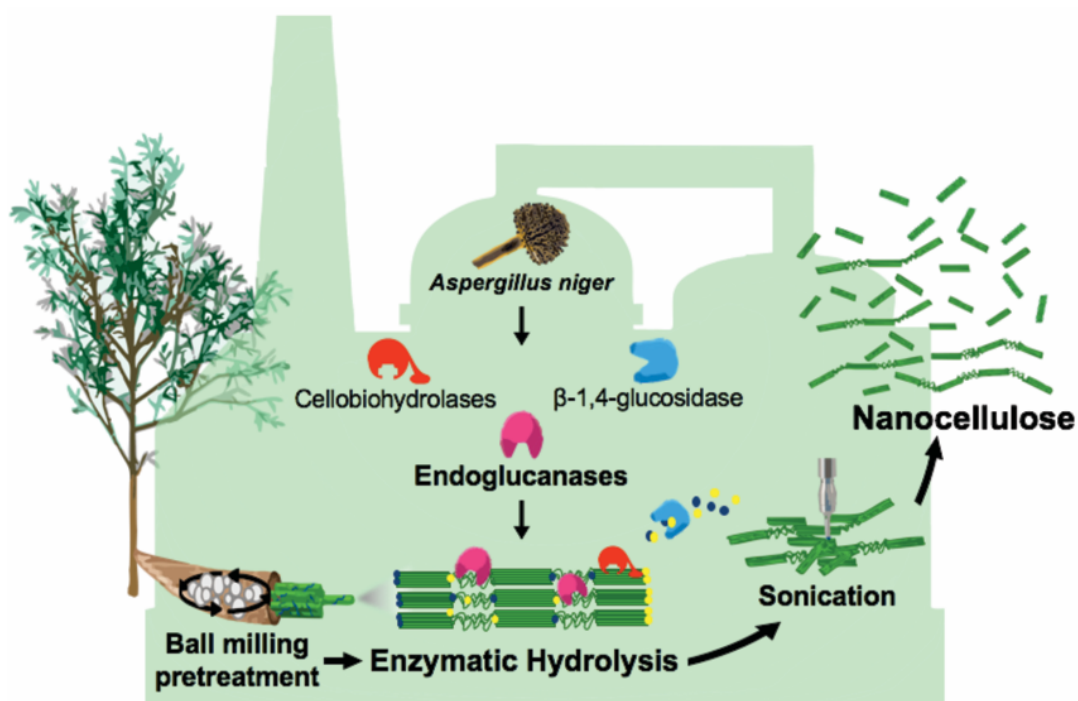
context. Considering the advantages of using enzymes, such as milder temperature and pH operating conditions, no generation of harmful co-products, high selectivity, the possibility of tuning the nanocellulose properties, e.g., controlling the size, increasing the uniformity, thermal stability, crystallinity, the applications of enzyme-mediated nanocellulose should be more explored.

Chapter 3

Production of non-commercial enzymes and their application to isolate cellulose nanomaterials

* The content of this chapter is an adaptation of the scientific article entitled: “**Nanocellulose production in future biorefineries: an integrated approach using tailor-made enzymes**” by P. Squinca, S. Bilatto, A. C. Badino, C. S. Farinas, published in ACS Sustainable Chemistry & Engineering.

Reference: doi: 10.1021/acssuschemeng.9b06790



3.1 Abstract

The development of process engineering approaches to integrate the production of biofuels and high value-added bio-based products, such as enzymes and nanocellulose, is crucial to improve the financial performance and sustainability of lignocellulosic biomass biorefineries. Here, the feasibility of applying enzymes produced on-site to obtain nanocellulose was evaluated using eucalyptus cellulose pulp as a model feedstock. A systematic analysis of the structural properties of the nanomaterials obtained after hydrolysis using a cellulolytic enzymatic complex with high endoglucanase specific activity (17.09 IU/mg_{protein}), produced by *Aspergillus niger*, followed by sonication, revealed that longer ball milling pretreatment and reaction times favored extraction of the cellulose nanocrystals (CNCs). The highest yield (24.6%) of CNCs was achieved using 96 h of enzymatic hydrolysis of the ball-milled cellulose pulp, followed by sonication for 5 min. The CNCs presented an approximate length of 294.0 nm and diameter of 24.0 nm, and the crystallinity index increased from 57.5 to 78.3%, compared to the cellulose pulp that was only ball milled. These findings demonstrated that nanocelluloses could be successfully extracted using on-site produced enzymes and that the sustainable integrated process reported here could contribute to the development of the nascent bio-based economy.

3.2 Introduction

Currently, there is an urgent need to replace the widespread use of petroleum-derived products with biodegradable and/or bio-based substitutes, in order to contribute to a low-carbon and more sustainable economy. Lignocellulosic biomass could potentially partially replace petroleum as a feedstock to obtain a variety of products adapted to the demands of the market. This could be achieved with the implementation of biorefineries to enable the conversion of biomass into a wide spectrum of products (fuels, value-added co-products, and energy), in an approach analogous to petroleum refineries (CHERUBINI, 2010). However, despite significant research, the full potential of the biorefinery concept has not been exploited and these facilities still encounter bottlenecks related to feedstock logistics, limitations of conventional processing technologies, and uncertain market economics (HASSAN; WILLIAMS; JAISWAL, 2019). Recent studies have demonstrated the potential of using the solid residue remaining after the enzymatic hydrolysis of lignocellulosic biomass to produce

nanocellulose (BONDANCIA *et al.*, 2017; SONG *et al.*, 2014), a high added-value material that could contribute to the sustainability of future biorefineries.

Nanocellulose-based materials have attracted interest for applications in food packaging, biomedicine, mechanical reinforcement of matrices and membrane filtration, among many other uses (ABITBOL *et al.*, 2016; DUFRESNE, 2013; LIN; DUFRESNE, 2014). The hierarchical structure of cellulose enables nanocelluloses to be isolated from lignocellulosic biomass employing top-down processes that aim to disintegrate cellulose fibers into cellulose nanocrystals and cellulose nanofibrils, depending on the processing conditions (KLEMM *et al.*, 2011). Although mechanical treatments and acid hydrolysis are the most widely studied methods for obtaining CNFs and CNCs, respectively, these procedures have some economic and environmental drawbacks, such as the energy demand of the disintegration process and the high amounts of water required in the neutralization step (RIBEIRO *et al.*, 2019). In contrast, the use of enzymatic hydrolysis to produce nanocellulose may be a promising environmentally friendly and sustainable route. Enzymes have high substrate specificity, targeting specific lignocellulosic linkages. Furthermore, they do not generate toxic residues and the hydrolysis is performed under mild conditions, resulting in a less energy-intensive process (FRITZ *et al.*, 2015). Due to the advantages of enzymatic treatments, there is growing interest in the use of enzymes for nanocellulose production. Several studies have evaluated the use of enzymes combined with mechanical treatments to facilitate fibrillation of cellulose bundles and reduce energy requirements for nanocellulose isolation (DE CAMPOS *et al.*, 2013; HENRIKSSON *et al.*, 2007; JANARDHAN; SAIN, 2011; PAAKKO *et al.*, 2007). In addition, enzymatic treatments have also been explored to improve uniformity, control the length, and improve the thermal stability of nanocelluloses (FRITZ *et al.*, 2015).

In the biorefinery context, the integrated production of nanocellulose and biofuels by enzymatic routes was first reported by Zhu *et al.* (2011). Recently, Bondancia *et al.* (2017) demonstrated that it was possible to produce CNCs using only enzymatic hydrolysis of eucalyptus cellulose pulp, integrated with cellulosic ethanol production. Other studies have demonstrated the technical and economic feasibility of integrating nanocellulose and ethanol production. However, an important issue is that most commercial enzymatic cocktails do not favor nanocellulose production, because they are optimized for the hydrolysis of lignocellulosic biomass and the highest possible conversion of cellulose and hemicellulose into soluble sugars. Furthermore, it is not economically desirable to increase the requirement for commercial enzymatic cocktails

in the biorefinery. The on-site production of enzymes has been considered a promising strategy for reducing costs within the cellulosic ethanol biorefinery (JOHNSON, 2016; LIU; ZHANG; BAO, 2016). In this approach, the cellulase plant could be located adjacent to the ethanol plant, reducing the costs associated with enzyme purification, addition of stabilizers, transportation, and storage (JOHNSON, 2016).

In this work, with the aim of increasing process integration and exploiting the advantages of on-site enzyme production, the feasibility of using non-commercial enzymes to extract nanocellulose by means of enzymatic hydrolysis was investigated using eucalyptus cellulose pulp as a model feedstock. The influence of the lignocellulosic biomass structural characteristics resulting from different ball milling pretreatment and sonication times on the nanocellulose properties were investigated using a central composite rotational design as a statistical tool. The cellulose nanomaterials were fully characterized by field emission scanning electron microscopy, X-ray diffraction, Fourier transform infrared spectroscopy, zeta potential measurements, and thermogravimetric analysis. The results demonstrated that the hydrolysis using on-site produced enzymes was effective in extracting nanocellulose, offering a potential green and sustainable route that can be applied in future biorefineries.

3.3 Experimental section

3.3.1 Material

Eucalyptus cellulose kraft pulp was kindly supplied by Suzano Pulp and Paper Company (São Paulo, Brazil). The pulp chemical composition was $75.6 \pm 2.3\%$ cellulose, $14.6 \pm 0.6\%$ hemicellulose, $6.7 \pm 1.2\%$ lignin, and $1.1 \pm 0.2\%$ ash, as previously determined in the laboratory (BONDANCIA *et al.*, 2017). The pulp was reduced to a particle size smaller than 2 mm, using a 500 W Wiley knife mill (Solab), and this material was used for the ball milling pretreatment and as substrate in the enzymatic reactions without any further treatment.

3.3.2 Microorganism

The wild-type *Aspergillus niger* A12 strain, obtained from the Embrapa Food Technology collection (Rio de Janeiro, Brazil), was used to produce the cellulolytic enzymatic complex. The strain was kept at $-18\text{ }^{\circ}\text{C}$ in a 30% (w/w) glycerol/water solution and was activated on potato dextrose agar slants for 4 days at $32\text{ }^{\circ}\text{C}$. Suspensions of spores

were prepared by the addition of Tween 80 (0.3% v/v). The spore concentrations were determined using a Neubauer chamber.

3.3.3 Solid state fermentation

The *Aspergillus niger* fungus was cultivated using solid state fermentations in 1 L Erlenmeyer flasks, with 20 g of wheat bran as solid substrate. After sterilization at 120 °C for 15 min, the medium was inoculated with 10^7 spores/g of substrate. The initial moisture content of the substrate was adjusted to 60% (w/v), using a solution of 0.9% (w/v) ammonium sulfate in 0.1 mol/L HCl, and cultivations were performed at 32 °C for 72 h (FARINAS *et al.*, 2011). After the cultivation period, the enzymes were extracted by the addition of 1:10 (w/v) 50 mM sodium acetate buffer solution (pH 4.8) and shaking the suspension at 120 rpm and 32 °C for 40 min. The enzymatic extracts were vacuum filtered and centrifuged at 10,000 rpm for 20 min at 4 °C. In order to further reduce the particulate matter and impurities, the enzymatic extracts were submitted to two sequential microfiltration steps using mixed cellulose esters membranes (StarTech) with average pore diameters of 0.45 and 0.22 μm .

3.3.4 Ball milling pretreatment

Prior to the enzymatic hydrolysis reactions, the eucalyptus cellulose pulp was mechanically pretreated in a planetary ball mill (model CT-12241, Servitech) consisting of a porcelain jar and alumina balls. The ball to material weight ratio (BMR) adopted was 12:1 and the weight ratio of balls with 8 and 4 mm diameters was 5:4. The milling time was defined by the experimental design methodology (Table 3.1).

3.3.5 Central composite design

The experiments to obtain the cellulose nanomaterials were performed according to a central composite rotatable design (CCRD) comprising 11 runs, with four cube points, four axial points, and three central points, in random order. The independent variables (factors) were the ball milling time ($t_{\text{ball milling}}$) and the sonication time applied after the enzymatic hydrolysis reaction ($t_{\text{sonication}}$). The analyzed response variables were the nanocellulose yield, zeta potential, and crystallinity index. The factors and levels investigated, which were defined in preliminary tests, are shown in Table 3.1. Statsoft v. 7.0 software was used for data analysis, including the effect estimates and analysis of variance (ANOVA) at 10% significance.

Table 3.1. Design of experiment matrix.

Run	t _{ball milling} (min)	t _{sonication} (min)
1	-1 (13)	-1 (1)
2	+1 (77)	-1 (1)
3	-1 (13)	+1 (9)
4	+1 (77)	+1 (9)
5	-1.41 (0)	0 (5)
6	+1.41 (90)	0 (5)
7	0 (45)	-1.41 (0)
8	0 (45)	+1.41 (10)
9	0 (45)	0 (5)
10	0 (45)	0 (5)
11	0 (45)	0 (5)

3.3.6 Extraction of nanocellulose

The enzymatic hydrolysis reactions were carried out in 125 mL Erlenmeyer flasks containing cellulose pulp at a solids loading of 2% (w/v) and 50 mL of the non-commercial enzymes preparation, at 50 °C and 200 rpm, using an orbital shaker. The enzyme loading was 20 mg_{protein}/g_{solid} and the reactions were conducted for 48 and 96 h, in order to respect the kinetics of the process. Glucose concentrations were quantified during the hydrolysis using an enzymatic kit for glucose measurement (Glicose Liquiform, Brazil). At the end of the reaction, the enzymes were denatured by boiling the suspension at 100 °C for 10 min. The residual pulp was washed with deionized water, the solid was separated by centrifuging for 20 min at 8,000 rpm and 4 °C and suspended in deionized water. This washing procedure was repeated several times to remove the released soluble sugars. After this step, a suspension of nanocellulose was obtained, diluted about 5-fold, and subsequently sonicated (Q1375 sonicator, QSonica) while immersed in an ice bath to prevent heating. The sonicator was operated at 50% amplitude (1375 Watts) for 1, 5, 9, and 10 min, according to the conditions defined in the experimental design methodology (Table 3.1).

3.3.7 Cellulose conversion

The cellulose conversion into glucose (C_c) was determined as follows:

$$C_c(\%) = \frac{(m_g^t - m_g^0) \times 0.9}{m_p^0 \times y_c} \times 100 \quad (3.1)$$

where m_g^t is the glucose mass at time t , m_g^0 is the initial glucose mass, m_p^0 is the initial pulp mass, y_c is the percentage of cellulose in the pulp, and 0.9 is the ratio of the molecular weights of anhydroglucan present in the cellulose chain (162.14 g/mol) and the glucose released during the hydrolysis (180.15 g/mol).

3.3.8 Characterization

3.3.8.1 Scanning electron microscopy

Morphological analyses of the kraft eucalyptus pulp, before and after ball milling pretreatment for different times, were performed using a scanning electron microscope (JSM-6510/GS, JEOL Ltd, Japan) operating at 10 kV, with a 10 mm working distance. The samples were dispersed onto aluminum specimen stubs using double-sided adhesive carbon tapes, followed by coating with a thin gold layer in an ionization chamber (MED 020, Baltec), in order to improve conductivity.

3.3.8.2 Field emission scanning electron microscopy

The morphology of the nanocellulose was examined using a Zeiss Sigma scanning electron microscope equipped with a field emission gun. A drop of diluted sample was deposited on a silicon plate and mounted onto an aluminum stub using carbon tape. The analyses were performed using a 4 kV acceleration voltage, with a 6 mm working distance.

3.3.8.3 Transmission electron microscopy

The morphology of the CNCs obtained in run 6 was evaluated using a Tecnai G2 F20 microscope (FEI, Hillsboro, OR, USA). A drop of diluted CNC suspension with 1% uranyl acetate was placed on a 400-mesh carbon-Cu grid and dried at room temperature. The CNCs diameter and length were estimated using Image J software and presented as an average of 100 individual measurements.

3.3.8.4 Nanocellulose yield

The nanocellulose suspensions were previously homogenized for 10 min in an ultrasonic bath, followed by drying 4 mL of each sample at 50 °C for 24 h. The yield of

nanocellulose was calculated by Equation 2:

$$Y(\%) = \frac{(m_s^f - m_s^i) \times R}{(m_p^0 \times y_c - m_g^f)} \times 100 \quad (3.2)$$

where m_s^f is the sample mass after drying, m_s^i is the sample mass before drying, m_p^0 is the initial pulp mass, y_c is the percentage of cellulose in the pulp, m_g^f is the glucose mass at the end of hydrolysis reaction and R is the ratio of the total volume used in the hydrolysis reaction and the sample volume.

3.3.8.5 Zeta potential

The surface charge of the nanocellulose was measured using a Zetasizer (Malvern Instruments Ltd., UK), at room temperature (25 °C), in quadruplicate. Prior to the measurements, the samples were diluted to 0.025% (w/v) with deionized water.

3.3.8.6 Fourier transform infrared spectroscopy

Analysis of the functional groups present in the kraft eucalyptus pulp and the nanocellulose suspensions was performed using a Vertex 70-RAM II spectrophotometer (Bruker Scientific Instruments, USA). Attenuated total reflection Fourier transform infrared (ATR-FTIR) spectra were acquired at a resolution of 2 cm^{-1} , in the range between 4000 and 400 cm^{-1} , with a total of 32 scans.

3.3.8.7 X-ray diffraction (XRD)

X-ray patterns were obtained in the 2θ range from 5° to 40°, at a scan rate of 2° min^{-1} , using a Shimadzu LabX XRD-6000 diffractometer operating with Cu K_α radiation ($\lambda = 0.15428 \text{ nm}$), at 30 kV and 30 mA. The crystallinity index (CI(XRD)) was calculated according to the method of Segal et al. (1959), as follows:

$$CI(XRD) = \frac{I_{200} - I_{am}}{I_{200}} \times 100 \quad (3.3)$$

where I_{200} is the peak height for the (200) crystal planes and I_{am} is the amorphous contribution.

3.3.8.8 Thermogravimetric analysis

The thermal behavior was analyzed using a thermogravimetric analyzer (TGA-Q500, TA Instruments, USA), under an atmosphere of nitrogen at a flow rate of 50 mL/min. Approximately 8 mg of sample were weighed out into a platinum pan and heated from 20 to 700 °C, at 10 °C/min.

3.3.9 Analytical methods

Endoglucanase and β -glucosidase activities were assayed in the presence of carboxymethylcellulose (Sigma, USA) and cellobiose (Sigma, USA), respectively, using the standard method proposed by Ghose (1987). Xylanase activity was measured using the method described by Bailey and Poutanen (1989), in the presence of beechwood xylan (Sigma, USA). The reducing sugar concentration was determined by the dinitrosalicylic acid (DNS) method (MILLER, 1959). In the case of β -glucosidase activity, the glucose released was quantified with an enzymatic kit for glucose measurement (Glucose Liquiform, Brazil). All the enzymatic analyses were carried out in triplicate. One unit of endoglucanase, β -glucosidase, or xylanase activity corresponded to 1 μ mol of reducing sugars released per minute of reaction. The total protein concentration in the enzymatic cocktails was determined by the method described by Bradford (1976), using bovine serum as a standard.

3.4 Results and discussion

3.4.1 Nanocellulose production by enzymatic hydrolysis

In this work, cellulose nanomaterials were obtained from the hydrolysis of eucalyptus cellulose pulp using a non-commercial enzymatic cocktail produced by the cultivation of *A. niger* under solid state fermentation. After the microfiltration step, the cocktail contained a total protein concentration of 0.331 ± 0.009 mg_{protein}/mL, with 5.66 ± 0.2 , 1.21 ± 0.33 and 16.20 ± 0.26 IU/mL of endoglucanase, β -glucosidase and xylanase activities, respectively.

Despite the relatively low protein concentration values, compared to commercial preparations, the specific activity of endoglucanase obtained here was 17.09 IU/mg_{protein} which could be more favorable for nanocellulose extraction, compared to commercial enzymes developed to maximize the hydrolysis of lignocellulosic biomass into soluble sugars. For example, values of 2.26 and 1.24 IU/mg_{protein} have been reported for the

specific activities of endoglucanase in commercial preparations of Cellic CTec 2 and 3 supplied by Novozymes (SUN *et al.*, 2015).

Cellulases are glycoside hydrolases with synergistic functions that efficiently cleave the glycosidic linkages of lignocellulose, resulting in its depolymerization (KUBICEK; KUBICEK, 2016). These enzymes include several subgroups. Endoglucanases (EC 3.2.1.4), or nonprocessive cellulases, randomly hydrolyze accessible intramolecular β -1,4-glucosidic linkages of cellulose chains, producing new chain ends and releasing short chain oligosaccharides. Cellobiohydrolases (EC 3.2.1.91), or processive cellulases, cleave the long-chain oligosaccharides obtained by the action of endoglucanases, producing short-chain oligosaccharides, mainly cellobiose. β -Glucosidases (EC 3.2.1.21) hydrolyze soluble cellobiose and oligosaccharides to glucose (BINOD *et al.*, 2019; ZHANG, Y-H Percival; HIMMEL; MIELENZ, 2006).

Among the cellulolytic enzymes, endoglucanases are mostly used for nanocellulose extraction, because they act preferentially on non-crystalline areas of cellulose and typically exhibit low activity on highly crystalline substrates such as microcrystalline cellulose (RAHIKAINEN *et al.*, 2019; THYGESEN *et al.*, 2011). These enzymes introduce internal and random cleavages to the cellulose chain and are commonly associated with a reduced degree of polymerization of the cellulose and increased crystallinity (PAAKKO *et al.*, 2007). Similarly, in controlled acid hydrolysis, the hydronium ions penetrate the cellulose amorphous domains and cleave the glycosidic bonds promoting the cellulose nanocrystals isolation (ABITBOL *et al.*, 2016).

In addition to cellulases, a few studies have evaluated the use of xylanase and lytic polysaccharide monooxygenases to improve the access of enzymes to cellulose and facilitate the production of nanocellulose (HASSAN *et al.*, 2018; HU *et al.*, 2018; LONG *et al.*, 2017; ZHOU; JOHN; ZHU, 2019). Zhou *et al.* (2019) demonstrated that although xylanase treatment is not as effective in obtaining nanoscale fibrils, compared to treatment using endoglucanase, the use of the former can facilitate the initial stage of fibrillation, producing microscale fibrils. Hence, the relatively high xylanase activity (16.20 IU/mL) in the enzymatic cocktail produced here could favor the extraction of nanocellulose.

The feasibility of using the non-commercial and endoglucanase-rich enzymatic cocktail produced by *A. niger* to obtain nanocellulose was investigated here using eucalyptus cellulose pulp as a model feedstock. Firstly, evaluation was made of the temporal profiles of glucose released (Figure 3.1) from reactions carried out with 20 mg_{protein}/g of the on-site produced enzymes and 2% (w/v) of pulp that had been ball milled

for 13, 45, 77, and 90 min. The cellulose conversions achieved in these reactions are shown in Figure 3.1 (inset).

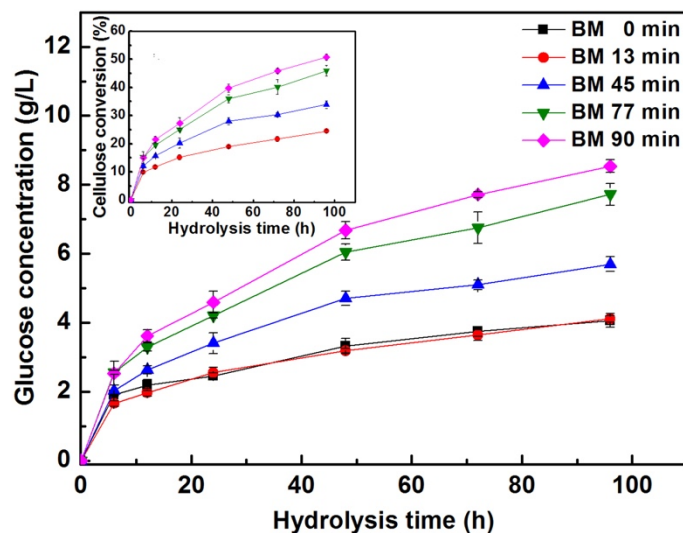


Figure 3.1. Glucose concentration and cellulose conversion (inset) obtained from enzymatic hydrolysis of cellulose pulp pretreated using different ball milling times (13, 45, 77, and 90 min).

It can be seen from Figure 3.1 that longer mechanical pretreatment times resulted in higher final glucose concentrations, indicating that access to the cellulose was improved. These findings were consistent with the work of Du *et al.* (2017) who reported that sufficient ball milling reduced the particle size and altered the fiber structure, consequently facilitating the action of enzymes and increasing the production of reducing sugars.

The final cellulose conversion yields ranged from 24.2 to 50.8% (Figure 3.1 inset), which were lower than those reported in many studies of enzymatic saccharification in the context of bioethanol production, where complete conversion of cellulose to soluble sugars is desired. However, lower cellulose conversion yields are beneficial for nanocellulose production, avoiding unwanted hydrolysis of the cellulose to glucose (YARBROUGH *et al.*, 2017). Furthermore, the rate of increase of pulp conversion was lower after 48 h of reaction. Considering the hydrolysis of the pulp that had been ball milled for 45 h, the cellulose conversion after 48 h of reaction was 28.0%, while after 96 h it was 33.9%. The small increase of cellulose conversion could be considered a positive result for nanocellulose production, since it suggested that only a small fraction of the

cellulose was converted to glucose during this period.

Therefore, the effects on the nanocellulose properties due to the process operational conditions, the ball milling pretreatment time ($t_{\text{ball milling}}$), and the sonication time after the enzymatic hydrolysis ($t_{\text{sonication}}$) were investigated for the samples obtained after the hydrolysis reactions carried out for both 48 and 96 h. The experimental conditions defined by the experimental design methodology are presented in Table 3.1. The nanocellulose samples were characterized by Fourier transform infrared spectroscopy, X-ray diffraction, zeta potential measurements, and field emission scanning electron microscopy, as discussed below.

3.4.2 Chemical composition

Figure 2 displays the FTIR spectra of the cellulose nanomaterials obtained after 48 and 96 h of hydrolysis under the different experimental conditions of the CCRD (Table 3.1).

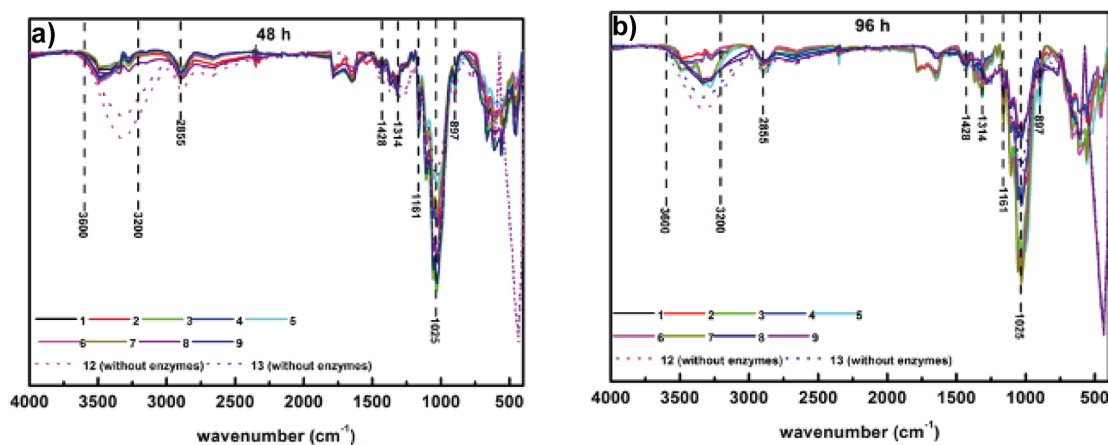


Figure 3.2. FTIR spectra of cellulose nanomaterials obtained using hydrolysis for a) 48 h and b) 96 h, under the different experimental conditions of the CCRD (Table 3.1).

The FTIR spectra of all the samples showed the presence of characteristic cellulose peaks, including a broad band between 3600 and 3200 cm^{-1} , attributed to O–H stretching vibration (PHANTHONG *et al.*, 2017), a peak at around 2885 cm^{-1} , corresponding to C–H stretching vibration (PHANTHONG *et al.*, 2017), and a peak between 1025 and 1161 cm^{-1} , due to antisymmetric in-phase C–O–C pyranose ring stretching vibration (SOFLA *et al.*, 2016).

There was also the presence of the bands at 1428 cm^{-1} , corresponding to symmetric CH_2 bending vibration (CIOLACU; CIOLACU; POPA, 2011), a peak at 1314

cm^{-1} corresponding to a wagging vibration of cellulose CH_2 (DO NASCIMENTO *et al.*, 2016), and a small peak at 897 cm^{-1} was indicative of the C-1 group or vibration of the glycosidic ring in amorphous domains (DO NASCIMENTO *et al.*, 2016). The different experimental conditions had no influence on the chemical compositions of the samples, as indicated by their similar FTIR spectra, possibly because the conditions involved variations of the same parameters.

3.4.3 Yield, zeta potential and crystallinity

Table 3.2 shows the yield (%), zeta potential (mV), and crystallinity index (%) values for the nanocellulose samples obtained from each experimental condition employed in the enzymatic hydrolyses (with different ball milling and sonication times). In addition to the conditions of the CCRD experimental design, runs were performed employing the conditions of run 6 (longer ball milling pretreatment time) and run 8 (longer sonication time), but without the addition of enzymes, for use as controls.

Table 3.2. Nanocellulose characterization results: yield (Y), zeta potential, (ZP) and crystallinity index (CrI).

Run	$t_{\text{ball milling}}$ (min)	$t_{\text{sonication}}$ (min)	48 h hydrolysis			96 h hydrolysis		
			Y (%)	ZP (mV)	CrI (%)	Y (%)	ZP (mV)	CrI (%)
1	-1 (13)	-1 (1)	2.3	-25.2	84.1	4.2	-27.4	83.4
2	+1 (77)	-1 (1)	5.1	-26.4	84.9	7.0	-28.6	77.0
3	-1 (13)	+1 (9)	3.3	-21.2	79.4	6.2	-19.2	80.7
4	+1 (77)	+1 (9)	6.6	-20.6	79.8	13.7	-19.4	82.7
5	-1.41 (0)	0 (5)	2.5	-25.5	80.4	3.2	-28.8	85.6
6	+1.41 (90)	0 (5)	11.0	-17.0	77.9	24.6	-18.2	78.3
7	0 (45)	-1.41 (0)	4.9	-22.5	78.2	9.5	-22.7	82.6
8	0 (45)	+1.41 (10)	7.4	-18.8	80.9	9.9	-18.1	77.2
9	0 (45)	0 (5)	7.4	-22.8	79.9	9.1	-21.0	81.6
10	0 (45)	0 (5)	8.1	-17.7	78.3	8.7	-19.8	83.8
11	0 (45)	0 (5)	6.9	-24.0	81.7	9.1	-20.0	83.0
12 ^a	+1.41 (90)	0 (5)	2.1	-18.7	71.9	2.0	-22.6	70.3
13 ^a	0 (45)	+1.41 (10)	2.2	-22.3	75.3	2.0	-21.3	74.5

^aControl conditions without enzymes.

The nanocellulose yields obtained in this set of experiments ranged from 2.2 to 11.0% and from 4.2 to 24.6% for the enzymatic hydrolysis durations of 48 and 96 h,

respectively. Extending the hydrolysis time from 48 to 96 h favored the production of nanocellulose and increased the crystallinity index, for all the experimental conditions evaluated. The highest yield of 24.6% was obtained under the conditions of run 6 (longer ball milling pretreatment time), after 96 h of hydrolysis and this value was about 12-fold higher than obtained for the control without enzyme (run 12), demonstrating that the enzymatic hydrolysis significantly increased nanocellulose production.

These yield values could be considered favorable, when compared to other reported works using the enzymatic hydrolysis route to obtain nanocellulose. Anderson *et al.* (2014) obtained a cellulose nanocrystals yield of 10% after 62 h digestion of kraft pulp using commercial cellulases. Cui *et al.* (2016) also evaluated the effect of enzymatic hydrolysis time and ultrasonic treatment on the extraction of cellulose nanocrystals, achieving a maximum CNCs yield of 22.57% after 120 h of hydrolysis, with 60 min of ultrasonic treatment every 12 h.

Since increasing the hydrolysis reaction time provided higher nanocellulose yields, the results obtained using hydrolysis for 96 h were further assessed by application of ANOVA (Table 3.3).

Table 3.3. Estimated effects and p-values of the variables ball milling pretreatment time ($t_{\text{ball milling}}$) and sonication time ($t_{\text{sonication}}$), considering the response variables nanocellulose yield, zeta potential, and crystallinity index.

Factor	Yield		Zeta potential		Crystallinity index	
	Effect	p-value	Effect	p-value	Effect	p-value
Mean	9.30	0.011	-20.12	0.000	82.75	0.000
$t_{\text{ball milling}}$	10.14	0.018	3.41	0.191	-3.71	0.056
$t_{\text{ball milling}}^2$	2.88	0.444	-4.11	0.181	-0.63	0.736
$t_{\text{sonication}}$	2.57	0.447	6.52	0.041	-1.04	0.538
$t_{\text{sonication}}^2$	-2.40	0.587	-1.53	0.649	-3.30	0.176
$t_{\text{ball milling}} \times t_{\text{sonication}}$	2.37	0.594	0.43	0.898	4.15	0.106
R^2	0.739		0.710		0.722	
F value	15.124		6.927		4.644	
$F_{\text{cal}}/F_{\text{listed}}$	4.501		2.256		1.382	

The statistical analysis revealed that the ball milling time was the only variable (within the ranges tested) that significantly influenced the nanocellulose yield ($p < 0.1$), with a linear positive effect. When the ball milling time was increased from level -1.41

(0 min) to +1.41 (90 min), the yield increased to the highest value of 24.6%. The observed behavior was consistent with the work of Phanthong *et al.* (2016), who reported a gradual increase in the nanocellulose yield as the ball milling time was increased. Higher yields obtained in the earlier work could be explained by the use of acid hydrolysis and cellulose-rich substrates (cellulose paper and cellulose powder).

The zeta potentials of the nanocellulose suspensions after 96 h of enzymatic hydrolysis varied from -28.8 to -18.1 mV. At the levels studied, the variable $t_{\text{sonication}}$ significantly affected this response variable ($p = 0.041$), with the effect being linear and positive, meaning that the shift of the sonication time between levels -1.41 (0 min) and +1.41 (10 min) increased the zeta potential values. The ZP values obtained were expected, because unlike sulfuric acid hydrolysis, enzymatic treatments do not install negatively charged groups on the surface. In addition, materials with lower negative zeta potentials are suitable for biomedical and related applications (FRITZ *et al.*, 2015).

The crystallinity index was only significantly affected by the variable $t_{\text{ball milling}}$ ($p = 0.056$), which exerted a negative linear effect, meaning that an increase of $t_{\text{ball milling}}$ between levels -1.41 (0 min) and +1.41 (90 min) decreased the index of crystallinity of the nanocelluloses. The slight decrease in the crystallinity index observed is probably due to the reduction of the pulp fibers to smaller sizes, consequently decreasing the crystalline region (FENG; HAN; OWEN, 2004). This is in agreement with previous studies showing a decrease in the crystallinity index of cellulose materials with the increase of ball milling time (PHANTHONG *et al.*, 2017, 2016).

3.4.4 Morphological analysis

Figure 3.3 shows SEM micrographs of the original and knife-milled cellulose pulp, and the pulp after 13, 45, 77 and 90 min of ball milling pretreatment, as defined by the CCRD experimental design. The crystallinity indexes of these materials are also shown in Figure 3.3.

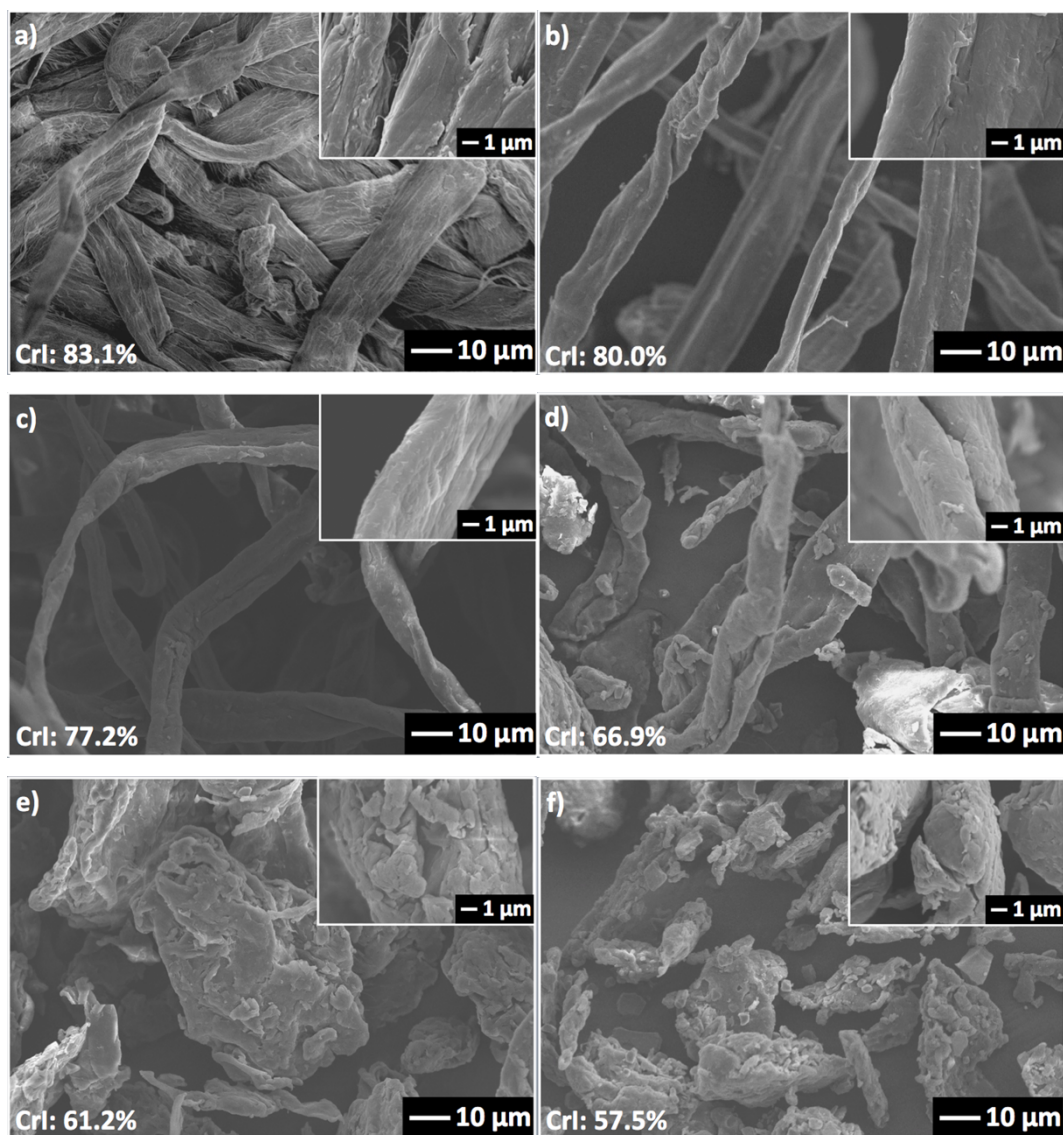


Figure 3.3. SEM images of a) the original cellulose pulp; b) the cellulose pulp after disintegration in the knife mill; and the cellulose pulp after ball milling for c) 13 min, d) 45 min, e) 77 min, and f) 90 min.

The cellulose fibers in the untreated pulp were regularly arranged and were aggregated in highly cohesive structures (Figure 3.3a). Ball milling produces high shear forces from the collisions between balls of different sizes, as well as due to the friction between the balls and the wall of the vessel, which contributes to decreasing both crystallinity and particle size (AVOLIO *et al.*, 2012; BAHETI; ABBASI; MILITKY, 2012; MOON *et al.*, 2011). After shorter ball milling pretreatments (13 and 45 min), the pulp fibers became cracked along the longitudinal axis and the macrofibril became more separated, as can be seen in Figures 3.3c and 3.3d. Increase of the ball milling time up to

90 min led to more severe structural changes. The cellulose fibers became spongy in appearance, with an abundance of small pores and a very broad particle size distribution (Figures 3.3e and 3.3f). In addition, compared to the original pulp (Figure 3.3a), the crystallinity of the ball-milled pulp decreased with increase of the ball milling time.

Figure 3.4 presents FE-SEM micrographs showing the morphologies of the nanocellulose suspensions obtained under the experimental conditions of runs 5, 6, 7, and 8 (Table 3.1).

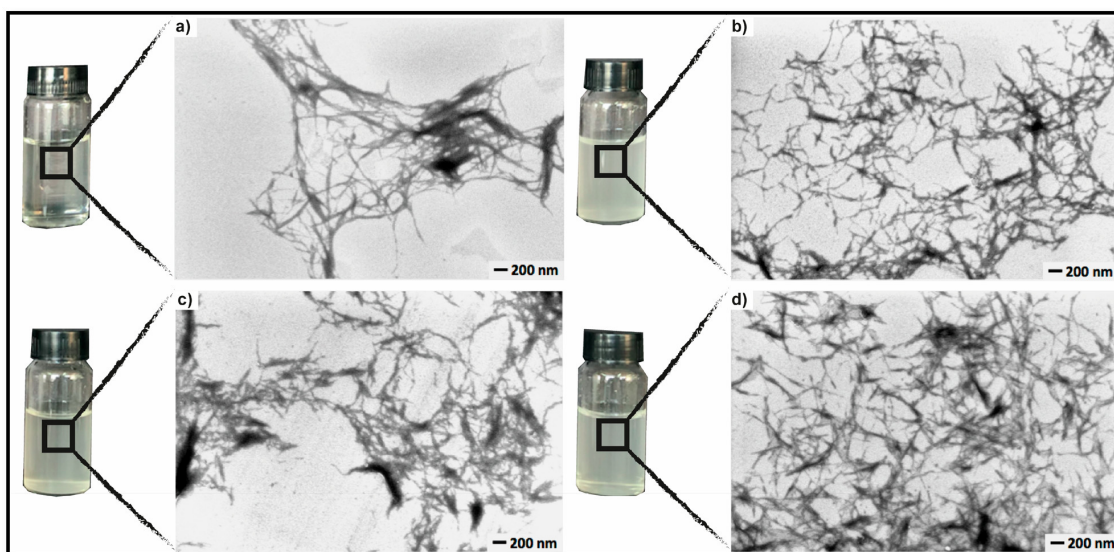


Figure 3.4. FE-SEM images and digital photos of the nanocelluloses obtained from a) run 5, b) run 6, c) run 7 and d) run 8.

These runs were selected based on the extreme values of the independent variables. In run 5, the pulp was not ball milled, while in run 6, the pulp was ball milled for 90 min. In run 7, there was no subsequent mechanical treatment, while in run 8, the sample was sonicated for 10 min. The images acquired for the other experimental conditions, including the control condition, are presented in Figure 3.7 (Supplementary data section).

The FE-SEM images confirmed the reduction of particles size after the enzymatic hydrolysis for all the conditions evaluated, suggesting the formation of cellulose nanofibers and nanocrystals. However, compared to the morphologies observed for the other conditions, the nanocelluloses in run 5 (hydrolysis using cellulose pulp without ball milling pretreatment) showed a more tangled aspect, which was probably due to the absence of milling. Moreover, the nanocellulose suspension from run 5 was the most

transparent (Figure 3.4a), probably because this sample presented the lowest yield. It is worth mentioning that in the control experiments without enzymes, it was difficult to identify these nanomaterials (Figure 3.7s and 3.7t), evidencing that enzymatic hydrolysis was required to obtain nanocellulose.

The highest nanocellulose yield was obtained in run 6, in which enzymatic hydrolysis was carried out for 96 h, using pulp that had been ball milled for 90 min, followed by 10 min of sonication. Therefore, the nanomaterials obtained using this experimental condition was further characterized in terms of their dimensions and thermal stability.

TEM images (Figure 3.5) were used to obtain the dimensions and aspect ratios of the cellulose nanocrystals.

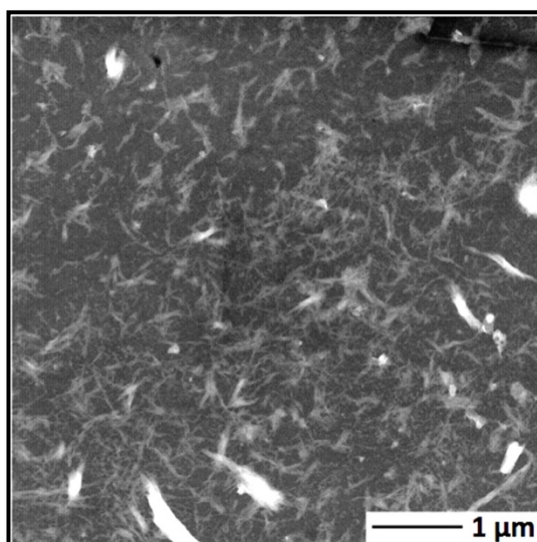


Figure 3.5. TEM images of the cellulose nanocrystals obtained using 96 h of enzymatic hydrolysis and the conditions of run 6.

The dimensions were calculated using Image J software. The cellulose nanocrystals obtained in run 6, with 96 h hydrolysis, presented a diameter of 24.0 ± 4.3 nm and a length of 294.0 ± 66.8 nm. Wang *et al.* (2015a) compared the cellulose nanofibrils obtained from hydrolysis of treated bleached eucalyptus pulp using a GH5 hyperthermostable endoglucanase and a commercial endoglucanase, combined with subsequent microfluidization. The CNFs obtained had lengths of 200-800 nm and diameters of 4-12 nm. Bondancia *et al.* (2017) produced CNCs with length of 260 nm and diameter of 15 nm, using only enzymatic hydrolysis of eucalyptus cellulose pulp. The

nanomaterials obtained here were larger than those prepared by hydrolysis using commercial enzymes. However, the conditions of run 6 were effective to provide a significant reduction in the diameter of the untreated eucalyptus cellulose pulp that was about $16 \pm 4 \mu\text{m}$ (BONDANCIA *et al.*, 2017).

3.4.5 Thermal properties

Knowledge of the thermal properties of natural materials is important for determining their compatibilities in specific applications, such as nano-filler for biocomposite (MORIANA; VILAPLANA; EK, 2016). Figure 3.6 shows the results of the thermogravimetric (TGA) and derivative thermogravimetric (DTG) analyses for the knife-milled pulp (KM), the pulp ball-milled for 90 min (BM 90 min), and the CNCs obtained from run 6 with enzymes (H 96 h - 6) and from run 12 without enzymes (H 96 h - 12).

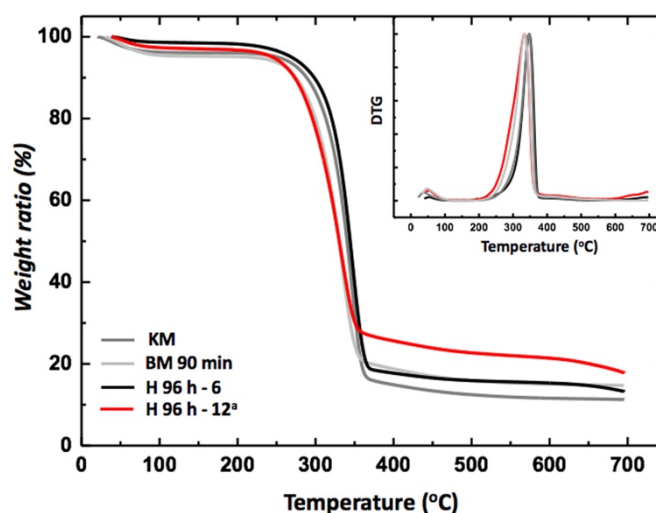


Figure 3.6. TGA curves for the original cellulose pulp and the cellulose nanocrystals obtained in runs 6 (96 h enzymatic hydrolysis) and 12 (control condition without enzymes).

All the samples presented small weight losses below 100 °C, which could be attributed to the desorption of physically and chemically bound water, or the evaporation of low molecular weight compounds remaining from the isolation procedures (ABRAHAM *et al.*, 2011). In thermal analysis, loss of hemicellulose mainly occurs between 220 and 315 °C, while cellulose decomposition starts at 310 °C and continues up

to 400 °C. Compared to cellulose and hemicellulose, lignin is more difficult to decompose, since its decomposition starts at 160 °C and extends up to 900 °C. These different behaviors are attributed to the specific chemical nature and structural characteristics of the three components (YANG *et al.*, 2007).

The samples showed significant mass loss between 300 and 350 °C, with the event peaks in the derivative weight loss curve probably being related to hemicellulose and cellulose degradation, due to processes such as depolymerization, dehydration, or decomposition of glycosyl units (ROMAN; WINTER, 2004). The decomposition events between 400 and 500 °C (Figure 3.6) were probably due to the decomposition of lignin. The small weight losses associated with these events could be explained by the low percentage of this lignocellulosic component in the pulp. Table 3.4 summarizes the values for the initial thermal degradation temperature (T_{onset}), the maximum degradation temperature (T_{max}), and the percentage of residue for the knife-milled pulp (KM), the pulp ball-milled for 90 min (BM 90 min), and the CNCs obtained from run 6 with enzymes (H 96 h - 6) and run 12 without enzymes (H 96 h - 12).

Table 3.4. Thermal properties of the pulp and the cellulose nanocrystals produced by enzymatic hydrolysis.

Samples	T_{onset}	T_{max}	Residue at 600 °C (%)
KM ^a	294.5	346.5	11.7
BM 90 min ^b	274.8	333.3	15.2
H96-6	300.5	347.4	15.2
H96-12 ^c	267.5	333.6	21.2

^a Knife-milled pulp;

^b Pulp ball-milled for 90 minutes;

^c Control condition without enzymes.

The values of T_{onset} for the KM and BM pulps were 294.5 and 274.8 °C, respectively. Decreases of thermal stability after ball milling treatment were reported previously by Rajinipriya *et al.* (2018). In comparison with the control sample (H 96 h - 12), T_{onset} for the CNCs obtained from run 6 increased from 267.5 to 300.5 °C, with the latter value being higher than T_{onset} for the ball-milled pulp (274.8 °C), which was the substrate used in the enzymatic hydrolysis.

These results demonstrated that the enzymatic treatment improved the thermal stability of the CNCs, which could have been due to the increase in crystallinity (Table

3.4). Xu and Chen (2019) investigated the optimal conditions for the preparation of CNCs with high purity and found that the nanoparticles started to degrade at 260 °C, which was slightly lower than the temperature found in the present work. Furthermore, the initial decomposition temperature of the nanocellulose obtained by enzymatic hydrolysis was higher than the temperatures of 228.2 and 130.0 °C reported by Yu *et al.* (2012) and Tian *et al.* (2016), respectively, for nanocellulose prepared by the sulfuric acid method. Lower thermal stability can result from the introduction of sulfated species on the nanocellulose fibers during the H₂SO₄ hydrolysis, due to the substitution of hydroxyl groups (O–H) by sulfate (O–SO₃H) (YAHYA *et al.*, 2019).

The maximum degradation temperature, T_{\max} , is the temperature at which the thermal degradation rate is fastest, corresponding to the peak value of the derivative weight curve. As shown in Table 3.4, T_{\max} for the CNCs obtained from run 6 (347.4 °C) was slightly higher than the values for the ball-milled pulp (333.3 °C) and the control sample (333.6 °C), which also indicated a positive effect in terms of the thermal stability of the CNCs. The residues remaining above 400 °C (Figure 3.6) varied between 11.7 and 21.2% for the original pulp and cellulose nanocrystals produced by enzymatic hydrolysis, respectively. The high crystallinity of the cellulose nanocrystals may be contributing to increase the proportion of carbon, increasing the residues by up to 81%, compared to the precursor material.

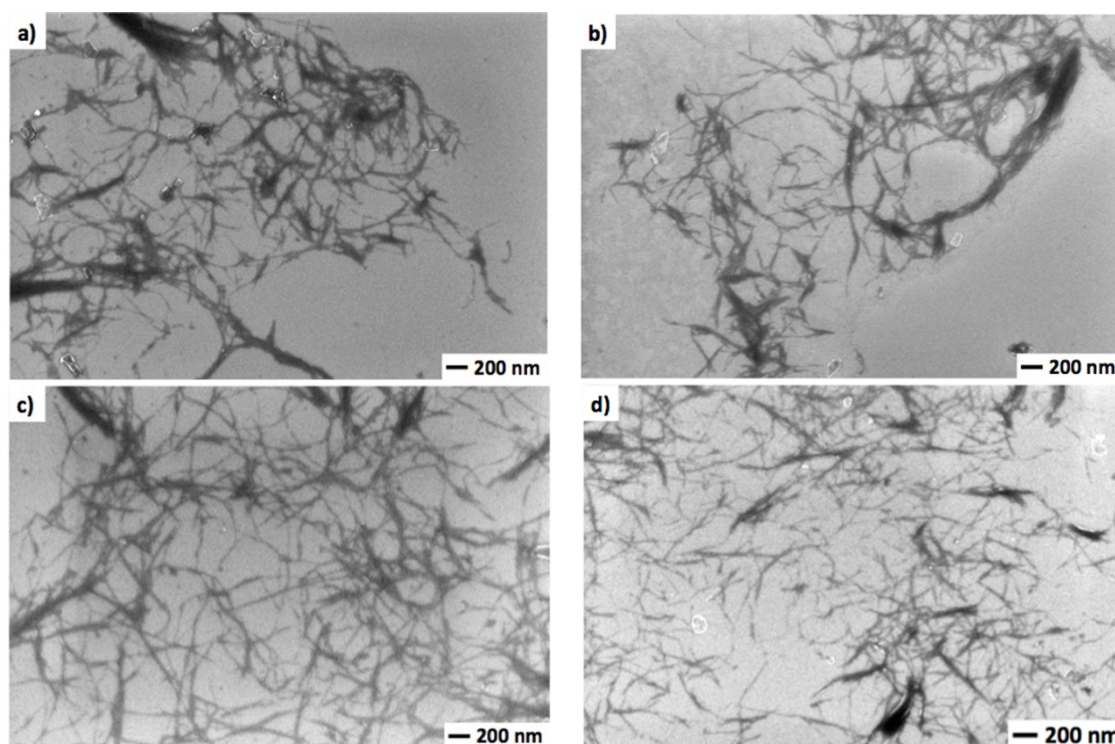
Considering the use of CNCs in the material science field, thermal stability is an important attribute, since the processing temperatures of most composite materials are usually above 200 °C (TADMOR; GOGOS, 2013). Therefore, enzymatic hydrolysis offers an attractive way to produce nanocelluloses with superior thermal stability, contributing to further expansion of their range of applications (TAO *et al.*, 2019). Overall, the results of this work demonstrated the viability of using a more sustainable route to extract cellulose nanocrystals, employing on-site produced enzymes in the context of an integrated biorefinery.

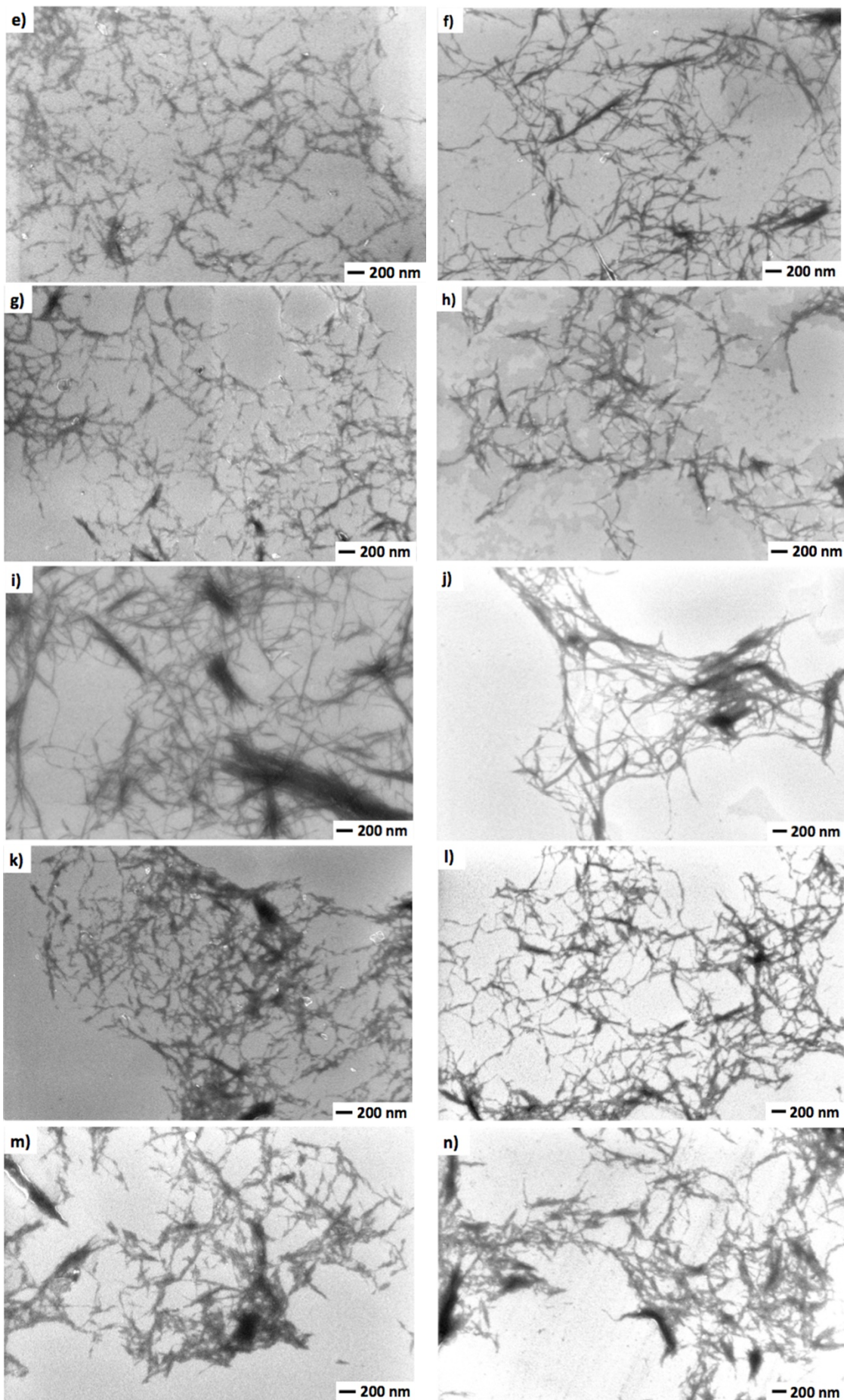
3.5 Conclusions

The findings demonstrated the feasibility of using cellulolytic enzymes produced on-site for the extraction of nanocellulose in future biorefineries. The enzymatic cocktail presented high endoglucanase specific activity of endoglucanase (17.09 IU/mg_{protein}), which is desirable for nanocellulose production. A longer ball milling pretreatment time (90 min) facilitated access to the cellulose, while increasing the hydrolysis reaction time

avored CNCs production. The highest cellulose nanocrystals yield was obtained using 96 h hydrolysis of the ball-milled pulp, followed by 5 min of sonication. The resulting nanomaterial presented a length of 294.0 ± 66.8 nm and a diameter of 24.0 ± 4.3 nm, which is within the range reported for this type of nanomaterial. The enzymatic treatment did not cause any significant changes in the cellulose surface chemistry, making the CNCs potentially suitable for use in biomedical applications. Moreover, the CNC obtained here using enzymatic hydrolysis presented superior thermal stability, compared to materials obtained by means of chemical hydrolysis reactions. The results demonstrated that use of the enzymatic hydrolysis route could be a potential strategy for the extraction of cellulose nanocrystals, offering a sustainable alternative to conventional chemical procedures. Furthermore, the integrated process reported here could be employed with different lignocellulosic feedstocks and tailor-made enzymatic cocktails, contributing to the development of a bio-based economy. Future studies on strategies to improve the enzymatic cocktail titer and its composition according to the desired end product (nanocellulose or biofuel) are encouraged to favor the economics of the proposed approach.

3.6 Supplementary data





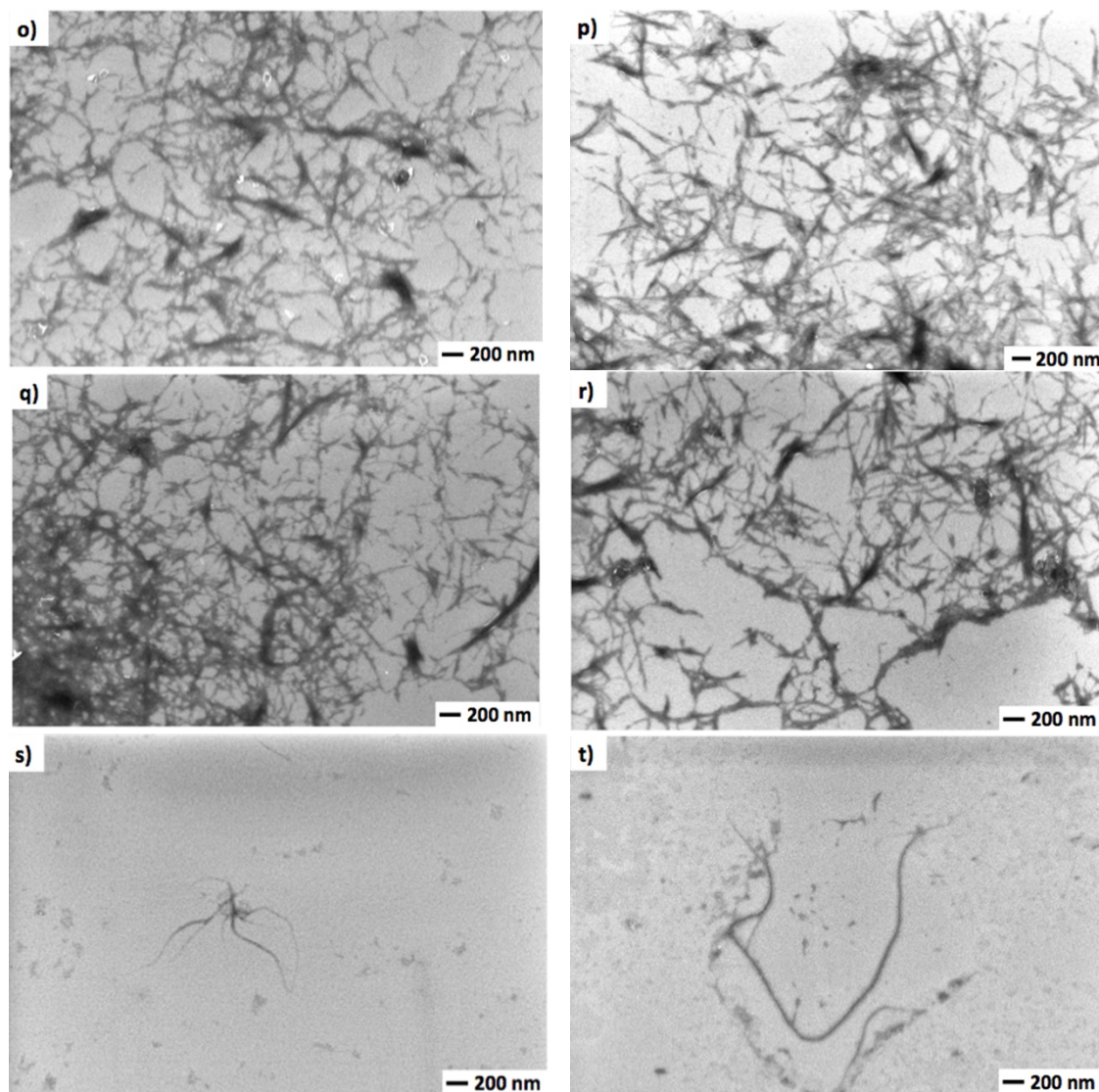


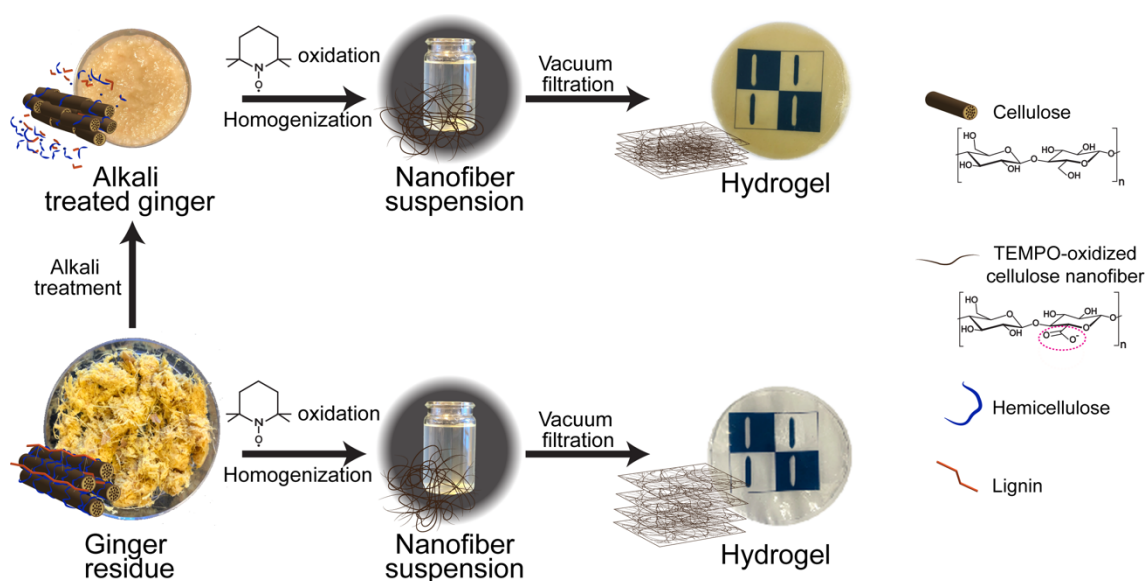
Figure 3.7. FE-SEM images of the nanocelluloses obtained from a) run 1, c) run 2, e) run 3, g) run 4, i) run 5, k) run 6, m) run 7, o) run 8, q) run 9 using 48 h of hydrolysis and from b) run 1, d) run 2, f) run 3, h) run 4, j) run 5, l) run 6, n) run 7, p) run 8 and r) run 9 using 96 h of hydrolysis. FE-SEM images of suspensions obtained from s) run 12 and t) run 13 (without enzymes).

Chapter 4

Use of ginger residue to isolate cellulose nanofibers

* The content of this chapter is an adaptation of the scientific article entitled: **“Multifunctional Ginger Nanofiber Hydrogels with Tunable Absorption – Potential for Advanced Wound Dressing Applications”** by P. Squinca, L. Berglund, K. Hanna, J. Rakar, J. Junker, H. Khalaf, C. S. Farinas and K. Oksman, published in Biomacromolecules.

Reference: doi: 10.1021/acs.biomac.1c00215



4.1 Abstract

In this study, ginger residue from juice production was evaluated as a raw material resource for preparation of nanofiber hydrogels with multifunctional properties for advanced wound dressing applications. Alkali treatment was applied to adjust the chemical composition of ginger fibers prior to nanofiber isolation. The effect of alkali treatment on hydrogel properties, assembled through vacuum filtration without addition of any chemical crosslinker was evaluated. Super absorption ability of 6200%, combined with excellent mechanical properties, tensile strength of 2.1 ± 0.2 MPa, elastic modulus of 15.3 ± 0.3 MPa and elongation at break of 25.1%, was achieved without alkali treatment. Furthermore, the absorption capacity was tunable by applying alkali treatment at different concentrations and by adjusting the hydrogel grammage. Cytocompatibility evaluation of the hydrogels showed no significant effect on human fibroblast proliferation *in vitro*. Ginger essential oil was used to functionalize the hydrogels by providing antimicrobial activity furthering its potential as a multifunctional wound dressing.

4.2 Introduction

Advanced wound dressings not only passively cover wounds, but also provide functions that promote healing or improve wound care. An ideal wound dressing should provide a moist environment, absorb exudates, protect against bacterial infection, while also being biocompatible and mechanically stable (DHIVYA; PADMA; SANTHINI, 2015; ZARRINTAJ *et al.*, 2017). It is generally accepted that a moist environment facilitates the healing of acute and chronic wounds (ALVAREZ; MERTZ; EAGLSTEIN, 1983; DOWSETT; AYELLO, 2004; SCHULTZ *et al.*, 2003) and also facilitates epidermal cell migration, increasing the rate of re-epithelialization and angiogenesis (OKAN *et al.*, 2007; SINGH *et al.*, 2013).

Hydrogels have been considered a suitable material for moist wound dressings since they absorb and retain water, which provides a moist environment for the wound. Hydrogels can have properties such as non-adhesion, bio-compatibility, and transparency. These properties can be leveraged to develop advanced wound dressings with superior and novel functions, such as enabling continuous monitoring of the wound without removal of the dressing (CALÓ; KHUTORYANSKIY, 2015; HOFFMAN, 2012; OKAN *et al.*, 2007; SLAUGHTER *et al.*, 2009). The low absorbent capability of some hydrogels geared toward wound dressings has encouraged the development of new

“superabsorbent” products that exhibit high degrees of swelling, often well over 10 times their dry mass (BUCHHOLZ; GRAHAM, 1997). This property may be useful for high rates of wound exudate absorption, which may be important for wound dressing applications (OPT VELD *et al.*, 2020). Degree of hydration can change the mechanical properties of hydrogels, often resulting in worse mechanical stability in a swollen state. This can limit their practical application as wound dressings (XIANG; SHEN; HONG, 2020).

TEMPO-oxidized cellulose nanofibers present attractive characteristics that distinguishes them from the non-oxidized nanofibers, such as, small and uniform widths (around 3 nm), high aspect ratio (higher than 150), that can provide transparent and strong network formation with increased mechanical performance (ISOGAI; BERGSTRÖM, 2018). In recent years, nanofiber based hydrogels have been exploited for wound dressing applications (CHENG *et al.*, 2017; CHENG *et al.*, 2020; CURVELLO; RAGHUWANSHI; GARNIER, 2019; GAO *et al.*, 2019; NORDLI *et al.*, 2019; WU *et al.*, 2018). However, to achieve desired multifunctional properties, such as swelling combined with mechanical stability, the preparation procedures of these hydrogels are often complex involving cellulose nanofibers in combination with several different components such as alginate (CHENG *et al.*, 2017) or chitosan (CHENG *et al.*, 2020; GAO *et al.*, 2019) and crosslinking agents (CHENG *et al.*, 2017; CHENG *et al.*, 2020) for the stability.

The use of silver nanoparticles in wound dressings is a well-known approach for minimizing microbial contamination of wounds, and one approach to achieve antimicrobial materials (WU *et al.*, 2018). However, silver nanoparticles can be difficult to control and their use is known to have side-effects on patient health (FERDOUS; NEMMAR, 2020). Bio-based materials with novel, nature-derived antimicrobial properties have recently been explored as an important advanced functionalization of wound dressings (LI *et al.*, 2018). This approach can reduce the microbial challenge to wounds, thereby minimizing the risks associated with wound infections, all the while avoiding further use of classical antibiotics as the use of which exasperates the threat of antimicrobial resistance (LI *et al.*, 2018).

Zingiber officinale Roscoe, commonly known as ginger, is extensively used as a spice, but it has also been used as traditional medicine due to its purported antioxidant, antiviral, antidiabetic, anti-inflammatory, anticancer, as well as antibacterial properties (ALI *et al.*, 2008; NICOLL; HENEIN, 2009; NILE; PARK, 2015; SEMWAL *et al.*, 2015;

SIVASOTHY *et al.*, 2011). Ginger is rich in constituents such as cellulose, starch and hemicellulose, but also includes several bioactive families of compounds such as gingerols, zingiberene and shogaols (BUTT; SULTAN, 2011). The essential oil extracted from ginger has also shown significant antimicrobial, antifungal and antioxidant activities and it is mainly constituted by geranial, α -zingiberene, (E,E)- α -farnesene, neral and ar-curcumene (EL-BAROTY *et al.*, 2010; SINGH *et al.*, 2008). Although the pharmacological properties have been supported by in vivo and in vitro experiments (SANG *et al.*, 2020), only a few studies have focused on using its nanofibers for the preparation of bionanocomposites (JACOB *et al.*, 2019a, b, 2018), films (ABRAL; ARIKSA; MAHARDIKA; HANDAYANI; AMINAH; SANDRAWATI; PRATAMA; *et al.*, 2020; ABRAL; ARIKSA; MAHARDIKA; HANDAYANI; AMINAH; SANDRAWATI; SAPUAN; *et al.*, 2020; ABRAL; ARIKSA; MAHARDIKA; HANDAYANI; AMINAH; SANDRAWATI; SUGIARTI; *et al.*, 2020) and aerogels (WANG *et al.*, 2019; WANG *et al.*, 2018). The potential use of ginger and its natural components for nanofiber extraction and their utilization for the preparation of completely ginger-based hydrogels have, so far, not been studied for wound dressing applications.

In this study, we investigated the potential use of ginger residue for nanofiber extraction and subsequent assembly into hydrogels aimed at wound dressing applications. The hydrogels were prepared by simple vacuum assisted filtration using only ginger nanofibers without any crosslinker, to maintain low energy requirements, minimize the components needed for sustainable production, and avoid the risk of introducing toxic side-effects. Alkali treatment was applied on ginger fibers before the TEMPO oxidation to modify their chemical composition, altering the liquid absorption capacity of the hydrogels. This is evaluated in water, bovine serum albumin (BSA) and phosphate buffered saline (PBS) solutions. The functionalization of ginger-based hydrogels with ginger essential oil seems like an advantageous strategy because it has the potential to leverage the antimicrobial properties of the plant to enhance the antimicrobial properties of the wound dressing, while being sourced from the same raw materials. The structural morphology, mechanical properties in wet conditions, cytocompatibility and antimicrobial properties of two versions of ginger nanofiber (GNF) hydrogels were quantified, supporting an initial evaluation of these materials for use in advanced wound dressing products.

4.3 Experimental section

4.3.1 Materials

Ginger roots were purchased from the local market, and the fibers were obtained after juicing to simulate residue condition and used as the feedstock in this study. Sodium chlorite (NaClO_2) high purity, with a sodium chlorite content of 77.5–82.5% (w/w) was purchased from VWR International AB (Stockholm, Sweden). Ginger essential oil, sodium hypochlorite (NaClO , 6–14% active chlorine), 2,2,6,6-tetramethylpiperidin-1-oxyl (TEMPO, 98%), bovine serum albumin lyophilized and phosphate buffered saline were purchased from Sigma-Aldrich, Sweden AB (Stockholm, Sweden). Glacial acetic acid (CH_3COOH , 100%) was purchased from Merck KGaA (Darmstadt, Germany). The BSA was used in a concentration of 50 g/L in distilled water without further treatment.

4.3.2 Alkali treatment

Alkali treatments were performed using 4 and 2% (w/w) NaOH solutions to alter the chemical composition of the ginger fibers. Treatments were performed at a liquor:dry matter ratio of 80:1, 80 °C for 2 h under magnetic stirring. Sequentially, alkali-treated ginger fibers were washed with distilled water until a neutral pH was reached.

4.3.3 Bleaching procedure

Ginger fibers, with and without alkali treatment were bleached with NaClO_2 (2.5% (w/w) in an acetic buffer (pH 4.5) at 80 °C for 2 h. After bleaching, materials were washed with distilled water until a neutral pH was reached. Sodium chlorite is the primary oxidant in the TEMPO/ NaClO / NaClO_2 -system, and bleaching treatments were performed to obtain samples that could be used for estimating the chemical composition of the ginger nanofibers, both with and without alkali treatment.

4.3.4 Chemical composition

The chemical composition of the raw material, after bleaching of ginger fibers with and without alkali treatment, was determined in accordance with the standard testing recommendations of the Technical Association of Pulp and Paper Industry (TAPPI). The extractive content was determined by Soxhlet extraction with acetone-alcohol 2:1 for 5 h following the methodology of T 204 cm-97 (TAPPI, 1997). Delignification of all materials was performed according to established protocols (WISE, 1946) in which three

additions of NaClO_2 (1 g/g_{dry matter}) and acetic acid (0.2 mL/g_{dry matter}) were added in intervals of 1h. The reactions were carried out at a liquor:dry matter ratio of 40:1 and 70 °C. After the delignification, materials were washed with distilled water until a neutral pH was reached. Holocellulose and α -cellulose contents were determined according the TAPPI standard T 203 cm-99 (TAPPI, Norma, 1999). Hemicellulose content was calculated as the subtraction of α -cellulose from holocellulose percentage. Klason lignin was determined in sulfuric acid solution at 72% (w/w) following the TAPPI standard T 222 om-02 (TAPPI, 2002). The presented component values are based on ten measurements for each sample, and tests were performed in triplicate.

4.3.5 Yield determination

The treatment yields (alkali treatment, bleaching and TEMPO oxidation) were calculated according to the following equation:

$$\text{Yield (\%)} = w_f/w_i \times 100 \quad (4.1)$$

where w_f indicates the dry weight of the sample after the alkali treatment, bleaching and TEMPO oxidation and w_i indicates the initial dry weight of the ginger fibers.

4.3.6 Optical microscopy

Characterizations of the ginger fibers before and after the alkali treatment and TEMPO oxidation were performed using an optical microscope (OM), Nikon Eclipse LV100N POL (Kanagawa, Japan) and the imaging software NIS-Elements D 4.30.

4.3.7 Ginger nanofiber production

The ginger nanofibers were obtained by TEMPO/ NaClO / NaClO_2 -system following a method described by *Saito et al.* (2009) with modifications and using either ginger fibers before or after alkali treatment. Firstly, NaClO_2 (5.0 g/g_{dry matter}) and TEMPO (17.5 mg/g_{dry matter}) were dissolved in the ginger fibers suspension at a liquor: dry matter ratio of 100:1 in the presence of sodium phosphate buffer (0.05 M, pH 6.8). The flask was sealed and submerged in an oil bath after which NaClO (1 mL/g_{dry matter}) was added and kept at a temperature of 60 °C for 72 h. After cooling the suspension to room temperature, the material was washed with distilled water until reaching a neutral pH. After the TEMPO-oxidation, the GNF suspension was diluted to 0.2% (w/w), homogenized with a

high shear fluid homogenizer APV 2000 (SPXFlow Inc, Delavan, USA) at 1000 bar and collected after 1 pass. Different GNF suspensions were prepared from ginger without alkali treatment, and after 2 and 4% (w/w) alkali treatment and they are denoted as T-GNF (TEMPO-treated GNF), AT 2%-GNF and AT 4%-GNF (Alkali and TEMPO-treated GNF with 2 or 4 % NaOH), respectively. The surface charge of the ginger nanofibers was measured using a Zetasizer Nano Z (Malvern Pan analytical Ltd, Malvern, UK), at room temperature (25 °C), in triplicate. Prior to the measurements, the samples were diluted to 0.05% (w/v) with distilled water.

4.3.8 Preparation of ginger nanofiber-based hydrogels

Hydrogels with different grammages (40, 80 and 120 g/m²) were prepared by vacuum-assisted filtration of ginger cellulose nanofibers on a filter paper (Whatman grade 54, 90 mm diameter) and metal wire sieve. Firstly, GNFs suspensions were diluted to 0.1% (w/w) in water and dispersed under magnetic stirring for 10 min. Suspensions were then degassed and poured in a Büchner funnel with filter paper and metal wire sieve. The suspension was filtered at room temperature (~20 °C) for 8 - 24 h depending on the grammage of the hydrogel. After the GNF network was formed, the hydrogel was put into water and peeled from the filter paper. Subsequently, hydrogels were dried at room temperature (~20 °C) and their swelling degree was adjusted according to the characterization condition tests. A reference hydrogel was prepared from wood-based nanofibers which were prepared using the TEMPO-oxidation and homogenization treatment described for ginger. The reference hydrogel was prepared at 40 g/m² following equivalent procedure and used for comparison of the swelling behavior. To enhance the antimicrobial properties of the dressing material, the hydrogels prepared with T-GNF and AT 4%-GNF were functionalized with ginger essential oil (GEO). Initially, the GNF suspensions were diluted to a concentration of 0.3% (w/w) in water and dispersed under magnetic stirring for 10 min. The solution was then placed in a thermostatic oil bath at 40 °C and the GEO (10% (w/w)) was added under constant stirring for 20 min. After that, the mixed solution was sonicated using an ultrasonic processor UP400s (Hielscher Ultrasonics GmbH, Teltow, Germany) for 2 min. The hydrogel was prepared by solution casting method and the mixed solution was casted on an acrylic plate (55 mm diameter). The hydrogel was subsequently dried at 50 °C for 12 h. For comparison, control hydrogels were also prepared by solution casting following the same procedure, but without adding the ginger essential oil.

4.3.9 Scanning electron microscopy

Morphology of ginger fiber raw material and cross-section of GNF hydrogel were examined using a SEM JEOL JSM 6460LV (JEOL Ltd, Tokyo, Japan) at an acceleration voltage of 15 kV. The samples were freeze-dried and coated with platinum using an EM ACE200 sputtering instrument (Leica, Wetzlar, Germany) prior to observation to avoid electron charging. The coating was performed in a vacuum of 6×10^{-5} mbar under a current of 100 mA resulting in a coating thickness of 15 nm.

4.3.10 Atomic force microscopy

GNF morphology and dimensions were further analyzed using a Veeco MultiMode Scanning Probe atomic force microscope (Bruker®, Santa Barbara, CA, USA) in tapping mode with a tip model TESPA (antimony (n) doped silicon) (Bruker, Camarillo, CA, USA). A drop of the diluted suspension (0.01% (w/w)) was placed on a clean mica surface and left to dry at 22-23 °C. The nanofiber width was determined from the height images using the Nanoscope V software, and the average values and deviations presented here are based on 100 different measurements.

4.3.11 Liquid absorption measurement

GNF hydrogels at dry state were immersed in distilled water, PBS and BSA (50 g/L) solutions at room temperature to study the liquid absorption over time. The wet weight of the hydrogels was recorded at regular intervals over 72 h. The excess liquid was removed before weighing by gently tapping the samples on a dry tissue paper. Liquid absorption was calculated as follows:

$$\text{Liquid absorption (\%)} = (w_t - w_d)/w_d \times 100 \quad (4.2)$$

in which w_d denotes the initial weight of the dried sample and w_t denotes the weight at time t after immersing samples in distilled water and PBS.

4.3.12 Hydrogel integrity measurement

Hydrogel structural integrity was evaluated by measuring its weight in BSA and PBS solutions at room temperature over time. Hydrogels were incubated either in BSA or PBS solution and the wet weight at the equilibrium state was taken as 100%. The wet weight of hydrogels was measured with regular intervals and the percentage of weight

remaining was determined by the following equation:

$$\text{Integrity (\%)} = w_w/w_{es} \times 100 \quad (4.3)$$

in which w_{es} denotes initial weight at the equilibrium state of the sample and w_w denotes wet weight of the sample.

4.3.13 Water retention capacity

Hydrogel samples with grammage of 40 g/m² were allowed to swell in distilled water until they reached equilibrium. Excess water was wiped off, then the hydrogels were left at ambient temperature for 24 h and weighed at regular intervals. The water retention capacity was calculated by the following equation:

$$\text{Water retention capacity (\%)} = w_r/w_{es} \times 100 \quad (4.4)$$

where w_{es} denotes initial weight at the equilibrium state of the sample and w_r denotes the weight retained after the sample was left to dry.

4.3.14 Mechanical testing

Compressive properties of hydrogels were performed using a Q800 dynamic mechanical analyzer (TA Instruments, New Castle, USA) with the compression configuration. Samples with dimensions of 5 × 5 mm and thicknesses ranging between 2 and 5 mm were tested in wet conditions (800% of swelling degree). Tests were carried out with a 1 mN preload and a strain rate of 5%/min. The compressive modulus was calculated from the slope of the initial linear region of the stress-strain curves (strain value lower than 5%). Ten measurements were taken for each sample, and averaged.

Tensile properties of the hydrogels were measured using a Shimadzu Autograph AG-X universal testing machine (Shimadzu Corp., Kyoto, Japan) equipped with a load cell of 1 kN. Tests were performed at a strain rate of 2 mm/min and with a gauge length of 20 mm. The samples were in the form of strips of 6 mm in width and 80 mm in length and were tested in wet conditions (800% of swelling degree for comparison under similar conditions). Ten measurements were taken for each sample, and averaged. Statistical analysis at 5% significance level based on the Levene's test was used to assess the equality of variances and ANOVA test was performed to compare the averages of the

mechanical properties.

4.3.15 Antibacterial activity study

The antibacterial activity assays were carried out by Dr. Hazem Khalaf and collaborates in the School of Medical Sciences laboratory (Örebro University, Sweden). *Staphylococcus aureus* and *Escherichia coli* were streaked onto a Luria Bertani (LB) agar plates and incubated at 37 °C overnight. Single bacterial colonies were picked and inoculated into 5 mL LB broth and cultivated overnight on a shaker (300 rpm) at 37 °C. The bacterial concentration was determined by viable count, which was adjusted to correspond to 10⁹ CFU/mL. The antimicrobial activity of ginger nanofibers was studied by spreading *S. aureus* and *E. coli* (10⁷ CFU in 100 µL) on Mueller Hinton Agar, and placing the hydrogels onto the bacterial lawn. The plates were incubated at 37 °C for 20 h and the zones of inhibition were visualized by acquiring images at a magnification of 12.5x using an Olympus SZX9 stereo zoom microscope, (Olympus, Solna, Sweden).

Direct antimicrobial activity of the ginger material (contact-dependent) was determined on Mueller Hinton Agar following addition of *S. aureus* and *E. coli* (10⁵ CFU in 10 µL) on top of the membranes. The plates were incubated at 37 °C for 20 h followed by image acquisition. The hydrogels were placed upside down on a new Mueller Hinton plate for 10 s and removed to determine bacterial viability. After 20 h of incubation, bacterial growth was visualized by capturing images using Olympus SZX9 at 12.5x magnification (Olympus, Solna, Sweden).

4.3.16 Cytocompatibility study

The experiments related to the cytocompatibility study were performed by Kristina Hanna, Dr. Jonathan Rakar, Dr. Johan Junker and collaborates in the Center for Disaster Medicine and Traumatology laboratory (Linköping, Sweden).

4.3.16.1 Primary cell isolation and cultures

Primary skin cells were isolated from human tissue obtained from healthy patients undergoing routine reduction abdominoplasty at the University Hospital in Linköping, Sweden. All human tissue and cells were handled in accordance with guidelines postulated by Linköping University under approval from the Swedish Ethical Review Authority (no. 2018/97-31). Briefly, human keratinocytes and fibroblasts were isolated by mechanical and enzymatic dissection of viable epidermis and dermis, under

sterile conditions. For isolation of fibroblasts, skin samples were repeatedly washed in sterile PBS then subcutaneous fat was mechanically removed. The remaining dermis was dissected into approximately two hundred $1 \times 3 \text{ mm}^2$ pieces, carefully avoiding epidermis and irregular structures such as large vessels, and placed in Dulbecco's modified Eagle's medium (DMEM, Gibco Thermo Fisher Scientific, Paisley, UK) with 165 U/mL collagenase (Gibco Thermo Fisher Scientific, Paisley, UK) and 2.5 mg/mL dispase (Gibco Thermo Fisher Scientific, Paisley, UK) and incubated at 37 °C, 5% CO₂, and 95% humidity for 12 h. After enzymatic digestion, the tissue is mostly dissolved and so the suspension is centrifuged for 5 min at $200 \times g$ and the resulting cell pellet re-suspended in fibroblast medium (DMEM containing 10% fetal calf serum, 50 U/mL Penicillin and 50/mg mL Streptomycin). This was repeated twice with fresh medium to wash the cells. The final cell pellet was dissociated, and the cells were seeded into 75 cm² culture flasks (Falcon, Corning Inc; Corning, NY, USA) in fibroblast medium and kept in an incubator at 37 °C, 5% CO₂, and 95% humidity. Medium was changed three times per week.

For isolation of keratinocytes, samples were processed according to a modification of the protocol described by Rheinwald and Green (1975). Briefly, samples were repeatedly washed in sterile PBS and subcutaneous fat was mechanically removed. The remaining tissue was cut into $5 \times 5 \text{ mm}^2$ pieces and placed in DMEM with 2.5 mg/mL dispase at 7 °C overnight. The epidermis was then manually removed from the dermis and placed in DMEM containing 0.02% versene/0.1% trypsin (Gibco Thermo Fisher Scientific, Paisley, UK) and incubated for 15 min at 37 °C, 5% CO₂, and 95% humidity. Pooled supernatants were centrifuged for 5 min at $365 \times g$ and the resulting cell pellet washed in DMEM (Gibco Thermo Fisher Scientific). Cells were seeded into 75 cm² culture flasks (Falcon, Corning Inc) with Keratinocyte Serum-Free Medium (KSFM; containing 1 mg/L epidermal growth factor, 25 mg/L bovine pituitary extract, 50 U/ml Penicillin and 50 mg/ml Streptomycin; Gibco Thermo Fisher Scientific) and kept in an incubator at 37 °C, 5% CO₂, and 95% humidity. Medium was changed three times per week.

Initial tests where cells were seeded on hydrogels were performed. Briefly, 200,000 keratinocytes or fibroblasts were seeded on 1 x 1 cm hydrogels. Following 48 h incubation at 37 °C, 5% CO₂, and 95% humidity, materials were fixed in 4% paraformaldehyde, dehydrated using an ethanol series (70%, 95% and 99.5%), and embedded in paraffin. 7 μm thick sections were mounted on microscopy slides and stained using AlexaFluor546-conjugated Phalloidin (Thermo Fisher Scientific) and 4',6-

diamidino-2-phenylindole (Thermo Fisher Scientific) to visualize cells. Samples were examined using a BX41 light/fluorescence microscope with a DP70 CCD camera (Olympus, Stockholm, Sweden), and cell nuclei were manually counted.

4.3.16.2 Cell Viability and Proliferation

Following establishment of primary cultures, cells were enzymatically detached using 0.02% versene/0.1% trypsin) and seeded in 6-well plates (Falcon, Corning Inc). Cells were allowed to adhere for 24 h and were subsequently covered with Ø 10 mm discs of T-GNF or AT 4%-GNF and cultured for 72 h. Keratinocyte and fibroblast cultures in three replicate wells without addition of material served as controls. Every 24 h, for 72 h in total, cells were detached using 0.02% versene/0.1% trypsin solution at 37 °C for approximately 10 min, stained with trypan blue to distinguish viable cells, and counted using an EVE™ Automated Cell Counter (NanoEnTek, Waltham, MA). All experiments were performed in biological triplicates (separate cell cultures) and methodological duplicates (staining and cell counting). Numbers of viable cells were recorded and analyzed using Prism 8.4.2 (Graphpad LLC, LaJolla, CA, US). A two-way ANOVA coupled with a Holm-Sidak post-test was used to compare cell numbers over time in all groups of the same cell type, and $p < 0.05$ was considered significant. Cell numbers in the treatment groups were normalized to non-treated controls and expressed as proliferative index according to the following equation:

$$\text{Proliferative Index} = C_T/C_{T0} \quad (4.5)$$

in which C_T denotes the mean number of viable cells at the analyzed timepoint and C_{T0} denotes the mean number of viable cells at the starting timepoint. All values are plotted as mean \pm standard deviation unless otherwise stated.

4.3.16.3 Cell Migration Assay

To assess effects of T-GNF or AT 4%-GNF on cell migration, fibroblasts and keratinocytes were seeded in separate triplicate 6-well plates as described above. Cells were cultured until confluency, and a denuded scratch was produced using a p200 pipette tip across the center of the wells. Cultures were covered with the hydrogels and examined at 0, 24, 48 and 72 h using an IX51 light microscope with a DP70 CCD camera (Olympus, Stockholm, Sweden). Photos were captured at 10x magnification and analyzed using

ImageJ 1.52p (NIH, USA) to measure remaining cell free area in the denuded streak. The areas were normalized to the area at time 0 according to the following equation:

$$\text{Scratch Closure (\%)} = A_t/A_{\text{start}} \times 100 \quad (4.6)$$

where A_t denotes mean remaining denuded area at experimental time and A_{start} denotes initial mean wound area. A mixed-effects restricted maximum likelihood model (REML) coupled with a Holm-Sidak post-test was used to compare cell numbers over time in all groups of the same cell type, and $p < 0.05$ was considered significant. All values are plotted as mean \pm standard deviation (SD) unless otherwise stated.

4.4 Results and discussion

4.4.1 Production and characterization of ginger nanofibers

Hydrogels with different liquid absorption capacities are interesting for wound dressing applications. Different types of wounds as well as different stages of the healing process may have different requirements for an optimal dressing. The process for material preparation can result in different material properties, and natural starting materials can have different advantageous properties. We sought to leverage this knowledge to develop a multifunctional material aimed at advanced wound dressings, sourced and produced with sustainability in mind.

Ginger nanofibers were produced by TEMPO-oxidation combined with high-pressure homogenization before and after alkali treatment. The effects of the different processing routes, and the nanofibers compositional varieties derived from the alkali treatments were further studied with regards to hydrogel properties (Figure 5.1). The chemical composition without applied alkali treatment was $25.1 \pm 0.5\%$ α -cellulose, $40.5 \pm 0.6\%$ hemicellulose, $5.5 \pm 0.9\%$ Klason lignin, and $5.1 \pm 1.3\%$ extractives. These results are in agreement with Abiral *et al.* (2020a) who found cellulose and hemicellulose content of 30 and 44% respectively. However, Zaki, Abdullah and Ahmad (2014) reported a higher value of cellulose (65.2%) and a lower hemicellulose value (10.1%). The differences in proportions of each individual component can be explained by a number of factors related to the analysis methodology or the sample itself. These factors include country of origin, harvesting conditions, industrial processing, and whether the ginger is fresh, dried, or processed (SCHWERTNER; RIOS; PASCOE, 2006). Besides the high

contents of cellulose and hemicellulose, ginger has a significant amount of starch varying between 30 to 60% (BRAGA; MORESCHI; MEIRELES, 2006; REYES *et al.*, 1982). It is generally accepted that alkali treatment changes the composition of the fibers by targeting the non-cellulosic components, such as, starch, hemicellulose, and pectin (BARTOS *et al.*, 2020). Alkali treatment was applied to ginger fibers before the TEMPO oxidation, aiming to reduce the hemicellulose content and alter the characteristics of the nanofibers. This directly influenced the properties of the hydrogels prepared with them. The content of hemicellulose after oxidation was $11.0 \pm 0.8\%$, which supports that the alkali treatment reduces non-cellulosic components. The process yields, with and without alkali-treated ginger as feedstock, are presented in Table 4.1.

Table 4.1. Total yield and weight after each step of the ginger nanofibers production process.

Samples	Initial weight (g)	Weight after alkali treatment (g)	Weight after TEMPO oxidation (g)	Total yield (%)
T-GNF	10	-	4.3	43.3
AT 4%-GNF	10	1.5	0.6	6.4

The lower yield (6.4%) reached using alkali-treated ginger is attributed to the material loss during the alkali step. However, this value is higher than the ginger nanofiber yield of 3.1% reported by Jacob *et al.* (2019) who also applied an alkali treatment under similar conditions on ginger fibers to reduce the non-cellulosic components.

The optical micrographs (OM) are presented in Figure 4.1, showing the raw material, the ginger fiber with and without alkali treatment, and GNFs, together with atomic force microscopy (AFM) height images (Figure 4.1-c2 and d2).

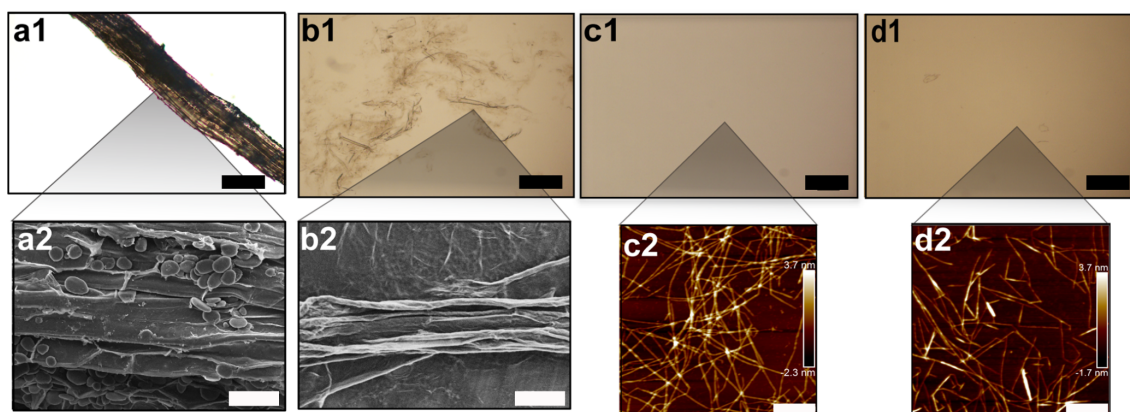


Figure 4.1. OM images of a1) ginger raw material before and b1) after alkali treatment step. OM images of homogenized nanofiber suspension c1) after only TEMPO treatment (T-GNF) and d1) after alkali and TEMPO treatment (AT 4%-GNF) (Scale bar: 200 μm). SEM images of dried ginger fibers a2) non-alkali treated and b2) after alkali treatment (Scale bar: 50 μm). AFM images of dried nanofiber suspensions c2) T-GNF and d2) AT 4%-GNF (Scale bar: 400 nm).

From Figure 4.1-c1, it is possible to note that alkali treatment generated micro-sized structures composed of fragments of parenchyma cells and fibers of different sizes. The representative SEM images before and after alkali-treatment are shown in Figure 4.1-a2 and b2, respectively. Starch granules can be observed with an oval shape and a smooth surface without fissures, typically found associated with fibers in ginger (BRAGA; MORESCHI; MEIRELES, 2006; POLICEGOUDRA; ARADHYA, 2008). Comparison between Figures 4.1-a2 and b2 indicates that besides reducing the hemicellulose content, the alkali treatment also reduced the starch content since the starch granules are absent in the alkali-treated fibers. Furthermore, the OMs of the GNF suspensions obtained from TEMPO oxidation directly followed by homogenization and after alkali-treatment of ginger, are presented in Figure 4.1-c1 and d1, respectively. In both conditions, it was not possible to observe any larger structures after the TEMPO treatment confirming that their size was reduced to the nanoscale.

The overview AFM images of GNFs together with their size distribution (Figure 5.8) are provided in Supplementary data. The size of the GNFs was measured from AFM height images (Figure 4.1-c2 and d2) and the averaged width values of T-GNFs and AT 4%-GNFs were 1.7 ± 0.7 nm and 2.0 ± 1.1 nm, respectively. Overall, it can be noted that the widths were comparable for both samples (Figure 4.8, Supplementary data section).

Additionally, the ginger nanofibers widths are in agreement with the values of TEMPO nanofibers isolated from wood reported elsewhere (JONASSON *et al.*, 2020; SAITO *et al.*, 2009).

4.4.2 Liquid absorption capacity of ginger nanofiber hydrogels

One of the most important properties of hydrogels for wound dressing applications is the water/liquid absorption, sometimes expressed as swelling degree, which directly reflects the hydration ability (HOLBACK; YEO; PARK, 2011). A moist environment allows cell migration – importantly, of epithelial cells and leukocytes – and distribution of growth factors, into including epithelial cells, and growth factors to migrate to the wound bed, thus facilitating the wound healing process (SOOD, Aditya; GRANICK; TOMASELLI, 2014).

The liquid absorptions over time of hydrogels prepared from GNFs isolated directly after TEMPO-treatment (T-GNF), and alkali-treatment using 2% (w/w) (AT 2%-GNF) and 4% (w/w) (AT 4%-GNF) of sodium hydroxide are shown in Figure 4.2.

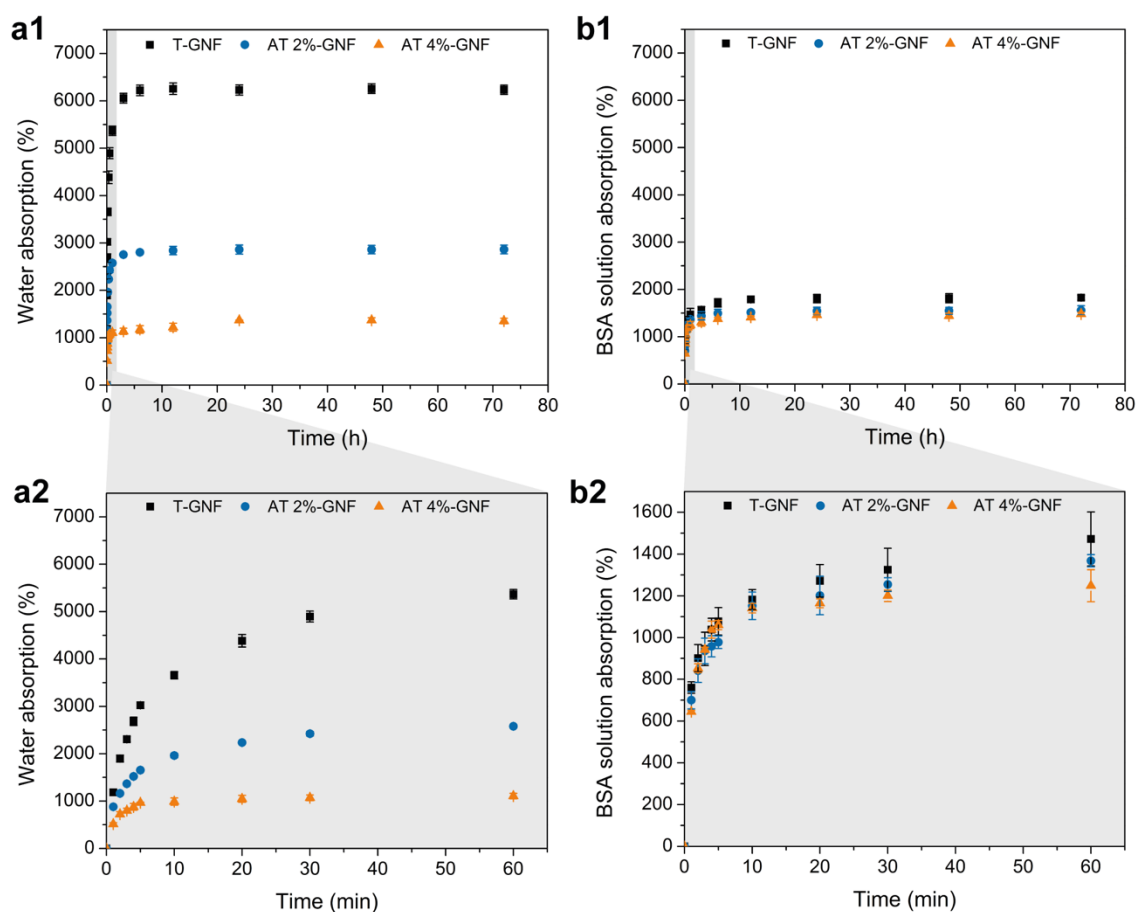


Figure 4.2. Liquid absorption of the hydrogels (40 g/m^2) in a1) water and b1) BSA

solution. Liquid absorption of hydrogels curves expanded for the first hour in a2) water and b2) BSA solution.

The highest water absorption capacity was obtained by T-GNF hydrogel (~6200%) which was about 5 times higher than the value obtained by AT 4%-GNF hydrogel (~1350%), as well as that measured for the reference hydrogel prepared from wood-based nanofibers (~1250%) (Figure 4.2-a1). From Figure 4.2-a2, it is evident that T-GNF hydrogel reached the same absorption capacity value of AT 4%-GNF at the equilibrium in the first minutes after immersion in water. It is worth highlighting that because the T-GNF hydrogel showed water absorption capacity of 62 times its dry weight T-GNF can be compared to a superabsorbent hydrogel (ALAM; ISLAM; CHRISTOPHER, 2019; HORIE *et al.*, 2004; POURJAVADI; AYYARI; AMINI-FAZL, 2008). This is an interesting result as the hydrogel was prepared from only natural polymer without using any crosslinker, swelling agent or highly hydrophilic synthetic polymer, and through a simple methodology. The high-water absorption of T-GNF is likely associated with the natural composition of ginger that is rich in both hemicellulose and starch, in contrast with AT 4%-GNF and wood-based reference material, where these components are reduced (and in case of wood the starch content is absent). Zhang *et al.* (2015) prepared a super-absorbent hydrogel based on the high swelling capacity of hemicellulose. Hydrophilic polymers, such as starch, carrageenan, and poly-acrylamide are commonly added into hydrogels to enhance their swelling capacity (YANG; FANG; TAN, 2006). These results suggest that the natural composition of ginger can be beneficial for the preparation of hydrogels with a high water absorption capacity. Additionally, alkali treatments can be used to effectively alter the liquid absorption capacity of the hydrogels by modifying the chemical composition of the raw materials.

The swelling behavior was also evaluated in BSA solution to more closely resemble the wound environment in terms of a higher abundance of proteins (Figure 4.2-b1 and b2). The difference between the hydrogel liquid absorption capacities was less pronounced in BSA solution, and the same behavior was also observed for PBS solution (Figure 4.9, Supplementary data section). However, the T-GNF hydrogel still showed the highest swelling degree at equilibrium when compared with AT 2%-GNF and AT 4%-GNF hydrogels. The swelling at equilibrium was overall lower in BSA than in water, which could be attributed to the repulsive electrostatic interactions between the BSA molecules and the hydrogels. The swelling behavior of neutral hydrogels is controlled by

opposing forces resulting from spontaneous mixing of the fluid molecules with the polymer chains and the retractive forces developed inside the structure. The equilibrium swelling state is reached when these forces balance. The presence of ionic groups in the hydrogel structure and ions in the surrounding media generate additional forces that affect the balance, thus influencing the liquid absorption properties (PEPPAS *et al.*, 2000). Both hydrogels are negatively charged as indicated by the negative zeta potentials: -44.8 ± 0.7 mV for T-GNF, and -65.6 ± 0.7 mV for AT 4%-GNF. All proteins contain positively and negatively charged groups and their effective charge is a result of the balance of those groups at a given pH. The BSA solution was prepared in water and the effective charge value at pH higher than the isoelectric point of BSA (4.7)(YON, 1972) has been reported to be around -7.0 mV (BÖHME; SCHELER, 2007). Thus, the ionic interactions between the carboxyl groups on the GNF surface with charged groups in the BSA molecules might have counteracted the swelling of the hydrogel structure resulting in decreased liquid absorption. Similarly, Kon, Oeda and Nakamura (2013) reported a reduction of the swelling degree due to the repulsive electrostatic interactions between the BSA molecules and the hydrogel which had carboxylate anions as the predominant charged species.

The structural integrity of the hydrogels was evaluated as weight remaining after immersing the samples either in BSA or PBS solution (Table 4.2 and 4.3, Supplementary data section). Within the 40 days, the wet weight remained constant for all the hydrogels indicating no material loss in either incubation conditions. It is noteworthy that the hydrogels maintained their structural integrity for long period of time. Water retention capacity reflects the ability of a dressing material to hold water molecules within its structure, which may be important for keeping the wound moist. The water retention capacity of T-GNF ($16 \pm 3.6\%$) and AT 4%-GNF ($12 \pm 3.3\%$) hydrogels were comparable, after exposure to air, at room temperature for 24 h (Figure 4.10, Supplementary data section).

Since the T-GNF hydrogel showed higher liquid absorption capacities, the influence of the hydrogel grammage on the water absorption was also investigated and presented in Figure 4.3.

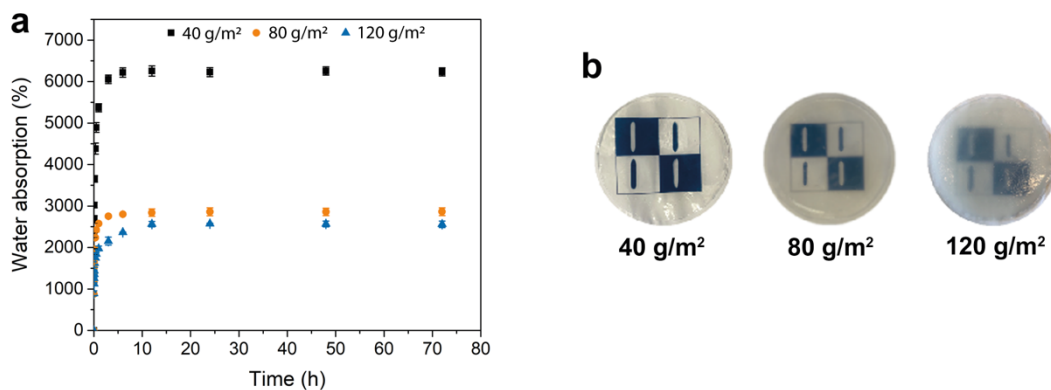


Figure 4.3. a) Water absorption as a function of time for T-GNF hydrogels at different grammages. b) Photographs of the T-GNF hydrogels at different grammages after the equilibrium swelling degree was reached.

From Figure 4.3, it is noted that the highest swelling degree was reached by the hydrogel with the lowest grammage (40 g/m^2). The increase in the grammage led to a significant decrease of the swelling. This behavior can be due to a higher degree of nanofibers which favors the formation of connected points and, in turn, increases the rigidity of the network and reduces the swelling capacity. It should be noted that controlling the hydrogel grammage could be another approach to adjust the liquid absorption capacity.

Comparing the hydrogels with different grammages (Figure 4.3-b), it is possible to observe that the transparency was reduced as the grammage increased. Thus, besides the highest swelling degree, the hydrogel produced with T-GNF at 40 g/m^2 presented good transparency, which is advantageous for dressing materials as it allows monitoring of the wound during the healing process (Figure 4.11, Supplementary data section).

The morphology of the hydrogels produced with T-GNFs and AT 4%-GNFs at a low swelling degree (800%) and after they reached the equilibrium swelling degree in water was investigated with SEM and presented in Figure 4.4.

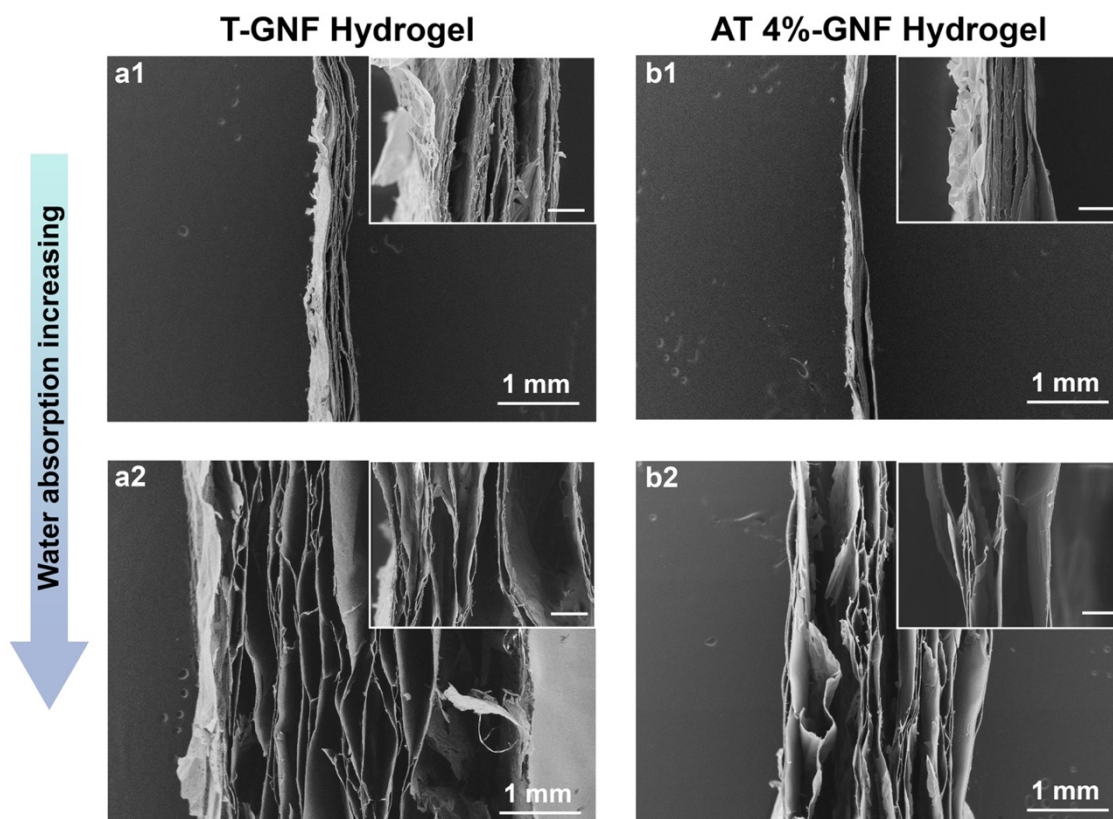


Figure 4.4. SEM images of ginger nanofiber hydrogels of 120 g/m^2 showing the swelling mechanism due to the water absorption. a1) T-GNF and b1) AT 4%-GNF at 800% of swelling degree; a2) T-GNF and b2) AT 4%-GNF at equilibrium swelling degree. Scale bar, inset: $100 \mu\text{m}$.

The cross-sections of both GNF hydrogels displayed a layer like structure after vacuum-assisted filtration assembly (Figure 4.4). The layered networks are formed as the water evaporates *via* fiber–fiber bonding due to secondary attraction forces, including hydrogen bonds, that develops between the nanofibers (OKSMAN *et al.*, 2016). This layered nanofiber network structure has been documented by other studies in the literature (BENSELFELT; ENGSTRÖM; WÅGBERG, 2018; BENSELFELT; WÅGBERG, 2019; BERGLUND *et al.*, 2017; JONOBI; MATHEW; OKSMAN, 2012; ZHAO *et al.*, 2018). Comparing the different conditions shown in Figure 4.4 it is possible to observe the swelling mechanism in which the layers have become more spaced with increasing water absorption. Additionally, it can be noted that the T-GNF hydrogel (Figure 4.4-a2) is thicker than the AT 4%-GNF hydrogel (Figure 4.4-b2) at the same swelling degrees which corroborate the higher liquid absorption capacity of the former.

4.4.3 Mechanical properties

The mechanical properties of the hydrogels and representative tensile and compressive stress–strain curves are displayed in Figure 4.5 and in Table 4.4 (Supplementary data section). The initial linear region of the stress-strain curves used to calculate the compressive modulus is available in Figure 4.12 (Supplementary data section). From Figure 4.5 it can be noted that the T-GNF hydrogel exhibited better compressive properties displaying a compressive modulus of 77.5 ± 3.6 kPa which is more than two times the value found for the AT 4%-GNF hydrogel (33.7 ± 4.7 kPa). It has been demonstrated that hemicellulose facilitates the nanofibrillation of wood and contributes to enhanced stiffness and strength of composites (IWAMOTO; ABE; YANO, 2008). Even though the length of nanofibers cannot be determined from AFM images, due to entanglements, the T-GNFs (Figure 4.1-c2) appears to have been isolated with a preserved length that allows increased interconnectivity compared to AT 4%-GNFs (Figure 4.1-d2) which showed shorter nanofibers. Longer nanofibers with high aspect ratio results in more entanglements and contact points, leading to stronger networks (JONOBI; MATHEW; OKSMAN, 2012). Tensile properties such as the strength and strain to failure, are important for wound dressings as the material should not break during the fixation process, wearing or removal (HAKKARAINEN *et al.*, 2016).

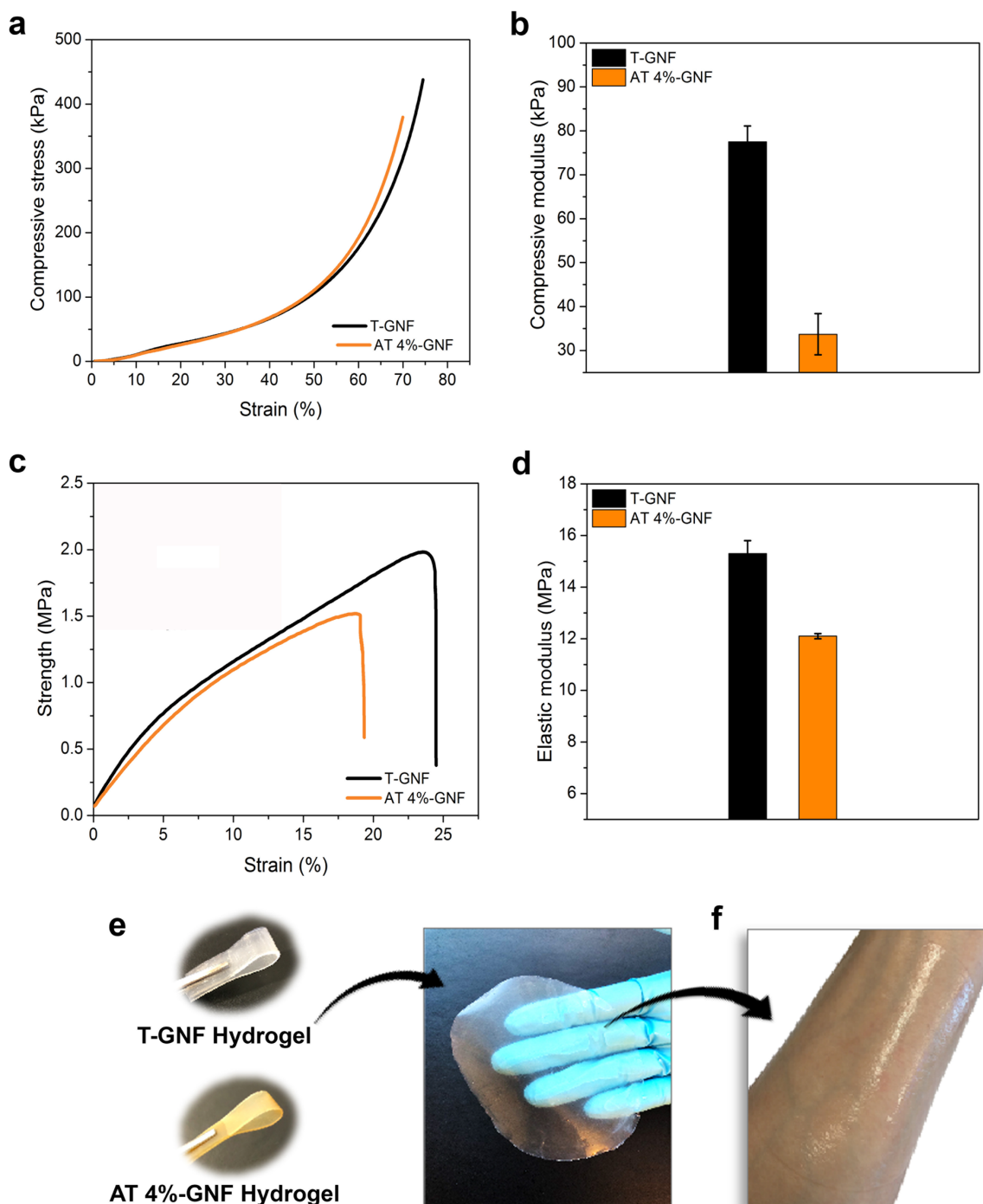


Figure 4.5. Mechanical properties and hydrogel appearance a) representative compressive stress-strain curves and b) the compressive modulus of the GNF hydrogels at 40 g/m^2 determined in wet conditions c) representative tensile stress-strain curves and d) tensile properties of the GNF hydrogels at 40 g/m^2 determined in wet conditions e) photographs of the T-GNF and AT 4%-GNF hydrogels and f) application of the T-GNF hydrogel on a forearm.

From Figure 4.5-c and d, The T-GNF hydrogel exhibited excellent mechanical

performance with a tensile strength of 2.1 ± 0.2 MPa and an elastic modulus of 15.3 ± 0.3 MPa, compared to AT 4%-GNF hydrogel with a tensile strength of 1.6 ± 0.1 MPa and an elastic modulus of 12.1 ± 0.1 MPa. Sun *et al.* (2017) reported elastic modulus in the range of 0.4 to 3.0 MPa and tensile strength less than 0.25 MPa measured in wet conditions of the TEMPO-oxidized cellulose nanofibers films obtained by solvent casting. These values were lower than what we show for GNF and the difference might be associated with the method used for cellulose nanofibers processing which affects the properties (e.g., mechanical, optical) of the resulting materials (WANG *et al.*, 2019). Studies in the literature comparing the effects of different processes such as casting and filtration on the mechanical properties, have reported that the filtration technique leads to mechanically stronger nanofiber network relative to the casting method (DU *et al.*, 2019; QING *et al.*, 2015; SEHAQUI *et al.*, 2010). According to Sehaqui *et al.* (2010) the network properties are very sensitive to nanofiber orientation, and the higher modulus and tensile strength are likely attributed to the increased in-plane orientation of nanofibers.

Moreover, the elastic modulus of skin reported in the literature varies considerably depending on the type and conditions of the mechanical test and for the tensile test it ranges from 4.6 MPa and 20 MPa (PAILLER-MATTEI; BEC; ZAHOUANI, 2008). Since the values reported here are within this range, hydrogels possess potential for wound dressing applications. Additionally, the hydrogels presented good flexibility (Figure 4.5-e), and shape retention and was gently pliant to the skin (Figure 4.5-f).

4.4.4 Hydrogels antibacterial effects

The results related to the hydrogels antibacterial activity were analyzed and discussed by Dr. Hazem Khalaf and collaborates from the School of Medical Sciences laboratory (Örebro University, Sweden).

To evaluate the antibacterial activity of hydrogels, microbiological assays were performed against gram-positive *Staphylococcus aureus* and gram-negative *Escherichia coli* (Figure 4.6), overview images and zone of inhibition are provided in Figure 4.13, Supplementary data section.

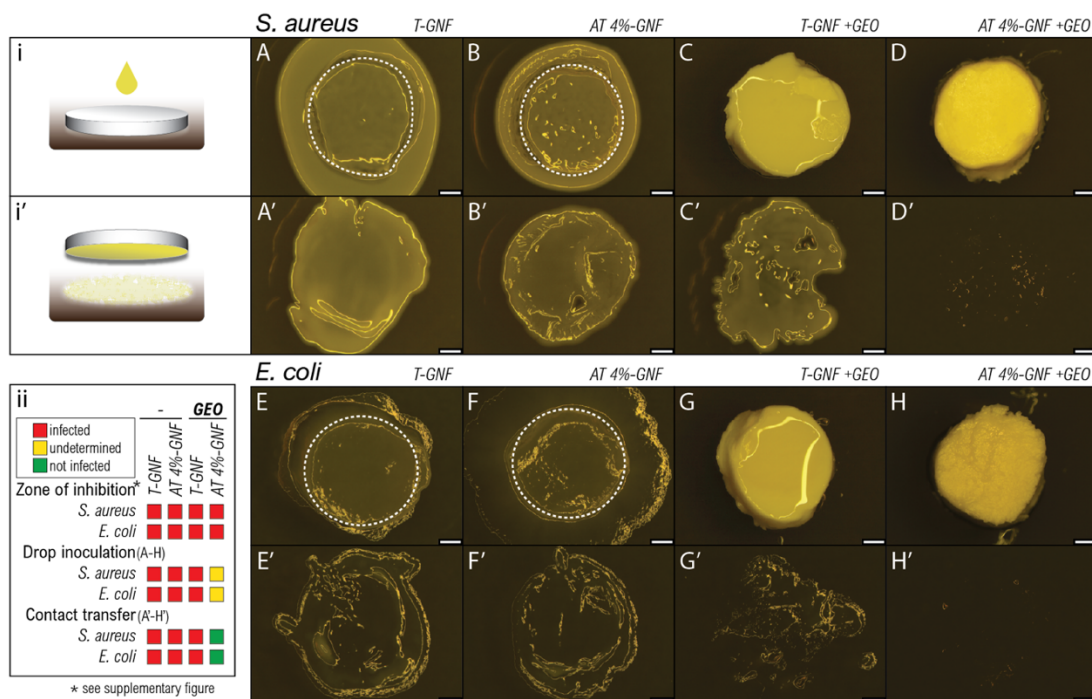


Figure 4.6. Images from microbiological assays against *S. aureus* and *E. coli* for T-GNF and AT 4%-GNF hydrogels before and after functionalization with ginger essential oil (GEO). Method sketches of (i) drop inoculation of hydrogels (upper rows: A-H), and (i') subsequent contact-dependent transfer of microbes to fresh agar (lower rows: A'-H'). (A-D) *S. aureus* infected hydrogels, (A'-D') contact transfer of *S. aureus*; (E-H) *E. coli* infected hydrogels, (E'-H') contact transfer of *E. coli*. Panel (ii) shows summary of antimicrobial results. *zone of inhibition assay is shown in Supporting Information section. Dashed lines approximate area of hydrogel beneath bacterial colony; scale bars show 1 mm.

Ginger essential oil (GEO) was chosen to functionalize the hydrogels since it has been reported to have antimicrobial activity (SINGH *et al.*, 2008). Before and after functionalization, no clear zone of inhibition could be observed for T-GNF and AT 4%-GNF hydrogels (Figure 4.13) indicating no measurable inhibitory activity against *S. aureus*, and *E. coli*.

In contrast, Abrial *et al.* (2020a) and Jacob *et al.* (2018) reported good antimicrobial performance of ginger nanofibers films against different bacteria species. There are many factors affecting the antibacterial activity of ginger such as processing methods, type of microorganisms (ABRAL; ARIKSA; MAHARDIKA; HANDAYANI; AMINAH; SANDRAWATI; PRATAMA; *et al.*, 2020), and/or raw material storage conditions (GHASEMZADEH; JAAFAR; RAHMAT, 2016). Plausible reasons for the

loss of antibacterial activity of the ginger nanofiber hydrogels in this study could be differences in nanofiber production methods or the use of raw material stored for longer time period as ginger is not growing in Sweden, compared to previously reported studies (JACOB *et al.*, 2018; SANG *et al.*, 2020). Bacterial growth could not be determined after drop inoculation of hydrogels (Figure 4.6 A-H). However, the subsequent contact-dependent transfer of microbes to fresh agar (Figure 4.6 A'-H') revealed a bactericidal effect after GEO functionalization, indicated by the absence of bacterial growth for AT 4%-GNF (Figure 4.6 D' and H'), compared to the bacterial growth pattern found in the other materials (Figure 4.6 A'-C' and E'-G').

The variation in chemical composition of the hydrogels might explain their different antibacterial activity. Overall, the GEO appears to contribute to antimicrobial hydrogels, hindering bacterial growth on the hydrogels, without releasing active antimicrobial substances under these conditions.

Infected wounds are commonly treated with antibiotics, and the rising problem of antibiotic resistance is alarming. The use of completely bio-based resources may be a safer way to obtain advanced wound dressing material with antimicrobial properties while minimizing cytotoxic side effects (CHEN *et al.*, 2017; MI *et al.*, 2018; WEISHAUP *et al.*, 2020). The use of GEO for antimicrobial activity enhancement of completely ginger-based hydrogels demonstrates the potential to utilize multiple intrinsic properties of a raw material to develop functional materials.

4.4.5 *In vitro* cytocompatibility study

The results related to the cytocompatibility study were analyzed and discussed by Kristina Hanna, Dr. Jonathan Rakar, Dr. Johan Junker and collaborates from the Center for Disaster Medicine and Traumatology laboratory (Linköping, Sweden).

The potential use of the GNF hydrogels for wound dressing application requires initial assessment of cytocompatibility. Since wound healing is primarily executed by the proliferation and migration of keratinocytes and fibroblasts, the migratory and proliferative behavior of primary keratinocytes and fibroblasts from human abdominal skin were separately evaluated in the presence of the T-GNF and AT 4%-GNF hydrogels by culturing them in direct contact with the two GNF hydrogels. Initial tests where cells were seeded on top of the hydrogels revealed a low degree of adhesion with no increase in cell numbers over time (Figure 4.14, Supplementary data section). This finding indicates that the hydrogels are unsuitable for use as cell-loaded scaffold material, but

suggest desirable properties for dressing applications, where incorporation of tissue from the healing wound may cause difficulties in dressing changes. A proliferation and viability assay where viable cells were counted over time, and a migration assay (scratch wound repopulation) were employed for the analysis of the cell cultures and the results are presented in Figure 4.7.

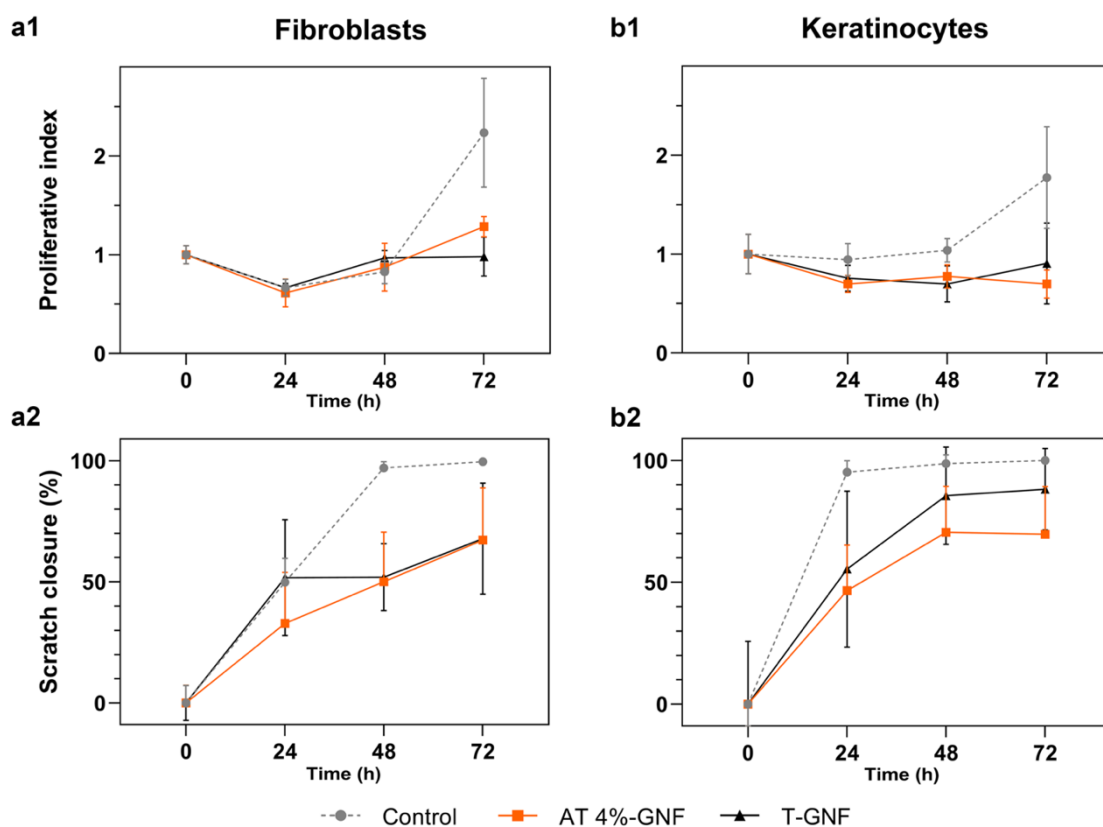


Figure 4.7. Effects of T-GNF and AT 4%-GNF hydrogels on: fibroblast a1) proliferation and a2) migration; keratinocytes b1) proliferation and b2) migration. n=4.

The proliferative index of keratinocytes and fibroblasts over time is shown in Figure 4.7 (a1, b1). The interpretation of the statistical analysis revealed that both time (49%, $p < 0.0001$) and treatment (7.8%, $p < 0.05$) significantly contribute to the total variation of the proliferative index. Neither T-GNF nor AT 4%-GNF hydrogels affected fibroblast or keratinocyte proliferation before the 72 h time point. Proliferation of fibroblasts was significantly impaired after 72 h (Figure 4.7-a1; $p < 0.05$), with a proliferative index of 0.98 ± 0.20 for T-GNF, 1.28 ± 0.10 for AT 4%-GNF and 2.23 ± 0.55 for control. Proliferation of keratinocytes was significantly impaired after 72 h (Figure 4.7-b1; $p < 0.05$), with a proliferative index of 0.91 ± 0.41 for T-GNF, $0.70 \pm$

0.14 for AT 4%-GNF and 1.77 ± 0.51 for control (Figure 4.7-a1).

The migration of fibroblasts and keratinocytes over time is shown in Figure 4.7 (a2, b2). Overall, significant differences were seen along both time and treatment ($p < 0.0001$). For fibroblasts, the scratch closure of the T-GNF group was significantly lower compared to control at 48 h ($52 \pm 14\%$ vs. $97 \pm 2.6\%$, $p < 0.005$). The AT 4%-GNF group was significantly reduced at 48 h ($50 \pm 20\%$ vs. $97 \pm 2.6\%$, $p < 0.001$) and 72 h ($67 \pm 22\%$ vs. $100 \pm 0.9\%$, $p < 0.05$).

For keratinocytes, the scratch closure for the T-GNF group was significantly reduced at 24 h ($55 \pm 32\%$ vs. $95 \pm 4.8\%$, $p < 0.005$) and 72 h (88 ± 17 vs. $100 \pm 0\%$, $p < 0.05$). For AT 4%-GNF, the scratch closure was significantly reduced at 24 h ($47 \pm 19\%$ vs. $95 \pm 4.8\%$, $p < 0.0001$), 48 h ($71 \pm 19\%$ vs. $99 \pm 3.6\%$, $p < 0.001$), and 72 h ($70 \pm 20\%$ vs. $100 \pm 0\%$, $p < 0.001$).

The method of placing the GNF hydrogels on top of the cells can itself interfere with normal culture conditions (PUSNIK *et al.*, 2016). The added barrier created by the GNF may interfere with the oxygen diffusion rate and the turn-over of soluble factors near the cells. In an *in vivo* situation, the skin is fed by nutrients from the vascularized underlying tissue but the *in vitro* model is limited by free diffusion of oxygen through, and soluble factors added into, the culture medium. This may explain some diminished migration and proliferation, and help explain some of the limits to scratch closure in the migration assay. In light of these results, the control group without hydrogels can be considered evidence of a viable and healthy primary cell population, but comparisons between results with and without hydrogels should be carefully employed. More interesting are any differences between the GNF hydrogels, and the overall viability and migratory capacity of the cells.

Overall, the GNF hydrogels did not display cytotoxicity (Figure 4.7; Figure 4.15 and 4.16 Supplementary data section). However, proliferation and migration of keratinocytes and fibroblasts were not increased, instead the covering of cultured resulted in somewhat decreased cell numbers. Wound healing is a complex process, and further evaluation both *in vitro* and *in vivo* would be imperative in future work to establish the suitability of GNF hydrogels as wound dressings and better understand the effects of T-GNF and AT 4%-GNF hydrogels on healing.

4.4.6 Conclusions

Hydrogels based on nanofibers extracted from ginger residue were successfully prepared via vacuum assisted filtration without any crosslinker and with advantageous properties for wound dressing applications. It was shown that the liquid absorption capacity of the hydrogels could be adjusted by altering the chemical composition of ginger fibers with alkali treatment prior to nanofiber isolation and subsequent hydrogel formation. Furthermore, the grammage of the hydrogels was shown to dictate the absorption capacity. The hydrogel produced with ginger without alkali treatment (T-GNF hydrogel) of 40 g/m² showed the highest water absorption of 62 times greater than its initial weight and reaching a value that was 5 times higher than the one obtained with the reference wood nanofiber hydrogel. The high swelling capacity was achieved by preserving the non-cellulosic components such as starch and hemicellulose naturally found in ginger when preparing the nanofibers and their hydrogels. Additionally, the T-GNF hydrogels showed good mechanical properties, with tensile strength of 2.1 ± 0.2 MPa and elastic modulus of 15.3 ± 0.3 MPa, respectively. The antimicrobial activity of ginger was not preserved after nanofiber separation, as observed from microbiological assays. However, functionalization using ginger essential oil improved antimicrobial performance against *S. aureus* and *E. coli*, and the absence of bacterial growth suggest that AT 4%-GNF hydrogel was bactericidal. However, additional experiments are needed to better understand and optimize the functionalization of ginger nanofiber hydrogels using essential oil. Cytocompatibility evaluation showed that T-GNF and AT 4%-GNF hydrogels did not significantly affect fibroblast proliferation. Meanwhile, the migration of keratinocytes was more beneficial in contact with the T-GNF hydrogel than the AT 4%-GNF.

The current study highlights an up-scalable environmentally friendly way to prepare completely ginger-based nanofiber hydrogels that combine functions attractive for wound dressing, such as tunable absorption, flexibility, and transparency, while being non-toxic and mechanically stable in moist conditions. Moreover, potential additional functionalization could further be explored with the aim at improving wound healing.

4.5 Supplementary data

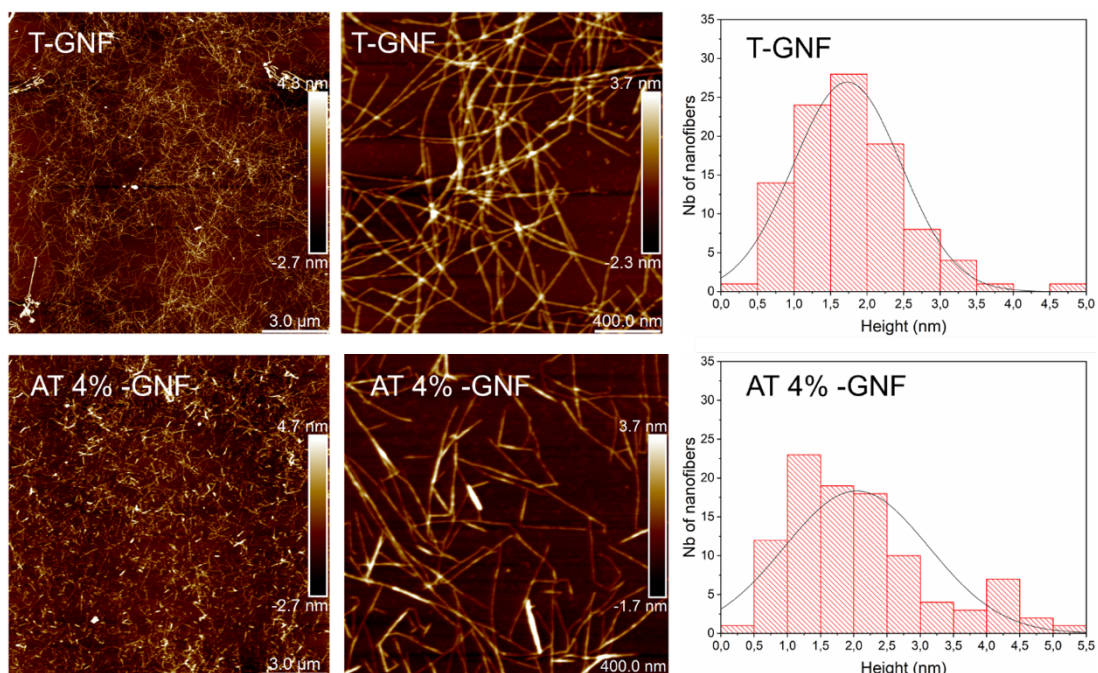


Figure 4.8. AFM height images and size distribution of the T-GNF and AT 4% -GNF, respectively.

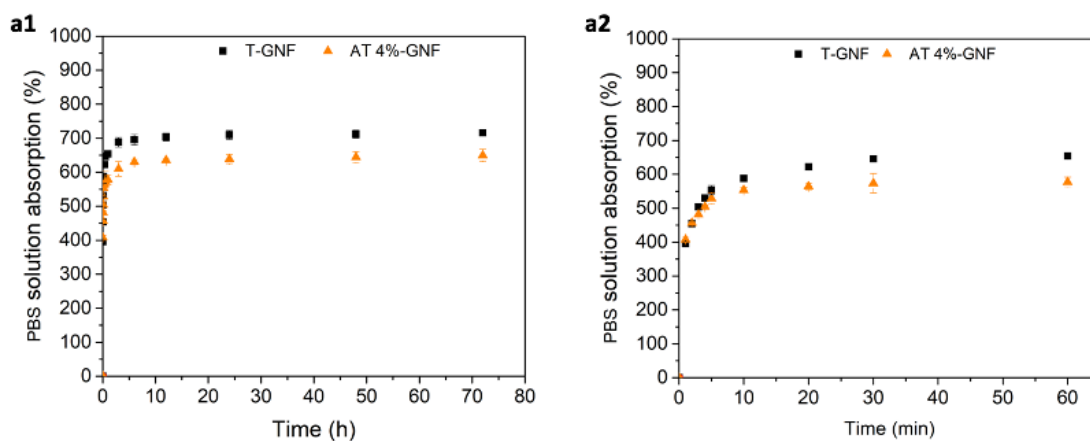


Figure 4.9. Liquid absorption of the hydrogels (40 g/m^2) in PBS solution. a2) Expanded curves (first hour) of the liquid absorption of hydrogels in PBS solution.

Table 4.2. Hydrogel integrity in BSA solution

Hydrogel	Days					
	1	5	10	15	20	40
T-GNF (%)	100	100.4 ± 0.8	101.7 ± 2.2	100.6 ± 3.4	102.1 ± 3.5	100.1 ± 0.7
4% AT-GNF (%)	100	102.4 ± 0.8	105.7 ± 4.6	112.1 ± 1.4	103.4 ± 1.9	102.2 ± 2.5

Table 4.3. Hydrogel integrity in PBS solution.

Hydrogel	Days					
	1	5	10	15	20	40
T-GNF (%)	100	100.7 ± 1.8	101.0 ± 0.7	100.5 ± 1.4	100.2 ± 0.4	100.7 ± 0.7
4% AT-GNF (%)	100	100.3 ± 1.0	100.6 ± 0.7	100.6 ± 0.7	100.3 ± 1.3	100.9 ± 0.5

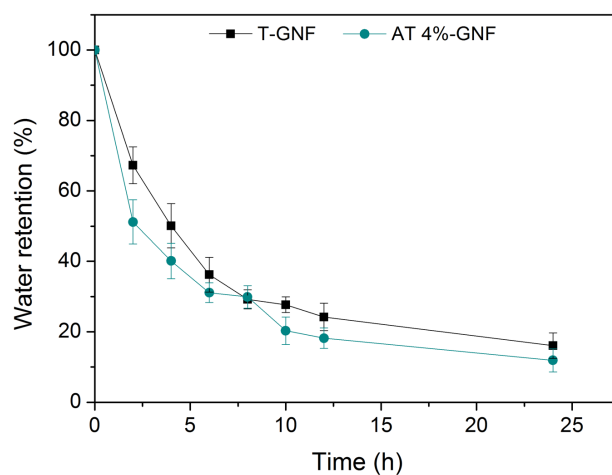
Figure 4.10. Water retention capacity of T-GNF and AT 4%-GNF hydrogels (40 g/m²).



Figure 4.11. Photographs of the T-GNF hydrogels at 40 g/m² after reaching the equilibrium state.

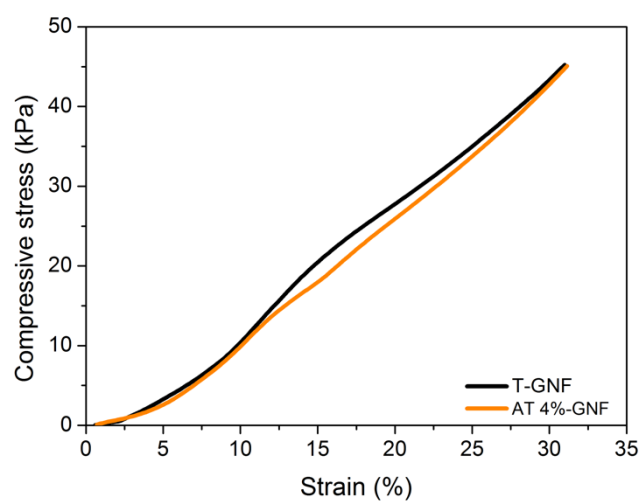


Figure 4.12. The representative compressive stress–strain curves enlarged at 30% strain.

Table 4.4. Mechanical properties of the hydrogels.

Hydrogel	Compressive Modulus (kPa)	Compressive strength (kPa)	E-modulus (MPa)	Tensile strength (MPa)	Elongation at break (%)
T-GNF	77.2 (1.6) ^a	445.9 (2.1) ^a	15.3 (0.5) ^a	2.1 (0.2) ^a	25.1 (1.4) ^a
AT 4%-GNF	33.7 (4.7) ^b	210.5 (5.6) ^b	12.1 (0.1) ^b	1.6 (0.1) ^b	17.8 (1.0) ^b

*Average values with different superscript letters in the same column are significantly different at 5% significance level ($p < 0.05$) based on ANOVA test. Results are expressed as the average value (Standard Deviation).

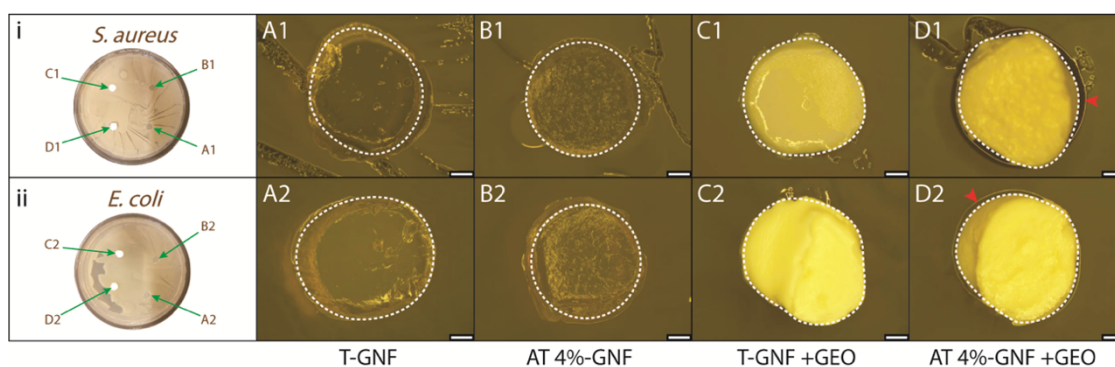


Figure 4.13. Overview images from microbiological assay for inhibition zones. Top row: i/1) *S. aureus* and bottom row ii/2) *E. coli*. A) T-GNF, B) AT 4%-GNF, C) T-GNF after functionalized with ginger essential oil (GEO), D) AT 4%-GNF with GEO. Red arrowheads indicate potential zone of inhibition. Dashed lines approximate hydrogel perimeters. Magnification 12.5x. (Scale bar: 1 mm).

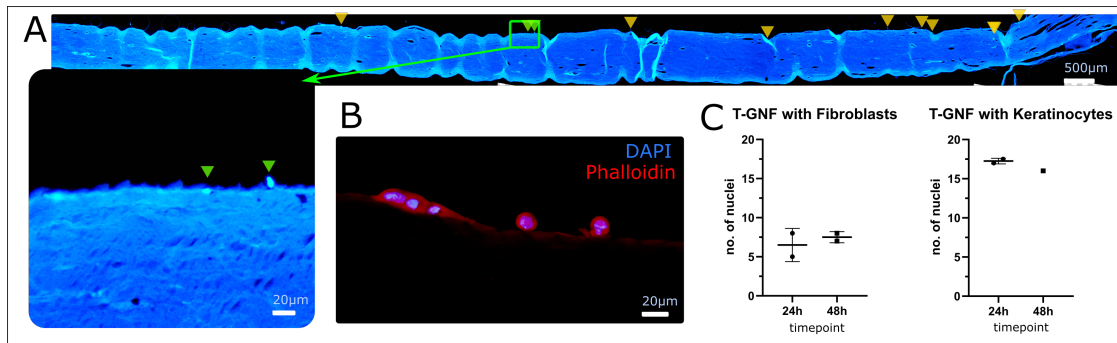


Figure 4.14. Investigation of cell attachment to the T-GNF hydrogel. A) acquired stitch at 10x magnification under UV-excitation along paraffin sectioned T-GNF hydrogel ($\sim 7 \mu\text{m}$ thick) with DAPI-labeled cells – inset: enlargement showing example of nuclei on the hydrogel surface (green arrowheads). B) Cells (keratinocytes shown) were labeled with DAPI and ALEXA546-conjugated Phalloidin. C) duplicate samples of fibroblasts and keratinocytes on T-GNF were quantified. Arrowheads indicate DAPI-stained nuclei.

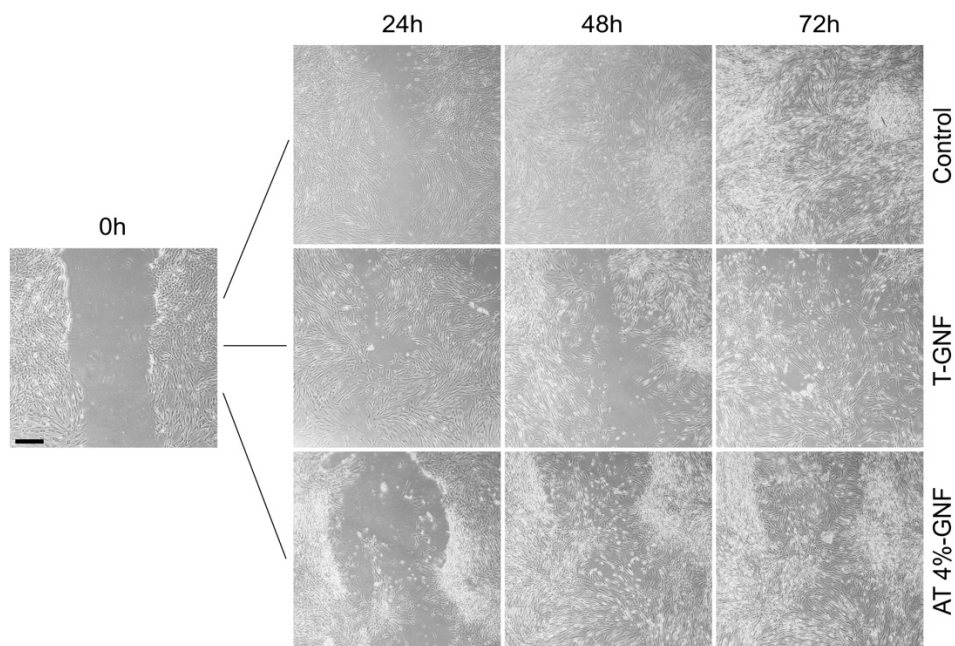


Figure 4.15. Images from scratch assay showing migration of fibroblasts at different time points. Scale bar corresponds to $\sim 100 \mu\text{m}$.

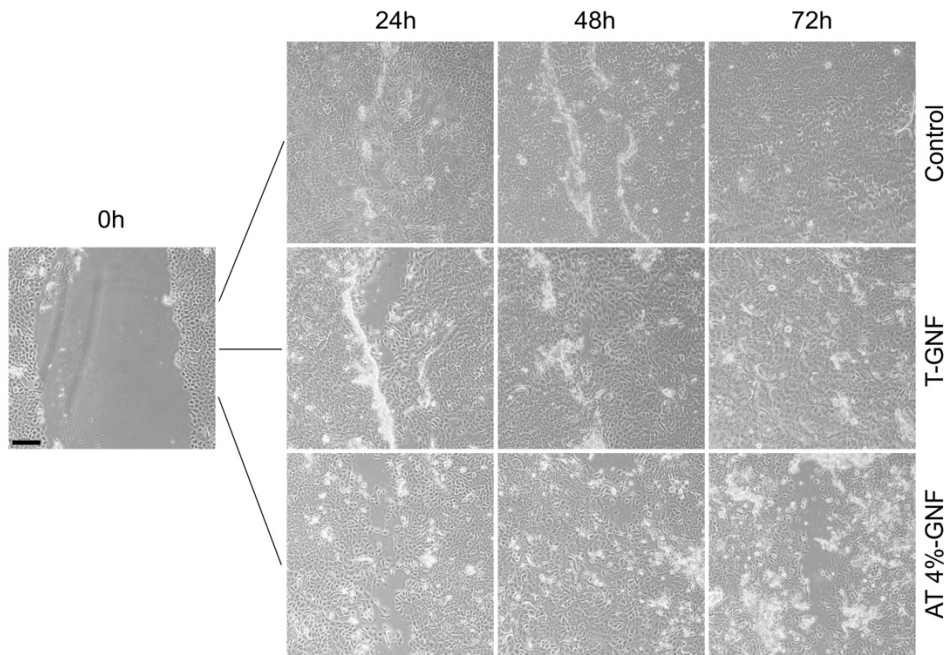
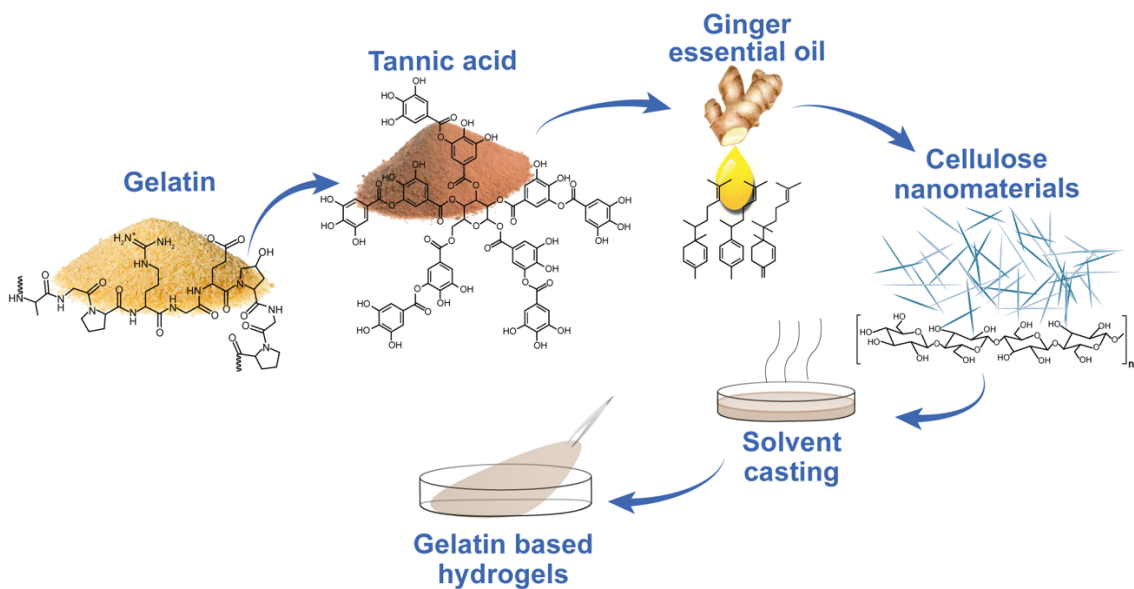


Figure 4.16. Images from scratch assay showing migration of keratinocytes at different time points. Scale bar corresponds to $\sim 50\mu\text{m}$.

Chapter 5

Comparison of cellulose nanomaterials produced with commercial and non-commercial enzymes and their application in gelatin-based hydrogels



5.1 Abstract

This chapter is focused on the comparison between cellulose nanomaterials produced by non-commercial and commercial enzymes and their application in the preparation of gelatin-based hydrogels. Cellulose nanomaterials (C-CNs) were obtained through 96 h of enzymatic hydrolysis using commercial enzymes of ball-milled cellulose pulp, followed by sonication (5 min). C-CNs presented a high crystallinity index ($\sim 73.2\%$), zeta potential of -23.8 ± 0.8 mV with initial thermal degradation temperature of ~ 203.0 °C and a production yield of $19.9 \pm 0.3\%$. The hydrogels were prepared by solvent casting using tannic acid as a cross-linking agent and ginger essential oil as a component to improve the antimicrobial activity. Tannic acid addition contributed to increasing the structural integrity of the hydrogels, but it was not enough to avoid their dissolution after 72 h submerged in water. Cellulose nanocrystal produced with non-commercial enzymes (NC-CNs) contributed better than their counterparts (NC-CNs) to the hydrogels structural integrity, maintaining it for more than two weeks. The hydrogels inhibited of growth *S. aureus* and *E. coli* mainly owing to the incorporation of tannic acid and ginger essential oil. However, it was not possible to quantify the individual contribution of each component to the antimicrobial activity. Although additional studies to better understand the interactions of the NC-CNs to the hydrogel network and further hydrogel characterizations are needed, this chapter presented a process with less environmental impact to prepare hydrogels with promising properties as part of an integrated biorefinery approach.

5.2 Introduction

In the last decades, the use of renewable and sustainable materials, such as biomass, has become immensely important for producing high-value products with low environmental impact to replace petroleum-based products. The biorefinery concept is attracting scientific, industrial and policy attention as a promising alternative for producing chemicals, biofuels, energy and high value-added products from biomass along with a reduction of the dependency on non-renewable feedstocks and environmental impacts (RABAÇAL *et al.*, 2017). Furthermore, multiple end products, for instance, pigments, biopolymers, acids, biosurfactants, could be obtained through integrated processes, which enables the biomass usage maximization in the biorefinery (LEE *et al.*, 2019).

Among the high value-added products, nanocellulose has been considered as an useful class of futuristic materials due to its physicochemical properties including low density, chemical inertness, high strength, excellent stiffness, low coefficient of thermal expansion, dimensional stability, ability to modify its surface chemistry, among others (FARINAS; MARCONCINI; MATTOSO, 2018; TRACHE *et al.*, 2020). Moreover, these cellulose nanomaterials can be used in different fields, such as nanocomposites and hydrogels as reinforcement agent, antimicrobial films and hydrogels, biomedical products, adhesives, supercapacitors, templates for electronic components, batteries, catalytic supports, electroactive polymers, food coatings, barrier/separation membranes, paper-making products, cosmetic, cements and many other applications (DHALI *et al.*, 2021; MOON; SCHUENEMAN; SIMONSEN, 2016; THOMAS *et al.*, 2018).

The increasing demand and the employment of new applications have encouraged academic researchers and the industry to exploit more uses of nanocellulose. Studies have been reporting the technical feasibility (BONDANCIA *et al.*, 2017; CAMARGO *et al.*, 2016; DE AGUIAR *et al.*, 2020; WANG, J *et al.*, 2021; ZHU; SABO; LUO, 2011) and economic advantages (DE ASSIS *et al.*, 2017; LEISTRITZ *et al.*, 2006; SONG *et al.*, 2014) of producing nanocellulose in the context of biorefinery. However, based on the articles found and analyzed in the systematic mapping presented in chapter 2, the evaluation of the application of cellulose nanomaterials produced in the context of biorefinery as a reinforcing agent of hydrogels has not been reported yet.

Hydrogels are three-dimensional network structures prepared with natural or synthetic polymers that can absorb and retain a significant amount of water without dissolving or losing their structural integrity (PEPPAS; MIKOS, 2019; SOOD *et al.*, 2016). The three-dimensional polymeric chain of hydrogels can be composed of hydrophilic homo- or heteropolymers. Crosslinkers (also known as tie-points or junctions) can be physical entanglements, covalent bonds or non-covalent interactions and they are mainly responsible for preventing the dissolution of hydrogels in water (BYRNE; SALIAN, 2008). Considering the cross-linking agents, hydrogels can be classified into chemical (or permanent) and physical (or temporary). In the first case, the crosslinking is derived from chemical reactions generally using a cross-linking agent leading to the formation of covalent bonds between the macromolecules. On the other hand, in physical crosslinkers, only intra or intermolecular physical interactions occur, such as, van der Waals forces (BUWALDA *et al.*, 2014). The hydrophilicity of hydrogels is due to the presence of hydrophilic groups -OH, -COOH, -CONH₂, -SO₃H, usually

present in its structure (AHMED, 2015). Hydrogels can be formed by natural polymers such as cellulose, gelatin, agar, hyaluronic acid, alginate, chitosan, among other examples, and synthetic polymers poly (ethylene glycol), poly (acrylic acid), polyacrylamide, poly (vinyl alcohol) and poly (N-isopropylacrylamide) and its copolymers (FU *et al.*, 2019).

Gelatin is a purified protein obtained from hydrolysis of collagen with high molecular weight. Because of its gelling, biocompatibility and thickening properties, gelatin has been widely used in food (dietary supplements and confectionaries), cosmetics (lotions, face-masks, and creams) and pharmaceutical products (capsule shells), medicine, and other fields (ROHMAN *et al.*, 2020). However, pure gelatin films and hydrogels present low mechanical strength, high degradability and strong hygroscopicity, hindering their applications. Two strategies that could be used to circumvent these limitations are the use of cellulose nanomaterials and tannic acid as reinforcement and cross-linking agents, respectively.

Tannic acid (TA) is a low-cost plant-derive polyphenol which can provide strong cohesiveness in the bulk of materials and strong adhesiveness to different substrates as it possesses several pyrogallol/catechol groups and dendritic structures. Additionally, it can offer several binding sites suitable for different types of interactions, such as hydrogen bonding, ionic and hydrophobic interactions (FAN; WANG; FENG; *et al.*, 2017; FAN; WANG; ZHANG; *et al.*, 2017; SHUTAVA *et al.*, 2005). Moreover, tannic acid is affirmed as Generally Recognized as Safe by Food and Drug Administrator and it is known by its attractive biological functions including antibacterial and astringent properties (BOŽIČ; GORGIEVA; KOKOL, 2012). Tannic acid has been used for preparing films and hydrogels in several studies (HEIDARIAN *et al.*, 2020; HU *et al.*, 2017; LEITE *et al.*, 2021; TAHERI *et al.*, 2020; WANG *et al.*, 2020).

The ginger essential oil (GEO) is mainly compost of geranial, α -zingiberene, (E,E)- α -farnesene, neral and ar-curcumene has also been reported to have significant antimicrobial and antioxidant activities (EL-BAROTY *et al.*, 2010; SINGH *et al.*, 2008). Bio-based materials with relevant properties including antibacterial activity, biodegradability combined with low toxicity and costs have promising application prospective in different fields, such as medical material, food, textile, chemical engineering and environmental protection (LIU *et al.*, 2019). Amalraj *et al.* (2020) reported that the bacteria growth was significantly inhibited by films containing ginger essential oil. To date, the combined effects between TA and GEO on the hydrogel

properties were not evaluated yet. Therefore, the ginger essential oil was also combined with gelatin and tannic acid to improve the antibacterial properties of the hydrogels.

In the previous study Squinca *et al.* (2020), the feasibility of producing cellulose nanocrystals using non-commercial enzymes was systematically analyzed and their production conditions were optimized. Although cellulose nanomaterials were successfully obtained using non-commercial enzymes showing to be a potential sustainable route that could be applied in future biorefineries, their application was not evaluated. Here, the properties of cellulose nanomaterials produced using non-commercial and commercial enzymatic preparation were compared in terms of yield, crystallinity index, thermal properties and surface charge. After that, cellulose nanomaterials were incorporated into gelatin-based hydrogels preparation in which tannic acid was used as a cross-linking agent and ginger essential oil was evaluated to improve their antimicrobial properties. The hydrogels produced were compared in terms of their water absorption capacity and antimicrobial properties. This study provided a proof of concept related to the application of CNs produced by non-commercial enzymes.

5.3 Materials and Methods

5.3.1 Materials

Eucalyptus cellulose kraft pulp was donated by Suzano Pulp and Paper Company (São Paulo, Brazil). The chemical composition of pulp was $75.6 \pm 2.3\%$ cellulose, $14.6 \pm 0.6\%$ hemicellulose, $6.7 \pm 1.2\%$ lignin, and $1.1 \pm 0.2\%$ ash, as previously determined in the laboratory (BONDANCIA *et al.*, 2017). The particle size of the pulp was reduced to a value smaller than 2 mm, using a 500 W Wiley knife mill (Solab). Cellulose nanocrystals were isolated from eucalyptus pulp by enzymatic hydrolysis using non-commercial enzymes, according to the process conditions that resulted in the highest yield determined by Squinca *et al.* (2020) and which is briefly described in the item 2.2 (SQUINCA *et al.*, 2020). Cellulase from *Aspergillus niger* (Carezyme, C2605), gelatin from bovine skin (type B), glycerol and tannic acid were purchased from Sigma-Aldrich (Brazil) and ginger essential oil from Now foods (Brazil). All chemicals were of analytical grade. *Staphylococcus aureus* (*S. aureus*) ATCC 25923 and *Escherichia coli* (*E. coli*) ATCC 25922 were supplied by Cefar Diagnóstica (Brazil).

5.3.2 Cellulose nanocrystals isolation

The eucalyptus cellulose pulp was mechanically pretreated in a planetary ball mill (model CT-12241, Servitech) at a ball to material weight ratio (BMR) of 12:1 for 90 minutes. The enzymatic hydrolysis reactions were performed using either non-commercial and commercial enzymes reactions at a dosage of 260 IU/g_{substrate} of endoglucanase activity (in both cases). The reactions were conducted at a solids loading of 2% (w/v) of cellulose pulp, 50 °C and 200 rpm for 96 h, using an orbital shaker. Glucose concentration was determined during the reaction using an enzymatic kit for glucose measurement (Glicose Liquiform, Brazil) and cellulose conversion was calculated as well. The reaction was stopped by boiling the suspension at 100 °C for 10 min. In sequence, the solid was separated by centrifuging at 8,000 rpm for 20 min and suspended in deionized water. This washing procedure was repeated to eliminate the released soluble sugars. After this step, the CN suspension was sonicated (Q1375 sonicator, QSonica) at 50% amplitude (1375 W) for 5 minutes. Cellulose nanomaterials produced by non-commercial and commercial enzymes were coded as NC-CNs and C-CNs.

5.3.3 Cellulose conversion

The cellulose conversion into glucose (C_c) was calculated according to the following equation:

$$C_c(\%) = \frac{(m_g^t - m_g^0) \times 0.9}{m_p^0 \times y_c} \times 100 \quad (5.1)$$

where m_g^t is the glucose mass at time t , m_g^0 is the initial glucose mass, m_p^0 is the initial pulp mass, y_c is the percentage of cellulose in the pulp, and 0.9 is the ratio of the molecular weights of anhydroglucan present (162.14 g/mol) and the glucose (180.15 g/mol).

5.3.4 Hydrogel preparation

Hydrogels were prepared following an adapted method described by Leite *et al.* (2021). A given amount of gelatin 8% (w/v) was dissolved Mili-Q water and kept hydrating at 24 °C for 5 min. After that, it was transferred to an oil bath and heated at 60 °C under mechanical stirring for 15 min. Glycerol (20% (w/w) on gelatin) was added under stirring at 60 °C for 5 min. Sequentially, ginger essential oil (10% (w/w) on gelatin)

was added and stirred for 40 minutes at 60 °C. After that, tannic acid solution prepared in Milli-Q water (6% (w/w) on gelatin) was slowly added and stirred for 1 h at 60 °C. Finally, CNCs suspensions (4.0 or 6.0% (w/w) based on gelatin) were added into the solution under constant stirring. After stirring for 1 hour, the hydrogel solution was poured into a Petri dish (90 mm diameter) and dried at 50 °C for 26 h. Pure gelatin, gelatin-TA and gelatin-TA-GEO hydrogels were prepared in the same way for comparison purposes. The samples were named GEL, GEL-TA, GEL-TA-GEO, GEL-TA-GEO-4%C, GEL-TA-GEO-6%C (using CNC produced by commercial enzymes), GEL-TA-GEO-4%NC and GEL-TA-GEO-6%NC (using CNC produced by non-commercial enzymes). It should be mentioned that the amount of gelatin used in the hydrogels preparation was initially determined by evaluating samples prepared following the same method but using only gelatin at different concentrations (4, 5, 6, 7, 8, 9 and 10% (w/v)). Figure 5.1 shows a schematic illustration representing the preparation of the hydrogels.

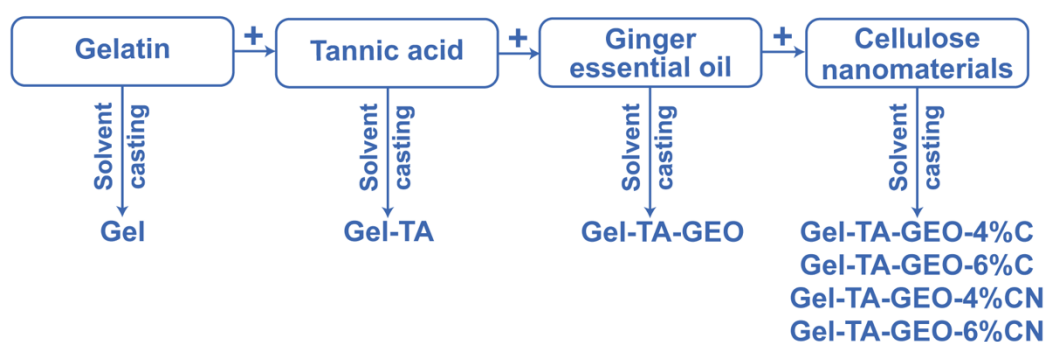


Figure 5.1. Schematic illustration showing the preparation process of the hydrogels.

5.3.5 Cellulose nanomaterials characterization

For comparison purposes, the CNCs obtained using commercial enzymes were characterized as follows.

5.3.5.1 Cellulose nanomaterials yield

The yield of cellulose nanomaterials was determined by drying 3 mL of the sample at 50 °C for 24 h and calculated by the following equation:

$$Y(\%) = \frac{(m_s^f - m_s^i) \times R}{(m_p^0 \times y_c - m_g^f)} \times 100 \quad (5.2)$$

where m_p^0 is the initial pulp mass, m_s^f is the after drying mass, m_s^i is the sample mass before drying, y_c is the percentage of cellulose in the pulp, m_g^f is the glucose mass at the end of hydrolysis reaction and R is the ratio of the total volume used in the hydrolysis reaction and volume of the sample.

5.3.5.2 Zeta potential

The CNCs surface charge was determined by using a Zetasizer (Malvern Instruments Ltd., UK), at room temperature (25 °C), in quadruplicate. Before the measurements, the samples were diluted to 0.025% (w/v) using deionized water

5.3.5.3 X-ray diffraction

The crystallinity index was obtained using a Shimadzu LabX XRD-6000 diffractometer operating at 30 kV and 30 mA with Cu K_α radiation ($\lambda = 0.15428$ nm). Scattered radiation was detected in the 2θ range from 5° to 40°, at a scan rate of 2°/min. The CrI was calculated according to the method of Segal et al. (1959) using the following equation:

$$CI(XRD) = \frac{I_{200} - I_{am}}{I_{200}} \times 100 \quad (5.3)$$

where I_{200} is height for the (200) crystal planes and I_{am} represents the amorphous component.

5.3.5.4 Thermogravimetric analysis

The thermal properties were evaluated using a thermogravimetric analyzer (TGA-Q500, TA Instruments, USA), under an atmosphere of nitrogen at a flow rate of 50 mL/min. Samples of approximately 8 mg were weighed, placed in a platinum pan and heated from 20 to 700 °C, at 10 °C/min.

5.3.6 Hydrogels characterization

5.3.6.1 Water absorption measurement

The dried hydrogels were previously weighted and immersed in distilled water at

room temperature to study the water absorption over time. The wet weight of the hydrogels was recorded at regular intervals. The excess of water was removed by gently tapping the samples on a dry tissue paper before being weighed. The water absorption was calculated as follows:

$$\text{Water absorption (\%)} = \frac{(W_t - W_d)}{W_d} \times 100 \quad (5.4)$$

in which W_d denotes the dried weight of the sample and W_t denotes the weight at time t after immersing samples in water.

5.3.6.2 Antibacterial activity measurement

The antibacterial activity of the hydrogels was assessed by the disk diffusion method using *Staphylococcus aureus* and *Escherichia coli*, as model Gram-positive and Gram-negative bacteria, respectively. The bacteria were cultured in Muller-Hinton Broth medium (MHB) and incubated overnight at 35 °C. The ensuing inoculum of each bacterium and its concentrations were adjusted to 1×10^6 CFU/mL (turbidity = 0.5, McFarland barium sulfate standard). After that, a volume of 100 μ L of the inoculum was spread over solid Muller-Hinton Agar (MHA) Petri dishes. Hydrogel sample disks (10 mm) were placed onto the inoculated Petri dishes and incubated overnight at 35 °C for optimum bacterial growth. The antibacterial activity was investigated by the presence of inhibition zones (colony-free areas) on the film disks.

5.3.7 Analytical methods

Endoglucanase and β -glucosidase activities were determined using carboxymethylcellulose (Sigma, USA) and cellobiose (Sigma, USA), respectively as substrate and according to the standard method proposed by Ghose (1987). Xylanase activity was analyzed following the method described by Bailey and Poutanen (1989), using beechwood xylan (Sigma, USA) as substrate. The reducing sugar concentration was measured by the dinitrosalicylic acid (DNS) method (MILLER, 1959) whereas the glucose released from the β -glucosidase activity measurement was quantified with an enzymatic kit for glucose measurement (Glicose Liquiform, Brazil). All the analyses were measured in triplicate. One unit of endoglucanase, β -glucosidase, or xylanase activity

corresponded to 1 μmol of reducing sugars released per minute of reaction. The total protein concentration was determined as described by Bradford (1976), using bovine serum as a standard.

5.4 Results and discussions

5.4.1 Enzymatic hydrolysis using non-commercial and commercial enzymes

To compare cellulose nanocrystals produced by non-commercial and commercial enzymes, cellulases from *A. niger* (Sigma) were chosen to be used in hydrolysis of eucalyptus cellulose pulp following the methodology described in (SQUINCA *et al.*, 2020). The experimental conditions used were those that had resulted in the highest yield of CNs obtained with non-commercial enzymes. Additionally, it was chosen to offer the same endoglucanase activity since this enzyme is preferably used for nanocellulose extraction (RAHIKAINEN *et al.*, 2019). Firstly, the commercial enzymes were characterized, and their total protein concentration and specific enzymatic activities were compared with the non-commercial enzymes (Table 5.1).

Table 5.1 Total Protein concentration and specific enzymatic activities of non-commercial and commercial enzymes.

Enzymes	Total protein concentration (mg/mL)	Specific activities			Reference
		Endoglucanase (IU/mg)	β -glucosidase (IU/mg)	Xylanase (IU/mg)	
Non-commercial	0.331	17.100	3.66	48.943	Squinca et al. (2020)
Commercial	3.766	101.561	0.004	0.977	This study

Commercial preparation has a protein concentration around 11 times higher than its non-commercial counterpart and a specific endoglucanase activity is also superior (around 6 times higher). These results might be related to the concentration step of the commercial production processes. On the other hand, the specific activities of β -glucosidase e xylanase of the commercial enzymes were lower than the non-commercial ones. In fact, the commercial cellulases used here can be considered an endoglucase-rich preparation.

Considering this work is not focused on the evaluation of the enzymatic hydrolysis

products but providing comparisons with the results reported in Squinca *et al.* (2020), the amount of glucose released during the reaction was determined. Figure 5.2 shows the temporal profile of glucose concentration released and cellulose conversion (inset).

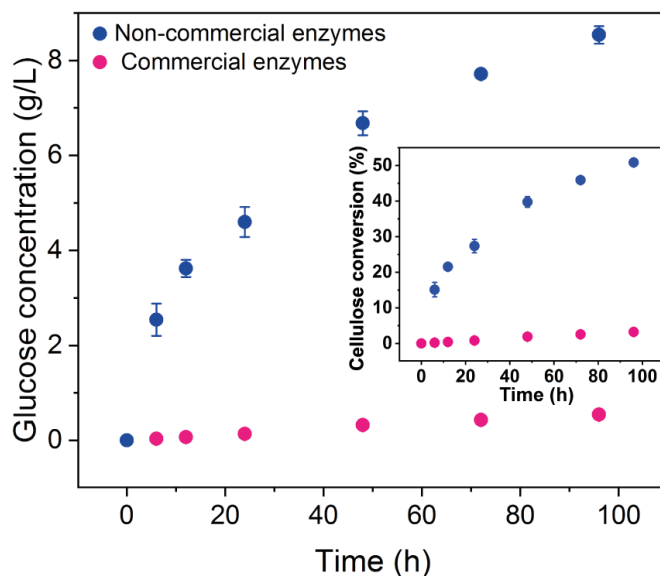


Figure 5.2. Glucose concentration and cellulose conversion (inset) obtained from enzymatic hydrolysis using commercial and non-commercial enzymes. Glucose concentration and cellulose conversion values derived from the reactions using non-commercial enzymes were obtained from Squinca *et al.* (2020) with permission provided by American Chemical Society and Copyright Clearance Center.

Enzymatic hydrolysis performed with non-commercial enzymes resulted in higher final glucose concentrations and cellulose conversion values compared with the commercial enzymes. Although it was offered the same load of endoglucanase, the lower β -glycosidases activity of the commercial preparation resulted in a reduced amount of glucose. Other studies that used endoglucanase-rich enzymes also reported low values of cellulose conversion into glucose (DAI *et al.*, 2018; WANG *et al.*, 2015; ZHU, SABO; CLEMONS, 2014). On the contrary, an enzymatic cocktail composed of all three classes of cellulases results in higher values of cellulose degradation, reaching almost 80% (BONDANCIA *et al.*, 2017). It has been shown that endoglucanases act more selectively on the amorphous regions of cellulose without compromising the crystalline cellulose domains, while the cocktails, especially the commercial ones which were designed to reach high yields of cellulose conversion into monosaccharides, can lead to complete hydrolysis of cellulose into monosaccharides (DAI *et al.*, 2018).

5.4.2 Main properties of cellulose nanomaterials produced by non-commercial and commercial enzymes

Cellulose nanomaterials were obtained from the hydrolysis of eucalyptus cellulose pulp using commercial enzymes as it can be confirmed by the structures in the nanoscale observed in Figure 5.3.

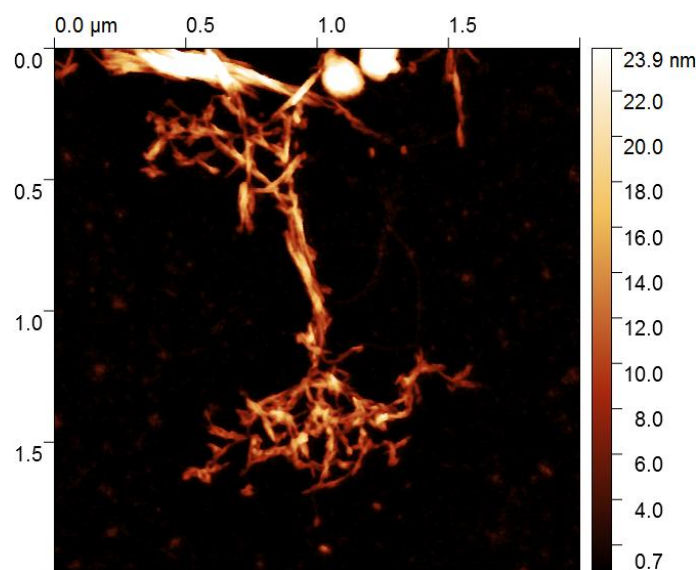


Figure 5.3. AFM images of cellulose nanomaterials produced using commercial enzymes.

Table 5.2 presents the values of yield, crystallinity index, thermal properties, zeta potential of the CNs produced by non-commercial and commercial enzymes.

Table 5.2. Yield, crystallinity index, thermal properties, zeta potential of the CNs produced by non-commercial and commercial enzymes.

Enzymes	Yield (%)	CrI (%)	Zeta potential (mV)	Thermal properties			Reference
				T _{onset} (°C)	T _{máx} (°C)	Residue at 600 °C (%)	
Non-commercial	24.6 ± 0.4	78.3	-18.2 ± 0.6	300.5	347.4	15.2	Squinca et al. (2020)
Commercial	19.9 ± 0.3	73.2	-23.8 ± 0.8	203.0	326.1	10.1	This study

The yield of NC-CN was slightly higher, 24.6% than the value of C-NC (19.9%).

This could be due to higher xylanase specific activity (48.9 IU/mg) in the non-commercial enzymatic cocktail compared to the commercial preparation (0.98 IU/mg) could have favored the extraction of nanocellulose. It has been reported that xylanases can facilitate the initial stage of separating fibrils not only by removing the xylan but also by provoking changes in fiber morphology including the increase of fiber porosity and fiber swelling (LONG *et al.*, 2017; ZHOU; JOHN; ZHU, 2019). Thus, higher xylanase activity might have contributed for the nanocellulose isolation, increasing the yield by improving cellulose accessibility.

The crystallinity index of NC-CNs and C-CNs were 78.3 and 73.2%, respectively. As expected, the values were close since the substrate used in the hydrolysis with non-commercial and commercial enzymes was subjected to the same conditions of ball-milling pretreatment. The zeta potential of C-CN was -23.8 mV which is close to the value CNC (-18.2 mV) produced using similar conditions and found by Squinca *et al.* (2020) and it is within the range of values reported elsewhere by Arantes *et al.* (2020), ranging from -31.37 to -11.4 mV.

Thermal stability is a very important parameter for cellulose nanomaterials applications since a lower degradation temperature limits their use while a higher extends their range of application (DUFRESNE, 2013). The initial thermal degradation temperature (T_{onset}) is defined as the temperature at which the sample mass loss begins to change significantly whereas the maximum thermal degradation rate temperature (T_{max}) corresponds to the temperature in which the sample is most rapidly degraded (NAIR; YAN, 2015). The C-CNs showed an onset temperature of degradation (T_{onset}) at around 203.0 °C and a maximum degradation temperature (T_{max}) of 336.1 °C, while the NC-CNs showed T_{onset} around 300.5 °C and T_{max} of 347.4 °C. The superior thermal properties of the NC-CNs could be associated with the higher xylanases activity of the non-commercial enzymatic preparation. The xylanase treatment reduces the hemicellulose fraction which has a lower thermal degradation temperature than those of the cellulose and the lignin, thus improving the thermal stability of the cellulose nanomaterials (DEMIRBAŞ, 2000; TAO *et al.*, 2019). Although the C-CNs began to degrade at a lower temperature than the NC-CNs, it is still higher than the degradation of the CNC obtained using sulfuric acid which has been reported to start at lower temperatures, such as, 122 °C (OKSMAN *et al.*, 2011) and 184 °C (GEORGE *et al.*, 2008). The lower thermal stability of CNC obtained by acid hydrolysis is commonly associated with the sulfate groups, introduced during hydrolysis with sulfuric acid, which induce the degradation of cellulose at lower

temperatures (ROMAN; WINTER, 2004).

5.4.3 Preparation and characterization of hydrogels

As the first step of hydrogel preparation, the effect of different gelatin concentrations (4, 5, 6, 7, 8, 9 and 10%) without adding crosslinking on the hydrogel network formation and its water absorption were evaluated (Figure 5.4).

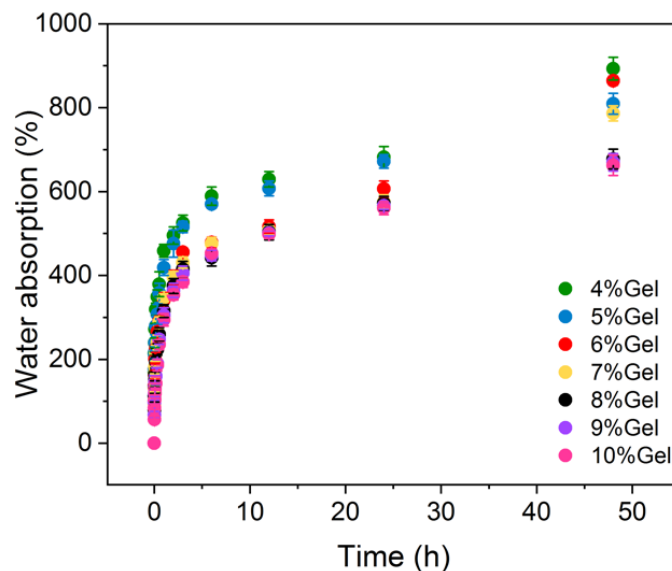


Figure 5.4. Water absorption of hydrogels prepared with different gelatin concentrations

Samples prepared with lower gelatin concentration reached higher water absorption within the first 24 hours. It can also be observed from Figure 5.4 that none of the samples reached the swelling equilibrium plateau which might be associated with the absence of crosslinking. Moreover, the hydrogels prepared with 4, 5, 6, 7% broke down after 48 hours as it can be confirmed by the abrupt increase in the swelling degree value. Therefore, the concentration of 8% was chosen to be used as it was the hydrogel with the lower amount of gelatin that kept its structural integrity after 48 hours.

After selecting the amount of gelatin, the incorporation tannic acid as crosslinking agent, ginger essential oil as a bactericidal compound and cellulose nanomaterials to increase the structural stability in the preparation of hydrogels. As mentioned before, the hydrogels were prepared following an adapted method described by Leite *et al.* (2021) who evaluated the interactions among the components (gelatin, tannic acid and cellulose crystals) that are affected by the order of adding them to the forming solution and confirmed that glycerol performed as a chemically inert plasticizer.

Figure 5.5 shows the water absorption of the gelatin-based hydrogels with by adding tannic acid and ginger essential oil.

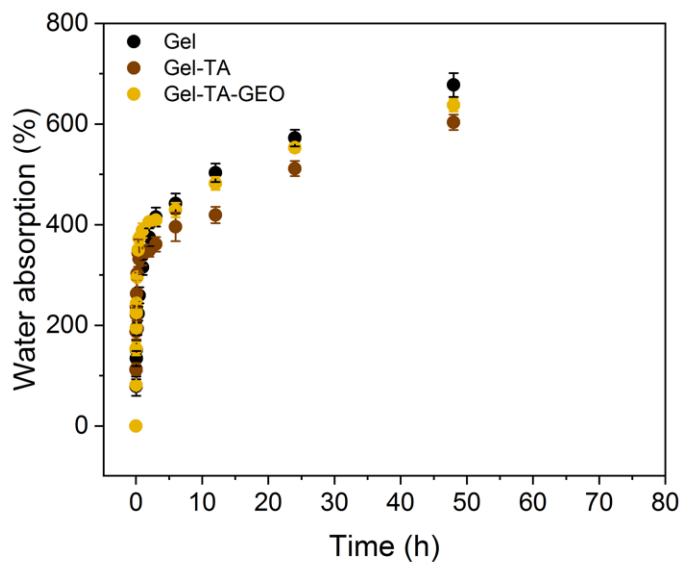


Figure 5.5. Water absorption of gelatin-based hydrogels with tannic acid and ginger essential oil.

The content of water absorbed by the Gel-TA and Gel-TA-GEO within 48 hours were $603.5 \pm 18.4\%$ and $637.6 \pm 12.7\%$, respectively. The amount of water absorbed by Gel-TA-GEO and Gel-TA hydrogels was similar indicating the ginger essential oil may not have hindered the interaction between gelatin and tannic acid. This result is important since GEO was added to the gelatin solution before the tannic acid and it could have reduced the number of physical interaction and/or cross-linking reaction that occurs between the gelatin amine groups and the catechol groups of TA (MUHOZA; XIA; ZHANG, 2019). Additionally, it can be seen from Figure 5.5 that the tannic acid addition reduced the water absorption compared with the hydrogels prepared only with gelatin which indicates some improvement of the hydrogel structural integrity. However, the equilibrium state was not reached and after 72 hours the hydrogels dissolved. Following this, the effect of the addition of 4 and 6% of cellulose nanomaterial produced with both, commercial and non-commercial enzymes, on the water absorption was evaluated (Figure 4.6).

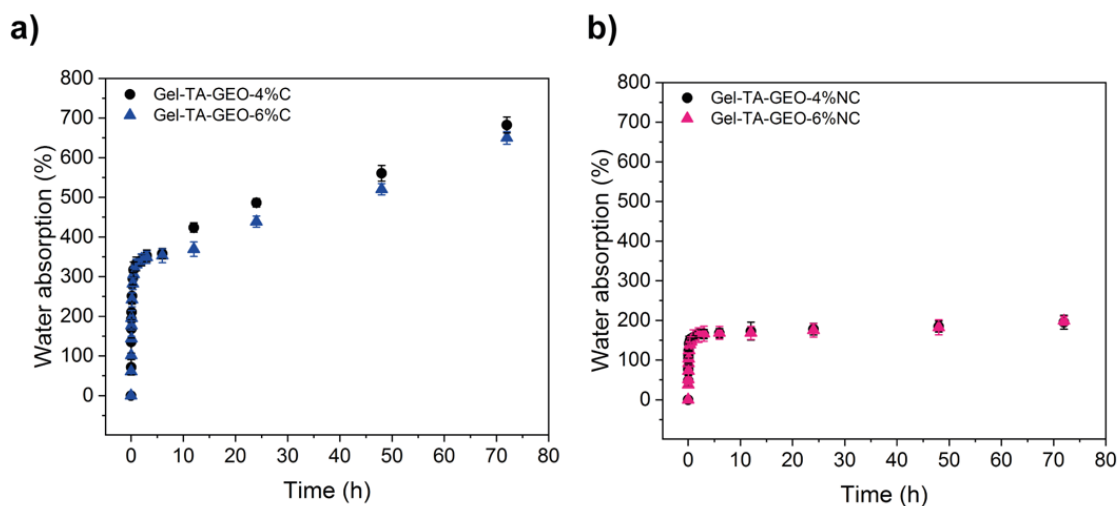


Figure 5.6. Water absorption of gelatin-based hydrogels with adding of cellulose nanomaterials prepared with a) commercial and b) non-commercial enzymes.

From Figure 5.6, it can be observed a higher swelling rate during the first 6 hours for C-NCs and NC-CNs hydrogels and the increase of cellulose nanomaterials concentration did not significantly affect the water absorption. The hydrogels with 4 and 6% of C-CNs reached 560.6 ± 19.9 and $520.4 \pm 14.3\%$ of water absorption, while those with 4 and 6% of NC-CNs reached 184.7 ± 13.8 and $182.7 \pm 13.8\%$, respectively in 48 hours. After this time, C-CNs hydrogels continue to absorb water and dissolved after 72 hours. Whereas the NC-CNs hydrogels reached the equilibrium indicating an improved stability. Although NC-CN hydrogels have reached lower values of water absorption, these nanomaterials contributed more to the maintenance of the structure preventing the hydrogels from dissolving for a much longer period of time which was not observed for any of the hydrogels prepared. Figure 5.7 displays the appearance of the all samples prepared in this work, that is, GEL, GEL-TA, GEL-TA-GEO, GEL-TA-GEO-4%C, GEL-TA-GEO-6%C, GEL-TA-GEO-4%NC and GEL-TA-GEO-6%NC hydrogels in wet state.

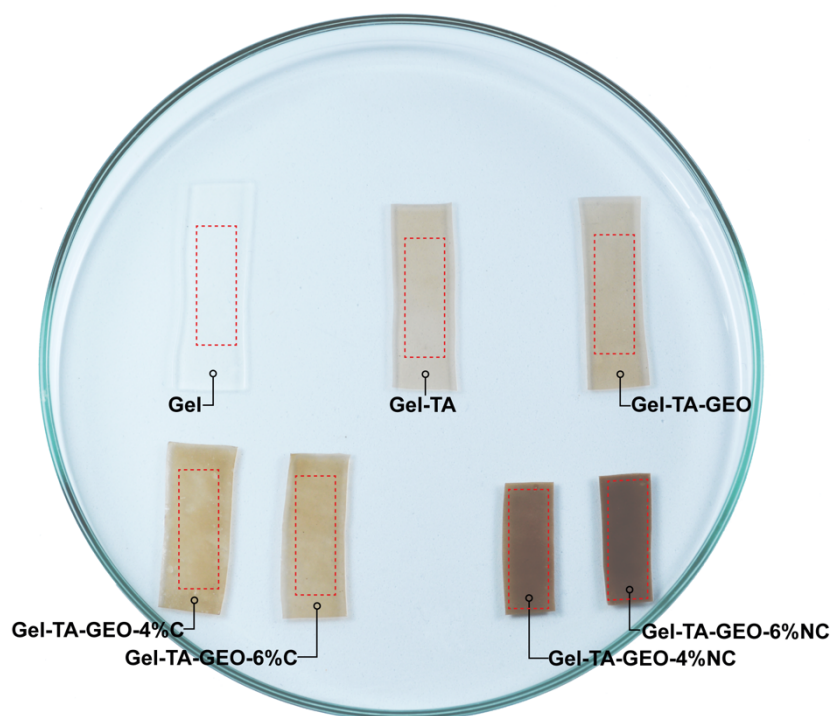


Figure 5.7. Photographs of the hydrogels prepared in this work showing their appearance after submersion in water for 4 hours. All samples were cut in dry state and with dimensions of 0.8×2.4 cm indicated by red dashed rectangles.

The smaller size and more brownish color of the samples with NC-CNs compared to others, mainly the hydrogel prepared only with gelatin (Gel), are likely related to their lower water absorption since all samples had initially the same dimensions in dry state and were kept in water during the same time. The more rigid network, the lower water uptake capacity (DASH; FOSTON; RAGAUSKAS, 2013). Taheri *et al.* (2020) also reported a considerable decline in the water absorption capacity associated with the presence of nanocellulose in gelatin-based networks containing tannic acid. These promising results need to be further evaluated to better understand the interactions and contributions of the NC-CNs to the hydrogel network.

5.5 Antimicrobial activity tests

Based on the Standard SNV 195920-1992, a material can be classified with regards antibacterial properties into “good”, when an inhibition zone $>$ than 1 mm is observed around and “fairly good”, when it is $<$ 1 mm; “sufficient” when there is no

growth on the sample; “limited” when a limited bacterial growth is observed on the sample and “not sufficient” when the sample is partially (50%) or totally covered by the bacteria (POLLINI *et al.*, 2009). Figure 5.8 presents the results of the antibacterial activity tests against *S. aureus* and *E. coli* of all samples prepared in this work, that is, GEL, GEL-TA, GEL-TA-GEO, GEL-TA-GEO-4%C, GEL-TA-GEO-6%C, GEL-TA-GEO-4%NC and GEL-TA-GEO-6%NC hydrogels.

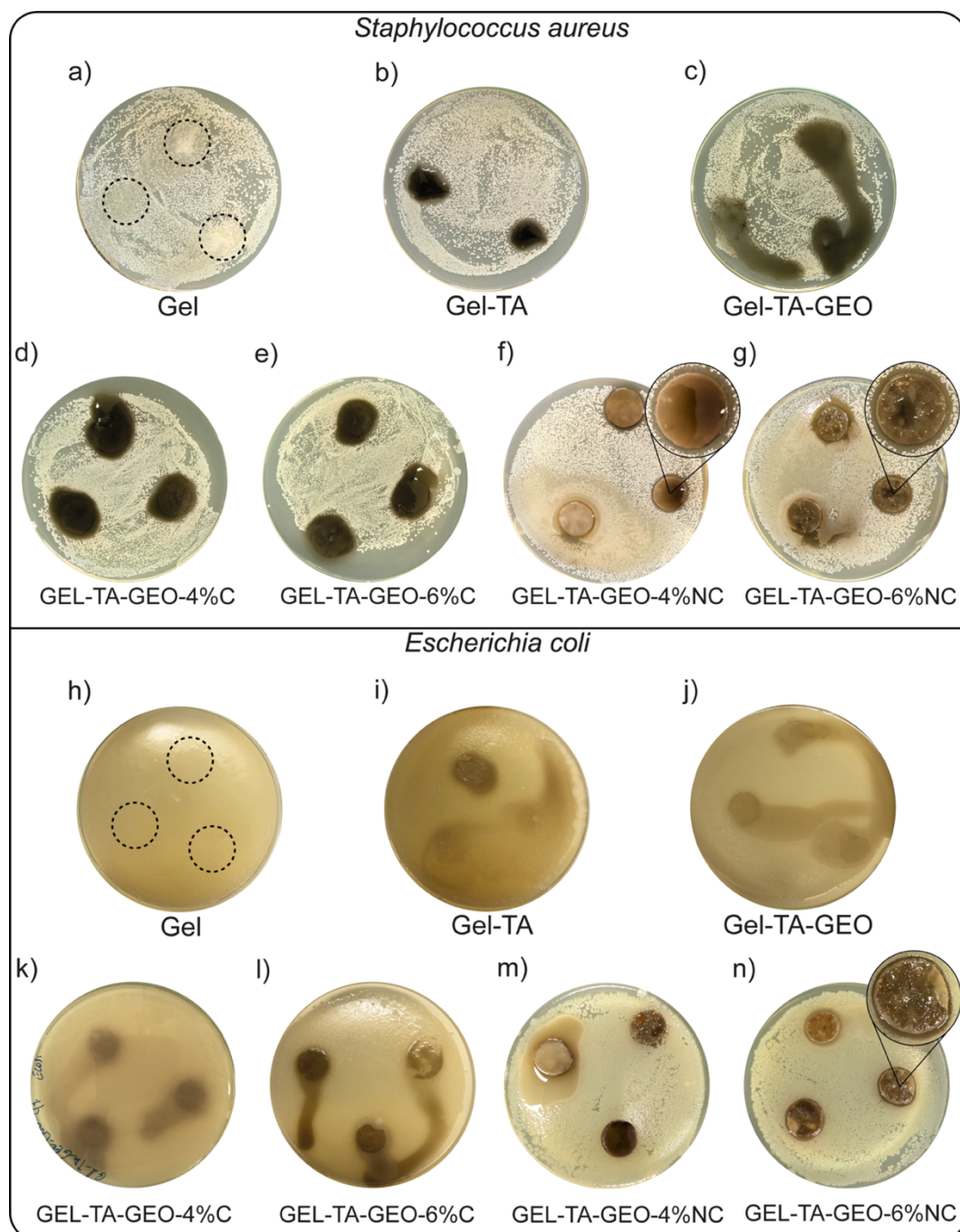


Figure 5.8. Images from antimicrobial assays with the gelatin-based hydrogels discs

against (a–g) *S. aureus* and (h–n) *E. coli*. Insets show the growth inhibition area observed around samples.

From Figure 5.8 it is possible to observe that hydrogels prepared only with gelatin (Figure 5.8a) were totally covered by bacteria indicating that they do not have antibacterial capacity. Meanwhile, the addition of tannic acid, ginger essential oil and cellulose nanomaterials, resulted in samples that displayed some antimicrobial effect against both bacteria, *S. aureus* and *E. coli*, and Gel-TA, Gel-TA-GEO, Gel-TA-GEO-4%C and Gel-TA-GEO-6%C were considered “sufficient” based on Standard SNV 195920-1992. Additionally, it is possible to observe narrow inhibitory zones (< 1 mm) around the Gel-TA-GEO-4%NC samples against *S. aureus* (inset Figure 5.8f) and around the Gel-TA-GEO-6%NC samples against both bacteria (insets Figure 5.8g and 5.8n). Thus, TA-GEO-6%NC hydrogel can be classified as fairly good. It should be mentioned that some hydrogels, especially those that were not reinforced with cellulose nanomaterials, dissolved during the experiment and left a “path” where no bacteria growth was observed. This dissolving issue might be due to the temperature of incubation which was above the sol-gel transition temperature of gelatin (TAKAHASHI; CHOI, 1996). Leite *et al.* (2021) also observed a similar tendency.

Besides, it was difficult to quantify the improving effect of the GEO addition on the antimicrobial properties comparing the Gel-TA and Gel-TA-GEO hydrogels performances. The reason for this is related to the fact that the samples with GEO and without cellulose nanomaterials were the most affected samples by the dissolving issue, which is likely due to the presence of oil that hindered the mechanical properties. It has been reported that the incorporation of ginger essential oil may slightly weaken the polymeric network, which in turn, could be associated with an increase in material heterogeneity and the appearance of more cavities (AMALRAJ *et al.*, 2020). Moreover from Figure 5.8, it is also worth to be highlighted that the reinforcement with cellulose nanocrystals produced by non-commercial enzymes resulted in hydrogels with higher stability as the integrity shape of Gel-TA-GEO-4%NC (Figure 5.8f and 5.8n) and Gel-TA-GEO-6%NC (Figure 5.8g and 5.8m) were more preserved in comparison to the other samples. Overall the hydrogels prepared with all-natural components could be further explored as they hold potential to be used as functional materials, for instance, wound dressings.

5.6 Conclusions

This chapter reports on the comparison between cellulose nanomaterials produced using non-commercial and commercial enzymes and the evaluation of their application in gelatin-based hydrogels. The results showed that the nanomaterials presented similar yield, crystallinity index and surface charge. However, NC-CNs presented superior thermal stability which could be attributed to the a lower amount of hemicellulose resulting in higher specific xylanase presented in the non-commercial enzymes. Gelatin-based hydrogels were prepared by solvent casting using tannic acid as a crosslinking agent, ginger essential oil as bactericidal a compound, and cellulose nanomaterials to increase their structural stability.

The incorporation of NC-CNs led to the formation of three-dimensional networks with higher structural integrity, but reduced the water absorption capacity compared with the other hydrogels prepared. The hydrogels inhibited the growth *S. aureus* and *E. coli* mainly due to the incorporation of tannic acid and ginger essential oil. Although further characterizations are needed, the feasibility of applying cellulose nanomaterials produced by non-commercial enzymes in the preparation was demonstrated. The bio-based materials obtained through an environmentally friendly and sustainable methodology could be explored in order to contribute to the economic viability of biorefineries and the development of the bioeconomy.

Chapter 6

Conclusions and future works

This PhD thesis was motivated by the growing interest to design environmentally sustainable products. This work demonstrated sustainable process strategies using fungal enzymes and ginger residue to produce cellulose nanomaterials via enzymatic and mechanical routes for application in the manufacture of hydrogels. The following conclusions can be drawn based on the results achieved in this thesis:

- There is a relevant growth in the annual number of publications related to the cellulose nanomaterials whose production process included the use of enzymes during the last decade, and especially during the last eight years (2013–2021). The most used feedstocks were derived from hardwood, softwood and residues, mainly from agro-industries, such as sugarcane straw and bagasse, corn cob, oat husks, lemongrass leaves, oil palm empty fruit bunch, rice straw, among others. To date, there is no commercial enzymatic preparation especially designed for nanocellulose production. Nanocelluloses whose production process included the use of enzymes have been more often applied for the preparation of films among the selected articles in the systematic map conducted. Furthermore, the production of cellulose nanomaterials using enzymatic hydrolysis has been explored in the context of integrated biorefinery, but no work evaluated the application of these nanomaterials;
- A non-commercial enzymatic preparation was obtained by cultivating *A. niger* under solid-state fermentation showing a high endoglucanase specific activity value of 17.09 IU/mg protein and it was used to obtain the cellulose nanocrystals (CNCs). The highest yield (24.6%) of CNCs was achieved using 96 hours of enzymatic hydrolysis of the ball-milled cellulose pulp for 90 minutes, followed by sonication for 5 min. The CNCs presented approximate lengths of 294.0 nm and diameters of 24.0 nm, and the crystallinity index increased from 57.5 to 78.3%, compared to the

cellulose pulp that was only ball-milled. Besides, the enzymatic hydrolysis using non-commercial enzymes resulted in cellulose nanomaterials good thermal stability as the T_{onset} and T_{max} for the CNCs obtained from the condition that resulted in the highest yield were 300.5 and 347.4 °C, respectively.

- Ginger residue was used as a raw material feedstock to isolate cellulose nanofibers by high-pressure homogenization. Hydrogels were successfully prepared via vacuum-assisted filtration without any cross-linker and with important properties for wound dressing applications. Alkali pre-treatment was used to adjust the liquid absorption capacity of the hydrogels by altering the chemical composition of ginger fibers before hydrogel formation. The hydrogel prepared with ginger without any pre-treatment of 40 g/m² grammage showed the highest water absorption of 62 times its initial weight. This result is likely associated with the presence of the noncellulosic components such as starch and hemicellulose naturally found in ginger when preparing the nanofibers and their hydrogels. Additionally, the hydrogels showed good mechanical properties with a tensile strength of 2.1 ± 0.2 MPa and elastic modulus of 15.3 ± 0.3 MPa. Although the intrinsic antimicrobial activity of ginger was not observed after isolation of cellulose nanofibers, the hydrogels were functionalized using ginger essential oil which improved antimicrobial performance against *S. aureus* and *E. coli*. However, additional experiments are needed to better understand and optimize the functionalization of ginger nanofiber hydrogels using essential oil. Cytocompatibility evaluation showed that hydrogels did not significantly affect fibroblast proliferation whereas the migration of keratinocytes was more beneficial when in contact with the hydrogel prepared with ginger without any pre-treatment.
- Enzymatic hydrolysis using commercial enzymes resulted in a yield of cellulose nanomaterials slightly lower (19.9%) than the value obtained with the non-commercial enzymes (24.6%) but the values of crystallinity index and zeta potential were similar. The use of non-commercial enzymes produced cellulose nanocrystal with superior thermal stability which can be associated with a lower amount of hemicellulose resulted in higher specific xylanase presented in this enzymatic cocktail. Sequentially, the nanomaterials were incorporated into gelatin-based hydrogels prepared by solvent casting using tannic acid as crosslinking and ginger essential oil. Tannic acid addition contributed improving the structural integrity of

the gelatin-based hydrogels but it was not enough to avoid their dissolution after 72 hours submerged in water. The incorporation of cellulose nanomaterials produced by non-commercial enzymes better contributed to the structural integrity of the hydrogels keeping them cohesive for more than two weeks. The hydrogels inhibited the growth *S. aureus* and *E. coli* mainly owing to the incorporation of tannic acid and ginger essential oil. Although, it was not possible to quantify the contribution of each component to the antimicrobial activity.

Cellulose-based materials likely have a bright future. The development of new biomaterials is fundamental to tackle climate change and to make the transition towards an economy based on renewable resources. Although promising results were obtained, there are interesting topics derived from this work it should be deeply investigated. For instance, it was demonstrated that the non-commercial enzymes produced cellulose nanomaterials with superior properties when compared to those isolated using commercial enzymes. It would be interesting to investigate the strategies to increase the enzymatic cocktail titer with higher endoglucanase and xylanase activities and the production scale, besides evaluating different lignocellulosic feedstocks to produce the enzymes and the cellulose nanomaterials.

Regarding the gelatin-based hydrogels, some adjustments in the protocol might be needed to improve their structural integrity when submerged in water for longer period. Moreover, additional studies and hydrogel characterizations are necessary to better understand the interactions among the components and define the best application for these hydrogels. With regards to the ginger nanofiber-based hydrogels, it would be interesting to further explore the functionalization step with ginger essential oil to improve their antimicrobial properties.

REFERENCES

- ABDELRAHMAN, T.; NEWTON, H. Wound dressings: Principles and practice. **Surgery**, vol. 29, no. 10, p. 491–495, 2011. DOI 10.1016/j.mpsur.2011.06.007.
- ABDULLA, H.; SMITH, K.; ATHERTON, P. J.; IDRIS, I. Role of insulin in the regulation of human skeletal muscle protein synthesis and breakdown: a systematic review and meta-analysis. **Diabetologia**, vol. 59, no. 1, p. 44–55, 2016.
- ABITBOL, T.; RIVKIN, A.; CAO, Y.; NEVO, Y.; ABRAHAM, E.; BEN-SHALOM, T.; LAPIDOT, S.; SHOSEYOV, O. Nanocellulose, a tiny fiber with huge applications. **Current opinion in biotechnology**, vol. 39, p. 76–88, 2016.
- ABRAHAM, E.; DEEPA, B.; POTHAN, L. A.; JACOB, M.; THOMAS, S.; CVELBAR, U.; ANANDJIWALA, R. Extraction of nanocellulose fibrils from lignocellulosic fibres: A novel approach. **Carbohydrate Polymers**, vol. 86, no. 4, p. 1468–1475, 2011.
- ABRAL, H.; ARIKSA, J.; MAHARDIKA, M.; HANDAYANI, D.; AMINAH, I.; SANDRAWATI, N.; PRATAMA, A. B.; FAJRI, N.; SAPUAN, S. M.; ILYAS, R. A. Transparent and antimicrobial cellulose film from ginger nanofiber. **Food Hydrocolloids**, vol. 98, no. May 2019, p. 105266, 2020. DOI 10.1016/j.foodhyd.2019.105266.
- ABRAL, H.; ARIKSA, J.; MAHARDIKA, M.; HANDAYANI, D.; AMINAH, I.; SANDRAWATI, N.; SAPUAN, S. M.; ILYAS, R. A. Highly transparent and antimicrobial PVA based bionanocomposites reinforced by ginger nanofiber. **POLYMER TESTING**, vol. 81, Jan. 2020. <https://doi.org/10.1016/j.polymertesting.2019.106186>.
- ABRAL, H.; ARIKSA, J.; MAHARDIKA, M.; HANDAYANI, D.; AMINAH, I.; SANDRAWATI, N.; SUGIARTI, E.; MUSLIMIN, A. N.; ROSANTI, S. D. Effect of heat treatment on thermal resistance, transparency and antimicrobial activity of sonicated ginger cellulose film. **CARBOHYDRATE POLYMERS**, vol. 240, Jul. 2020. <https://doi.org/10.1016/j.carbpol.2020.116287>.
- AFRIN, S.; KARIM, Z. Isolation and Surface Modification of Nanocellulose: Necessity of Enzymes over Chemicals. **ChemBioEng Reviews**, vol. 4, no. 5, p. 289–303, 2017. <https://doi.org/10.1002/cben.201600001>.
- AGBLEVOR, F. A.; IBRAHIM, M. M.; EL-ZAWAWY, W. K. Coupled acid and enzyme mediated production of microcrystalline cellulose from corn cob and cotton gin waste. **CELLULOSE**, vol. 14, no. 3, p. 247–256, Jun. 2007. <https://doi.org/10.1007/s10570-006-9103-y>.
- AHMED, E. M. Hydrogel: Preparation, characterization, and applications: A review. **Journal of Advanced Research**, vol. 6, no. 2, p. 105–121, 2015. DOI <https://doi.org/10.1016/j.jare.2013.07.006>.
- AL-DULAIMI, A. A.; WANROSLI, W. D. Isolation and characterization of

nanocrystalline cellulose from totally chlorine free oil palm empty fruit bunch pulp. **Journal of Polymers and the Environment**, vol. 25, no. 2, p. 192–202, 2017.

ALAM, M. N.; ISLAM, M. S.; CHRISTOPHER, L. P. Sustainable Production of Cellulose-Based Hydrogels with Superb Absorbing Potential in Physiological Saline. **ACS Omega**, vol. 4, no. 5, p. 9419–9426, 2019. <https://doi.org/10.1021/acsomega.9b00651>.

ALI, B. H.; BLUNDEN, G.; TANIRA, M. O.; NEMMAR, A. Some phytochemical, pharmacological and toxicological properties of ginger (*Zingiber officinale* Roscoe): A review of recent research. **Food and Chemical Toxicology**, vol. 46, no. 2, p. 409–420, 2008. DOI <https://doi.org/10.1016/j.fct.2007.09.085>.

ALVAREZ, O. M.; MERTZ, P. M.; EAGLSTEIN, W. H. The effect of occlusive dressings on collagen synthesis and re-epithelialization in superficial wounds. **Journal of Surgical Research**, vol. 35, no. 2, p. 142–148, 1983. DOI [https://doi.org/10.1016/0022-4804\(83\)90136-1](https://doi.org/10.1016/0022-4804(83)90136-1).

AMALRAJ, A.; HAPONIUK, J. T.; THOMAS, S.; GOPI, S. Preparation, characterization and antimicrobial activity of polyvinyl alcohol/gum arabic/chitosan composite films incorporated with black pepper essential oil and ginger essential oil. **International Journal of Biological Macromolecules**, vol. 151, p. 366–375, 2020. DOI [10.1016/j.ijbiomac.2020.02.176](https://doi.org/10.1016/j.ijbiomac.2020.02.176).

ANDERSON, S. R.; ESPOSITO, D.; GILLETTE, W.; ZHU, J. Y.; BAXA, U.; MCNEIL, S. E. Enzymatic preparation of nanocrystalline and microcrystalline cellulose. **TAPPI JOURNAL**, vol. 13, no. 5, p. 35–42, 2014. <https://doi.org/10.32964/TJ13.5.35>.

ANDLAR, M.; REZIC, T.; MARĐETKO, N.; KRACHER, D.; LUDWIG, R.; ŠANTEK, B. Lignocellulose degradation: an overview of fungi and fungal enzymes involved in lignocellulose degradation. **Engineering in Life Sciences**, vol. 18, no. 11, p. 768–778, 2018.

ARACRI, E.; BARNETO, A. G.; VIDAL, T. Comparative study of the effects induced by different laccase-based systems on sisal cellulose fibers. **Industrial and Engineering Chemistry Research**, 2012. DOI [10.1021/ie2028206](https://doi.org/10.1021/ie2028206).

ARANTES, V.; DIAS, I. K. R.; BERTO, G. L.; PEREIRA, B.; MAROTTI, B. S.; NOGUEIRA, C. F. O. **The current status of the enzyme-mediated isolation and functionalization of nanocelluloses: production, properties, techno-economics, and opportunities.** [*S. l.: s. n.*], 2020. vol. 27, . <https://doi.org/10.1007/s10570-020-03332-1>.

AULIN, C.; GÄLLSTEDT, M.; LINDSTRÖM, T. Oxygen and oil barrier properties of microfibrillated cellulose films and coatings. **Cellulose**, vol. 17, no. 3, p. 559–574, 2010.

AUTHORITY, E. G. for those carrying out systematic reviews E. F. S. Application of systematic review methodology to food and feed safety assessments to support decision making. **EFSA journal**, vol. 8, no. 6, p. 1637, 2010.

AVOLIO, R.; BONADIES, I.; CAPITANI, D.; ERRICO, M. E.; GENTILE, G.; AVELLA, M. A multitechnique approach to assess the effect of ball milling on cellulose. **Carbohydrate Polymers**, vol. 87, no. 1, p. 265–273, 2012.

BAHETI, V.; ABBASI, R.; MILITKY, J. Ball milling of jute fibre wastes to prepare nanocellulose. **World Journal of Engineering**, 2012.

BAILEY, M. J.; POUTANEN, K. Production of xylanolytic enzymes by strains of *Aspergillus*. **Applied Microbiology and Biotechnology**, vol. 30, no. 1, p. 5–10, 1989.

BAJAJ, P.; MAHAJAN, R. Cellulase and xylanase synergism in industrial biotechnology. **Applied microbiology and biotechnology**, vol. 103, no. 21, p. 8711–8724, 2019.

BANVILLET, G.; DEPRES, G.; BELGACEM, N.; BRAS, J. Alkaline treatment combined with enzymatic hydrolysis for efficient cellulose nanofibrils production. **Carbohydrate Polymers**, 2021. DOI 10.1016/j.carbpol.2020.117383.

BARTOS, A.; ANGGONO, J.; FARKAS, Á. E.; KUN, D.; SOETAREDJO, F. E.; MÓCZÓ, J.; ANTONI; PURWANINGSIH, H.; PUKÁNSZKY, B. Alkali treatment of lignocellulosic fibers extracted from sugarcane bagasse: Composition, structure, properties. **Polymer Testing**, vol. 88, no. April, p. 106549, 2020. <https://doi.org/10.1016/j.polymertesting.2020.106549>.

BATES, S.; CLAPTON, J.; COREN, E. Systematic maps to support the evidence base in social care. **Evidence & Policy: A Journal of Research, Debate and Practice**, vol. 3, no. 4, p. 539–551, 2007.

BENSELFELT, T.; ENGSTRÖM, J.; WÅGBERG, L. Supramolecular double networks of cellulose nanofibrils and algal polysaccharides with excellent wet mechanical properties. **Green Chemistry**, vol. 20, no. 11, p. 2558–2570, 2018.

BENSELFELT, T.; WÅGBERG, L. Unidirectional Swelling of Dynamic Cellulose Nanofibril Networks: A Platform for Tunable Hydrogels and Aerogels with 3D Shapeability. **Biomacromolecules**, vol. 20, no. 6, p. 2406–2412, 10 Jun. 2019. DOI 10.1021/acs.biomac.9b00401.

BENZIE, I. F. F.; WACHTEL-GALOR, S. Herbal medicine: biomolecular and clinical aspects. 2011.

BERGLUND, L.; ANUGWOM, I.; HEDENSTRÖM, M.; AITOMÄKI, Y.; MIKKOLA, J.-P.; OKSMAN, K. Switchable ionic liquids enable efficient nanofibrillation of wood pulp. **Cellulose**, vol. 24, no. 8, p. 3265–3279, 2017.

BIAN, H.; CHEN, L.; DAI, H.; ZHU, J. Y. Integrated production of lignin containing cellulose nanocrystals (LCNC) and nanofibrils (LCNF) using an easily recyclable dicarboxylic acid. **Carbohydrate Polymers**, vol. 167, p. 167–176, 2017.

BIAN, H.; LI, G.; JIAO, L.; YU, Z.; DAI, H. Enzyme-Assisted Mechanical Fibrillation of Bleached Spruce Kraft Pulp to Produce Well-Dispersed and Uniform-Sized Cellulose Nanofibrils. **BioResources**, vol. 11, no. 4, p. 10483–10496, 2016. DOI 10.15376/biores.11.4.10483-10496.

BINOD, P.; GNANSOUNOU, E.; SINDHU, R.; PANDEY, A. Enzymes for second generation biofuels: recent developments and future perspectives. **Bioresource Technology Reports**, vol. 5, p. 317–325, 2019.

BÖHME, U.; SCHELER, U. Effective charge of bovine serum albumin determined by electrophoresis NMR. **Chemical Physics Letters**, vol. 435, no. 4–6, p. 342–345, 2007. <https://doi.org/10.1016/j.cplett.2006.12.068>.

BONDANCIA, T. J.; DE AGUIAR, J.; BATISTA, G.; CRUZ, A. J. G.; MARCONCINI, J. M.; MATTOSO, L. H. C.; FARINAS, C. S. Production of nanocellulose using citric acid in a biorefinery concept: effect of the hydrolysis reaction time and techno-economic analysis. **Industrial & Engineering Chemistry Research**, vol. 59, no. 25, p. 11505–11516, 2020.

BONDANCIA, T. J.; MATTOSO, L. H. C.; MARCONCINI, J. M.; FARINAS, C. S. A new approach to obtain cellulose nanocrystals and ethanol from eucalyptus cellulose pulp via the biochemical pathway. **Biotechnology Progress**, vol. 33, no. 4, p. 1085–1095, 2017.

BONDESON, D.; MATHEW, A.; OKSMAN, K. Optimization of the isolation of nanocrystals from microcrystalline cellulose by acid hydrolysis. **Cellulose**, vol. 13, no. 2, p. 171, 2006. DOI 10.1007/s10570-006-9061-4.

BOŽIČ, M.; GORGIEVA, S.; KOKOL, V. Homogeneous and heterogeneous methods for laccase-mediated functionalization of chitosan by tannic acid and quercetin. **Carbohydrate polymers**, vol. 89, no. 3, p. 854–864, 2012.

BRADFORD, M. M. A rapid and sensitive method for the quantitation of microgram quantities of protein utilizing the principle of protein-dye binding. **Analytical biochemistry**, vol. 72, no. 1–2, p. 248–254, 1976.

BRAGA, M. E. M.; MORESCHI, S. R. M.; MEIRELES, M. A. A. Effects of supercritical fluid extraction on *Curcuma longa* L. and *Zingiber officinale* R. starches. **Carbohydrate Polymers**, vol. 63, no. 3, p. 340–346, 2006. <https://doi.org/10.1016/j.carbpol.2005.08.055>.

BRINCHI, L.; COTANA, F.; FORTUNATI, E.; KENNY, J. M. Production of nanocrystalline cellulose from lignocellulosic biomass: technology and applications. **Carbohydrate polymers**, vol. 94, no. 1, p. 154–169, 2013.

BROWN JR, R. M. The biosynthesis of cellulose. **Journal of Macromolecular Science, Part A: Pure and Applied Chemistry**, vol. 33, no. 10, p. 1345–1373, 1996.

BUCHHOLZ, F. L.; GRAHAM, A. T. **Modern superabsorbent polymer technology**. 1st ed. New York: Wiley-VCH, 1997.

BUTT, M. S.; SULTAN, M. T. Ginger and its health claims: Molecular aspects. **Critical Reviews in Food Science and Nutrition**, vol. 51, no. 5, p. 383–393, 2011. <https://doi.org/10.1080/10408391003624848>.

BUWALDA, S. J.; BOERE, K. W. M.; DIJKSTRA, P. J.; FEIJEN, J.; VERMONDEN, T.; HENNINK, W. E. Hydrogels in a historical perspective: From simple networks to smart materials. **Journal of controlled release**, vol. 190, p. 254–273, 2014. .

BYRNE, M. E.; SALIAN, V. Molecular imprinting within hydrogels II: Progress and analysis of the field. **International Journal of Pharmaceutics**, vol. 364, no. 2, p. 188–

212, 2008. <https://doi.org/10.1016/j.ijpharm.2008.09.002>.

CALÓ, E.; KHUTORYANSKIY, V. V. Biomedical applications of hydrogels: A review of patents and commercial products. **European Polymer Journal**, vol. 65, p. 252–267, 2015. <https://doi.org/10.1016/j.eurpolymj.2014.11.024>.

CAMARERO ESPINOSA, S.; KUHNT, T.; FOSTER, E. J.; WEDER, C. Isolation of Thermally Stable Cellulose Nanocrystals by Phosphoric Acid Hydrolysis. **Biomacromolecules**, vol. 14, no. 4, p. 1223–1230, 8 Apr. 2013. DOI 10.1021/bm400219u.

CAMARGO, L. A.; PEREIRA, S. C.; CORREA, A. C.; FARINAS, C. S.; MARCONCINI, J. M.; MATTOSO, L. H. C. C. Feasibility of Manufacturing Cellulose Nanocrystals from the Solid Residues of Second-Generation Ethanol Production from Sugarcane Bagasse. **Bioenergy Research**, vol. 9, no. 3, p. 894–906, 2016. DOI 10.1007/s12155-016-9744-0.

CAO, Y.; TAN, H. Effects of cellulase on the modification of cellulose. **Carbohydrate Research**, vol. 337, no. 14, p. 1291–1296, 2002.

CEBREIROS, F.; SEILER, S.; DALLI, S. S.; LAREO, C.; SADDLER, J. Enhancing cellulose nanofibrillation of eucalyptus Kraft pulp by combining enzymatic and mechanical pretreatments. **Cellulose**, 2021. DOI 10.1007/s10570-020-03531-w.

CHANDEL, A. K.; GARLAPATI, V. K.; JEEVAN KUMAR, S. P.; HANS, M.; SINGH, A. K.; KUMAR, S. The role of renewable chemicals and biofuels in building a bioeconomy. **Biofuels, Bioproducts and Biorefining**, vol. 14, no. 4, p. 830–844, 2020. .

CHANG, C.; ZHANG, L. Cellulose-based hydrogels: Present status and application prospects. **Carbohydrate Polymers**, vol. 84, no. 1, p. 40–53, 2011. DOI 10.1016/j.carbpol.2010.12.023.

CHARREAU, H.; CAVALLO, E.; FORESTI, M. L. Patents involving nanocellulose: Analysis of their evolution since 2010. **Carbohydrate Polymers**, vol. 237, no. December 2019, p. 116039, 2020. DOI 10.1016/j.carbpol.2020.116039. Available at: <https://doi.org/10.1016/j.carbpol.2020.116039>.

CHEBLI, Y.; KANEDA, M.; ZERZOUR, R.; GEITMANN, A. The cell wall of the Arabidopsis pollen tube-spatial distribution, recycling, and network formation of polysaccharides. **Plant Physiology**, 2012. DOI 10.1104/pp.112.199729.

CHEN, C.; HU, L. Nanocellulose toward advanced energy storage devices: structure and electrochemistry. **Accounts of chemical research**, vol. 51, no. 12, p. 3154–3165, 2018. .

CHEN, L.; ZHU, J. Y.; BAEZ, C.; KITIN, P.; ELDER, T. Highly thermal-stable and functional cellulose nanocrystals and nanofibrils produced using fully recyclable organic acids. **Green Chemistry**, vol. 18, no. 13, p. 3835–3843, 2016. .

CHEN, Y.; FAN, D.; HAN, Y.; LI, G.; WANG, S. Length-controlled cellulose nanofibrils produced using enzyme pretreatment and grinding. **Cellulose**, 2017. DOI 10.1007/s10570-017-1499-z.

CHEN, Y.; HE, Y.; FAN, D.; HAN, Y.; LI, G.; WANG, S. An efficient method for cellulose nanofibrils length shearing via environmentally friendly mixed cellulase pretreatment. **Journal of Nanomaterials**, 2017. DOI 10.1155/2017/1591504.

CHEN, Yue; XU, M.; ZHANG, J.; MA, J.; GAO, M.; ZHANG, Z.; XU, Y.; LIU, S. Genome-Wide DNA Methylation Variations upon Exposure to Engineered Nanomaterials and Their Implications in Nanosafety Assessment. **Advanced Materials**, vol. 29, no. 6, p. 1604580, 2017. <https://doi.org/10.1002/adma.201604580>.

CHENG, F.; LIU, C.; WEI, X.; YAN, T.; LI, H.; HE, J.; HUANG, Y. Preparation and Characterization of 2,2,6,6-Tetramethylpiperidine-1-oxyl (TEMPO)-Oxidized Cellulose Nanocrystal/Alginate Biodegradable Composite Dressing for Hemostasis Applications. **ACS Sustainable Chemistry and Engineering**, vol. 5, no. 5, p. 3819–3828, 2017. <https://doi.org/10.1021/acssuschemeng.6b02849>.

CHENG, H.; XIAO, D.; TANG, Y.; WANG, B.; FENG, X.; LU, M.; VANCOSO, G. J.; SUI, X. Sponges with Janus Character from Nanocellulose: Preparation and Applications in the Treatment of Hemorrhagic Wounds. **Advanced Healthcare Materials**, vol. 9, no. 17, p. 1–8, 2020. <https://doi.org/10.1002/adhm.201901796>.

CHERUBINI, F. The biorefinery concept: using biomass instead of oil for producing energy and chemicals. **Energy conversion and management**, vol. 51, no. 7, p. 1412–1421, 2010.

CIOLACU, D.; CIOLACU, F.; POPA, V. I. Amorphous cellulose—structure and characterization. **Cellulose chemistry and technology**, vol. 45, no. 1, p. 13, 2011. .

CUI, S.; ZHANG, S.; GE, S.; XIONG, L.; SUN, Q. Green preparation and characterization of size-controlled nanocrystalline cellulose via ultrasonic-assisted enzymatic hydrolysis. **Industrial Crops and Products**, 2016. DOI 10.1016/j.indcrop.2016.01.019.

CUNHA, F. M.; VASCONCELLOS, V. M.; FLORENCIO, C.; BADINO, A. C.; FARINAS, C. S. On-site production of enzymatic cocktails using a non-conventional fermentation method with agro-industrial residues as renewable feedstocks. **Waste and biomass valorization**, vol. 8, no. 2, p. 517–526, 2017. <https://doi.org/10.1007/s12649-016-9609-y>.

CURVELLO, R.; RAGHUWANSHI, V. S.; GARNIER, G. Engineering nanocellulose hydrogels for biomedical applications. **Advances in Colloid and Interface Science**, vol. 267, p. 47–61, 2019. DOI 10.1016/j.cis.2019.03.002.

DAI, J.; CHAE, M.; BEYENE, D.; DANUMAH, C.; TOSTO, F.; BRESSLER, D. C. Co-production of cellulose nanocrystals and fermentable sugars assisted by endoglucanase treatment of wood pulp. **Materials**, 2018. DOI 10.3390/ma11091645.

DASH, R.; FOSTON, M.; RAGAUSKAS, A. J. Improving the mechanical and thermal properties of gelatin hydrogels cross-linked by cellulose nanowhiskers. **Carbohydrate polymers**, vol. 91, no. 2, p. 638–645, 2013.

DE AGUIAR, J.; BONDANCIA, T. J.; CLARO, P. I. C.; MATTOSO, L. H. C.; FARINAS, C. S.; MARCONCINI, J. M. Enzymatic Deconstruction of Sugarcane

Bagasse and Straw to Obtain Cellulose Nanomaterials. **ACS Sustainable Chemistry and Engineering**, vol. 8, no. 5, p. 2287–2299, 2020. DOI 10.1021/acssuschemeng.9b06806.

DE ASSIS, C. A.; HOUTMAN, C.; PHILLIPS, R.; BILEK, E. M.; ROJAS, O. J.; PAL, L.; PERESIN, M. S.; JAMEEL, H.; GONZALEZ, R. Conversion economics of forest biomaterials: risk and financial analysis of CNC manufacturing. **Biofuels, Bioproducts and Biorefining**, vol. 11, no. 4, p. 682–700, 2017.

DE CAMPOS, A.; CORREA, A. C.; CANNELLA, D.; DE M TEIXEIRA, E.; MARCONCINI, J. M.; DUFRESNE, A.; MATTOSO, L. H. C. C.; CASSLAND, P.; SANADI, A. R. Obtaining nanofibers from curauá and sugarcane bagasse fibers using enzymatic hydrolysis followed by sonication. **Cellulose**, vol. 20, no. 3, p. 1491–1500, 2013. <https://doi.org/10.1007/s10570-013-9909-3>.

DELGADO AGUILAR, M.; GONZÁLEZ TOVAR, I.; TARRÉS FARRÉS, J. A.; ALCALÀ VILAVELLA, M.; PÈLACH SERRA, M. À.; MUTJÉ PUJOL, P.; DELGADO-AGUILAR, M.; GONZÁLEZ, I.; TARRÉS, Q.; ALCALÀ, M.; PÈLACH, M. À.; MUTJÉ, P. Approaching a low-cost production of cellulose nanofibers for papermaking applications. **BioResources**, 2015. DOI 10.15376/biores.10.3.5330-5344.

DEMIRBAŞ, A. Mechanisms of liquefaction and pyrolysis reactions of biomass. **Energy conversion and management**, vol. 41, no. 6, p. 633–646, 2000.

DHALI, K.; GHASEMLOU, M.; DAVER, F.; CASS, P.; ADHIKARI, B. A review of nanocellulose as a new material towards environmental sustainability. **Science of the Total Environment**, vol. 775, p. 145871, 2021. DOI 10.1016/j.scitotenv.2021.145871.

DHIVYA, S.; PADMA, V. V.; SANTHINI, E. Wound dressings - a review. **BioMedicine**, vol. 5, no. 4 ed. 2015/11/28, p. 22, Dec. 2015. DOI 10.7603/s40681-015-0022-9. Available at: <https://pubmed.ncbi.nlm.nih.gov/26615539>.

DI GRUTTOLA, F.; BORELLO, D. Analysis of the EU Secondary Biomass Availability and Conversion Processes to Produce Advanced Biofuels: Use of Existing Databases for Assessing a Metric Evaluation for the 2025 Perspective. **Sustainability**, vol. 13, no. 14, p. 7882, 2021.

DIMIDA, S.; DEMITRI, C.; DE BENEDICTIS, V. M.; SCALERA, F.; GERVASO, F.; SANNINO, A. Genipin-cross-linked chitosan-based hydrogels: Reaction kinetics and structure-related characteristics. **Journal of Applied Polymer Science**, vol. 132, no. 28, 2015.

DLOUHÁ, J.; POSPÍŠILOVÁ, M. Education for Sustainable Development Goals in public debate: The importance of participatory research in reflecting and supporting the consultation process in developing a vision for Czech education. **Journal of Cleaner Production**, vol. 172, p. 4314–4327, 2018.

DO NASCIMENTO, D. M.; ALMEIDA, J. S.; VALE, M. do S.; LEITÃO, R. C.; MUNIZ, C. R.; DE FIGUEIRÊDO, M. C. B.; MORAIS, J. P. S.; ROSA, M. de F. A comprehensive approach for obtaining cellulose nanocrystal from coconut fiber. Part I: Proposition of technological pathways. **Industrial Crops and Products**, vol. 93, p. 66–75, 2016.

DONALDSON, L. Cellulose microfibril aggregates and their size variation with cell wall type. **Wood science and technology**, vol. 41, no. 5, p. 443–460, 2007.

DOWSETT, C.; AYELLO, E. TIME principles of chronic wound bed preparation and treatment. **British journal of nursing (Mark Allen Publishing)**, England, vol. 13, no. 15, p. S16-23, Aug. 2004. <https://doi.org/10.12968/bjon.2004.13.Sup3.15546>.

DU, H.; LIU, W.; ZHANG, M.; SI, C.; ZHANG, X.; LI, B. Cellulose nanocrystals and cellulose nanofibrils based hydrogels for biomedical applications. **Carbohydrate Polymers**, vol. 209, no. November 2018, p. 130–144, 2019. DOI 10.1016/j.carbpol.2019.01.020.

DU, L.; WANG, J.; ZHANG, Y.; QI, C.; WOLCOTT, M. P.; YU, Z. A co-production of sugars, lignosulfonates, cellulose, and cellulose nanocrystals from ball-milled woods. **BIORESOURCE TECHNOLOGY**, vol. 238, p. 254–262, 2017. <https://doi.org/10.1016/j.biortech.2017.03.097>.

DUFRESNE, A. Cellulose nanomaterials as green nanoreinforcements for polymer nanocomposites. **Philosophical Transactions of the Royal Society A: Mathematical, Physical and Engineering Sciences**, vol. 376, no. 2112, p. 20170040, 2018.

DUFRESNE, A. Nanocellulose: a new ageless bionanomaterial. **Materials today**, vol. 16, no. 6, p. 220–227, 2013.

DUFRESNE, A. **Nanocellulose: from nature to high performance tailored materials**. [S. l.]: Walter de Gruyter GmbH & Co KG, 2017.

DUFRESNE, A. Nanocellulose Processing Properties and Potential Applications. **Current Forestry Reports**, 2019. <https://doi.org/10.1007/s40725-019-00088-1>.

EL-BAROTY, G. S.; ABD EL-BAKY, H. H.; FARAG, R. S.; SALEH, M. A. Characterization of antioxidant and antimicrobial compounds of cinnamon and ginger essential oils. **African journal of biochemistry research**, vol. 4, no. 6, p. 167–174, 2010.

ESPINOSA, E.; TARRÉS, Q.; DELGADO-AGUILAR, M.; GONZÁLEZ, I.; MUTJÉ, P.; RODRÍGUEZ, A. Suitability of wheat straw semichemical pulp for the fabrication of lignocellulosic nanofibres and their application to papermaking slurries. **Cellulose**, vol. 23, no. 1, p. 837–852, 2016.

FAN, H.; WANG, J.; ZHANG, Q.; JIN, Z. Tannic acid-based multifunctional hydrogels with facile adjustable adhesion and cohesion contributed by polyphenol supramolecular chemistry. **ACS omega**, vol. 2, no. 10, p. 6668–6676, 2017.

FAN, H.; WANG, L.; FENG, X.; BU, Y.; WU, D.; JIN, Z. Supramolecular hydrogel formation based on tannic acid. **Macromolecules**, vol. 50, no. 2, p. 666–676, 2017.

FARINAS, C Scarpelini; SCARPELINI, L. M.; MIRANDA, E. A.; BERTUCCI NETO, V. Evaluation of operational parameters on the precipitation of endoglucanase and xylanase produced by solid state fermentation of *Aspergillus niger*. **Brazilian Journal of Chemical Engineering**, vol. 28, p. 17–26, 2011.

FARINAS, Cristiane S; MARCONCINI, J. M.; MATTOSO, L. H. C. Enzymatic

Conversion of Sugarcane Lignocellulosic Biomass as a Platform for the Production of Ethanol, Enzymes and Nanocellulose. **Journal of Renewable Materials**, vol. 6, no. 2, p. 203–216, 2018. <https://doi.org/10.7569/JRM.2017.6341578>.

FENG, Y. T.; HAN, K.; OWEN, D. R. J. Discrete element simulation of the dynamics of high energy planetary ball milling processes. **Materials Science and Engineering: A**, vol. 375, p. 815–819, 2004. .

FENGEL, D.; WEGENER, G. **Wood: chemistry, ultrastructure, reactions**. [S. l.]: Walter de Gruyter, 1989.

FERDOUS, Z.; NEMMAR, A. Health impact of silver nanoparticles: a review of the biodistribution and toxicity following various routes of exposure. **International journal of molecular sciences**, vol. 21, no. 7, p. 2375, 2020.

FERNANDES, A. N.; THOMAS, L. H.; ALTANER, C. M.; CALLOW, P.; FORSYTH, V. T.; APPERLEY, D. C.; KENNEDY, C. J.; JARVIS, M. C. Nanostructure of cellulose microfibrils in spruce wood. **Proceedings of the National Academy of Sciences**, vol. 108, no. 47, p. E1195–E1203, 2011.

FIorentino, G.; RIPA, M.; ULGIATI, S. Chemicals from biomass: technological versus environmental feasibility. A review. **Biofuels, Bioproducts and Biorefining**, vol. 11, no. 1, p. 195–214, 2017. DOI <https://doi.org/10.1002/bbb.1729>.

FITZPATRICK, M.; CHAMPAGNE, P.; CUNNINGHAM, M. F.; WHITNEY, R. A. A biorefinery processing perspective: treatment of lignocellulosic materials for the production of value-added products. **Bioresource technology**, vol. 101, no. 23, p. 8915–8922, 2010.

FRANCE, K. J. De; HOARE, T.; CRANSTON, E. D.; DE FRANCE, K. J.; HOARE, T.; CRANSTON, E. D. Review of Hydrogels and Aerogels Containing Nanocellulose. **Chemistry of materials**, vol. 29, no. 11, p. 4609–4631, Jun. 2017. DOI [10.1021/acs.chemmater.7b00531](https://doi.org/10.1021/acs.chemmater.7b00531).

FREITAS, J. V; BILATTO, S.; SQUINCA, P.; PINTO, A. S. S.; BRONDI, M. G.; BONDANCIA, T. J.; BATISTA, G.; KLAIC, R.; FARINAS, C. S. Sugarcane biorefineries: potential opportunities towards shifting from wastes to products. **Industrial Crops and Products**, vol. 172, p. 114057, 2021.

FRITZ, C.; JEUCK, B.; SALAS, C.; GONZALEZ, R.; JAMEEL, H.; ROJAS, O. J. Nanocellulose and proteins: exploiting their interactions for production, immobilization, and synthesis of biocompatible materials. **Cellulose Chemistry and Properties: Fibers, Nanocelluloses and Advanced Materials**. [S. l.]: Springer, 2015. p. 207–224.

FU, L. H.; QI, C.; MA, M. G.; WAN, P. Multifunctional cellulose-based hydrogels for biomedical applications. **Journal of Materials Chemistry B**, vol. 7, no. 10, p. 1541–1562, 2019. <https://doi.org/10.1039/c8tb02331j>.

GAO, H.; ZHONG, Z.; XIA, H.; HU, Q.; YE, Q.; WANG, Y.; CHEN, L.; DU, Y.; SHI, X.; ZHANG, L. Construction of cellulose nanofibers/quaternized chitin/organic rectorite composites and their application as wound dressing materials. **Biomaterials Science**, vol. 7, no. 6, p. 2571–2581, 2019. <https://doi.org/10.1039/c9bm00288j>.

GAO, J.; HUANG, X.; ZHANG, L. *tsinghua edu cn*. Comparative analysis between international research hotspots and national-level policy keywords on artificial intelligence in China from 2009 to 2018. **Sustainability (Switzerland)**, vol. 11, no. 23, p. 1–18, 2019. <https://doi.org/10.3390/su11236574>.

GAO, X.; SADASIVUNI, K. K.; KIM, H.-C.; MIN, S.-K.; KIM, J. Designing pH-responsive and dielectric hydrogels from cellulose nanocrystals. **Journal of Chemical Sciences**, vol. 127, no. 6, p. 1119–1125, 2015.

GARCÍA, A.; GANDINI, A.; LABIDI, J.; BELGACEM, N.; BRAS, J. Industrial and crop wastes: A new source for nanocellulose biorefinery. **Industrial Crops and Products**, vol. 93, p. 26–38, 2016.

GEORGE, J.; SAJEEVKUMAR, V. A.; KUMAR, R.; RAMANA, K. V.; SABAPATHY, S. N.; BAWA, A. S. Enhancement of thermal stability associated with the chemical treatment of bacterial (*Gluconacetobacter xylinus*) cellulose. **Journal of applied polymer science**, vol. 108, no. 3, p. 1845–1851, 2008.

GHASEMZADEH, A.; JAAFAR, H. Z. E.; RAHMAT, A. Changes in antioxidant and antibacterial activities as well as phytochemical constituents associated with ginger storage and polyphenol oxidase activity. **BMC Complementary and Alternative Medicine**, vol. 16, no. 1, p. 1–11, 2016. <https://doi.org/10.1186/s12906-016-1352-1>.

GHOSE, T. K. Measurement of cellulase activities. **Pure and applied Chemistry**, vol. 59, no. 2, p. 257–268, 1987.

GÍRIO, F. M.; FONSECA, C.; CARVALHEIRO, F.; DUARTE, L. C.; MARQUES, S.; BOGEL-ŁUKASIK, R. Hemicelluloses for fuel ethanol: a review. **Bioresource technology**, vol. 101, no. 13, p. 4775–4800, 2010.

GONÇALVES, M. C. P.; KIECKBUSCH, T. G.; PERNA, R. F.; FUJIMOTO, J. T.; MORALES, S. A. V.; ROMANELLI, J. P. Trends on enzyme immobilization researches based on bibliometric analysis. **Process biochemistry**, vol. 76, p. 95–110, 2019.

GONÇALVES, M. C. P.; ROMANELLI, J. P.; GUIMARÃES, J. R.; VIEIRA, A. C.; DE AZEVEDO, B. P.; TARDIOLI, P. W. Reviewing research on the synthesis of CALB-catalyzed sugar esters incorporating systematic mapping principles. **Critical Reviews in Biotechnology**, vol. 0, no. 0, p. 1–23, 2021. DOI 10.1080/07388551.2021.1888071.

HABIBI, Y.; LUCIA, L. A.; ROJAS, O. J. Cellulose nanocrystals: chemistry, self-assembly, and applications. **Chemical reviews**, vol. 110, no. 6, p. 3479–3500, 2010. .

HAKKARAINEN, T.; KOIVUNIEMI, R.; KOSONEN, M.; ESCOBEDO-LUCEA, C.; SANZ-GARCIA, A.; VUOLA, J.; VALTONEN, J.; TAMMELA, P.; MÄKITIE, A.; LUUKKO, K.; YLIPERTTULA, M.; KAVOLA, H. Nanofibrillar cellulose wound dressing in skin graft donor site treatment. **Journal of Controlled Release**, vol. 244, p. 292–301, 2016. DOI 10.1016/j.jconrel.2016.07.053. Available at: <http://dx.doi.org/10.1016/j.jconrel.2016.07.053>.

HASSAN, M.; BERGLUND, L.; HASSAN, E.; ABOU-ZEID, R.; OKSMAN, K. Effect of xylanase pretreatment of rice straw unbleached soda and neutral sulfite pulps on isolation of nanofibers and their properties. **Cellulose**, vol. 25, no. 5, p. 2939–2953, 2018.

HASSAN, S. S.; WILLIAMS, G. A.; JAISWAL, A. K. Lignocellulosic biorefineries in Europe: current state and prospects. **Trends in biotechnology**, vol. 37, no. 3, p. 231–234, 2019.

HAYASHI, N.; KONDO, T.; ISHIHARA, M. Enzymatically produced nano-ordered short elements containing cellulose I-beta crystalline domains. **Carbohydrate Polymers**, vol. 61, no. 2, p. 191–197, 2005. <https://doi.org/10.1016/j.carbpol.2005.04.018>.

HEIDARIAN, P.; KOUZANI, A. Z.; KAYNAK, A.; PAULINO, M.; NASRI-NASRABADI, B.; VARLEY, R. Double dynamic cellulose nanocomposite hydrogels with environmentally adaptive self-healing and pH-tuning properties. **Cellulose**, vol. 27, no. 3, p. 1407–1422, 2020.

HEIMANN, T. Bioeconomy and SDGs: Does the bioeconomy support the achievement of the SDGs? **Earth's Future**, vol. 7, no. 1, p. 43–57, 2019.

HENRIKSSON, M.; HENRIKSSON, G.; BERGLUND, L. A.; LINDSTRÖM, T. An environmentally friendly method for enzyme-assisted preparation of microfibrillated cellulose (MFC) nanofibers. **European Polymer Journal**, vol. 43, no. 8, p. 3434–3441, 2007.

HIGGINS, J. P. T.; ALTMAN, D. G.; GÖTZSCHE, P. C.; JÜNI, P.; MOHER, D.; OXMAN, A. D.; SAVOVIĆ, J.; SCHULZ, K. F.; WEEKS, L.; STERNE, J. A. C. The Cochrane Collaboration's tool for assessing risk of bias in randomised trials. **Bmj**, vol. 343, 2011.

HIGGINS, J. P. T.; THOMAS, J.; CHANDLER, J.; CUMPSTON, M.; LI, T.; PAGE, M. J.; WELCH, V. A. **Cochrane handbook for systematic reviews of interventions**. [S. l.]: John Wiley & Sons, 2019.

HOFFMAN, A. S. Hydrogels for biomedical applications. **Advanced Drug Delivery Reviews**, vol. 64, no. SUPPL., p. 18–23, 2012. DOI 10.1016/j.addr.2012.09.010.

HOLBACK, H.; YEO, Y.; PARK, K. **Hydrogel swelling behavior and its biomedical applications**. [S. l.]: Woodhead Publishing Limited, 2011. DOI 10.1533/9780857091383.1.3.

HORIE, K.; BARÓN, M.; FOX, R. B.; HE, J.; HESS, M.; KAHOVEC, J.; KITAYAMA, T.; KUBISA, P.; MARÉCHAL, E.; MORMANN, W. Definitions of terms relating to reactions of polymers and to functional polymeric materials (IUPAC Recommendations 2003). **Pure and Applied Chemistry**, vol. 76, no. 4, p. 889–906, 2004.

HSIEH, M.-C.; KIM, C.; NOGI, M.; SUGANUMA, K. Electrically conductive lines on cellulose nanopaper for flexible electrical devices. **Nanoscale**, vol. 5, no. 19, p. 9289–9295, 2013.

HU, J.; TIAN, D.; RENNECKAR, S.; SADDLER, J. N. Enzyme mediated nanofibrillation of cellulose by the synergistic actions of an endoglucanase, lytic polysaccharide monooxygenase (LPMO) and xylanase. **Scientific reports**, vol. 8, no. 1, p. 1–8, 2018.

HU, X.; WANG, Y.; ZHANG, L.; XU, M. Morphological and mechanical properties of

tannic acid/PAAm semi-IPN hydrogels for cell adhesion. **Polymer testing**, vol. 61, p. 314–323, 2017.

HUANG, J.; ZHU, H.; CHEN, Y.; PRESTON, C.; ROHRBACH, K.; CUMINGS, J.; HU, L. Highly transparent and flexible nanopaper transistors. **ACS nano**, vol. 7, no. 3, p. 2106–2113, 2013.

INNVENTIA. Innventia World's First Pilot Plant for Production of Nanocellulose Inaugurated. 2011.

ISHIHARA, M.; NAKANISHI, K.; ONO, K.; SATO, M.; KIKUCHI, M.; SAITO, Y.; YURA, H.; MATSUI, T.; HATTORI, H.; UENOYAMA, M. Photocrosslinkable chitosan as a dressing for wound occlusion and accelerator in healing process. **Biomaterials**, vol. 23, no. 3, p. 833–840, 2002.

ISO. ISO/TS 20477: 2017: Nanotechnologies—Standard terms and Their Definition for Cellulose Nanomaterial. 2017.

ISOGAI, A. Wood nanocelluloses: fundamentals and applications as new bio-based nanomaterials. **Journal of wood science**, vol. 59, no. 6, p. 449–459, 2013.

ISOGAI, A.; BERGSTRÖM, L. Preparation of cellulose nanofibers using green and sustainable chemistry. **Current Opinion in Green and Sustainable Chemistry**, vol. 12, p. 15–21, 2018. DOI 10.1016/j.cogsc.2018.04.008.

IWAMOTO, S.; ABE, K.; YANO, H. The effect of hemicelluloses on wood pulp nanofibrillation and nanofiber network characteristics. **Biomacromolecules**, vol. 9, no. 3, p. 1022–1026, 2008. <https://doi.org/10.1021/bm701157n>.

JACOB, J.; HAPONIUK, J. T.; THOMAS, S.; PETER, G.; GOPI, S. Use of ginger nanofibers for the preparation of cellulose nanocomposites and their antimicrobial activities. **Fibers**, vol. 6, no. 4, p. 1–11, 2018. <https://doi.org/10.3390/fib6040079>.

JACOB, J.; PETER, G.; THOMAS, S.; HAPONIUK, J. T.; GOPI, S. Chitosan and polyvinyl alcohol nanocomposites with cellulose nanofibers from ginger rhizomes and its antimicrobial activities. **International Journal of Biological Macromolecules**, vol. 129, p. 370–376, 2019a. DOI 10.1016/j.ijbiomac.2019.02.052.

JACOB, J.; PETER, G.; THOMAS, S.; HAPONIUK, J. T.; GOPI, S. In-situ synthesis and characterization of biocompatible magnetic ginger nanofiber composites for copper (II) removal from water. **Materials Today Communications**, vol. 21, no. September, p. 100690, 2019b. DOI 10.1016/j.mtcomm.2019.100690.

JAMES, K. L.; RANDALL, N. P.; HADDAWAY, N. R. A methodology for systematic mapping in environmental sciences. **Environmental Evidence**, vol. 5, no. 1, p. 1–13, 2016. <https://doi.org/10.1186/s13750-016-0059-6>.

JANARDHANAN, S.; SAIN, M. Bio-Treatment of Natural Fibers in Isolation of Cellulose Nanofibres: Impact of Pre-Refining of Fibers on Bio-Treatment Efficiency and Nanofiber Yield. **Journal of Polymers and the Environment**, vol. 19, no. 3, p. 615–621, 2011. <https://doi.org/10.1007/s10924-011-0312-6>.

JANARDHANAN, S.; SAIN, M. M. Isolation of cellulose microfibrils—an enzymatic approach. **Bioresources**, vol. 1, no. 2, p. 176–188, 2006.

JANG, J. H. J.-H.; HAYASHI, N.; HAN, S. Y. S.-Y.; PARK, C.-W. C. W.; FEBRIANTO, F.; LEE, S.-H. S. H.; KIM, N. H. N.-H. Changes in the dimensions of lignocellulose nanofibrils with different lignin contents by enzymatic hydrolysis. **Polymers**, vol. 12, no. 10, 2020. DOI 10.3390/POLYM12102201. 85092429386&doi=10.3390%2FPOLYM12102201&partnerID=40&md5=fb2c3054180ee66d874a7dc7badc8519.

JAUŠOVEC, D.; VOGRINČIČ, R.; KOKOL, V. Introduction of aldehyde vs. carboxylic groups to cellulose nanofibers using laccase/TEMPO mediated oxidation. **Carbohydrate polymers**, vol. 116, p. 74–85, 2015.

JIANG, F.; LI, T.; LI, Y.; ZHANG, Y.; GONG, A.; DAI, J.; HITZ, E.; LUO, W.; HU, L. Wood-based nanotechnologies toward sustainability. **Advanced Materials**, vol. 30, no. 1, p. 1703453, 2018.

JIANG, J.; CHEN, H.; LIU, L.; YU, J.; FAN, Y.; SAITO, T.; ISOGAI, A. Influence of chemical and enzymatic TEMPO-mediated oxidation on chemical structure and nanofibrillation of lignocellulose. **ACS Sustainable Chemistry & Engineering**, vol. 8, no. 37, p. 14198–14206, 2020. <https://doi.org/10.1021/acssuschemeng.0c05291>.

JIANG, J.; CHEN, H.; YU, J.; LIU, L.; FAN, Y.; SAITO, T.; ISOGAI, A. Rate-Limited Reaction in TEMPO/Laccase/O₂ Oxidation of Cellulose. **Macromolecular Rapid Communications**, vol. 42, no. 3, p. 2000501, 2021.

JOHNSON, E. Integrated enzyme production lowers the cost of cellulosic ethanol. **Biofuels, Bioproducts and Biorefining**, vol. 10, no. 2, p. 164–174, 1 Mar. 2016. DOI 10.1002/bbb.1634. Available at: <https://doi.org/10.1002/bbb.1634>.

JONASSON, S.; BÜNDER, A.; NIITYLÄ, T.; OKSMAN, K. Isolation and characterization of cellulose nanofibers from aspen wood using derivatizing and non-derivatizing pretreatments. **Cellulose**, vol. 27, no. 1, p. 185–203, 2020. <https://doi.org/10.1007/s10570-019-02754-w>.

JONOBI, M.; MATHEW, A. P.; OKSMAN, K. Producing low-cost cellulose nanofiber from sludge as new source of raw materials. **Industrial Crops and Products**, vol. 40, p. 232–238, 2012.

JONOBI, M.; OLADI, R.; DAVOUDPOUR, Y.; OKSMAN, K.; DUFRESNE, A.; HAMZEH, Y.; DAVOODI, R. Different preparation methods and properties of nanostructured cellulose from various natural resources and residues: a review. **Cellulose**, vol. 22, no. 2, p. 935–969, 2015. <https://doi.org/10.1007/s10570-015-0551-0>.

KABOORANI, A.; AUCLAIR, N.; RIEDL, B.; LANDRY, V. Physical and morphological properties of UV-cured cellulose nanocrystal (CNC) based nanocomposite coatings for wood furniture. **Progress in organic coatings**, vol. 93, p. 17–22, 2016.

KALIA, S.; BOUFI, S.; CELLI, A.; KANGO, S. Nanofibrillated cellulose: surface modification and potential applications. **Colloid and Polymer Science**, vol. 292, no. 1, p. 5–31, 2014.

KARGARZADEH, H.; IOELOVICH, M.; AHMAD, I.; THOMAS, S.; DUFRESNE, A. Methods for extraction of nanocellulose from various sources. **Handbook of nanocellulose and cellulose nanocomposites**, vol. 1, p. 1–51, 2017.

KARGARZADEH, H.; MARIANO, M.; GOPAKUMAR, D.; AHMAD, I.; THOMAS, S.; DUFRESNE, A.; HUANG, J.; LIN, N. Advances in cellulose nanomaterials. **Cellulose**, vol. 25, no. 4, p. 2151–2189, 2018. DOI 10.1007/s10570-018-1723-5. Available at: <https://doi.org/10.1007/s10570-018-1723-5>.

KARGARZADEH, H.; MARIANO, M.; HUANG, J.; LIN, N.; AHMAD, I.; DUFRESNE, A.; THOMAS, S. Recent developments on nanocellulose reinforced polymer nanocomposites: A review. **Polymer**, vol. 132, p. 368–393, 2017. DOI 10.1016/j.polymer.2017.09.043.

KIM, Y.; KIM, Y. K.; KIM, S.; HARBOTTLE, D.; LEE, J. W. Nanostructured potassium copper hexacyanoferrate-cellulose hydrogel for selective and rapid cesium adsorption. **Chemical Engineering Journal**, vol. 313, p. 1042–1050, 2017.

KITCHENHAM, B. A.; BUDGEN, D.; BRERETON, O. P. Using mapping studies as the basis for further research—a participant-observer case study. **Information and Software Technology**, vol. 53, no. 6, p. 638–651, 2011.

KITCHENHAM, B.; BRERETON, O. P.; BUDGEN, D.; TURNER, M.; BAILEY, J.; LINKMAN, S. Systematic literature reviews in software engineering—a systematic literature review. **Information and software technology**, vol. 51, no. 1, p. 7–15, 2009.

KITCHENHAM, B.; BRERETON, P.; BUDGEN, D. The educational value of mapping studies of software engineering literature. 2010. **Proceedings of the 32nd ACM/IEEE International Conference on Software Engineering-Volume 1** [...]. [*S. l.*: *s. n.*], 2010. p. 589–598.

KLEMM, D.; CRANSTON, E. D.; FISCHER, D.; GAMA, M.; KEDZIOR, S. A.; KRALISCH, D.; KRAMER, F.; KONDO, T.; LINDSTRÖM, T.; NIETZSCHE, S. Nanocellulose as a natural source for groundbreaking applications in materials science: Today's state. **Materials Today**, vol. 21, no. 7, p. 720–748, 2018.

KLEMM, D.; KRAMER, F.; MORITZ, S.; LINDSTRÖM, T.; ANKERFORS, M.; GRAY, D.; DORRIS, A. Nanocelluloses: a new family of nature-based materials. **Angewandte Chemie International Edition**, vol. 50, no. 24, p. 5438–5466, 2011.

KLEMM, D.; PETZOLD-WELCKE, K.; KRAMER, F.; RICHTER, T.; RADDATZ, V.; FRIED, W.; NIETZSCHE, S.; BELLMANN, T.; FISCHER, D. Biotech Nanocellulose: A review on progress in product design and today's state of technical and medical applications. **Carbohydrate Polymers**, vol. 254, no. October 2020, p. 117313, 2020. <https://doi.org/10.1016/j.carbpol.2020.117313>.

KLEMM, D.; PHILPP, B.; HEINZE, T.; HEINZE, U.; WAGENKNECHT, W. **Comprehensive cellulose chemistry. Volume 1: Fundamentals and analytical methods**. [*S. l.*]: Wiley-VCH Verlag GmbH, 1998.

KONO, H.; OEDA, I.; NAKAMURA, T. The preparation, swelling characteristics, and albumin adsorption and release behaviors of a novel chitosan-based polyampholyte

hydrogel. **Reactive and Functional Polymers**, vol. 73, no. 1, p. 97–107, 2013. DOI 10.1016/j.reactfunctpolym.2012.08.016.

KUBICEK, C. P.; KUBICEK, E. M. Enzymatic deconstruction of plant biomass by fungal enzymes. **Current opinion in chemical biology**, vol. 35, p. 51–57, 2016. .

KUMAR, D.; MURTHY, G. S. Stochastic molecular model of enzymatic hydrolysis of cellulose for ethanol production. **Biotechnology for Biofuels**, vol. 6, no. 1, 2013. DOI 10.1186/1754-6834-6-63. 84876867404&doi=10.1186%2F1754-6834-6-63&partnerID=40&md5=954dbfda828b7c519b38b12df26559a6.

KUMAR, R.; RAI, B.; GAHLYAN, S.; KUMAR, G. A comprehensive review on production, surface modification and characterization of nanocellulose derived from biomass and its commercial applications. **Express Polymer Letters**, vol. 15, no. 2, 2021.

KUUTTI, L.; PAJARI, H.; ROVIO, S.; KOKKONEN, J.; NUOPPONEN, M. Chemical recovery in TEMPO oxidation. **BioResources**, vol. 11, no. 3, p. 6050–6061, 2016. <https://doi.org/10.15376/biores.11.3.6049-6061>.

LAADILA, M. A.; SURESH, G.; ROUISSI, T.; KUMAR, P.; BRAR, S. K.; CHEIKH, R. Ben; ABOKITSE, K.; GALVEZ-COLTIER, R.; JACOB, C. Biocomposite fabrication from enzymatically treated nanocellulosic fibers and recycled polylactic acid. **Energies**, vol. 13, no. 4, 2020. <https://doi.org/10.3390/en13041003>.

LAURICHESSE, S.; AVÉROUS, L. Chemical modification of lignins: Towards biobased polymers. **Progress in polymer science**, vol. 39, no. 7, p. 1266–1290, 2014. .

LAVANYA, D.; KULKARNI, P. K.; DIXIT, M.; RAAVI, P. K.; KRISHNA, L. N. V. Sources of cellulose and their applications—A review. **International Journal of Drug Formulation and Research**, vol. 2, no. 6, p. 19–38, 2011.

LAVOINE, N.; DESLOGES, I.; DUFRESNE, A.; BRAS, J. Microfibrillated cellulose—Its barrier properties and applications in cellulosic materials: A review. **Carbohydrate polymers**, vol. 90, no. 2, p. 735–764, 2012.

LEE, S. Y.; KIM, H. U.; CHAE, T. U.; CHO, J. S.; KIM, J. W.; SHIN, J. H.; KIM, D. I.; KO, Y.-S.; JANG, W. D.; JANG, Y.-S. A comprehensive metabolic map for production of bio-based chemicals. **Nature Catalysis**, vol. 2, no. 1, p. 18–33, 2019.

LEISTRITZ, F. L.; SENECHAL, D. M.; STOWERS, M. D.; MCDONALD, W. F.; SAFFRON, C. M.; HODUR, N. M. **Preliminary feasibility analysis for an integrated biomaterials and ethanol biorefinery using wheat straw feedstock**. [*S. l.: s. n.*], 2006.

LEITE, L. S. F.; PHAM, C.; BILATTO, S.; AZEREDO, H. M. C.; CRANSTON, E. D.; MOREIRA, F. K.; MATTOSO, L. H. C.; BRAS, J. Effect of Tannic Acid and Cellulose Nanocrystals on Antioxidant and Antimicrobial Properties of Gelatin Films. **ACS Sustainable Chemistry & Engineering**, 2021.

LI, F.; MASCHERONI, E.; PIERGIOVANNI, L. The potential of nanocellulose in the packaging field: a review. **Packaging Technology and Science**, vol. 28, no. 6, p. 475–508, 2015.

- LI, James; SOLHI, L.; GODDARD-BORGER, E. D.; MATHIEU, Y.; WAKARCHUK, W. W.; WITHERS, S. G.; BRUMER, H. Four cellulose-active lytic polysaccharide monooxygenases from *Cellulomonas* species. **Biotechnology for biofuels**, vol. 14, no. 1, p. 1–19, 2021.
- LI, Juanjuan; CHA, R.; MOU, K.; ZHAO, X.; LONG, K.; LUO, H.; ZHOU, F.; JIANG, X. Nanocellulose-Based Antibacterial Materials. **Advanced healthcare materials**, vol. 7, no. 20, p. 1800334, 2018.
- LIIMATAINEN, H.; VISANKO, M.; SIRVIÖ, J.; HORMI, O.; NIINIMÄKI, J. Sulfonated cellulose nanofibrils obtained from wood pulp through regioselective oxidative bisulfite pre-treatment. **Cellulose**, vol. 20, no. 2, p. 741–749, 2013.
- LIN, N.; DUFRESNE, A. Nanocellulose in biomedicine: Current status and future prospect. **European Polymer Journal**, vol. 59, p. 302–325, 2014.
- LIU, G.; ZHANG, J.; BAO, J. Cost evaluation of cellulase enzyme for industrial-scale cellulosic ethanol production based on rigorous Aspen Plus modeling. **Bioprocess and Biosystems Engineering**, vol. 39, no. 1, p. 133–140, 2016. <https://doi.org/10.1007/s00449-015-1497-1>.
- LIU, H.; LIU, D.; YAO, F.; WU, Q. Fabrication and properties of transparent polymethylmethacrylate/cellulose nanocrystals composites. **Bioresource technology**, vol. 101, no. 14, p. 5685–5692, 2010.
- LIU, S.; QAMAR, S. A.; QAMAR, M.; BASHARAT, K.; BILAL, M. Engineered nanocellulose-based hydrogels for smart drug delivery applications. **International Journal of Biological Macromolecules**, 2021.
- LIU, X.; JIANG, Y.; SONG, X.; QIN, C.; WANG, S.; LI, K. A bio-mechanical process for cellulose nanofiber production – Towards a greener and energy conservation solution. **Carbohydrate Polymers**, vol. 208, no. November 2018, p. 191–199, 2019. DOI 10.1016/j.carbpol.2018.12.071.
- LIU, X.; JIANG, Y.; WANG, L.; SONG, X.; QIN, C.; WANG, S. Tuning of size and properties of cellulose nanofibers isolated from sugarcane bagasse by endoglucanase-assisted mechanical grinding. **Industrial Crops and Products**, vol. 146, no. July 2019, p. 112201, 2020. DOI 10.1016/j.indcrop.2020.112201.
- LIU, Y.; YU, Y.; WANG, Q.; XU, J.; FAN, X.; WANG, P.; YUAN, J. Biological–chemical modification of cellulose nanocrystal to prepare highly compatible chitosan-based nanocomposites. **Cellulose**, vol. 26, no. 9, p. 5267–5279, 2019. DOI 10.1007/s10570-019-02486-x.
- LONG, L.; TIAN, D.; HU, J.; WANG, F.; SADDLER, J. A xylanase-aided enzymatic pretreatment facilitates cellulose nanofibrillation. **Bioresource technology**, vol. 243, p. 898–904, 2017.
- LUO, L.; VAN DER VOET, E.; HUPPES, G. Biorefining of lignocellulosic feedstock– Technical, economic and environmental considerations. **Bioresource technology**, vol. 101, no. 13, p. 5023–5032, 2010.

LYND, L. R.; WEIMER, P. J.; ZYL, W. H. Van; ISAK, S. Microbial Cellulose Utilization: Fundamentals and Biotechnology Microbial Cellulose Utilization: Fundamentals and Biotechnology Downloaded from <http://mibr.asm.org/> on February 6, 2013 by INDIAN INSTITUTE OF TECHNOLOGY MADRAS. **Microbiology and Molecular Biology Reviews**, vol. 66, no. 3, p. 506–577, 2002. <https://doi.org/10.1128/MMBR.66.3.506>.

MA, H.; HSIAO, B. S.; CHU, B. Ultrafine cellulose nanofibers as efficient adsorbents for removal of UO₂²⁺ in water. **ACS Macro Letters**, vol. 1, no. 1, p. 213–216, 2012.

MADAGHIELE, M.; DEMITRI, C.; SANNINO, A.; AMBROSIO, L. Polymeric hydrogels for burn wound care: Advanced skin wound dressings and regenerative templates. **Burns & trauma**, vol. 2, no. 4, p. 2321–3868, 2014.

MANSFIELD, S. D.; MEDER, R. Cellulose hydrolysis—the role of monocomponent cellulases in crystalline cellulose degradation. **Cellulose**, vol. 10, no. 2, p. 159–169, 2003.

MARIANO, M.; EL KISSI, N.; DUFRESNE, A. Cellulose nanocrystals and related nanocomposites: review of some properties and challenges. **Journal of Polymer Science Part B: Polymer Physics**, vol. 52, no. 12, p. 791–806, 2014.

MARKETS AND MARKETS. Market research report. 2020. **Nanocellulose Market by Type (MFC & NFC, CNC/NCC, and Others), Application (Pulp&paper, composites, biomedical & pharmaceutical, electronics & sensors, and others), Region (Europe, North America, APAC, and Rest of World) - Global Forecast to 2025**.

MCCORMICK, K.; KAUTTO, N. The bioeconomy in Europe: An overview. **Sustainability**, vol. 5, no. 6, p. 2589–2608, 2013.

MERINO, S.; CHERRY, J. Progress and challenges in enzyme development for biomass utilization. **Advances in biochemical engineering/biotechnology**, vol. 108, p. 95–120, 2007.

MI, G.; SHI, D.; WANG, M.; WEBSTER, T. J. Reducing bacterial infections and biofilm formation using nanoparticles and nanostructured antibacterial surfaces. **Advanced healthcare materials**, vol. 7, no. 13, p. 1800103, 2018.

MICHELIN, M.; GOMES, D. G.; ROMANÍ, A.; POLIZELI, M. de L. T. M.; TEIXEIRA, J. A. Nanocellulose production: Exploring the enzymatic route and residues of pulp and paper industry. **Molecules**, vol. 25, no. 15, p. 1–36, 2020. <https://doi.org/10.3390/molecules25153411>.

MILLER, G. L. Use of dinitrosalicylic acid reagent for determination of reducing sugar. **Analytical chemistry**, vol. 31, no. 3, p. 426–428, 1959.

MILLER, J. **Nanocellulose: Producers, Products, and Applications: A Guide for End Users**. [S. l.]: TAPPI Press, 2017.

MOHAMMED, N.; GRISHKEWICH, N.; BERRY, R. M.; TAM, K. C. Cellulose nanocrystal–alginate hydrogel beads as novel adsorbents for organic dyes in aqueous solutions. **Cellulose**, vol. 22, no. 6, p. 3725–3738, 2015.

- MOHAMMED, N.; GRISHKEWICH, N.; WAEIJEN, H. A.; BERRY, R. M.; TAM, K. C. Continuous flow adsorption of methylene blue by cellulose nanocrystal-alginate hydrogel beads in fixed bed columns. **Carbohydrate polymers**, vol. 136, p. 1194–1202, 2016.
- MOKHENA, T. C.; JOHN, M. J. Cellulose nanomaterials: New generation materials for solving global issues. **Cellulose**, vol. 27, no. 3, p. 1149–1194, 2020.
- MOOHAN, J.; STEWART, S. A.; ESPINOSA, E.; ROSAL, A.; RODRÍGUEZ, A.; LARRAÑETA, E.; DONNELLY, R. F.; DOMÍNGUEZ-ROBLES, J. Cellulose nanofibers and other biopolymers for biomedical applications. A review. **Applied Sciences**, vol. 10, no. 1, p. 65, 2020. <https://doi.org/10.3390/app10010065>.
- MOON, R. J.; MARTINI, A.; NAIRN, J.; SIMONSEN, J.; YOUNGBLOOD, J. Cellulose nanomaterials review: structure, properties and nanocomposites. **Chemical Society Reviews**, vol. 40, no. 7, p. 3941–3994, 2011.
- MOON, R. J.; SCHUENEMAN, G. T.; SIMONSEN, J. Overview of cellulose nanomaterials, their capabilities and applications. **Jom**, vol. 68, no. 9, p. 2383–2394, 2016.
- MOREAU, C.; TAPIN-LINGUA, S.; GRISEL, S.; GIMBERT, I.; LE GALL, S.; MEYER, V.; PETIT-CONIL, M.; BERRIN, J.-G.; CATHALA, B.; VILLARES, A. Lytic polysaccharide monooxygenases (LPMOs) facilitate cellulose nanofibrils production. **Biotechnology for Biofuels**, vol. 12, Jun. 2019. <https://doi.org/10.1186/s13068-019-1501-0>.
- MORIANA, R.; VILAPLANA, F.; EK, M. Cellulose nanocrystals from forest residues as reinforcing agents for composites: A study from macro-to nano-dimensions. **Carbohydrate polymers**, vol. 139, p. 139–149, 2016.
- MUHOZA, B.; XIA, S.; ZHANG, X. Gelatin and high methyl pectin coacervates crosslinked with tannic acid: The characterization, rheological properties, and application for peppermint oil microencapsulation. **Food Hydrocolloids**, vol. 97, p. 105174, 2019.
- NAIR, S. S.; YAN, N. Effect of high residual lignin on the thermal stability of nanofibrils and its enhanced mechanical performance in aqueous environments. **Cellulose**, vol. 22, no. 5, p. 3137–3150, 2015.
- NANDI, S.; GUHA, P. A review on preparation and properties of cellulose nanocrystal-incorporated natural biopolymer. **Journal of Packaging Technology and Research**, vol. 2, no. 2, p. 149–166, 2018.
- NECHYPORCHUK, O.; BELGACEM, M. N.; BRAS, J. Production of cellulose nanofibrils: A review of recent advances. **Industrial Crops and Products**, vol. 93, p. 2–25, 2016. DOI 10.1016/j.indcrop.2016.02.016.
- NICOLL, R.; HENEIN, M. Y. Ginger (*Zingiber officinale* Roscoe): A hot remedy for cardiovascular disease? **International Journal of Cardiology**, vol. 131, no. 3, p. 408–409, 2009. DOI 10.1016/j.ijcard.2007.07.107.
- NILE, S. H.; PARK, S. W. Chromatographic analysis, antioxidant, anti-inflammatory,

and xanthine oxidase inhibitory activities of ginger extracts and its reference compounds. **Industrial Crops and Products**, vol. 70, p. 238–244, 2015. DOI 10.1016/j.indcrop.2015.03.033.

NISHIYAMA, Y.; LANGAN, P.; CHANZY, H. Crystal structure and hydrogen-bonding system in cellulose I β from synchrotron X-ray and neutron fiber diffraction. **Journal of the American Chemical Society**, vol. 124, no. 31, p. 9074–9082, 2002.

NORDLI, H. R.; PUKSTAD, B.; CHINGA-CARRASCO, G.; ROKSTAD, A. M. Ultrapure Wood Nanocellulose - Assessments of Coagulation and Initial Inflammation Potential. **ACS Applied Bio Materials**, vol. 2, no. 3, p. 1107–1118, 2019. <https://doi.org/10.1021/acsabm.8b00711>.

NORRRAHIM, M. N. F.; NURAZZI, N. M.; JENOL, M. A.; FARID, M. A. A.; JANUDIN, N.; UJANG, F. A.; YASIM-ANUAR, T. A. T.; SYED NAJMUDDIN, S. U. F.; ILYAS, R. A. Emerging development of nanocellulose as an antimicrobial material: An overview. **Materials Advances**, vol. 2, no. 11, p. 3538–3551, 2021. <https://doi.org/10.1039/d1ma00116g>.

O'SULLIVAN, A. C. Cellulose: the structure slowly unravels. **Cellulose**, vol. 4, no. 3, p. 173–207, 1997.

OKAN, D.; WOO, K.; AYELLO, E. A.; SIBBALD, G. The role of moisture balance in wound healing. **Advances in skin & wound care**, vol. 20, no. 1, p. 39–53, 2007. <https://doi.org/10.1097/00129334-200701000-00013>.

OKSMAN, K.; AITOMÄKI, Y.; MATHEW, A. P.; SIQUEIRA, G.; ZHOU, Q.; BUTYLINA, S.; TANPICHAI, S.; ZHOU, X.; HOOSHMAND, S. Review of the recent developments in cellulose nanocomposite processing. **Composites Part A: Applied Science and Manufacturing**, vol. 83, p. 2–18, 2016. DOI 10.1016/j.compositesa.2015.10.041.

OKSMAN, K.; ETANG, J. A.; MATHEW, A. P.; JONOBI, M. Cellulose nanowhiskers separated from a bio-residue from wood bioethanol production. **Biomass and Bioenergy**, vol. 35, no. 1, p. 146–152, 2011. DOI 10.1016/j.biombioe.2010.08.021.

OOI, S. Y.; AHMAD, I.; AMIN, M. C. I. M. Cellulose nanocrystals extracted from rice husks as a reinforcing material in gelatin hydrogels for use in controlled drug delivery systems. **Industrial Crops and Products**, vol. 93, p. 227–234, 2016. DOI <https://doi.org/10.1016/j.indcrop.2015.11.082>.

OPT VELD, R. C.; WALBOOMERS, X. F.; JANSEN, J. A.; WAGENER, F. A. D. T. G. Design Considerations for Hydrogel Wound Dressings: Strategic and Molecular Advances. **Tissue Engineering - Part B: Reviews**, vol. 26, no. 3, p. 230–248, 2020. <https://doi.org/10.1089/ten.teb.2019.0281>.

OWOYOKUN, T.; BERUMEN, C. M. P.; LUÉVANOS, A. M.; CANTÚ, L.; CENICEROS, A. C. L. Cellulose Nanocrystals: Obtaining and Sources of a Promising Bionanomaterial for Advanced Applications. 2020.

PAAKKO, M.; ANKERFORS, M.; KOSONEN, H.; NYKANEN, A.; AHOLA, S.; OSTERBERG, M.; RUOKOLAINEN, J.; LAINE, J.; LARSSON, P. T.; IKKALA, O.;

LINDSTROM, T.; PÄÄKKO, M.; ANKERFORS, M.; KOSONEN, H.; NYKÄNEN, A.; AHOLA, S.; ÖSTERBERG, M.; RUOKOLAINEN, J.; LAINE, J.; ... IKKALA, O. Enzymatic hydrolysis combined with mechanical shearing and high-pressure homogenization for nanoscale cellulose fibrils and strong gels. **Biomacromolecules**, 1155 16TH ST, NW, WASHINGTON, DC 20036 USA, vol. 8, no. 6, p. 1934–1941, Jun. 2007. DOI 10.1021/bm061215p.

PAILLER-MATTEI, C.; BEC, S.; ZAHOUANI, H. In vivo measurements of the elastic mechanical properties of human skin by indentation tests. **Medical Engineering and Physics**, vol. 30, no. 5, p. 599–606, 2008. <https://doi.org/10.1016/j.medengphy.2007.06.011>.

PANDEY, A. Pharmaceutical and biomedical applications of cellulose nanofibers: a review. **Environmental Chemistry Letters**, , p. 1–13, 2021.

PANDEY, P.; KUILA, A.; TULI, D. K. Chapter 6 - Cellulase: An overview. *In*: TULI, D. K.; KUILA, A. B. T.-C. S. and F. S. of M. C. (eds.). [*S. l.*]: Elsevier, 2021. p. 95–113. DOI <https://doi.org/10.1016/B978-0-12-821882-2.00015-6>. Available at: <https://www.sciencedirect.com/science/article/pii/B9780128218822000156>.

PARK, N.-M.; CHOI, S.; OH, J. E.; HWANG, D. Y. Facile extraction of cellulose nanocrystals. **Carbohydrate polymers**, vol. 223, p. 115114, 2019.

PASQUI, D.; TORRICELLI, P.; DE CAGNA, M.; FINI, M.; BARBUCCI, R. Carboxymethyl cellulose—hydroxyapatite hybrid hydrogel as a composite material for bone tissue engineering applications. **Journal of Biomedical Materials Research Part A**, vol. 102, no. 5, p. 1568–1579, 2014.

PASQUINI, D.; DE MORAIS TEIXEIRA, E.; DA SILVA CURVELO, A. A.; BELGACEM, M. N.; DUFRESNE, A. Extraction of cellulose whiskers from cassava bagasse and their applications as reinforcing agent in natural rubber. **Industrial Crops and Products**, vol. 32, no. 3, p. 486–490, 2010. .

PAULY, M.; KEEGSTRA, K. Cell-wall carbohydrates and their modification as a resource for biofuels. **The Plant Journal**, vol. 54, no. 4, p. 559–568, 2008.

PAYNE, C. M.; KNOTT, B. C.; MAYES, H. B.; HANSSON, H.; HIMMEL, M. E.; SANDGREN, M.; STÅHLBERG, J.; BECKHAM, G. T. Fungal Cellulases. **Chemical Reviews**, vol. 115, no. 3, p. 1308–1448, 11 Feb. 2015. DOI 10.1021/cr500351c.

PENNELLS, J.; GODWIN, I. D.; AMIRALIAN, N.; MARTIN, D. J. Trends in the production of cellulose nanofibers from non-wood sources. **Cellulose**, vol. 27, no. 2, p. 575–593, 2020. DOI 10.1007/s10570-019-02828-9.

PEPPAS, N. A.; BURES, P.; LEOBANDUNG, W.; ICHIKAWA, H. Hydrogels in pharmaceutical formulations. **European Journal of Pharmaceutics and Biopharmaceutics**, vol. 50, no. 1, p. 27–46, 2000. [https://doi.org/10.1016/S0939-6411\(00\)00090-4](https://doi.org/10.1016/S0939-6411(00)00090-4).

PEPPAS, Nikolaos A; MIKOS, A. G. Preparation methods and structure of hydrogels. **Hydrogels in medicine and pharmacy**. [*S. l.*]: CRC Press, 2019. p. 1–26.

PERIĆ, M.; PUTZ, R.; PAULIK, C. 3D-printed pla filaments reinforced with nanofibrillated cellulose. **Journal of Renewable Materials**, 2020. DOI 10.32604/jrm.2020.09284.

PETERSEN, K.; VAKKALANKA, S.; KUZNIARZ, L. Guidelines for conducting systematic mapping studies in software engineering: An update. **Information and Software Technology**, vol. 64, p. 1–18, 2015. DOI 10.1016/j.infsof.2015.03.007. Available at: <http://dx.doi.org/10.1016/j.infsof.2015.03.007>.

PETROKOFISKY, G. Guidelines and Standards for Evidence Synthesis in Environmental Management: Version 5.0. 2018.

PHANTHONG, P.; GUAN, G.; MA, Y.; HAO, X.; ABUDULA, A. Effect of ball milling on the production of nanocellulose using mild acid hydrolysis method. **Journal of the Taiwan Institute of Chemical Engineers**, vol. 60, p. 617–622, 2016.

PHANTHONG, P.; KARNJANAKOM, S.; REUBROYCHAROEN, P.; HAO, X.; ABUDULA, A.; GUAN, G. A facile one-step way for extraction of nanocellulose with high yield by ball milling with ionic liquid. **Cellulose**, vol. 24, no. 5, p. 2083–2093, 2017.

PHANTHONG, P.; REUBROYCHAROEN, P.; HAO, X.; XU, G.; ABUDULA, A.; GUAN, G. Nanocellulose: Extraction and application. **Carbon Resources Conversion**, vol. 1, no. 1, p. 32–43, 2018.

POLICEGODRA, R. S.; ARADHYA, S. M. Structure and biochemical properties of starch from an unconventional source-Mango ginger (*Curcuma amada* Roxb.) rhizome. **Food Hydrocolloids**, vol. 22, no. 4, p. 513–519, 2008. <https://doi.org/10.1016/j.foodhyd.2007.01.008>.

POLIZELI, M.; RIZZATTI, A. C. S.; MONTI, R.; TERENCEZI, H. F.; JORGE, J. A.; AMORIM, D. S. Xylanases from fungi: properties and industrial applications. **Applied microbiology and biotechnology**, vol. 67, no. 5, p. 577–591, 2005.

POLLINI, M.; RUSSO, M.; LICCIULLI, A.; SANNINO, A.; MAFFEZZOLI, A. Characterization of antibacterial silver coated yarns. **Journal of Materials Science: Materials in Medicine**, vol. 20, no. 11, p. 2361–2366, 2009.

POURJAVADI, A.; AYYARI, M.; AMINI-FAZL, M. S. Taguchi optimized synthesis of collagen-g-poly(acrylic acid)/kaolin composite superabsorbent hydrogel. **European Polymer Journal**, vol. 44, no. 4, p. 1209–1216, 2008. <https://doi.org/10.1016/j.eurpolymj.2008.01.032>.

PULIDINDI, K.; PANDEY, H. Nanocellulose Market Size By Product (Nanofibrillated Cellulose, Nanocrystalline Cellulose), By Application (Composites, Paper Processing, Food & Beverages, Paints & Coatings, Oil & Gas, Personal Care), Industry Analysis Report, Regional Outlook, Growth P. 2020. Available at: <https://www.gminsights.com/pressrelease/nanocellulose-market>.

PULLIN, A. S.; STEWART, G. B. Guidelines for systematic review in conservation and environmental management. **Conservation biology**, vol. 20, no. 6, p. 1647–1656, 2006.

PUSNIK, M.; IMERI, M.; DEPIERRAZ, G.; BRUININK, A.; ZINN, M. The agar

diffusion scratch assay - A novel method to assess the bioactive and cytotoxic potential of new materials and compounds. **Scientific Reports**, vol. 6, no. 1, p. 20854, 2016. DOI 10.1038/srep20854. Available at: <https://doi.org/10.1038/srep20854>.

QING, Y.; SABO, R.; WU, Y.; ZHU, J. Y.; CAI, Z. Self-assembled optically transparent cellulose nanofibril films: effect of nanofibril morphology and drying procedure. **Cellulose**, vol. 22, no. 2, p. 1091–1102, 2015. <https://doi.org/10.1007/s10570-015-0563-9>.

RABAÇAL, M.; FERREIRA, A. F.; SILVA, C. A. M.; COSTA, M. **Biorefineries: targeting energy, high value products and waste valorisation**. [S. l.]: Springer, vol. 57, 2017.

RAGAUSKAS, A. J.; WILLIAMS, C. K.; DAVISON, B. H.; BRITOVSEK, G.; CAIRNEY, J.; ECKERT, C. A.; FREDERICK, W. J.; HALLETT, J. P.; LEAK, D. J.; LIOTTA, C. L. The path forward for biofuels and biomaterials. **science**, vol. 311, no. 5760, p. 484–489, 2006.

RAHIKAINEN, J.; CECCHERINI, S.; MOLINIER, M.; HOLOPAINEN-MANTILA, U.; REZA, M.; VÄISÄNEN, S.; PURANEN, T.; KRUIUS, K.; VUORINEN, T.; MALONEY, T. Effect of cellulase family and structure on modification of wood fibres at high consistency. **Cellulose**, vol. 26, no. 8, p. 5085–5103, 2019.

RAJINIPRIYA, M.; NAGALAKSHMAIAH, M.; ROBERT, M.; ELKOUN, S. Homogenous and transparent nanocellulosic films from carrot. **Industrial Crops and Products**, vol. 118, p. 53–64, 2018.

RAMOS, M. D. L. P.; PIRICH, C. L.; PICHETH, G. F.; FONTES, A. M.; DELGADO-AGUILAR, M.; RAMOS, L. P. Disruptive enzyme-based strategies to isolate nanocelluloses: a review. **Cellulose**, vol. 27, no. 10, p. 5457–5475, 2020. <https://doi.org/10.1007/s10570-020-03185-8>.

RANA, V.; ECKARD, A. D.; TELLER, P.; AHRING, B. K. On-site enzymes produced from *Trichoderma reesei* RUT-C30 and *Aspergillus saccharolyticus* for hydrolysis of wet exploded corn stover and loblolly pine. **Bioresource Technology**, vol. 154, p. 282–289, 2014. DOI 10.1016/j.biortech.2013.12.059.

REYES, F. G. R.; D'APPOLONIA, B. L.; CIACCO, C. F.; MONTGOMERY, M. W. Characterization of Starch from Ginger Root (*Zingiber officinale*). **Starch - Stärke**, vol. 34, no. 2, p. 40–44, 1982. <https://doi.org/10.1002/star.19820340203>.

RHEINWATD, J. G.; GREEN, H. Serial cultivation of strains of human epidermal keratinocytes: the formation keratinizing colonies from single cell is. **Cell**, vol. 6, no. 3, p. 331–343, 1975. DOI [https://doi.org/10.1016/S0092-8674\(75\)80001-8](https://doi.org/10.1016/S0092-8674(75)80001-8). Available at: <http://www.sciencedirect.com/science/article/pii/S0092867475800018>.

RHIM, J.-W.; PARK, H.-M.; HA, C.-S. Bio-nanocomposites for food packaging applications. **Progress in polymer science**, vol. 38, no. 10–11, p. 1629–1652, 2013.

RIBEIRO, R. S. A.; POHLMANN, B. C.; CALADO, V.; BOJORGE, N.; PEREIRA JR, N. Production of nanocellulose by enzymatic hydrolysis: Trends and challenges. **Engineering in Life Sciences**, vol. 19, no. 4, p. 279–291, 2019.

ROHMAN, A.; WINDARSIH, A.; ERWANTO, Y.; ZAKARIA, Z. Review on analytical methods for analysis of porcine gelatine in food and pharmaceutical products for halal authentication. **Trends in Food Science & Technology**, vol. 101, p. 122–132, 2020.

ROMAN, M.; WINTER, W. T. Effect of sulfate groups from sulfuric acid hydrolysis on the thermal degradation behavior of bacterial cellulose. **Biomacromolecules**, vol. 5, no. 5, p. 1671–1677, 2004.

ROMANELLI, J. P.; MELI, P.; NAVES, R. P.; ALVES, M. C.; RODRIGUES, R. R. Reliability of evidence-review methods in restoration ecology. **Conservation Biology**, vol. 35, no. 1, p. 142–154, 2021.

ROSALES-CALDERON, O.; ARANTES, V. A review on commercial-scale high-value products that can be produced alongside cellulosic ethanol. **Biotechnology for biofuels**, vol. 12, no. 1, p. 1–58, 2019.

ROSALES-CALDERON, O.; PERIRA, B.; ARANTES, V. Economic assessment of the conversion of Bleached Eucalyptus Kraft Pulp into cellulose nanocrystals in a stand-alone facility via acid and enzymatic hydrolysis. **Biofuels, Bioproducts & Biorefining (Accepted)**, , p. 1–14, 2021. <https://doi.org/10.1002/bbb.2277>.

ROSSI, B. R.; PELLEGRINI, V. O. A.; CORTEZ, A. A.; CHIROMITO, E. M. S.; CARVALHO, A. J. F.; PINTO, L. O.; REZENDE, C. A.; MASTELARO, V. R.; POLIKARPOV, I. Cellulose nanofibers production using a set of recombinant enzymes. **Carbohydrate Polymers**, vol. 256, Mar. 2021. <https://doi.org/10.1016/j.carbpol.2020.117510>.

SAITO, T.; HIROTA, M.; TAMURA, N.; KIMURA, S.; FUKUZUMI, H.; HEUX, L.; ISOGAI, A. Individualization of nano-sized plant cellulose fibrils by direct surface carboxylation using TEMPO catalyst under neutral conditions. **Biomacromolecules**, vol. 10, no. 7, p. 1992–1996, 2009. <https://doi.org/10.1021/bm900414t>.

SAITO, T.; KIMURA, S.; NISHIYAMA, Y.; ISOGAI, A. Cellulose nanofibers prepared by TEMPO-mediated oxidation of native cellulose. **Biomacromolecules**, vol. 8, no. 8, p. 2485–2491, 2007.

SANG, S.; SNOOK, H. D.; TAREQ, F. S.; FASINA, Y. Precision Research on Ginger: The Type of Ginger Matters. **Journal of agricultural and food chemistry**, vol. 68, no. 32, p. 8517–8523, 2020. <https://doi.org/10.1021/acs.jafc.0c03888>.

SHELLER, H. V.; ULVSKOV, P. Hemicelluloses. **Annual review of plant biology**, vol. 61, p. 263–289, 2010.

SCHULTZ, G. S.; SIBBALD, R. G.; FALANGA, V.; AYELLO, E. A.; DOWSETT, C.; HARDING, K.; ROMANELLI, M.; STACEY, M. C.; TEOT, L.; VANSCHIEDT, W. Wound bed preparation: a systematic approach to wound management. **Wound repair and regeneration : official publication of the Wound Healing Society [and] the European Tissue Repair Society**, United States, vol. 11 Suppl 1, p. S1-28, Mar. 2003. <https://doi.org/10.1046/j.1524-475x.11.s2.1.x>.

SCHWERTNER, H. A.; RIOS, D. C.; PASCOE, J. E. Variation in Concentration and Labeling of Ginger Root Dietary Supplements. **Obstetrics & Gynecology**, vol. 107, no.

6, p. 1337–1343, 2006.

SEGAL, L.; CREELY, J. J.; MARTIN JR, A. E.; CONRAD, C. M. An empirical method for estimating the degree of crystallinity of native cellulose using the X-ray diffractometer. **Textile research journal**, vol. 29, no. 10, p. 786–794, 1959.

SEHAQUI, H.; LIU, A.; ZHOU, Q.; BERGLUND, L. A. Fast Preparation Procedure for Large, Flat Cellulose and Cellulose/Inorganic Nanopaper Structures. **Biomacromolecules**, vol. 11, no. 9, p. 2195–2198, 13 Sep. 2010. DOI 10.1021/bm100490s.

SEMWAL, R. B.; SEMWAL, D. K.; COMBRINCK, S.; VILJOEN, A. M. Gingerols and shogaols: Important nutraceutical principles from ginger. **Phytochemistry**, vol. 117, p. 554–568, 2015. DOI 10.1016/j.phytochem.2015.07.012.

SHATKIN, J. A.; WEGNER, T. H.; BILEK, E. M. T.; COWIE, J. Market projections of cellulose nanomaterial-enabled products-Part 1: Applications. **TAPPI Journal, Volume 13, Number 5, 2014; pp. 9-16.**, vol. 13, no. 5, p. 9–16, 2014.

SHLONSKY, A.; NOONAN, E.; LITTELL, J. H.; MONTGOMERY, P. The Role of Systematic Reviews and the Campbell Collaboration in the Realization of Evidence-Informed Practice. **Clinical Social Work Journal**, vol. 39, no. 4, p. 362–368, 2011. DOI 10.1007/s10615-010-0307-0. Available at: <https://doi.org/10.1007/s10615-010-0307-0>.

SHOJAEIARANI, J.; BAJWA, D.; SHIRZADIFAR, A. A review on cellulose nanocrystals as promising biocompounds for the synthesis of nanocomposite hydrogels. **Carbohydrate polymers**, vol. 216, p. 247–259, 2019.

SHUTAVA, T.; PROUTY, M.; KOMMIREDDY, D.; LVOV, Y. pH responsive decomposable layer-by-layer nanofilms and capsules on the basis of tannic acid. **Macromolecules**, vol. 38, no. 7, p. 2850–2858, 2005.

SINGH, G.; KAPOOR, I. P. S.; SINGH, P.; DE HELUANI, C. S.; DE LAMPASONA, M. P.; CATALAN, C. A. N. Chemistry, antioxidant and antimicrobial investigations on essential oil and oleoresins of *Zingiber officinale*. **Food and Chemical Toxicology**, vol. 46, no. 10, p. 3295–3302, 2008. DOI 10.1016/j.fct.2008.07.017. Available at: <http://dx.doi.org/10.1016/j.fct.2008.07.017>.

SINGH, M. R.; SARAF, S.; VYAS, A.; JAIN, V.; SINGH, D. Innovative approaches in wound healing: Trajectory and advances. **Artificial Cells, Nanomedicine and Biotechnology**, vol. 41, no. 3, p. 202–212, 2013. <https://doi.org/10.3109/21691401.2012.716065>.

SIRÓ, I.; PLACKETT, D. Microfibrillated cellulose and new nanocomposite materials: a review. **Cellulose**, vol. 17, no. 3, p. 459–494, 2010.

SIVASOTHY, Y.; CHONG, W. K.; HAMID, A.; ELDEEN, I. M.; SULAIMAN, S. F.; AWANG, K. Essential oils of *Zingiber officinale* var. *rubrum* Theilade and their antibacterial activities. **Food Chemistry**, vol. 124, no. 2, p. 514–517, 2011. DOI 10.1016/j.foodchem.2010.06.062.

SJOSTROM, E. **Wood chemistry: fundamentals and applications**. [S. l.]: Gulf

professional publishing, 1993.

SLAUGHTER, B. V.; KHURSHID, S. S.; FISHER, O. Z.; KHADEMHOSEINI, A.; PEPPAS, N. A. Hydrogels in regenerative medicine. **Advanced Materials**, vol. 21, no. 32–33, p. 3307–3329, 2009. <https://doi.org/10.1002/adma.200802106>.

SOFLA, M. R. K.; BROWN, R. J.; TSUZUKI, T.; RAINEY, T. J. A comparison of cellulose nanocrystals and cellulose nanofibres extracted from bagasse using acid and ball milling methods. **Advances in Natural Sciences: Nanoscience and Nanotechnology**, vol. 7, no. 3, p. 35004, 2016.

SONG, H.-T.; GAO, Y.; YANG, Y.-M.; XIAO, W.-J.; LIU, S.-H.; XIA, W.-C.; LIU, Z.-L.; YI, L.; JIANG, Z.-B. Synergistic effect of cellulase and xylanase during hydrolysis of natural lignocellulosic substrates. **Bioresource technology**, vol. 219, p. 710–715, 2016.

SONG, Q.; WINTER, W. T.; BUJANOVIC, B. M.; AMIDON, T. E. Nanofibrillated Cellulose (NFC): A High-Value Co-Product that Improves the Economics of Cellulosic Ethanol Production. **ENERGIES**, vol. 7, no. 2, p. 607–618, 2014. <https://doi.org/10.3390/en7020607>.

SONI, B.; SCHILLING, M. W.; MAHMOUD, B. Transparent bionanocomposite films based on chitosan and TEMPO-oxidized cellulose nanofibers with enhanced mechanical and barrier properties. **Carbohydrate polymers**, vol. 151, p. 779–789, 2016.

SOOD, A.; GRANICK, M. S.; TOMASELLI, N. L. Wound Dressings and Comparative Effectiveness Data. **Advances in Wound Care**, vol. 3, no. 8, p. 511–529, 2014. <https://doi.org/10.1089/wound.2012.0401>.

SOOD, N.; BHARDWAJ, A.; MEHTA, S.; MEHTA, A. Stimuli-responsive hydrogels in drug delivery and tissue engineering. **Drug delivery**, vol. 23, no. 3, p. 748–770, 2016.

SØRENSEN, A.; TELLER, P. J.; LÜBECK, P. S.; AHRING, B. K. Onsite enzyme production during bioethanol production from biomass: screening for suitable fungal strains. **Applied biochemistry and biotechnology**, vol. 164, no. 7, p. 1058–1070, 2011. <https://doi.org/10.1007/s12010-011-9194-2>.

SPENCE, K. L.; VENDITTI, R. A.; ROJAS, O. J.; HABIBI, Y.; PAWLAK, J. J. A comparative study of energy consumption and physical properties of microfibrillated cellulose produced by different processing methods. **Cellulose**, vol. 18, no. 4, p. 1097–1111, 2011.

SPINELLA, S.; MAIORANA, A.; QIAN, Q.; DAWSON, N. J.; HEPWORTH, V.; MCCALLUM, S. A.; GANESH, M.; SINGER, K. D.; GROSS, R. A. Concurrent cellulose hydrolysis and esterification to prepare a surface-modified cellulose nanocrystal decorated with carboxylic acid moieties. **ACS Sustainable Chemistry & Engineering**, vol. 4, no. 3, p. 1538–1550, 2016. .

SQUINCA, P.; BERGLUND, L.; HANNA, K.; RAKAR, J.; JUNKER, J.; KHALAF, H.; FARINAS, C. S.; OKSMAN, K. Multifunctional Ginger Nanofiber Hydrogels with Tunable Absorption: The Potential for Advanced Wound Dressing Applications. **Biomacromolecules**, vol. 22, no. 8, p. 3202–3215, 2021.

SQUINCA, P.; BILATTO, S.; BADINO, A. C.; FARINAS, C. S. Nanocellulose Production in Future Biorefineries: An Integrated Approach Using Tailor-Made Enzymes. **ACS Sustainable Chemistry and Engineering**, vol. 8, no. 5, p. 2277–2286, 2020. <https://doi.org/10.1021/acssuschemeng.9b06790>.

SUN, B.; PENG, G.; DUAN, L.; XU, A.; LI, X. Pretreatment by NaOH swelling and then HCl regeneration to enhance the acid hydrolysis of cellulose to glucose. **BIORESOURCE TECHNOLOGY**, vol. 196, p. 454–458, Nov. 2015. <https://doi.org/10.1016/j.biortech.2015.08.009>.

SUN, F. F.; HONG, J.; HU, J.; SADDLER, J. N.; FANG, X.; ZHANG, Z.; SHEN, S. Accessory enzymes influence cellulase hydrolysis of the model substrate and the realistic lignocellulosic biomass. **Enzyme and microbial technology**, vol. 79, p. 42–48, 2015.

SUN, F.; NORDLI, H. R.; PUKSTAD, B.; GAMSTEDT, E. K.; CHINGA-CARRASCO, G.; KRISTOFER GAMSTEDT, E.; CHINGA-CARRASCO, G. Mechanical characteristics of nanocellulose-PEG bionanocomposite wound dressings in wet conditions. **Journal of the Mechanical Behavior of Biomedical Materials**, vol. 69, no. January, p. 377–384, 2017. DOI 10.1016/j.jmbbm.2017.01.049. Available at: <http://dx.doi.org/10.1016/j.jmbbm.2017.01.049>.

TADMOR, Z.; GOGOS, C. G. **Principles of polymer processing**. [S. l.]: John Wiley & Sons, 2013.

TAHERI, P.; JAHANMARDI, R.; KOOSHA, M.; ABDI, S. Physical, mechanical and wound healing properties of chitosan/gelatin blend films containing tannic acid and/or bacterial nanocellulose. **International journal of biological macromolecules**, vol. 154, p. 421–432, 2020.

TAKAHASHI, H.; CHOI, P.-K. Sol–Gel Transition in Gelatin Observed with Surface Waves. **Japanese Journal of Applied Physics**, vol. 35, no. Part 1, No. 5B, p. 2939–2943, 1996. DOI 10.1143/jjap.35.2939. Available at: <http://dx.doi.org/10.1143/JJAP.35.2939>.

TANG, Y.; SHEN, X.; ZHANG, J.; GUO, D.; KONG, F.; ZHANG, N. Extraction of cellulose nano-crystals from old corrugated container fiber using phosphoric acid and enzymatic hydrolysis followed by sonication. **Carbohydrate Polymers**, 2015. DOI 10.1016/j.carbpol.2015.02.063.

TAO, P.; WU, Z.; XING, C.; ZHANG, Q.; WEI, Z.; NIE, S. Effect of enzymatic treatment on the thermal stability of cellulose nanofibrils. **Cellulose**, 2019. DOI 10.1007/s10570-019-02634-3.

TAPPI, N. T203 cm-99. “**Alpha-, beta-and gamma-cellulose in pulp**, 1999. .

TAPPI, T. 204 cm-97. **Solvent extractives of wood and pulp**, 1997.

TAPPI, T. 222 om-02: Acid-insoluble lignin in wood and pulp. **2002–2003 TAPPI Test Methods**, 2002.

TEJADO, A.; ALAM, M. N.; ANTAL, M.; YANG, H.; VAN DE VEN, T. G. M. Energy requirements for the disintegration of cellulose fibers into cellulose nanofibers. **Cellulose**, vol. 19, no. 3, p. 831–842, 2012.

TEODORO, K. B. R.; SANFELICE, R. C.; MIGLIORINI, F. L.; PAVINATTO, A.; FACURE, M. H. M.; CORREA, D. S. A Review on the Role and Performance of Cellulose Nanomaterials in Sensors. **ACS Sensors**, vol. 6, no. 7, p. 2473–2496, 23 Jul. 2021. DOI 10.1021/acssensors.1c00473.

THAKUR, V.; GULERIA, A.; KUMAR, S.; SHARMA, S.; SINGH, K. Recent advances in nanocellulose processing, functionalization and applications: A review. **Materials Advances**, vol. 2, no. 6, p. 1872–1895, 2021. <https://doi.org/10.1039/d1ma00049g>.

THOMAS, B.; RAJ, M. C.; JOY, J.; MOORES, A.; DRISKO, G. L.; SANCHEZ, C. Nanocellulose, a versatile green platform: from biosources to materials and their applications. **Chemical reviews**, vol. 118, no. 24, p. 11575–11625, 2018.

THYGESEN, L. G.; HIDAYAT, B. J.; JOHANSEN, K. S.; FELBY, C. Role of supramolecular cellulose structures in enzymatic hydrolysis of plant cell walls. **Journal of Industrial Microbiology and Biotechnology**, vol. 38, no. 8, p. 975–983, 2011. DOI 10.1007/s10295-010-0870-y.

TIAN, C.; YI, J.; WU, Y.; WU, Q.; QING, Y.; WANG, L. Preparation of highly charged cellulose nanofibrils using high-pressure homogenization coupled with strong acid hydrolysis pretreatments. **Carbohydrate polymers**, vol. 136, p. 485–492, 2016.

TONG, X.; SHEN, W.; CHEN, X.; JIA, M.; ROUX, J.-C. Preparation and mechanism analysis of morphology-controlled cellulose nanocrystals via compound enzymatic hydrolysis of eucalyptus pulp. **Journal of Applied Polymer Science**, 2020. DOI 10.1002/app.48407.

TRACHE, D.; HUSSIN, M. H.; HAAFIZ, M. K. M.; THAKUR, V. K. Recent progress in cellulose nanocrystals: sources and production. **Nanoscale**, vol. 9, no. 5, p. 1763–1786, 2017.

TRACHE, D.; TARCHOUN, A. F.; DERRADJI, M.; HAMIDON, T. S.; MASRUCHIN, N.; BROSSE, N.; HUSSIN, M. H. **Nanocellulose: From Fundamentals to Advanced Applications**. [*S. l.: s. n.*], 2020. vol. 8, . <https://doi.org/10.3389/fchem.2020.00392>.

TSUKAMOTO, J.; DURÁN, N.; TASIC, L. Nanocellulose and bioethanol production from orange waste using isolated microorganisms. **Journal of the Brazilian Chemical Society**, vol. 24, no. 9, p. 1537–1543, 2013.

UNITED NATIONS. **The Sustainable Development Goals Report 2016**. [*S. l.: s. n.*], 2016. Available at: <https://unstats.un.org/sdgs/report/2016/The Sustainable Development Goals Report 2016.pdf>. Accessed on: 10 Jan. 2021.

VALENZUELA, S. V.; VALLS, C.; SCHINK, V.; SÁNCHEZ, D.; RONCERO, M. B.; DIAZ, P.; MARTÍNEZ, J.; PASTOR, F. I. J.; SANCHEZ, D.; BLANCA RONCERO, M.; DIAZ, P.; MARTINEZ, J.; JAVIER PASTOR, F. I. Differential activity of lytic polysaccharide monoxygenases on celluloses of different crystallinity. Effectiveness in the sustainable production of cellulose nanofibrils. **CARBOHYDRATE POLYMERS**, vol. 207, no. July 2018, p. 59–67, Mar. 2019. <https://doi.org/10.1016/j.carbpol.2018.11.076>.

VALLS, C.; JAVIER PASTOR, F. I.; BLANCA RONCERO, M.; VIDAL, T.; DIAZ, P.;

MARTÍNEZ, J.; VALENZUELA, S. V. Assessing the enzymatic effects of cellulases and LPMO in improving mechanical fibrillation of cotton linters. **Biotechnology for Biofuels**, vol. 12, p. 1–14, 2019. DOI 10.1186/s13068-019-1502-z.

VAN DEN BRINK, J.; MAITAN-ALFENAS, G. P.; ZOU, G.; WANG, C.; ZHOU, Z.; GUIMARÃES, V. M.; DE VRIES, R. P. Synergistic effect of *Aspergillus niger* and *Trichoderma reesei* enzyme sets on the saccharification of wheat straw and sugarcane bagasse. **Biotechnology Journal**, vol. 9, no. 10, p. 1329–1338, 1 Oct. 2014. DOI <https://doi.org/10.1002/biot.201400317>.

VAN ECK, N. J.; WALTMAN, L. Software survey: VOSviewer, a computer program for bibliometric mapping. **scientometrics**, vol. 84, no. 2, p. 523–538, 2010.

VANDERFLEET, O. M.; CRANSTON, E. D. Production routes to tailor the performance of cellulose nanocrystals. **Nature Reviews Materials**, vol. 6, no. 2, p. 124–144, 2021.

VASCONCELOS, N. F.; FEITOSA, J. P. A.; DA GAMA, F. M. P.; MORAIS, J. P. S.; ANDRADE, F. K.; DE SOUZA, M. de S. M.; DE FREITAS ROSA, M. Bacterial cellulose nanocrystals produced under different hydrolysis conditions: properties and morphological features. **Carbohydrate polymers**, vol. 155, p. 425–431, 2017.

VILLARES, A.; MOREAU, C.; BENNATI-GRANIER, C.; GARAJOVA, S.; FOUCAT, L.; FALOURD, X.; SAAKE, B.; BERRIN, J.-G.; CATHALA, B. Lytic polysaccharide monooxygenases disrupt the cellulose fibers structure. **Scientific Reports**, vol. 7, 2017. DOI 10.1038/srep40262.

VOELKER, S. L.; LACHENBRUCH, B.; MEINZER, F. C.; STRAUSS, S. H. Reduced wood stiffness and strength, and altered stem form, in young antisense 4CL transgenic poplars with reduced lignin contents. **New Phytologist**, vol. 189, no. 4, p. 1096–1109, 2011.

WANG, D.-C.; YU, H.-Y.; QI, D.; RAMASAMY, M.; YAO, J.; TANG, F.; TAM, K. (Michael) C.; NI, Q. Supramolecular Self-Assembly of 3D Conductive Cellulose Nanofiber Aerogels for Flexible Supercapacitors and Ultrasensitive Sensors. **ACS APPLIED MATERIALS & INTERFACES**, vol. 11, no. 27, p. 24435–24446, Jul. 2019. <https://doi.org/10.1021/acsami.9b06527>.

WANG, D.; YU, H.; FAN, X.; GU, J.; YE, S.; YAO, J.; NI, Q. High Aspect Ratio Carboxylated Cellulose Nanofibers Cross-linked to Robust Aerogels for Superabsorption–Flocculants: Paving Way from Nanoscale to Macroscale. **ACS Applied Materials & Interfaces**, vol. 10, no. 24, p. 20755–20766, 20 Jun. 2018. DOI 10.1021/acsami.8b04211.

WANG, J.; CHAE, M.; BEYENE, D.; SAUVAGEAU, D.; BRESSLER, D. C. Co-production of ethanol and cellulose nanocrystals through self-cycling fermentation of wood pulp hydrolysate. **Bioresource Technology**, 2021. DOI 10.1016/j.biortech.2021.124969.

WANG, Q.; YAO, Q.; LIU, J.; SUN, J.; ZHU, Q.; CHEN, H. **Processing nanocellulose to bulk materials: a review**. [S. l.]: Springer Netherlands, 2019. vol. 26, . DOI 10.1007/s10570-019-02642-3.

WANG, R.; CHEN, L.; ZHU, J. Y.; YANG, R. Tailored and integrated production of carboxylated cellulose nanocrystals (CNC) with nanofibrils (CNF) through maleic acid hydrolysis. **ChemNanoMat**, vol. 3, no. 5, p. 328–335, 2017.

WANG, W.; MOZUCH, M. D.; SABO, R. C.; KERSTEN, P.; ZHU, J. Y.; JIN, Y. Production of cellulose nanofibrils from bleached eucalyptus fibers by hyperthermostable endoglucanase treatment and subsequent microfluidization. **Cellulose**, 2015. DOI 10.1007/s10570-014-0465-2.

WANG, Wangxia; MOZUCH, M. D.; SABO, R. C.; KERSTEN, P.; ZHU, J. Y.; JIN, Y. Endoglucanase post-milling treatment for producing cellulose nanofibers from bleached eucalyptus fibers by a supermasscolloider. **Cellulose**, vol. 23, no. 3, p. 1859–1870, 2016.

WANG, Zhaohui; CARLSSON, D. O.; TAMMELA, P.; HUA, K.; ZHANG, P.; NYHOLM, L.; STRØMME, M. Surface modified nanocellulose fibers yield conducting polymer-based flexible supercapacitors with enhanced capacitances. **ACS nano**, vol. 9, no. 7, p. 7563–7571, 2015.

WANG, Zhenggang; FAN, X.; HE, M.; CHEN, Z.; WANG, Y.; YE, Q.; ZHANG, H.; ZHANG, L. Construction of cellulose–phosphor hybrid hydrogels and their application for bioimaging. **Journal of Materials Chemistry B**, vol. 2, no. 43, p. 7559–7566, 2014.

WANG, Zi; TANG, L.; LIN, F.; SHEN, Y.; CHEN, Y.; CHEN, X.; HUANG, B.; LU, B. Multi-Functional Edible Film with Excellent UV Barrier Performance and Accurate Instant Ion Printing Capability. **Advanced Sustainable Systems**, vol. 4, no. 7, p. 1–10, 2020. <https://doi.org/10.1002/adsu.202000043>.

WEI, Z.; WU, C.; LI, R.; YU, D.; DING, Q. Nanocellulose based hydrogel or aerogel scaffolds for tissue engineering. **Cellulose**, vol. 28, no. 12, p. 7497–7520, 2021. DOI 10.1007/s10570-021-04021-3.

WEISHAUPT, R.; ZÜND, J. N.; HEUBERGER, L.; ZUBER, F.; FACCIO, G.; ROBOTTI, F.; FERRARI, A.; FORTUNATO, G.; REN, Q.; MANIURA-WEBER, K.; GÜEX, A. G. Antibacterial, Cytocompatible, Sustainably Sourced: Cellulose Membranes with Bifunctional Peptides for Advanced Wound Dressings. **Advanced Healthcare Materials**, vol. 9, no. 7, p. 1–13, 2020. <https://doi.org/10.1002/adhm.201901850>.

WISE, L. E. Chlorite holocellulose, its fractionation and bearing on summative wood analysis and on studies on the hemicelluloses. **Paper Trade**, vol. 122, p. 35–43, 1946.

WOHLIN, C.; RUNESON, P.; HÖST, M.; OHLSSON, M. C.; REGNELL, B.; WESSLÉN, A. **Experimentation in software engineering**. [S. l.]: Springer Science & Business Media, 2012.

WOODCOCK, P.; PULLIN, A. S.; KAISER, M. J. Evaluating and improving the reliability of evidence syntheses in conservation and environmental science: a methodology. **Biological Conservation**, vol. 176, p. 54–62, 2014.

WU, C. N.; FUH, S. C.; LIN, S. P.; LIN, Y. Y.; CHEN, H. Y.; LIU, J. M.; CHENG, K. C. TEMPO-Oxidized Bacterial Cellulose Pellicle with Silver Nanoparticles for Wound Dressing. **Biomacromolecules**, vol. 19, no. 2, p. 544–554, 2018. <https://doi.org/10.1021/acs.biomac.7b01660>.

XIANG, J.; SHEN, L.; HONG, Y. Status and future scope of hydrogels in wound healing: Synthesis, materials and evaluation. **European Polymer Journal**, vol. 130, no. March, p. 109609, 2020. DOI 10.1016/j.eurpolymj.2020.109609. Available at: <https://doi.org/10.1016/j.eurpolymj.2020.109609>.

XU, C.; LIU, F.; ALAM, M. A.; CHEN, H.; ZHANG, Y.; LIANG, C.; XU, H.; HUANG, S.; XU, J.; WANG, Z. Comparative study on the properties of lignin isolated from different pretreated sugarcane bagasse and its inhibitory effects on enzymatic hydrolysis. **International journal of biological macromolecules**, vol. 146, p. 132–140, 2020.

XU, J.-T.; CHEN, X.-Q. Preparation and characterization of spherical cellulose nanocrystals with high purity by the composite enzymolysis of pulp fibers. **Bioresource Technology**, 2019. DOI 10.1016/j.biortech.2019.121842.

YAHYA, M.; CHEN, Y. W.; LEE, H. V.; HOCK, C. C.; HASSAN, W. H. W. A New Protocol for Efficient and High Yield Preparation of Nanocellulose from *Elaeis guineensis* Biomass: A Response Surface Methodology (RSM) Study. **JOURNAL OF POLYMERS AND THE ENVIRONMENT**, vol. 27, no. 4, p. 678–702, 2019. <https://doi.org/10.1007/s10924-019-01373-7>.

YANG, H.; YAN, R.; CHEN, H.; LEE, D. H.; ZHENG, C. Characteristics of hemicellulose, cellulose and lignin pyrolysis. **Fuel**, vol. 86, no. 12–13, p. 1781–1788, 2007.

YANG, J.; FANG, L.; TAN, T. Synthesis and characterization of superabsorbent hydrogels composites based on polysuccinimide. **Journal of Applied Polymer Science**, vol. 102, no. 1, p. 550–557, 2006. <https://doi.org/10.1002/app.24282>.

YANG, T.; GUO, Y.; GAO, N.; LI, X.; ZHAO, J. Modification of a cellulase system by engineering *Penicillium oxalicum* to produce cellulose nanocrystal. **CARBOHYDRATE POLYMERS**, vol. 234, no. September 2019, p. 115862, 2020. DOI 10.1016/j.carbpol.2020.115862.

YARBROUGH, J. M.; ZHANG, R.; MITTAL, A.; VANDER WALL, T.; BOMBLE, Y. J.; DECKER, S. R.; HIMMEL, M. E.; CIESIELSKI, P. N. Multifunctional cellulolytic enzymes outperform processive fungal cellulases for coproduction of nanocellulose and biofuels. **Acs Nano**, vol. 11, no. 3, p. 3101–3109, 2017.

YON, R. J. Chromatography of lipophilic proteins on adsorbents containing mixed hydrophobic and ionic groups. **The Biochemical journal**, vol. 126, no. 3, p. 765–767, 1972. <https://doi.org/10.1042/bj1260765>.

YU, H.-Y.; QIN, Z.-Y.; LIU, Y.-N.; CHEN, L.; LIU, N.; ZHOU, Z. Simultaneous improvement of mechanical properties and thermal stability of bacterial polyester by cellulose nanocrystals. **Carbohydrate polymers**, vol. 89, no. 3, p. 971–978, 2012.

YU, H.; ABDALKARIM, S. Y. H.; ZHANG, H.; WANG, C.; TAM, K. C. Simple process to produce high-yield cellulose nanocrystals using recyclable citric/hydrochloric acids. **ACS Sustainable Chemistry & Engineering**, vol. 7, no. 5, p. 4912–4923, 2019.

YUE, Y.; HAN, J.; HAN, G.; FRENCH, A. D.; QI, Y.; WU, Q. Cellulose nanofibers reinforced sodium alginate-polyvinyl alcohol hydrogels: Core-shell structure formation

- and property characterization. **Carbohydrate polymers**, vol. 147, p. 155–164, 2016.
- YUEN, J. D.; WALPER, S. A.; MELDE, B. J.; DANIELE, M. A.; STENGER, D. A. Electrolyte-sensing transistor decals enabled by ultrathin microbial nanocellulose. **Scientific reports**, vol. 7, no. 1, p. 1–9, 2017.
- ZAKI, F. A.; ABDULLAH, I.; AHMAD, I. The physical and chemical natures of cellulose extracted from torch ginger stems. **International Journal of Materials Engineering Innovation**, vol. 5, no. 1, p. 48–60, 2014.
- ZARRINTAJ, P.; MOGHADDAM, A. S.; MANOUCHEHRI, S.; ATOUFI, Z.; AMIRI, A.; AMIRKHANI, M. A.; NILFOROUSHZADEH, M. A.; SAEB, M. R.; HAMBLIN, M. R.; MOZAFARI, M. Can regenerative medicine and nanotechnology combine to heal wounds? The search for the ideal wound dressing. **Nanomedicine**, vol. 12, no. 19, p. 2403–2422, 2017.
- ZHANG, C.; WU, M.; YANG, S.; SONG, X.; XU, Y. Combined mechanical grinding and enzyme post-treatment leading to increased yield and size uniformity of cellulose nanofibrils. **Cellulose**, vol. 27, no. 13, p. 7447–7461, 2020. DOI 10.1007/s10570-020-03335-y.
- ZHANG, W.; REN, G.; XU, H.; ZHANG, J.; LIU, H.; MU, S.; CAI, X.; WU, T. Genipin cross-linked chitosan hydrogel for the controlled release of tetracycline with controlled release property, lower cytotoxicity, and long-term bioactivity. **Journal of Polymer Research**, vol. 23, no. 8, p. 156, 2016. DOI 10.1007/s10965-016-1059-5.
- ZHANG, Y.-H. P.; HIMMEL, M. E.; MIELENZ, J. R. Outlook for cellulase improvement: screening and selection strategies. **Biotechnology advances**, vol. 24, no. 5, p. 452–481, 2006.
- ZHAO, M.; ANSARI, F.; TAKEUCHI, M.; SHIMIZU, M.; SAITO, T.; BERGLUND, L. A.; ISOGAI, A. Nematic structuring of transparent and multifunctional nanocellulose papers. **Nanoscale Horizons**, vol. 3, no. 1, p. 28–34, 2018.
- ZHOU, C.; WU, Q.; LEI, T.; NEGULESCU, I. I. Adsorption kinetic and equilibrium studies for methylene blue dye by partially hydrolyzed polyacrylamide/cellulose nanocrystal nanocomposite hydrogels. **Chemical Engineering Journal**, vol. 251, p. 17–24, 2014.
- ZHOU, H.; JOHN, F. S.; ZHU, J. Y. Xylanase pretreatment of wood fibers for producing cellulose nanofibrils: a comparison of different enzyme preparations. **Cellulose**, vol. 26, no. 1, p. 543–555, 2019.
- ZHU, J.; SABO, R.; CLEMONS, C. Methods for integrated conversion of lignocellulosic material to sugars or biofuels and nano-cellulose. 16 Sep. 2014.
- ZHU, J. Y.; SABO, R.; LUO, X. Integrated production of nano-fibrillated cellulose and cellulosic biofuel (ethanol) by enzymatic fractionation of wood fibers. **Green Chemistry**, vol. 13, no. 5, p. 1339–1344, 2011.

APPENDIX A

Related to the systematic mapping reported in chapter 2, this appendix presents:

- List of excluded articles during the final selection and the reasons for exclusion;
- List of included articles during the final selection and the terms that were assigned to them to provide a “fingerprint” of each article;
- List of the substrates used in the included articles and their occurrence percentage;
- List of the commercial and non-commercial enzymes used in the included articles and their occurrence percentage;
- References of the included articles.

TABLE OF CONTENT

Excluded articles during the final selection.....	177
Included articles during the final selection.....	182
Substrates used in the included articles.....	203
Commercial enzymes used in the included articles.....	206
Non-commercial enzymes used in the included articles.....	209
References.....	212

Table A. 1. Excluded articles during the final selection step and the reasons for exclusion.

Title	DOI	Reasons for exclusion
A Bottom-Up Synthesis of Vinyl-Cellulose Nanosheets and Their Nanocomposite Hydrogels with Enhanced Strength	10.1021/acs.biomac.7b01224	Not directly related to cellulosic CN production
A comparative study of enzymatic and fenton pretreatment applied to a birch kraft pulp used for mfc production in a pilot scale high-pressure homogenizer	10.32964/tj15.6.375	Journal impact factor lower than 1.5
An environment-friendly method to prepare microcrystalline cellulose	-	Conference paper
Biodegradation of crystalline cellulose nanofibers by means of enzyme immobilized-alginate beads and microparticles	10.3390/polym12071522	Not directly related to cellulosic CN production
Biorefining via solid-state fermentation of rice and sunflower by-products employing novel monosporic strains from <i>Pleurotus sapidus</i>	10.1016/j.biortech.2019.121692	CN produced by chemical treatment
Catalytic transformation of cellulose into short rod-like cellulose nanofibers and platform chemicals over lignin-based solid acid	10.1016/j.apcatb.2020.118732	CN produced by chemical treatment
Cellulose Microfibril Formation by Surface-Tethered Cellulose Synthase Enzymes	10.1021/acsnano.5b05648	Not directly related to cellulosic CN production
Characterization of Adhesion Surface of Cellulosic Fibers Extracted from Agro Wastes	10.1080/15440478.2014.1002148	Not directly related to cellulosic CN production
Characterization of Microcrystalline Cellulose Obtained from Enzymatic Hydrolysis of Alpha-Cellulose and its Application	10.5530/jyp.2018.2s.17	Journal impact factor lower than 1.5
Chemo-enzymatic preparation and characterization of cellulose nanofibers-graft-poly(lactic acid)s	10.1016/j.eurpolymj.2019.02.036	CN produced by chemical treatment
Comparative Study of the Effects Induced by Different Laccase-Based Systems on Sisal Cellulose Fibers	10.1021/ie2028206	Not directly related to cellulosic CN production
Comprehensive utilization strategy of cellulose in a facile, controllable, high-yield preparation process of cellulose nanocrystals using aqueous tetrabutylphosphonium hydroxide	10.1039/d0gc04370b	CN produced by chemical treatment

Continuous Metal-Organic Framework Biomineralization on Cellulose Nanocrystals: Extrusion of Functional Composite Filaments	10.1021/acssuschemeng.8b06713	CN produced by chemical treatment
Conversion of Potato Starch and Peel Waste to High Value Nanocrystals	10.1007/s11540-018-9381-4	CN produced by chemical treatment
Covalent immobilization of cyclodextrin glucanotransferase on kenaf cellulose nanofiber and its application in ultrafiltration membrane system	10.1016/j.procbio.2017.01.025	CN produced by chemical treatment
Development of Lignin and Nanocellulose Enhanced Bio PU Foams for Automotive Parts	10.1007/s10924-013-0631-x	Not related to CN production
Direct observation of endoglucanase fibrillation and rapid thickness identification of cellulose nanoplatelets using constructive interference	10.1016/j.carbpol.2020.117463	Not related to CN production
Dual nanofibrillar-based bio-sorbent films composed of nanocellulose and lysozyme nanofibrils for mercury removal from spring waters	10.1016/j.carbpol.2020.116210	Not related to CN production
Eco-friendly cellulose nano fibers via first reported Egyptian Humicola fuscoatra Egyptia X4: Isolation and characterization	10.1016/j.enmm.2018.10.004	Low quality
Effects of cellulose micro/nanofibers as paper additives in kraft and kraft-NaBH ₄ pulps	10.3183/NPPRJ-2016-31-04-p561-572	Journal impact factor lower than 1.5
Effects of enzyme mixture and beating treatment on the properties of pulp fibers	10.7584/jktappi.2020.10.52.5.101	Journal impact factor lower than 1.5
Effects of residual lignin and heteropolysaccharides on the bioconversion of softwood lignocellulose nanofibrils obtained by SO ₂ -ethanol-water fractionation	10.1016/j.biortech.2014.03.025	Not directly related to cellulosic CN production
Enhancement of anaerobic digestion of microcrystalline cellulose (MCC) using natural micronutrient sources	10.1590/0104-6632.20140312s00002689	Not directly related to cellulosic CN production
Enzymatic Conversion of Sugarcane Lignocellulosic Biomass as a Platform for the Production of Ethanol, Enzymes and Nanocellulose	10.7569/jrm.2017.6341578	Review article
Enzymatic hydrolysis of cellulose nanoplatelets as a source of sugars with the concomitant production of cellulose nanofibrils	10.1016/j.carbpol.2019.01.055	Not directly related to cellulosic CN production

Enzymatic production of cellulose nanofibers from oil palm empty fruit bunch (EFB) with crude cellulase of <i>Trichoderma</i> sp	10.1088/2053-1591/aab449	Low quality
Enzymatic refining and cellulose nanofiber addition in papermaking processes from recycled and deinked slurries	10.15376/biores.10.3.5730-5743	Not directly related to cellulosic CN production
Enzymatic Transformations of Cellulose Assessed by Quantitative High-Throughput Fourier Transform Infrared Spectroscopy (QHT-FTIR)	10.1002/bit.23098	Not directly related to cellulosic CN production
Enzymatic treatment of lyocell - Clarification of depilling mechanisms	10.1177/004051750007000807	Not directly related to cellulosic CN production
EXAMINING THE EFFICIENCY OF MECHANIC/ENZYMATIC PRETREATMENTS IN MICRO/NANOFIBRILLATED CELLULOSE PRODUCTION	10.4067/s0718-221x2018005001601	Low quality
Extraction and modification of cellulose nanofibers derived from biomass for environmental application	10.1039/c7ra06713e	Review article
Extraction of High Crystalline Nanocellulose from Biorenewable Sources of Vietnamese Agricultural Wastes	10.1007/s10924-020-01695-x	CN produced by chemical treatment
Fast and efficient nanoshear hybrid alkaline pretreatment of corn stover for biofuel and materials production	10.1016/j.biombioe.2012.12.037	Not directly related to cellulosic CN production
Formation of biocompatible nanoparticles by self-assembly of enzymatic hydrolysates of chitosan and carboxymethyl cellulose	10.1271/bbb.69.1637	Not directly related to cellulosic CN production
Fractionation of Nanocellulose by Foam Filter	10.1080/01496395.2012.661825	Not directly related to cellulosic CN production
Gel structure phase behavior in micro nanofibrillated cellulose containing in situ precipitated calcium carbonate	10.1002/app.43486	Not directly related to cellulosic CN production
Green synthesis of cellulosic nanofiber in enset woven fabric structures via enzyme treatment and mechanical hammering	10.32710/tekstilvekonfeksiyon.764976	Journal impact factor lower than 1.5
Influence of Xyloglucan Molar Mass on Rheological Properties of Cellulose Nanocrystal/Xyloglucan Hydrogels	10.32604/jrm.2019.07838	Low quality

Isolation of cellulolytic fungi and utilization of its cellulolytic activity for microcrystalline cellulose preparation from water hyacinth (<i>Eichhornia crassipes</i>)	10.5530/pj.2018.6.183	Journal impact factor lower than 1.5
Lignocellulosic fibres from enzyme-treated tomato plants: Characterisation and application in paperboard manufacturing	10.1016/j.ijbiomac.2020.06.077	Not directly related to cellulosic CN production
Multi-layer nanopaper based composites	10.1007/s10570-017-1220-2	CN produced by mechanical treatment
Nanocellulose isolation from <i>Amorpha fruticosa</i> by an enzyme-assisted pretreatment	10.26789/AEB.2017.01.005	Journal impact factor lower than 1.5
Nanocellulose production using ionic liquids with enzymatic pretreatment	10.3390/ma14123264	Low quality
Nanocrystals of cellulose allomorphs have different adsorption of cellulase and subsequent degradation	10.1016/j.indcrop.2017.12.052	Not directly related to cellulosic CN production
Optimizing the isolation of microfibrillated bamboo in high pressure enzymatic Hydrolysis	10.15376/biores.10.3.5305-5316	Duplicate article
Potential of cellulase of <i>Chaetomium globosum</i> for preparation and characterization of microcrystalline cellulose from water hyacinth (<i>Eichhornia crassipes</i>)	10.22159/ijap.2019v11i4.31081	Journal impact factor lower than 1.5
Preparation and characterization of nano crystalline cellulose from Bamboo fibers by controlled cellulase hydrolysis	10.3993/jfbi09201204	Journal impact factor lower than 1.5
Preparation of Microcrystalline Cellulose from Water Hyacinth Powder by Enzymatic Hydrolysis Using Cellulase of Local Isolate	10.5530/jyp.2017.1s.6	Journal impact factor lower than 1.5
Preparation of nanocellulose from steam exploded poplar wood by enzymolysis assisted sonication	10.1088/2053-1591/ab7b28	Low quality
Pretreatment of microcrystalline cellulose flakes with CaCl ₂ increases the surface area, and thus improves enzymatic saccharification	10.1016/j.carres.2008.03.007	Not directly related to cellulosic CN production
Processable polyaniline suspensions through in situ polymerization onto nanocellulose	10.1016/j.eurpolymj.2012.10.026	CN produced by mechanical treatment

Production of green biocellulose nanofibers by <i>Gluconacetobacter xylinus</i> through utilizing the renewable resources of agriculture residues	10.1007/s00449-013-0948-9	Bacterial nanocellulose production
Production of nanotubes in delignified porous cellulosic materials after hydrolysis with cellulase	10.1016/j.biortech.2016.03.065	Not directly related to cellulosic CN production
Solid- and Nano-Catalysts Pretreatment and Hydrolysis Techniques	10.1007/978-3-642-32735-3_15	Chapter of a book
Sound-absorbing green composites based on cellulose ultra-short/ultra-fine fibers	10.1177/0040517514553873	Low quality
Study on the anti-biodegradation property of tunicate cellulose	10.3390/polym12123071	Not directly related to cellulosic CN production
Substrate docking and molecular dynamic simulation for prediction of fungal enzymes from <i>Trichoderma</i> species-assisted extraction of nanocellulose from oil palm leaves	10.1080/07391102.2019.1679667	Not directly related to cellulosic CN production
Synergistic effects on process parameters to enhance enzymatic hydrolysis of alkaline oil palm fronds	10.1016/j.indcrop.2018.06.037	Not directly related to cellulosic CN production
Taguchi orthogonal design for optimizing a unified ternary process to valorize oil palm leaves for nanocellulose isolation	10.11113/jurnalteknologi.v83.15109	Journal impact factor lower than 1.5
Thermogravimetry study of xylanase- and laccase/mediator-treated eucalyptus pulp fibres	10.1016/j.biortech.2011.07.061	Not directly related to cellulosic CN production
X-ray Diffraction Study of Bacterial Nanocellulose Produced by <i>Medusomyces Gisevii</i> Sa-12 Cultured in Enzymatic Hydrolysates of <i>Miscanthus</i>	10.1134/s1063774519060026	Bacterial nanocellulose production
Xyloglucan adsorption for measuring the specific surface area on various never-dried cellulose nanofibers	10.1515/npprj-2018-3034	Not directly related to cellulosic CN production

Table A. 2. Included articles during the final selection and the terms that were assigned to them to provide a “fingerprint” of each article.

Title	Process conditions and purposes*	Applications**	References
3D-Printed PLA Filaments Reinforced with Nanofibrillated Cellulose	Pretreatment step; Nanofibrillation enhancement	Reinforcement agent nanocomposites	(PERIĆ; PUTZ; PAULIK, 2020)
A bio-mechanical process for cellulose nanofiber production - Towards a greener and energy conservation solution	Pretreatment step; Reaction conditions optimization without DOE; Nanofibrillation enhancement	Films preparation	(LIU <i>et al.</i> , 2019)
A co-production of sugars, lignosulfonates, cellulose, and cellulose nanocrystals from ball-milled woods	Pretreatment step; Biorefinery	N.E.	(DU <i>et al.</i> , 2017)
A comparative study of cellulose nanofibrils disintegrated via multiple processing approaches	Pretreatment step; different pretreatments	Films preparation	(QING <i>et al.</i> , 2013)
A comparison of cellulose nanofibrils produced from <i>Cladophora glomerata</i> algae and bleached eucalyptus pulp	Pretreatment step; different feedstocks	N.E.	(XIANG <i>et al.</i> , 2016)
A comprehensive study on nanocelluloses in papermaking: the influence of common additives on filler retention and paper strength	Pretreatment step; different pretreatments	Reinforcement agent hand-sheets	(LOURENÇO <i>et al.</i> , 2020)
A New Approach to Obtain Cellulose Nanocrystals and Ethanol from Eucalyptus Cellulose Pulp via the Biochemical Pathway	Main step; Biorefinery	N.E.	(BONDANCIA <i>et al.</i> , 2017)
A novel enzymatic approach to nanocrystalline cellulose preparation	Pretreatment step; Reaction conditions optimization with doe	N.E.	(BELTRAMINO <i>et al.</i> , 2018)
A Novel Nano Cellulose Preparation Method and Size Fraction by Cross Flow Ultra-Filtration	Pretreatment step; different pretreatments	N.E.	(ZHU <i>et al.</i> , 2012)

A novel process for synthesis of spherical nanocellulose by controlled hydrolysis of microcrystalline cellulose using anaerobic microbial consortium	Main step; Reaction conditions optimization without doe	N.E.	(SATYAMURTHY; VIGNESHWARAN, 2013)
A xylanase-aided enzymatic pretreatment facilitates cellulose nanofibrillation	Pretreatment step; Nanofibrillation enhancement; different feedstocks	N.E.	(LONG <i>et al.</i> , 2017)
Alkaline treatment combined with enzymatic hydrolysis for efficient cellulose nanofibrils production	Pretreatment step; Nanofibrillation enhancement	N.E.	(BANVILLET; DEPRES; <i>et al.</i> , 2021)
An efficient method for cellulose nanofibrils length shearing via environmentally friendly mixed cellulase pretreatment	Pretreatment step; size control; homogeneity increase; different enzyme concentrations; different reaction times; size control	N.E.	(CHEN <i>et al.</i> , 2017)
An environmentally friendly method for enzyme-assisted preparation of microfibrillated cellulose (MFC) nanofibers	Pretreatment step; Nanofibrillation enhancement; different enzyme concentrations	N.E.	(HENRIKSSON <i>et al.</i> , 2007)
An environmentally friendly xylanase-assisted pretreatment for cellulose nanofibrils isolation from sugarcane bagasse by high-pressure homogenization	Pretreatment step; different enzyme concentrations	N.E.	(SAELEE <i>et al.</i> , 2016)
Application of cellulose nanocrystals prepared from agricultural wastes for synthesis of starch-based hydrogel nanocomposites: Efficient and selective nanoadsorbent for removal of cationic dyes from water	Pretreatment step	nanofiller hydrogels	(MOHARRAMI; MOTAMEDI, 2020)
Approaching a low-cost production of cellulose nanofibers for papermaking applications	Pretreatment step; different pretreatments	Reinforcement agent paper-sheets	(DELGADO AGUILAR <i>et al.</i> , 2015)
Assessing the enzymatic effects of cellulases and LPMO in improving mechanical fibrillation of cotton linters	Pretreatment step; Nanofibrillation enhancement; different enzymes	Films preparation	(VALLS <i>et al.</i> , 2019)

Banana starch nanocomposite with cellulose nanofibers isolated from banana peel by enzymatic treatment: In vitro cytotoxicity assessment	Pretreatment step; different feedstock concentrations	Films preparation	(TIBOLLA <i>et al.</i> , 2019)
Bacterial cellulose nanocrystals exhibiting high thermal stability and their polymer nanocomposites	Main step; thermal stability	nanocomposites preparation	(GEORGE <i>et al.</i> , 2011)
Bio-Treatment of Natural Fibers in Isolation of Cellulose Nanofibres: Impact of Pre-Refining of Fibers on Bio-Treatment Efficiency and Nanofiber Yield	Main step	N.E.	(JANARDHAN; SAIN, 2011)
Biocomposite fabrication from enzymatically treated nanocellulosic fibers and recycled polylactic acid	Posttreatment step; size control; crystallinity increase	N.E.	(LAADILA <i>et al.</i> , 2020)
Biological-chemical modification of cellulose nanocrystal to prepare highly compatible chitosan-based nanocomposites	Posttreatment step; Functionalization	CNC; reinforcement agent films	(LIU <i>et al.</i> , 2019)
Biomimetic foams of high mechanical performance based on nanostructured cell walls reinforced by native cellulose nanofibrils	Pretreatment step	reinforcement agent foams	(SVAGAN; SAMIR; BERGLUND, 2008)
Cardboard boxes as raw material for high-performance papers through the implementation of alternative technologies: More than closing the loop	Pretreatment step	reinforcement agent paper-sheets	(TARRES <i>et al.</i> , 2017)
Cellulose fibers deconstruction by twin-screw extrusion with in situ enzymatic hydrolysis via bioextrusion	Pretreatment step; Nanofibrillation enhancement; bioextrusion	Films preparation	(BANVILLET <i>et al.</i> , 2021)
Cellulose micro and nanofibrils as coating agent for improved printability in office papers	Pretreatment step; different pretreatments	coating agent	(LOURENÇO <i>et al.</i> , 2020)
Cellulose nanocrystals from rice and oat husks and their application in aerogels for food packaging	Pretreatment step	aerogels preparation	(DE OLIVEIRA <i>et al.</i> , 2019)
Cellulose nanofibers from lignocellulosic biomass of lemongrass using enzymatic hydrolysis: characterization and cytotoxicity assessment	Main step	N.E.	(KUMARI <i>et al.</i> , 2019)

Cellulose Nanofibers from Softwood, Hardwood, and Tunicate: Preparation-Structure-Film Performance Interrelation	Pretreatment step; different pretreatments; different feedstocks	N.E.	(ZHAO <i>et al.</i> , 2017)
Cellulose nanofibers produced from banana peel by chemical and enzymatic treatment	Main step; different methods	N.E.	(TIBOLLA; PELISSARI; MENEGALLI, 2014)
Cellulose nanofibers produced from banana peel by enzymatic treatment: Study of process conditions	Main step; Reaction conditions optimization with doe	N.E.	(TIBOLLA <i>et al.</i> , 2017)
Cellulose nanofibers production using a set of recombinant enzymes	Pretreatment step; different enzymes; Different reaction times; Nanofibrillation enhancement	N.E.	(ROSSI <i>et al.</i> , 2021)
Cellulose nanofibrils as reinforcing agents for PLA-based nanocomposites: An in situ approach	Pretreatment step	reinforcement agent nanocomposites	(GAZZOTTI <i>et al.</i> , 2019)
Cellulose nanofibrils filled poly(lactic acid) biocomposite filament for FDM 3D printing	Pretreatment step	nanofiller nanocomposites	(WANG <i>et al.</i> , 2020)
Cellulose nanostructures from wood waste with low input consumption	Main step	N.E.	(BAULI <i>et al.</i> , 2019)
Cellulosic nanofibrils from eucalyptus, acacia and pine fibers	Pretreatment step; different feedstocks	Films preparation	(FALL; BURMAN; WAGBERG, 2014)
Changes in the Dimensions of Lignocellulose Nanofibrils with Different Lignin Contents by Enzymatic Hydrolysis	Posttreatment step; size control; crystallinity increase	N.E.	(JANG <i>et al.</i> , 2020)
Characteristic microcrystalline cellulose extracted by combined acid and enzyme hydrolysis of sweet sorghum	Posttreatment step; different enzyme concentrations; different reaction times	N.E.	(REN <i>et al.</i> , 2019)
Cleaner production of lignocellulosic nanofibrils: Potential of mixed enzymatic treatment	Posttreatment step; different pretreatments; different enzyme concentrations	Films preparation	(BIAN <i>et al.</i> , 2020)
Co-Production of Cellulose Nanocrystals and Fermentable Sugars Assisted by Endoglucanase Treatment of Wood Pulp	Pretreatment step; different enzyme concentrations;	N.E.	(DAI <i>et al.</i> , 2018)

	different enzymes		
Co-production of ethanol and cellulose nanocrystals through self-cycling fermentation of wood pulp hydrolysate	Pretreatment step; biorefinery	N.E.	(WANG <i>et al.</i> , 2021)
Combined effect of sodium carboxymethyl cellulose, cellulose nanofibers and drainage aids in recycled paper production process	Pretreatment step	reinforcement agent paper-sheets	(TARRÉS <i>et al.</i> , 2018)
Combined mechanical grinding and enzyme post-treatment leading to increased yield and size uniformity of cellulose nanofibrils	Posttreatment step; yield improvement; size control	N.E.	(ZHANG <i>et al.</i> , 2020)
Combining biomass wet disk milling and endoglucanase/beta-glucosidase hydrolysis for the production of cellulose nanocrystals	Main step; Different feedstocks	N.E.	(SOBRAL TEIXEIRA <i>et al.</i> , 2015)
Comparative analysis of physical and functional properties of cellulose nanofibers isolated from alkaline pre-treated wheat straw in optimized hydrochloric acid and enzymatic processes	Main step; different methods; reaction conditions optimization with DOE	N.E.	(CEASER; CHIMPHANGO, 2021)
Comparison Between Chitosan Nanoparticles and Cellulose Nanofibers as Reinforcement Fillers in Papaya Puree Films: Effects on Mechanical, Water Vapor Barrier, and Thermal Properties	Pretreatment step	reinforcement agent films	(DE BARROS-ALEXANDRINO; TOSI; ASSIS, 2019)
Comparison of mixed enzymatic pretreatment and post-treatment for enhancing the cellulose nanofibrillation efficiency	Pretreatment step; Posttreatment step; Different feedstocks	N.E.	(BIAN <i>et al.</i> , 2019)
Comparison of the properties of cellulose nanocrystals and cellulose nanofibrils isolated from bacteria, tunicate, and wood processed using acid, enzymatic, mechanical, and oxidative methods	Pretreatment step; different pretreatments	N.E.	(SACUI <i>et al.</i> , 2014)
Composite films of ecofriendly lignocellulosic nanostructures in biodegradable polymeric matrix	Main step	reinforcement agent films	(BAULI; ROCHA; ROSA, 2019)

Controlled enzymolysis preparation of nanocrystalline cellulose from pretreated cotton fibers	Main step; different methods	N.E.	(CHEN <i>et al.</i> , 2012)
Controlling the Size and Film Strength of Individualized Cellulose Nanofibrils Prepared by Combined Enzymatic Pretreatment and High Pressure Microfluidization	Pretreatment step; different enzyme concentrations	films preparation	(WANG <i>et al.</i> , 2016)
Coupled acid and enzyme mediated production of microcrystalline cellulose from corn cob and cotton gin waste	Main step; different methods; Different feedstocks; different reaction times	N.E.	(AGBLEVOR; IBRAHIM; EL-ZAWAWY, 2007)
Deconstruction of cellulosic fibers to fibrils based on enzymatic pretreatment	Pretreatment step; reaction conditions optimization with doe	N.E.	(WANG <i>et al.</i> , 2018)
Differential activity of lytic polysaccharide monoxygenases on celluloses of different crystallinity. Effectiveness in the sustainable production of cellulose nanofibrils	Pretreatment step; Nanofibrillation enhancement; Different enzyme concentrations; different reaction times	N.E.	(VALENZUELA <i>et al.</i> , 2019)
Eco-Efficient Process Improvement at the Early Development Stage: Identifying Environmental and Economic Process Hotspots for Synergetic Improvement Potential	Pretreatment step; Life cycle assessment	N.E.	(PICCINNO <i>et al.</i> , 2018)
Effect of endoglucanase and high-pressure homogenization post-treatments on mechanically grinded cellulose nanofibrils and their film performance	Posttreatment step	films preparation	(XU <i>et al.</i> , 2021)
Effect of endoglucanases from different glycoside hydrolase families on enzymatic preparation of cellulose nanocrystal	Main step; different enzymes	N.E.	(YANG <i>et al.</i> , 2020)
Effect of enzymatic treatment on the thermal stability of cellulose nanofibrils	Pretreatment step; thermal stability	N.E.	(TAO <i>et al.</i> , 2019)

Effect of enzyme beating on grinding method for microfibrillated cellulose preparation as a paper strength enhancer	Pretreatment step	reinforcement agent hand-sheets	(KIM <i>et al.</i> , 2017)
Effect of Nanofibrillated Cellulose Made from Enzyme-pretreated Bamboo Pulp on Paper Strength	Pretreatment step; different enzyme concentrations	reinforcement agent hand-sheets	(JO <i>et al.</i> , 2021)
Effect of pretreatment of bagasse fibers on the properties of chitosan/microfibrillated cellulose nanocomposites	Pretreatment step	reinforcement agent nanocomposites	(HASSAN; HASSAN; OKSMAN, 2011)
Effect of Pulp Concentration during Cellulase Pretreatment on Microfibrillated Cellulose and Its Film Properties	Pretreatment step; different feedstock concentrations	films preparation	(ZHANG <i>et al.</i> , 2016)
Effect of retention rate of fluorescent cellulose nanofibrils on paper properties and structure	Pretreatment step	reinforcement agent paper-sheets	(DING <i>et al.</i> , 2018)
Effect of the chemical and structural characteristics of pulps of Eucalyptus and Pinus on the deconstruction of the cell wall during the production of cellulose nanofibrils	Pretreatment step; rheological behavior; different feedstocks	N.E.	(ANDRADE <i>et al.</i> , 2021)
Effective and simple methodology to produce nanocellulose-based aerogels for selective oil removal	Main step; different methods	Aerogels preparation	(TARRÉS <i>et al.</i> , 2016)
Endoglucanase post-milling treatment for producing cellulose nanofibers from bleached eucalyptus fibers by a supermasscolloider	Posttreatment step; different enzymes; different enzyme concentrations	N.E.	(WANG <i>et al.</i> , 2016)
Endoglucanase recycling for disintegrating cellulosic fibers to fibrils	Pretreatment step	N.E.	(WANG <i>et al.</i> , 2019)
Enhanced Materials from Nature: Nanocellulose from Citrus Waste	Main step	N.E.	(MARIÑO <i>et al.</i> , 2015)
Enhancing cellulose nanofibrillation of eucalyptus Kraft pulp by combining enzymatic and mechanical pretreatments	Pretreatment step; Nanofibrillation enhancement; different feedstocks; different enzyme concentrations	N.E.	(CEBREIROS <i>et al.</i> , 2021)

Enzymatic-mediated production of cellulose nanocrystals from recycled pulp	Main step; reaction conditions optimization with DOE	N.E.	(FILSON; DAWSON-ANDOH; SCHWEGLER-BERRY, 2009)
Enzymatic and cold alkaline pretreatments of sugarcane bagasse pulp to produce cellulose nanofibrils using a mechanical method	Pretreatment step; thermal stability; different enzymes	N.E.	(NIE <i>et al.</i> , 2018)
Enzymatic Deconstruction of Sugarcane Bagasse and Straw to Obtain Cellulose Nanomaterials	Main step; Biorefinery	N.E.	(DE AGUIAR <i>et al.</i> , 2020)
Enzymatic engineering of nanometric cellulose for sustainable polypropylene nanocomposites	Posttreatment step; size control	nanofiller nanocomposites	(ZIELINSKA <i>et al.</i> , 2021)
Enzymatic extract of <i>Aspergillus fumigatus</i> CCT 7873 for hydrolysis of sugarcane bagasse and generation of cellulose nanocrystals (CNC)	Main step; different feedstocks	N.E.	(DE OLIVEIRA JUNIOR <i>et al.</i> , 2020)
Enzymatic hydrolysis combined with mechanical shearing and high-pressure homogenization for nanoscale cellulose fibrils and strong gels	Pretreatment step	N.E.	(PAAKKO <i>et al.</i> , 2007)
Enzymatic Hydrolysis in the Green Production of Bacterial Cellulose Nanocrystals	Main step; Different enzyme concentrations; different reaction times	N.E.	(ROVERA <i>et al.</i> , 2018)
Enzymatic Hydrolysis of Bacterial Cellulose for the Production of Nanocrystals for the Food Packaging Industry	Main step; different reaction times	oxygen barrier agent nanocomposites	(ROVERA <i>et al.</i> , 2020)
Enzymatic nanocellulose in papermaking - The key role as filler flocculant and strengthening agent	Pretreatment step; different enzymes	reinforcement agent hand-sheets	(LOURENÇO <i>et al.</i> , 2019)
Enzymatic preparation of nanocrystalline and microcrystalline cellulose	Main step; different enzymes; different reaction times	N.E.	(ANDERSON <i>et al.</i> , 2014)
Enzymatic pretreatment for cellulose nanofibrils isolation from bagasse pulp: Transition of cellulose crystal structure	Pretreatment step; different pretreatments	N.E.	(TAO <i>et al.</i> , 2019)

Enzymatic production of cellulose nanofibers and sugars in a stirred-tank reactor: determination of impeller speed, power consumption, and rheological behavior	Main step; reaction conditions optimization without DOE; biorefinery	N.E.	(BONDANCIA <i>et al.</i> , 2018)
Enzymatically assisted isolation of high-quality cellulose nanoparticles from water hyacinth stems	Posttreatment step; different reaction times	N.E.	(JUÁREZ-LUNA <i>et al.</i> , 2019)
Enzymatically hydrolyzed and TEMPO-oxidized cellulose nanofibers for the production of nanopapers: morphological, optical, thermal and mechanical properties	Pretreatment step; different pretreatments; different enzyme concentrations	films preparation	(TARRÉS <i>et al.</i> , 2017)
Enzymatically produced cellulose nanocrystals as reinforcement for waterborne polyurethane and its applications	Main step	reinforcement agent nanocomposites	(ALONSO-LERMA <i>et al.</i> , 2021)
Enzymatically produced nano-ordered short elements containing cellulose I-beta crystalline domains	Main step; different feedstocks; different enzyme concentrations	N.E.	(HAYASHI; KONDO; ISHIHARA, 2005)
Enzyme-assisted isolation of microfibrillated cellulose from date palm fruit stalks	Pretreatment step; different enzyme concentrations	films preparation	(HASSAN <i>et al.</i> , 2014)
Enzyme-Assisted Mechanical Fibrillation of Bleached Spruce Kraft Pulp to Produce Well-Dispersed and Uniform-Sized Cellulose Nanofibrils	Pretreatment step; different pretreatments; Nanofibrillation enhancement	N.E.	(BIAN <i>et al.</i> , 2016)
Enzyme-assisted mechanical grinding for cellulose nanofibers from bagasse: energy consumption and nanofiber characteristics	Pretreatment step; Nanofibrillation enhancement; different feedstocks	films preparation	(LIU <i>et al.</i> , 2018)
Enzyme-assisted mechanical production of cellulose nanofibrils: thermal stability	Pretreatment step; thermal stability; different enzyme concentrations	N.E.	(ZHANG <i>et al.</i> , 2018)
Enzyme-assisted mechanical production of microfibrillated cellulose from Northern Bleached Softwood Kraft pulp	Pretreatment step; different enzymes	N.E.	(TIAN <i>et al.</i> , 2017)
Enzymatically-mediated co-production of cellulose nanocrystals and fermentable sugars	Pretreatment step; reaction conditions	N.E.	(BEYENE <i>et al.</i> , 2017)

	optimization without doe		
Enzyme mediated nanofibrillation of cellulose by the synergistic actions of an endoglucanase, lytic polysaccharide monooxygenase (LPMO) and xylanase	Pretreatment step; different enzymes	N.E.	(HU <i>et al.</i> , 2018)
Evaluation of the effects of chemical composition and refining treatments on the properties of nanofibrillated cellulose films from sugarcane bagasse	Pretreatment step; different pretreatments	Nanocomposites preparation	(SANTUCCI <i>et al.</i> , 2016)
Exploring the action of endoglucanases on bleached eucalyptus kraft pulp as potential catalyst for isolation of cellulose nanocrystals	Main step; different enzymes	N.E.	(SIQUEIRA; DIAS; ARANTES, 2019)
Extraction of cellulose nanocrystals from old corrugated container fiber using phosphoric acid and enzymatic hydrolysis followed by sonication	Pretreatment step; rheological behavior; different reaction times	N.E.	(TANG <i>et al.</i> , 2015)
Fabricating cellulose nanofibril from licorice residues and its cellulose composite incorporated with natural nanoparticles	Pretreatment step; different reaction times; different enzyme concentrations	nanocomposite films preparation	(WANG <i>et al.</i> , 2020)
Facile one-pot fabrication of cellulose nanocrystals and enzymatic synthesis of its esterified derivative in mixed ionic liquids	Posttreatment step; functionalization; different enzyme concentrations	N.E.	(ZHAO <i>et al.</i> , 2017)
Feasibility of Manufacturing Cellulose Nanocrystals from the Solid Residues of Second-Generation Ethanol Production from Sugarcane Bagasse	Pretreatment step; biorefinery; different feedstocks; different enzyme concentrations	N.E.	(CAMARGO <i>et al.</i> , 2016)
Feasibility of nanocrystalline cellulose production by endoglucanase treatment of natural bast fibers	Pretreatment step; different feedstocks	N.E.	(XU <i>et al.</i> , 2013)

Fluorescently labeled cellulose nanofibrils for detection and loss analysis	Pretreatment step	N.E.	(REID; KARLSSON; ABITBOL, 2020)
Green preparation and characterization of size-controlled nanocrystalline cellulose via ultrasonic-assisted enzymatic hydrolysis	Main step; different reaction times	N.E.	(CUI <i>et al.</i> , 2016)
Green synthesis of cellulose nanofibers using immobilized cellulase	Main step; immobilized enzymes	N.E.	(YASSIN <i>et al.</i> , 2019)
High performance crystalline nanocellulose using an ancestral endoglucanase	Pretreatment step; different reaction times	Nanocomposites preparation; films preparation	(ALONSO-LERMA <i>et al.</i> , 2020)
High value-added products from the orange juice industry waste	Pretreatment step; biorefinery	N.E.	(CYPRIANO; DA SILVA; TASIC, 2018)
High yield production of nanocrystalline cellulose by microwave-assisted dilute-acid pretreatment combined with enzymatic hydrolysis	Main step; different reaction times	N.E.	(QIAN <i>et al.</i> , 2021)
High yielding, one-step mechano-enzymatic hydrolysis of cellulose to cellulose nanocrystals without bulk solvent	Main step; reaction conditions optimization without doe	N.E.	(ZHANG <i>et al.</i> , 2021)
Hydrolytic activities of artificial nanocellulose synthesized via phosphorylase-catalyzed enzymatic reactions	Main step; artificial nanocellulose synthesis	N.E.	(SERIZAWA <i>et al.</i> , 2016)
Impact of pretreatment methods on production of bioethanol and nanocrystalline cellulose	Pretreatment step; biorefinery; different enzyme concentrations	N.E.	(KO <i>et al.</i> , 2020)
Improving the production of nanofibrillated cellulose from bamboo pulp by the combined cellulase and refining treatment	Pretreatment step; Nanofibrillation enhancement; different enzyme concentrations	N.E.	(YUAN; WEI; WEN, 2019)
In Vitro Synthesis and Self-Assembly of Cellulose II Nanofibrils Catalyzed by the Reverse Reaction of Clostridium thermocellum Cellodextrin Phosphorylase	Main step; artificial nanocellulose synthesis; different feedstock concentrations; different enzyme concentrations	N.E.	(PYLKKÄNEN <i>et al.</i> , 2020)
Increasing yield of nanocrystalline cellulose	Pretreatment step;	N.E.	(BELTRAMINO <i>et al.</i> , 2015)

preparation process by a cellulase pretreatment	Nanofibrillation enhancement		
Influence of Chemical and Enzymatic TEMPO-Mediated Oxidation on Chemical Structure and Nanofibrillation of Lignocellulose	Posttreatment step; functionalization; different feedstocks; different methods	N.E.	(JIANG <i>et al.</i> , 2020)
Innovative Nanofibrillated Cellulose from Rice Straw as Dietary Fiber for Enhanced Health Benefits Prepared by a Green and Scale Production Method	Main step; different methods	N.E.	(YAN <i>et al.</i> , 2018)
Integrated production of nanofibrillated cellulose and cellulosic biofuel (ethanol) by enzymatic fractionation of wood fibers	Pretreatment step; biorefinery; Different reaction times	N.E.	(ZHU; SABO; LUO, 2011)
Interfacial properties of cellulose nanoparticles obtained from acid and enzymatic hydrolysis of cellulose	Main step; different methods	Pickering emulsions Preparation	(DOMINGUES <i>et al.</i> , 2016)
Introduction of aldehyde vs. carboxylic groups to cellulose nanofibers using laccase/TEMPO mediated oxidation	Posttreatment step; functionalization; Different reaction times; different enzyme concentrations	N.E.	(JAUŠOVEC; VOGRINČIČ; KOKOL, 2015)
Laccase aided modification of nanofibrillated cellulose with dodecyl gallate	Posttreatment step; functionalization; rheological behavior	N.E.	(SAASTAMOINEN <i>et al.</i> , 2012)
Length-controlled cellulose nanofibrils produced using enzyme pretreatment and grinding	Pretreatment step; size control; homogeneity increase; Different reaction times; different enzyme concentrations; size control	N.E.	(CHEN; FAN; <i>et al.</i> , 2017)
Life Cycle Assessment of a New Technology To Extract, Functionalize and Orient Cellulose Nanofibers from Food Waste	Pretreatment step; Life cycle assessment	N.E.	(PICCINNO <i>et al.</i> , 2015)

Life Cycle Assessment of Cellulose Nanofibrils Production by Mechanical Treatment and Two Different Pretreatment Processes	Pretreatment step; Life cycle assessment	N.E.	(ARVIDSSON; NGUYEN; SVANSTRÖM, 2015)
Long and entangled native cellulose i nanofibers allow flexible aerogels and hierarchically porous templates for functionalities	Pretreatment step	aerogels preparation	(PÄÄKKÖ <i>et al.</i> , 2008)
Lytic Polysaccharide Monoxygenase-Assisted Preparation of Oxidized-Cellulose Nanocrystals with a High Carboxyl Content from the Tunic of Marine Invertebrate <i>Ciona intestinalis</i>	Pretreatment step; Posttreatment step; tunicates	N.E.	(KARNAOURI <i>et al.</i> , 2020)
Lytic polysaccharide monoxygenases (LPMOs) facilitate cellulose nanofibrils production	Pretreatment step	N.E.	(MOREAU <i>et al.</i> , 2019)
Lytic polysaccharide monoxygenase (LPMO) mediated production of ultra-fine cellulose nanofibres from delignified softwood fibres	Pretreatment step; different enzymes	films preparation	(KOSKELA <i>et al.</i> , 2019)
Mechanical properties of natural rubber nanocomposites reinforced with cellulosic nanoparticles obtained from combined mechanical shearing, and enzymatic and acid hydrolysis of sisal fibers	Pretreatment step; Different enzymes; different enzyme concentrations	reinforcement agent films	(SIQUEIRA <i>et al.</i> , 2011)
Microcrystalline cellulose property-structure effects in high-pressure fluidization: microfibril characteristics	Pretreatment step	N.E.	(VANHATALO <i>et al.</i> , 2016)
Modification of a cellulase system by engineering <i>Penicillium oxalicum</i> to produce cellulose nanocrystal	Main step; reaction conditions optimization without doe	N.E.	(YANG <i>et al.</i> , 2020)
Morphological investigation of nanoparticles obtained from combined mechanical shearing, and enzymatic and acid hydrolysis of sisal fibers	Pretreatment step; different pretreatments	N.E.	(SIQUEIRA <i>et al.</i> , 2010)
Morphological properties of nanofibrillated cellulose produced using wet grinding as an ultimate fibrillation process	Pretreatment step; different enzyme concentrations	N.E.	(NECHYPORCHUK; PIGNON; BELGACEM, 2015)

Multifunctional Cellulolytic Enzymes Outperform Processive Fungal Cellulases for Coproduction of Nanocellulose and Biofuels	Main step; different enzymes	N.E.	(YARBROUGH <i>et al.</i> , 2017)
Nanocellulose and Bioethanol Production from Orange Waste using Isolated Microorganisms	Pretreatment step; biorefinery	N.E.	(TSUKAMOTO; DURÁN; TASIC, 2013)
Nanocellulose as functional filler in starch/polyvinyl alcohol film for preparation of urea biosensor	Main step	nanofiller nanocomposites	(SATYAMURTHY; NADANATHANGAM, 2018)
Nanocellulose Production in Future Biorefineries: An Integrated Approach Using Tailor-Made Enzymes	Main step; biorefinery; reaction conditions optimization with DOE	N.E.	(SQUINCA <i>et al.</i> , 2020)
Nanocelluloses and their phosphorylated derivatives for selective adsorption of Ag ⁺ , Cu ²⁺ and Fe ³⁺ from industrial effluents	Posttreatment step; functionalization	metal ion removal	(LIU <i>et al.</i> , 2015)
Nanocelluloses from phormium (<i>Phormium tenax</i>) fibers	Pretreatment step; different pretreatments	N.E.	(DI GIORGIO <i>et al.</i> , 2020)
Nanofibers Produced from Agro-Industrial Plant Waste Using Entirely Enzymatic Pretreatments	Pretreatment step; different enzymes	N.E.	(HOLLAND <i>et al.</i> , 2019)
Nanofibrillated cellulose (NFC): A high-value co-product that improves the economics of cellulosic ethanol production	Pretreatment step; biorefinery; different feedstocks	N.E.	(SONG <i>et al.</i> , 2014)
New findings about the lipase acetylation of nanofibrillated cellulose using acetic anhydride as acyl donor	Posttreatment step; functionalization; rheological behavior; Different reaction times	N.E.	(BOŽIČ <i>et al.</i> , 2015)
Obtaining nanofibers from curauá and sugarcane bagasse fibers using enzymatic hydrolysis followed by sonication	Pretreatment step; different feedstocks; different enzyme concentrations	N.E.	(DE CAMPOS <i>et al.</i> , 2013)
Optical haze regulation of cellulose nanopaper via morphological tailoring and nano-hybridization of cellulose nanoparticles	Pretreatment step; different pretreatments	films preparation	(LI <i>et al.</i> , 2020)

Optimization of cellulose nanofiber production from oil palm empty fruit bunch using <i>Trichoderma</i> sp. with the solid state fermentation method	Main step; reaction conditions optimization without DOE	N.E.	(ADITIAWATI <i>et al.</i> , 2019)
Optimized extraction of cellulose nanocrystals from pristine and carded hemp fibres	Pretreatment step; different pretreatments	N.E.	(LUZI <i>et al.</i> , 2014)
Optimizing the isolation of microfibrillated bamboo in high pressure enzymatic Hydrolysis	Main step; reaction conditions optimization with DOE	N.E.	(SRI APRILIA <i>et al.</i> , 2015)
Oriented Cellulose Nanopaper (OCNP) based on bagasse cellulose nanofibrils	Main step	films preparation	(DJAFARI PETROUDY; RASOOLY GARMAROODY; RUDI, 2017)
Oriented polyvinyl alcohol films using short cellulose nanofibrils as a reinforcement	Pretreatment step	reinforcement agent nanocomposites	(PENG <i>et al.</i> , 2015)
Partition usage of cellulose by coupling approach of supercritical carbon dioxide and cellulase to reducing sugar and nanocellulose	Pretreatment step; Different reaction times	N.E.	(LI, L <i>et al.</i> , 2020)
Pilot-Scale Twin Screw Extrusion and Chemical Pretreatment as an Energy-Efficient Method for the Production of Nanofibrillated Cellulose at High Solid Content	Pretreatment step; Different pretreatments	N.E.	(ROL <i>et al.</i> , 2017)
Poly(dimethyldiallylammonium chloride) (polyDADMAC) assisted cellulase pretreatment for microfibrillated cellulose (MFC) preparation and MFC analysis	Pretreatment step	N.E.	(ZHANG <i>et al.</i> , 2018)
Potential of Xylanases to Reduce the Viscosity of Micro/Nanofibrillated Bleached Kraft Pulp	Posttreatment step; rheological behavior	N.E.	(TIAN <i>et al.</i> , 2020)
Potential to Produce Sugars and Lignin-Containing Cellulose Nanofibrils from Enzymatically Hydrolyzed Chemi-Thermomechanical Pulps	Pretreatment step	films preparation	(HAN <i>et al.</i> , 2020)
Predicting the environmental impact of a future nanocellulose production at industrial scale: Application of the life cycle assessment scale-up framework	Pretreatment step; Life cycle assessment	N.E.	(PICCINNO <i>et al.</i> , 2018)

Preparation and characterization of cellulose nanowhiskers from cotton fibres by controlled microbial hydrolysis	main step; Different reaction times	N.E.	(SATYAMURTHY <i>et al.</i> , 2011)
Preparation and characterization of spherical cellulose nanocrystals with high purity by the composite enzymolysis of pulp fibers	Main step; different enzyme concentrations; different enzymes	N.E.	(XU, J.-T.; CHEN, 2019)
Preparation and characterization of the ribbon-like cellulose nanocrystals by the cellulase enzymolysis of cotton pulp fibers	main step; Different reaction times; different enzyme concentrations	N.E.	(CHEN <i>et al.</i> , 2019)
Preparation and characterization of the spherical nanosized cellulose by the enzymatic hydrolysis of pulp fibers	main step; Different reaction times; different enzyme concentrations	N.E.	(CHEN <i>et al.</i> , 2018)
Preparation and mechanism analysis of morphology-controlled cellulose nanocrystals via compound enzymatic hydrolysis of eucalyptus pulp	main step; size control; reaction conditions optimization without doe	N.E.	(TONG <i>et al.</i> , 2020)
Preparation by combined enzymatic and mechanical treatment and characterization of nanofibrillated cotton fibers	Pretreatment step; different enzyme concentrations; different feedstock concentrations	films preparation	(HIDENO <i>et al.</i> , 2016)
Preparation of cellulose nanocrystals through a sequential process of cellulase pretreatment and acid hydrolysis	Pretreatment step; Nanofibrillation enhancement; different enzyme concentrations	N.E.	(AN <i>et al.</i> , 2016)
Preparation of Composites from Natural Rubber and Oil Palm Empty Fruit Bunch Cellulose: Effect of Cellulose Morphology on Properties	Main step; different methods	reinforcement agent nanocomposites	(FIOROTE <i>et al.</i> , 2019)
Preparation of Unmodified Cellulose Nanocrystals from <i>Phyllostachys heterocycla</i> and their Biocompatibility Evaluation	Main step; Different reaction times	N.E.	(MA <i>et al.</i> , 2014)

Production and Characterization of Cellulose Nanofibers from Wood Pulp	Pretreatment step; Nanofibrillation enhancement; different enzyme concentrations; different feedstock concentrations	N.E.	(SIDDIQI <i>et al.</i> , 2011)
Production of cellulose nanocrystals integrated into a biochemical sugar platform process via enzymatic hydrolysis at high solid loading	Main step; biorefinery; reaction conditions optimization without doe	N.E.	(PEREIRA; ARANTES, 2020)
Production of cellulose nanofibrils from bleached eucalyptus fibers by hyperthermostable endoglucanase treatment and subsequent microfluidization	Pretreatment step; different enzymes; different enzyme concentrations	N.E.	(WANG <i>et al.</i> , 2015)
Production of High Solid Nanocellulose by Enzyme-Aided Fibrillation Coupled with Mild Mechanical Treatment	Main step; rheological behavior	N.E.	(PERE <i>et al.</i> , 2020)
Production of lignocellulose nanofibers from wheat straw by different fibrillation methods. Comparison of its viability in cardboard recycling process	Pretreatment step; different pretreatments	reinforcement agent paper-sheets	(ESPINOSA <i>et al.</i> , 2019)
Production of nanocellulose by enzymatic treatment for application in polymer composites	Main step; different feedstocks	films preparation	(ZIELIŃSKA <i>et al.</i> , 2021)
Properties of cellulose micro/nanofibers obtained from eucalyptus pulp fiber treated with anaerobic digestate and high shear mixing	Pretreatment step	N.E.	(TONOLI <i>et al.</i> , 2016)
Properties of cellulose nanofibril produced from wet ball milling after enzymatic treatment vs. mechanical grinding of bleached softwood kraft fibers	Pretreatment step; Nanofibrillation enhancement	N.E.	(ZENG <i>et al.</i> , 2020)
Rapidly growing vegetables as new sources for lignocellulose nanofibre isolation: Physicochemical, thermal and rheological characterization	Pretreatment step; different pretreatments	N.E.	(ESPINOSA; SÁNCHEZ; <i>et al.</i> , 2017)

Rate-Limited Reaction in TEMPO/Laccase/O ₂ Oxidation of Cellulose	Posttreatment step; functionalization; different methods	N.E.	(JIANG <i>et al.</i> , 2021)
Reinforcement of enzyme hydrolyzed longer jute microcrystals in polylactic acid	Main step; Different reaction times	reinforcement agent nanocomposites	(MAQSOOD <i>et al.</i> , 2018)
Remarkable increase of paper strength by combining enzymatic cellulose nanofibers in bulk and TEMPO-oxidized nanofibers as coating	Pretreatment step; different pretreatments	reinforcement agent paper-sheets	(TARRÉS <i>et al.</i> , 2016)
Revalorization of barley straw and husk as precursors for cellulose nanocrystals extraction and their effect on PVA-CH nanocomposites	Pretreatment step; different pretreatments	reinforcement agent nanocomposites	(FORTUNATI <i>et al.</i> , 2016)
Rheological properties of micro-/nanofibrillated cellulose suspensions: Wall-slip and shear banding phenomena	Pretreatment step; different pretreatments; rheological behavior; different enzyme concentrations	N.E.	(NECHYPORCHUK; BELGACEM; PIGNON, 2014)
Role of dispersion time on the properties of enzymatic-treated bamboo cellulose nanofibers	Pretreatment step	N.E.	(SRI APRILIA <i>et al.</i> , 2018)
Short cellulose nanofibrils as reinforcement in polyvinyl alcohol fiber	Pretreatment step	reinforcement agent nanocomposites	(PENG <i>et al.</i> , 2014)
Single-Step Fiber Pretreatment with Monocomponent Endoglucanase: Defibrillation Energy and Cellulose Nanofibril Quality	Pretreatment step; Nanofibrillation enhancement; reaction conditions optimization with doe	N.E.	(BERTO <i>et al.</i> , 2021)
Soybean straw nanocellulose produced by enzymatic or acid treatment as a reinforcing filler in soy protein isolate films	Pretreatment step; different pretreatments	reinforcement agent nanocomposites	(MARTELLI-TOSI <i>et al.</i> , 2018)
Spherical cellulose nanoparticles preparation from waste cotton using a green method	Main step; thermal stability	N.E.	(FATTAHI MEYABADI <i>et al.</i> , 2014)
Spherical vs rod-like cellulose nanocrystals from enzymolysis: A comparative study as reinforcing agents on polyvinyl alcohol	Main step; different reaction times	reinforcement agent nanocomposites	(XU <i>et al.</i> , 2021)

Statistical analysis of the crystallinity index of nanocellulose produced from Kraft pulp via controlled enzymatic hydrolysis	main step; reaction conditions optimization with DOE	N.E.	(RIBEIRO; BOJORGE; PEREIRA JR., 2020)
Structure and properties of polylactic acid biocomposite films reinforced with cellulose nanofibrils	Pretreatment step; different pretreatments	Nanocomposites preparation	(WANG <i>et al.</i> , 2020)
Surface properties of distinct nanofibrillated celluloses assessed by inverse gas chromatography	Main step; different methods	N.E.	(GAMELAS <i>et al.</i> , 2015)
Sustainable production of cellulose nanofiber gels and paper from sugar beet waste using enzymatic pre-treatment	Pretreatment step; different pretreatments	films preparation	(PERZON; JØRGENSEN; ULVSKOV, 2020)
Sustained release of an essential oil by a hybrid cellulose nanofiber foam system	Pretreatment step; different pretreatments; different enzyme concentrations	foams preparation	(ZHANG <i>et al.</i> , 2020)
The Effect of Mechano-enzymatic Treatment on the Characteristics of Cellulose Nanofiber Obtained from Kenaf (<i>Hibiscus cannabinus</i> L.) Bark	Pretreatment step	N.E.	(NARKPIBAN <i>et al.</i> , 2019)
The effect of pre-treatment on the production of lignocellulosic nanofibers and their application as a reinforcing agent in paper	Pretreatment step; different pretreatments	reinforcement agent paper-sheets	(ESPINOSA <i>et al.</i> , 2017)
The feasibility of incorporating cellulose micro/nanofibers in papermaking processes: the relevance of enzymatic hydrolysis	Pretreatment step; Nanofibrillation enhancement; reaction conditions optimization without DOE	N.E.	(TARRÉS <i>et al.</i> , 2016)
Tunicate cellulose nanocrystals: Preparation, neat films and nanocomposite films with glucomannans	Pretreatment step; different pretreatments; tunicates	Films preparation; nanocomposites preparation	(ZHAO <i>et al.</i> , 2015)
Tuning of size and properties of cellulose nanofibers isolated from sugarcane bagasse by endoglucanase-assisted mechanical grinding	Pretreatment step; size control; different enzyme concentrations	films preparation	(LIU <i>et al.</i> , 2020)

Use of Endoglucanase and Accessory Enzymes to Facilitate Mechanical Pulp Nanofibrillation	Pretreatment step; different enzymes	N.E.	(HAN <i>et al.</i> , 2021)
Using Commercial Enzymes to Produce Cellulose Nanofibers from Soybean Straw	Main step	N.E.	(MARTELLI-TOSI <i>et al.</i> , 2016)
Valorization and extraction of cellulose nanocrystals from North African grass: <i>Ampelodesmos mauritanicus</i> (Diss)	Pretreatment step; different pretreatments	N.E.	(LUZI <i>et al.</i> , 2019)
Valorization of alkaline peroxide mechanical pulp by metal chloride-assisted hydrotropic pretreatment for enzymatic saccharification and cellulose nanofibrillation	Pretreatment step; biorefinery	N.E.	(BIAN <i>et al.</i> , 2019)
Valorization of Enzymatic Hydrolysis Residues from Corncob into Lignin-Containing Cellulose Nanofibrils and Lignin Nanoparticles	Pretreatment step; residual lignin; Different reaction times	N.E.	(XU <i>et al.</i> , 2021)
Wood cell wall mimicking for composite films of spruce nanofibrillated cellulose with spruce galactoglucomannan and arabinoglucuronoxylan	Pretreatment step; different enzyme concentrations	films preparation	(STEVANIC <i>et al.</i> , 2014)
Xylanase pretreatment of energy cane enables facile cellulose nanocrystal isolation	Pretreatment step; different enzyme concentrations	N.E.	(MEESUPTHONG <i>et al.</i> , 2021)
Xylanase pretreatment of wood fibers for producing cellulose nanofibrils: a comparison of different enzyme preparations	Pretreatment step; different enzyme concentrations	films preparation	(ZHOU; JOHN; ZHU, 2019)

Legend:

*Process conditions and purposes

Pre-treatment step: Enzymatic hydrolysis was used as a pre-treatment step

Main step: Enzymatic hydrolysis was used as the main step

Post-treatment: Enzymatic hydrolysis was used as a post-treatment step

Different methods: Comparison of different methods to isolate CNs

Different enzymes: Comparison of different enzymes

Different enzyme concentrations: Comparison of different enzyme concentrations

Different reaction times: Comparison of different reaction times

Different pretreatments: Comparison of different pretreatments to isolate CNs

Different feedstocks: Comparison of different feedstocks

Different feedstock concentrations: Comparison of different feedstock concentrations

Reaction condition optimization without doe: Reaction conditions were optimized without using design of experiments

Reaction condition optimization with doe: Reaction conditions were optimized through a design of experiments.

Immobilized enzymes: CNs were isolated using immobilized enzymes

Bioextrusion: CNs were produced by twin-screw extrusion with in situ enzymatic hydrolysis

Life cycle assessment studies: A life cycle assessment was performed

Biorefinery: CNs were produced within the biorefinery context

Nanofibrillation enhancement: Enzymatic hydrolysis was used to facilitate cellulose nanofibrillation

Size control: Enzymatic hydrolysis was used to control the size of CNs

Functionalization: Enzymatic hydrolysis was used to functionalize CNs

Crystallinity increase: Enzymatic hydrolysis was used to crystallinity increase of CNs

Homogeneity increase: Enzymatic hydrolysis was used to increase the homogeneity of CNs

Yield improvement: Enzymatic hydrolysis was used to improve the yield of CNs

Artificial nanocellulose increase: Enzymatic hydrolysis was used for artificial cellulose nanomaterials synthesis

Thermal stability: Evaluation of the enzymatic hydrolysis effects on the thermal stability of CNs

Rheological behavior: Evaluation of the enzymatic hydrolysis effects on the rheological behavior of CNs

****Applications**

N.E.: Not evaluated

Films preparation: CNs were applied in preparation of films

Reinforcement agent in nanocomposites: CNs were used as reinforcement agent in nanocomposites

Reinforcement agent paper-sheets: CNs were used as reinforcement agent in paper-sheets

Nanocomposites preparation: CNs were applied in preparation of nanocomposites

Reinforcement agent films: CNs were used as reinforcement agent in films

Reinforcement agent hand-sheets: CNs were used as reinforcement agent in hand-sheets

Aerogels preparation: CNs were applied in preparation of aerogels

Nanofiller nanocomposites: CNs were used as nanofiller in nanocomposites

Reinforcement agent foams: CNs were used as reinforcement agent in foams

Coating agent: CNs were used as coating agent

Foams preparation: CNs were applied in preparation of foams

Nanofiller hydrogels: CNs were used as nanofiller in hydrogels

Metal ion removal: CNs were used for metal ion removal

Oxygen barrier agent: CNs were used as oxygen barrier agent

Pickering emulsions preparation: CNs were applied in preparation of pickering emulsions

Table A. 3. Feedstocks used in the selected articles and their occurrences.

Feedstocks	Percentage (%)
Crops	
Cotton boll	0.46
Cotton fibers	1.37
Cotton pulp	0.46
Curauá fibers	0.46
Flax ECF bleached fibers	0.46
Flax fiber	0.46
Hemp fiber	0.46
Hemp fibres	0.91
Leucaena (growing vegetables)	0.46
Phormium tenax	0.46
Rice grains	0.46
Tagasaste (growing vegetables)	0.46
Grasses	
Bamboo chips	0.91
Bamboo culms	0.46
Bambooo fibers	0.46
Betung bamboo	0.46
Bleached bamboo Kraft pulp	0.46
Bleached bamboo pulp	0.46
Diss stems (<i>Ampelodesmos mauritanicus</i> is a large grass plant)	0.46
Energy cane	0.46
<i>kenaf bark</i>	0.46
Sweet sorghum	0.46
Sweet sorghum stalk	0.46
Hardwoods	
Bleached Acacia Kraft pulp - hardwood	0.46
Bleached birchwood Kraft pulp	0.46

Bleached Eucalyptus Kraft pulp	12.79
Bleached Eucalyptus pulp	1.37
Bleached hardwood Kraft pulp	3.65
Bleached Poplar Kraft pulp (hardwood)	0.46
Delignified Eucalyptus holocellulos	0.46
Eucalyptus Kraft pulp	0.91
Eucalyptus mechanical pulp	0.46
Eucalyptus pulp	0.46
Eucalyptus pulpboard	0.91
Formosan alder - biomass (hardwoods)	0.46
Hardwood	0.46
Hardwood pulp	0.91
Northern bleached hardwood Kraft pulp	1.83
Poplar wood chips	0.46
Unbleached Eucalyptus Kraft pulp	0.46
Unbleached hardwood pulp	0.46
Others	
Bacterial cellulose	1.83
Cladophora glomerata (alga)	0.46
Cladophora sp - algae	0.46
Alkaline peroxide mechanical pulp	0.46
Arbocel nanocellulose type UFC 100	0.46
Bisulfite pulp	0.46
D- cellobiose acceptor	0.46
D-glucose acceptor	0.46
Dissolving Pulp Plus	0.46
Microcrystalline cellulose	5.02
Microfibrillated celluloses	0.46
Nanofibrillated cellulose	0.46
Micrometric cellulose Sigmacell Type 101	0.46
Micrometric cellulose Sigmacell Type 20	0.46
Sisal fibers	0.91
Whatman filter paper	0.91
Recycled pulp	0.46
Ciona intestinalis - tunicados	1.37
Ozone treated softwood kraft pulp	0.46

Residues

Bleached bagasse	0.46
Bleached bagasse Kraft pulp	0.46
Bleached bagasse pulp	0.91
Cellulose sludge	1.37
Citrus bagasse	1.37
Corn cob residue	0.46
Cotton gin waste	0.91
Cotton linters	1.37
Corn cob	0.46
Date palm fruit stalks	0.46
Jute fibrous waste	0.46
Lemongrass leaves	0.46
Licorice residues	0.46
Liquid hot water treated sugarcane bagasse	0.46
Oat husks	0.46
Oil palm empty fruit bunch	0.91
Old corrugated container	0.46
Potato pulp	0.46
Pulp and paper solid waste	0.46
Rice straw	0.46
Soybean straw	0.91
Steam exploded sugarcane bagasse	0.46
Sugar beet pulp	0.91
Sugar beet waste	0.46
Sugarcane bagasse	4.57
Sugarcane straw	0.46
Unbleached bagasse pulp	1.83
Unripe banana peel	1.37
Untreated sugarcane bagasse	0.46
Water hyacinth stems	0.46
Wheat straw	0.91

Softwoods

Bisulfite softwood pulp	0.46
Bleached Pine Kraft pulp	0.46
Bleached Pinus Kraft pulp	0.46

Bleached softwood chemi-thermomechanical pulp	0.91
Bleached softwood Kraft pulp	4.57
Bleached softwood sulphite pulp	1.37
Bleached Spruce sulphite pulp	0.46
Masson pine chemical pulp	0.46
Northern Bleached Softwood Kraft pulp	1.83
Northern bleached softwood pulp	0.46
Pine Kraft pulp (softwood)	0.46
Pinus taeda sawdust residue (softwood)	0.46
Pinus taeda wood flour - softwood	0.46
Softwood Kraft pulp	1.37
Softwood pulp	0.46
Softwood thermomechanical pulp	0.46
Spruce dissolving pulp (softwood)	0.46
Spruce pulp (softwood)	0.91
Spruce sulphite pulp (softwood)	0.46
Unbleached Picea abies Kraft pulp - softwood	0.46
Unbleached Pine Kraft pulp	0.46

Table A. 4. Percentual of each commercial enzyme related to the total number of occurrences.

Commercial enzymes	Percentage (%)
Cellulases	
Accellerase 1500	0.48
Carezyme (Sigma–Aldrich)	0.48
Cellic CTec2	4.31
CellicCTec3	2.39
Celluclast® 1.5 L	7.18
Cellulase (Fungal Bioproducts®)	0.96
Cellulase (Marugoto D)	0.48
Cellulase (n.i.)	0.96
Cellulase (Novozyme)	1.91
Cellulase (Sukahana)	1.44
Cellulase (Yuanye Biotechnology Co)	0.48

Cellulase (Sertec20)	0.48
Cellulase 50013 (Novozyme)	0.96
Cellulase CL- 8000 (Biofornnoon Bio-Engineering Co.)	0.48
Cellulase fom <i>Aspergillus niger</i> (Ningxia Xiasheng Industrial Group)	1.44
Cellulase from <i>Aspergillus niger</i> (Shandong Xindeli Biotechnology Co.)	0.48
Cellulase from <i>Aspergillus niger</i> (Sigma)	1.44
Cellulase from <i>Trichoderma Viride G</i> (Shanghai Kaiyang Biological Co., Ltd.)	0.48
Cellulase produced by <i>Trichoderma reesei</i> (Sigma)	0.96
Cellulase produced by <i>Trichoderma reesei</i> (Ningxia Sunson Biotechnology Co.,)	0.48
Cellulase produced by <i>Trichoderma viride</i> (Chinese Medicine Group)	0.48
Cellulases from <i>Aspergillus niger</i> (Aladdin Reagent)	0.48
Cellulases from <i>Trichoderma longibrachiatum</i> (Ningxia Heshibi)	0.48
Cellulases (Domestic company)	0.48
Cellulases from <i>Trichoderma reesei</i> ATCC 26921 (Sigma- Aldrich)	2.87
Cellulyve 50LC	0.96
Commercial cellulase (Giant A)	0.48
Ecopulp Energy (Eco) (AB Enzymes)	1.44
Commercial enzymes (n.i.)	0.96
FiberZyme™ LBR (Dyadic International Inc.)	0.48
FiberZyme™ CS (Dyadic International Inc.)	0.48
Meicelase: Cellulases prepared by <i>Trichoderma viride</i> (Meiji Seika Co. Ltd, Japan)	0.48
Multifect B (Genencor)	0.48
Optimash™ VR (DuPont, USA)	1.44
Pulpzyme HA (Novozyme)	0.48
S22086 cellulase complex (Novozymes)	0.48
Spezyme CP (Genencor)	0.48
TEXAZYM AP cellulase enzyme (INOTEX)	0.48
Viscozyme (Sigma- Aldrich)	3.35
Cellulase and xylanase (Imperial Jade Bio-technology Co., Ltd)	0.48

Cellulase enzyme (Qingdao Vland Biotech Inc.)	0.48
Endoglucanase-rich enzymes	
Commercial endoglucanase (n.i.)	0.48
Endoglucanase EcoPulp RÒ (RAOL Oyj)	0.48
Endoglucanase (Banzyme 2900)	1.44
Endocellulase (Novozymes)	0.48
Endoglucanase (Novozymes)	1.91
Endodoglucanase (n.i.)	0.48
Endoglucanase from <i>Bacillus amyloliquefaciens</i> (Megazyme)	0.48
Endoglucanase from <i>Thermobifida halotolerans</i> (Megazyme)	0.48
Endoglucanases from <i>Trichoderma longibrachiatum</i> (Megazyme)	0.48
Enzymes from <i>Trichoderma viride</i> (Sinopharm Chemical Reagent Co.)	0.48
Fibercare® R	11.48
Mono-component endoglucanase (Novozymes)	0.48
Novozym 476	10.53
Quimizime B (endoglucanase-rich)	0.48
Laccases	
Laccase from <i>Trametes versicolor</i> (Sigma-Aldrich)	1.91
Laccase from <i>Trametes versicolor</i> (VTT)	0.48
Laccase (Laccase SUKALacc) from <i>Aspergillus</i> (Bio-Technology Co.)	0.48
Others	
Amano Lipase A from <i>A. niger</i> (Aldrich)	0.48
Lipase from <i>Candida rugosa</i> , type VII (Sigma- Aldrich)	0.48
Aquazym 240 (Novozymes)	0.48
Aquazym 240 L (Novozymes)	0.48
Hexokinase enzyme from <i>Saccharomyces</i> (Sigma- Aldrich)	0.48
Mannanase (Novozymes),	0.48
Pecllyve EXG	0.96
Pectinex Ultra Clear (Novozymes)	0.48
Pectinex® (Sigma–Aldrich)	0.96
Pectinase (Sigma-Aldrich)	0.48
β -galactosidase from <i>Aspergillus oryzae</i> (Sigma)	0.48

LPMOs

LPMO (Novozymes) 0.48

Xylanase-rich enzymes

Biobrite (Novozymes) 0.48

Biofeed (Novo Nordisk) 0.48

Cellic HTec2 1.44

Cellic Htec 1.91

Feedlyve AXC 0.48

Multifect (Genencor) 0.48

Pulpzyme HC (Novozymes) 0.48

Xylanase (BIOTEC, Thailand) 0.48

Xylanase (Macklin Biochemical Co) 0.48

Xylanase (Novozymes) 2.87

Xylanase (Sigma-Aldrich) 0.96

Xylanase from *Trichoderma reesei* (Beijing Shibojiaying Bio-Technology Co.) 0.48

Xylanase from *Trichoderma reesei* (Ningxia Sunson Biotechnology Co.,) 0.48

xylanase from *Trichoderma Viride* G (Shandong Xindeli Biotechnology Co.) 0.48

Xylanase *Trichoderma Viride* G (Ningxia Xiasheng Industrial Group) 0.96

Xylanase X2753 (Novozymes) 0.48

Xylanase X2753 (Sigma- Aldrich) 0.48

Table A. 5. Percentual of each non-commercial enzyme related to the total number of occurrences.

Method***	Non-commercial enzymes	Percentage (%)
Cellulases		
PHE	Cellulases from an anaerobic microbial consortium expressed in <i>E. coli</i>	2.00
MPE	Cellulases produced by <i>Aspergillus niger</i>	2.00
MPE	Cellulases produced by an anaerobic microbial consortium	2.00
MPE	Cellulases produced by <i>Aspergillus fumigatus</i> CCT 7873	2.00
MPE	Cellulases produced by <i>T. reesei</i> QM6a	2.00

MPE	Cellulases produced by <i>Trichoderma reesei</i> (ATCC 13631)	4.00
MPE	Cellulases produced by <i>Trichoderma sp</i>	4.00
NEP	NS 51129	4.00
NEP	‘Meicelase’: Cellulases prepared by <i>Trichoderma viride</i> (Meiji Seika Co. Ltd, Japan)	2.00

Enzymes

EHE	Enzymes from genetically modified fungus isolated from fungus infected Dutch elm tree	4.00
MPE	Enzymes produced by bacteria	2.00
MPE	Enzymes produced by <i>C. bescii</i>	2.00
MPE	Enzymes produced by <i>Xanthomonas axonopodis pv. citri</i> strain 306	4.00

Endoglucanase-rich enzymes

PHE	Ancestor endoglucanase with a carbohydrate-binding module from firmicutes expressed in <i>E. coli</i>	4.00
PHE	Ancestor endoglucanase without a carbohydrate-binding module from firmicutes expressed in <i>E. coli</i>	2.00
PHE	Endoglucanase from <i>Paenibacillus barcinonensis</i> expressed in <i>E. coli</i>	2.00
PHE	Endoglucanase and exoglucanase enzymes from yak rumen metagenome expressed in <i>E. coli</i>	2.00
PHE	endoglucanase Cel9B from <i>P. barcinonensis</i> expressed in <i>E. coli</i>	2.00
PHE	Endoglucanase from <i>Aspergillus oryzae</i> expressed in <i>Pichia pastoris</i>	2.00
PHE	Endoglucanase from <i>Fervidobacterium nodosum</i> expressed in <i>E. coli</i>	2.00
PHE	Endoglucanase from <i>Pyrococcus horikoshi</i> expressed in <i>E. coli</i>	6.00
NEP	Endoglucanase with cellulose-binding domain (NS 51137)	2.00
EHE	endoglucanases (GH5, GH7, GH12, and GH45) from <i>Penicillium oxalicum</i> were expressed in <i>Pichia pastoris</i>	2.00
EHE	Endoglucanases (Cel7B, Cel5B, and Cel12A) from <i>P. oxalicum</i> were expressed in <i>Pichia pastoris</i>	2.00
EHE	Engoglucanase produced by <i>chimeric termite</i>	2.00

	GH7 endoglucanase from <i>Trichoderma</i>	
EHE	<i>harzianum</i> expressed in <i>Aspergillus niger</i>	2.00
	Mutant Endoglucanase without cellulose-binding	
NEP	domain (NS 51172)	2.00
Laccases		
	Lacase (Institute of Chemical Engineering at Nanjing	
NEP	Forestry University)	2.00
MPE	Laccase produced by <i>Trametes versicolor</i> (ATCC-20869)	2.00
Others		
	Cellobiohydrolase and swollenin from <i>P. oxalicum</i> 114-2	
EHE	expressed in <i>Penicillium oxalicum</i> 114-2	2.00
	Cellodextrin phosphorylase from <i>C.</i>	
EHE	<i>thermocellum</i> expression in <i>Saccharomyces cerevisiae</i>	2.00
EHE	Swollenin from <i>T. reesei</i> expressed in <i>P. oxalicum</i> 114-2	2.00
NEP	Swollenin from <i>T. reesei</i> (VTT)	2.00
PHE	β -glucosidase from <i>P. Furious.</i> expressed in <i>E. coli</i>	2.00
LPMOs		
	AA9 LPMO from <i>Thermothelomyces thermophilus</i>	
EHE	expressed in <i>Aspergillus nidulans</i>	2.00
	LPMO from <i>Podospora anserina</i> expressed in <i>Pichia</i>	
EHE	<i>pastoris</i>	2.00
	LPMO from <i>Thermothelomyces thermophila</i> expressed	
EHE	in <i>Pichia pastoris</i>	2.00
PHE	LPMOs from <i>Neurospora crassa</i> expressed in <i>E. coli</i>	2.00
	LPMO from <i>Streptomyces ambofaciens</i> expressed in <i>E.</i>	
PHE	<i>coli</i>	2.00
Xylanase-rich enzymes		
	GH10 xylanase from <i>Thermobacillus composti</i> expressed	
PHE	in <i>E. coli</i>	2.00
	Xylanase from <i>Aspergillus sp</i> (Enzyme Technology	
	Laboratory, National Center for Genetic Engineering and	
NEP	Biotechnology)	2.00
MPE	Xylanase produced by <i>Trichoderma reesei</i> NRRL 6156	2.00

***Production method: NEP: Non-commercial enzymatic formulations; PHE: Prokaryotic heterologous expression; EHE: Eukaryotic heterologous expression and MPE: Microbiological production of enzymes by fungus or bacteria

References

- ADITIAWATI, P.; DUNGANI, R.; FIKRI, R. M.; HARTATI, S. Optimization of cellulose nanofiber production from oil palm empty fruit bunch using *Trichoderma* sp. with the solid state fermentation method. **BioResources**, vol. 14, no. 2, p. 3688–3700, 2019. <https://doi.org/10.15376/biores.14.2.3688-3700>.
- AGBLEVOR, F. A.; IBRAHIM, M. M.; EL-ZAWAWY, W. K. Coupled acid and enzyme mediated production of microcrystalline cellulose from corn cob and cotton gin waste. **Cellulose**, vol. 14, no. 3, p. 247–256, Jun. 2007. <https://doi.org/10.1007/s10570-006-9103-y>.
- ALONSO-LERMA, B; LARRAZA, I.; BARANDIARAN, L.; UGARTE, L.; SARALEGI, A.; CORCUERA, M. A.; PEREZ-JIMENEZ, R.; ECEIZA, A. Enzymatically produced cellulose nanocrystals as reinforcement for waterborne polyurethane and its applications. **Carbohydrate Polymers**, 2021. DOI 10.1016/j.carbpol.2020.117478.
- ALONSO-LERMA, Borja; BARANDIARAN, L.; UGARTE, L.; LARRAZA, I.; REIFS, A.; OLMOS-JUSTE, R.; BARRUETABEÑA, N.; AMENABAR, I.; HILLENBRAND, R.; ECEIZA, A.; PEREZ-JIMENEZ, R. High performance crystalline nanocellulose using an ancestral endoglucanase. **Communications Materials**, vol. 1, no. 1, 2020. DOI 10.1038/s43246-020-00055-5.
- AN, X.; WEN, Y.; CHENG, D.; ZHU, X.; NI, Y. Preparation of cellulose nano-crystals through a sequential process of cellulase pretreatment and acid hydrolysis. **Cellulose**, vol. 23, no. 4, p. 2409–2420, 2016. <https://doi.org/10.1007/s10570-016-0964-4>.
- ANDERSON, S. R.; ESPOSITO, D.; GILLETTE, W.; ZHU, J. Y.; BAXA, U.; MCNEIL, S. E. Enzymatic preparation of nanocrystalline and microcrystalline cellulose. **TAPPI Journal**, vol. 13, no. 5, p. 35–42, 2014. <https://doi.org/10.32964/TJ13.5.35>.
- ANDRADE, A.; HENRÍQUEZ-GALLEGOS, S.; ALBORNOZ-PALMA, G.; PEREIRA, M. Effect of the chemical and structural characteristics of pulps of *Eucalyptus* and *Pinus* on the deconstruction of the cell wall during the production of cellulose nanofibrils. **Cellulose**, vol. 28, no. 9, p. 5387–5399, 2021. <https://doi.org/10.1007/s10570-021-03848-0>.
- ARVIDSSON, R.; NGUYEN, D.; SVANSTRÖM, M. Life cycle assessment of cellulose nanofibrils production by mechanical treatment and two different pretreatment processes. **Environmental Science and Technology**, vol. 49, no. 11, p. 6881–6890, 2015. DOI 10.1021/acs.est.5b00888.
- BANVILLET, G.; DEPRES, G.; BELGACEM, N.; BRAS, J. Alkaline treatment combined with enzymatic hydrolysis for efficient cellulose nanofibrils production. **Carbohydrate Polymers**, 2021. DOI 10.1016/j.carbpol.2020.117383.
- BANVILLET, G.; GATT, E.; BELGACEM, N.; BRAS, J. Cellulose fibers deconstruction by twin-screw extrusion with in situ enzymatic hydrolysis via bioextrusion. **Bioresource Technology**, 2021. DOI 10.1016/j.biortech.2021.124819.

BAULI, C R; ROCHA, D. B.; ROSA, D. S. Composite films of ecofriendly lignocellulosic nanostructures in biodegradable polymeric matrix. **SN Applied Sciences**, 2019. DOI 10.1007/s42452-019-0765-0.

BAULI, Clara R; ROCHA, D. B.; DE OLIVEIRA, S. A.; ROSA, D. S. Cellulose nanostructures from wood waste with low input consumption. **Journal of Cleaner Production**, vol. 211, p. 408–416, 2019. <https://doi.org/10.1016/j.jclepro.2018.11.099>.

BELTRAMINO, F; BLANCA RONCERO, M.; VIDAL, T.; VALLS, C. A novel enzymatic approach to nanocrystalline cellulose preparation. **Carbohydrate Polymers**, 2018. DOI 10.1016/j.carbpol.2018.02.015.

BELTRAMINO, Facundo; RONCERO, M. B.; VIDAL, T.; TORRES, A. L.; VALLS, C. Increasing yield of nanocrystalline cellulose preparation process by a cellulase pretreatment. **Bioresource Technology**, vol. 192, p. 574–581, 2015. DOI 10.1016/j.biortech.2015.06.007.

BERTO, G. L.; MATTOS, B. D.; ROJAS, O. J.; ARANTES, V. Single-Step Fiber Pretreatment with Monocomponent Endoglucanase: Defibrillation Energy and Cellulose Nanofibril Quality. **ACS Sustainable Chemistry and Engineering**, 2021. DOI 10.1021/acssuschemeng.0c08162.

BEYENE, D.; CHAE, M.; DAI, J.; DANUMAH, C.; TOSTO, F.; DEMESA, A. G.; BRESSLER, D. C. Enzymatically-mediated co-production of cellulose nanocrystals and fermentable sugars. **Catalysts**, vol. 7, no. 11, p. 1–13, 2017. <https://doi.org/10.3390/catal7110322>.

BIAN, H; WU, X.; LUO, J.; QIAO, Y.; FANG, G.; DAI, H. Valorization of alkaline peroxide mechanical pulp by metal chloride-assisted hydrotropic pretreatment for enzymatic saccharification and cellulose nanofibrillation. **Polymers**, 2019. DOI 10.3390/polym11020331.

BIAN, Huiyang; CHEN, L.; DONG, M.; FU, Y.; WANG, R.; ZHOU, X.; WANG, X.; XU, J.; DAI, H. Cleaner production of lignocellulosic nanofibrils: Potential of mixed enzymatic treatment. **Journal of Cleaner Production**, vol. 270, p. 122506, 2020. DOI 10.1016/j.jclepro.2020.122506.

BIAN, Huiyang; DONG, M.; CHEN, L.; ZHOU, X.; NI, S.; FANG, G.; DAI, H. Comparison of mixed enzymatic pretreatment and post-treatment for enhancing the cellulose nanofibrillation efficiency. **Bioresource Technology**, vol. 293, no. September, 2019. DOI 10.1016/j.biortech.2019.122171.

BIAN, Huiyang; LI, G.; JIAO, L.; YU, Z.; DAI, H. Enzyme-Assisted Mechanical Fibrillation of Bleached Spruce Kraft Pulp to Produce Well-Dispersed and Uniform-Sized Cellulose Nanofibrils. **BioResources**, vol. 11, no. 4, p. 10483–10496, 2016. DOI 10.15376/biores.11.4.10483-10496.

BONDANCIA, T J; CORRÊA, L. J.; CRUZ, A. J. G.; BADINO, A. C.; MATTOSO, L. H. C.; MARCONCINI, J. M.; FARINAS, C. S. Enzymatic production of cellulose nanofibers and sugars in a stirred-tank reactor: determination of impeller speed, power consumption, and rheological behavior. **Cellulose**, 2018. DOI 10.1007/s10570-018-1876-2.

BONDANCIA, Thalita J; MATTOSO, L. H. C.; MARCONCINI, J. M.; FARINAS, C. S. A new approach to obtain cellulose nanocrystals and ethanol from eucalyptus cellulose pulp via the biochemical pathway. **Biotechnology Progress**, vol. 33, no. 4, p. 1085–1095, 2017.

BOŽIČ, M.; VIVOD, V.; KAVČIČ, S.; LEITGEB, M.; KOKOL, V. New findings about the lipase acetylation of nanofibrillated cellulose using acetic anhydride as acyl donor. **Carbohydrate Polymers**, vol. 125, p. 340–351, 2015. <https://doi.org/10.1016/j.carbpol.2015.02.061>.

CAMARGO, L. A.; PEREIRA, S. C.; CORREA, A. C.; FARINAS, C. S.; MARCONCINI, J. M.; MATTOSO, L. H. C. C. Feasibility of Manufacturing Cellulose Nanocrystals from the Solid Residues of Second-Generation Ethanol Production from Sugarcane Bagasse. **Bioenergy Research**, vol. 9, no. 3, p. 894–906, 2016. DOI 10.1007/s12155-016-9744-0.

CEASER, R.; CHIMPHANGO, A. F. A. A. Comparative analysis of physical and functional properties of cellulose nanofibers isolated from alkaline pre-treated wheat straw in optimized hydrochloric acid and enzymatic processes. **International Journal of Biological Macromolecules**, vol. 171, p. 331–342, 2021. DOI 10.1016/j.ijbiomac.2021.01.018.

CEBREIROS, F.; SEILER, S.; DALLI, S. S.; LAREO, C.; SADDLER, J. Enhancing cellulose nanofibrillation of eucalyptus Kraft pulp by combining enzymatic and mechanical pretreatments. **Cellulose**, 2021. DOI 10.1007/s10570-020-03531-w.

CHEN, X.-Q.; DENG, X.-Y.; SHEN, W.-H.; JIA, M.-Y. Preparation and characterization of the spherical nanosized cellulose by the enzymatic hydrolysis of pulp fibers. **Carbohydrate Polymers**, 2018. DOI 10.1016/j.carbpol.2017.11.064.

CHEN, X.-Q.; PANG, G.-X.; SHEN, W.-H.; TONG, X.; JIA, M.-Y. Preparation and characterization of the ribbon-like cellulose nanocrystals by the cellulase enzymolysis of cotton pulp fibers. **Carbohydrate Polymers**, 2019. DOI 10.1016/j.carbpol.2018.12.042.

CHEN, X.; DENG, X.; SHEN, W.; JIANG, L. Controlled enzymolysis preparation of nanocrystalline cellulose from pretreated cotton fibers. **BioResources**, vol. 7, no. 3, p. 4237–4248, 2012. <https://doi.org/10.15376/biores.7.3.4237-4248>.

CHEN, Y.; FAN, D.; HAN, Y.; LI, G.; WANG, S. Length-controlled cellulose nanofibrils produced using enzyme pretreatment and grinding. **Cellulose**, 2017. DOI 10.1007/s10570-017-1499-z. z&partnerID=40&md5=612a97d7944e5a36925debc07641d6a6.

CHEN, Y.; HE, Y.; FAN, D.; HAN, Y.; LI, G.; WANG, S. An efficient method for cellulose nanofibrils length shearing via environmentally friendly mixed cellulase pretreatment. **Journal of Nanomaterials**, 2017. DOI 10.1155/2017/1591504.

CUI, S.; ZHANG, S.; GE, S.; XIONG, L.; SUN, Q. Green preparation and characterization of size-controlled nanocrystalline cellulose via ultrasonic-assisted enzymatic hydrolysis. **Industrial Crops and Products**, 2016. DOI 10.1016/j.indcrop.2016.01.019.

CYPRIANO, D. Z.; DA SILVA, L. L.; TASIC, L. High value-added products from the orange juice industry waste. **Waste Management**, 2018. DOI 10.1016/j.wasman.2018.07.028.

DAI, J.; CHAE, M.; BEYENE, D.; DANUMAH, C.; TOSTO, F.; BRESSLER, D. C. Co-production of cellulose nanocrystals and fermentable sugars assisted by endoglucanase treatment of wood pulp. **Materials**, 2018. DOI 10.3390/ma11091645.

DE AGUIAR, J.; BONDANCIA, T. J.; CLARO, P. I. C.; MATTOSO, L. H. C.; FARINAS, C. S.; MARCONCINI, J. M. Enzymatic Deconstruction of Sugarcane Bagasse and Straw to Obtain Cellulose Nanomaterials. **ACS Sustainable Chemistry and Engineering**, vol. 8, no. 5, p. 2287–2299, 2020. DOI 10.1021/acssuschemeng.9b06806.

DE BARROS-ALEXANDRINO, T. T.; TOSI, M. M.; ASSIS, O. B. G. Comparison Between Chitosan Nanoparticles and Cellulose Nanofibers as Reinforcement Fillers in Papaya Puree Films: Effects on Mechanical, Water Vapor Barrier, and Thermal Properties. **Polymer Engineering and Science**, vol. 59, p. E287–E292, 2019. DOI 10.1002/pen.24938.

DE CAMPOS, A.; CORREA, A. C.; CANNELLA, D.; DE M TEIXEIRA, E.; MARCONCINI, J. M.; DUFRESNE, A.; MATTOSO, L. H. C. C.; CASSLAND, P.; SANADI, A. R. Obtaining nanofibers from curauá and sugarcane bagasse fibers using enzymatic hydrolysis followed by sonication. **Cellulose**, vol. 20, no. 3, p. 1491–1500, 2013. <https://doi.org/10.1007/s10570-013-9909-3>.

DE OLIVEIRA, J. P.; BRUNI, G. P.; EL HALAL, S. L. M.; BERTOLDI, F. C.; DIAS, A. R. G.; ZAVAREZE, E. da R. Cellulose nanocrystals from rice and oat husks and their application in aerogels for food packaging. **International Journal of Biological Macromolecules**, vol. 124, p. 175–184, 2019. DOI 10.1016/j.ijbiomac.2018.11.205.

DE OLIVEIRA JUNIOR, S. D.; ASEVEDO, E. A.; DE ARAUJO, J. S.; BRITO, P. B.; DOS SANTOS CRUZ COSTA, C. L.; DE MACEDO, G. R.; DOS SANTOS, E. S.; DE OLIVEIRA JÚNIOR, S. D.; ASEVEDO, E. A.; DE ARAÚJO, J. S.; BRITO, P. B.; DOS SANTOS CRUZ COSTA, C. L.; DE MACEDO, G. R.; DOS SANTOS, E. S. Enzymatic extract of *Aspergillus fumigatus* CCT 7873 for hydrolysis of sugarcane bagasse and generation of cellulose nanocrystals (CNC). **Biomass Conversion and Biorefinery**, 2020. DOI 10.1007/s13399-020-01020-5.

DELGADO AGUILAR, M.; GONZÁLEZ TOVAR, I.; TARRÉS FARRÉS, J. A.; ALCALÀ VILAVELLA, M.; PÈLACH SERRA, M. À.; MUTJÉ PUJOL, P.; DELGADO-AGUILAR, M.; GONZÁLEZ, I.; TARRÉS, Q.; ALCALÀ, M.; PÈLACH, M. À.; MUTJÉ, P. Approaching a low-cost production of cellulose nanofibers for papermaking applications. **BioResources**, 2015. DOI 10.15376/biores.10.3.5330-5344.

DI GIORGIO, L.; SALGADO, P. R.; DUFRESNE, A.; MAURI, A. N. Nanocelluloses from phormium (*Phormium tenax*) fibers. **Cellulose**, vol. 27, no. 9, p. 4975–4990, 2020. <https://doi.org/10.1007/s10570-020-03120-x>.

DING, Q.; ZENG, J.; WANG, B.; GAO, W.; CHEN, K.; YUAN, Z.; XU, J.; TANG, D. Effect of retention rate of fluorescent cellulose nanofibrils on paper properties and structure. **Carbohydrate Polymers**, vol. 186, no. November 2017, p. 73–81, 2018. DOI

10.1016/j.carbpol.2018.01.040.

DJAFARI PETROUDY, S. R.; RASOOLY GARMAROODY, E.; RUDI, H. Oriented Cellulose Nanopaper (OCNP) based on bagasse cellulose nanofibrils. **Carbohydrate Polymers**, vol. 157, p. 1883–1891, 2017. DOI 10.1016/j.carbpol.2016.11.074.

DOMINGUES, A. A.; PEREIRA, F. V.; SIERAKOWSKI, M. R.; ROJAS, O. J.; PETRI, D. F. S. Interfacial properties of cellulose nanoparticles obtained from acid and enzymatic hydrolysis of cellulose. **Cellulose**, 2016. DOI 10.1007/s10570-016-0965-3.

DU, L.; WANG, J.; ZHANG, Y.; QI, C.; WOLCOTT, M. P.; YU, Z. A co-production of sugars, lignosulfonates, cellulose, and cellulose nanocrystals from ball-milled woods. **Bioresource Technology**, vol. 238, p. 254–262, 2017. <https://doi.org/10.1016/j.biortech.2017.03.097>.

ESPINOSA, E.; ROL, F.; BRAS, J.; RODRÍGUEZ, A. Production of lignocellulose nanofibers from wheat straw by different fibrillation methods. Comparison of its viability in cardboard recycling process. **Journal of Cleaner Production**, 2019. DOI 10.1016/j.jclepro.2019.118083.

ESPINOSA, Eduardo; DOMINGUEZ-ROBLES, J.; SANCHEZ, R.; TARRES, Q.; RODRIGUEZ, A. The effect of pre-treatment on the production of lignocellulosic nanofibers and their application as a reinforcing agent in paper. **Cellulose**, vol. 24, no. 6, p. 2605–2618, Jun. 2017. <https://doi.org/10.1007/s10570-017-1281-2>.

ESPINOSA, Eduardo; SÁNCHEZ, R.; GONZÁLEZ, Z.; DOMÍNGUEZ-ROBLES, J.; FERRARI, B.; RODRÍGUEZ, A. Rapidly growing vegetables as new sources for lignocellulose nanofibre isolation: Physicochemical, thermal and rheological characterisation. **Carbohydrate polymers**, vol. 175, p. 27–37, 2017. .

FALL, A. B.; BURMAN, A.; WAGBERG, L. Cellulosic nanofibrils from eucalyptus, acacia and pine fibers. **NORDIC PULP & PAPER RESEARCH JOURNAL**, vol. 29, no. 1, SI, p. 176–184, 2014. <https://doi.org/10.3183/npprj-2014-29-01-p176-184>.

FATTAHI MEYABADI, T.; DADASHIAN, F.; MIR MOHAMAD SADEGHI, G.; EBRAHIMI ZANJANI ASL, H. Spherical cellulose nanoparticles preparation from waste cotton using a green method. **Powder Technology**, vol. 261, p. 232–240, 2014. DOI 10.1016/j.powtec.2014.04.039.

FILSON, P. B.; DAWSON-ANDOH, B. E.; SCHWEGLER-BERRY, D. Enzymatic-mediated production of cellulose nanocrystals from recycled pulp. **Green Chemistry**, vol. 11, no. 11, p. 1808–1814, 2009. .

FIOROTE, J. A.; FREIRE, A. P.; RODRIGUES, D. de S.; MARTINS, M. A.; ANDREANI, L.; VALADARES, L. F. Preparation of Composites from Natural Rubber and Oil Palm Empty Fruit Bunch Cellulose: Effect of Cellulose Morphology on Properties. **Bioresources**, vol. 14, no. 2, p. 3168–3181, 2019. <https://doi.org/10.15376/biores.14.2.3168-3181>.

FORTUNATI, E.; BENINCASA, P.; BALESTRA, G. M.; LUZI, F.; MAZZAGLIA, A.; DEL BUONO, D.; PUGLIA, D.; TORRE, L. Revalorization of barley straw and husk as precursors for cellulose nanocrystals extraction and their effect on PVA_CH

nanocomposites. **Industrial Crops and Products**, 2016. DOI 10.1016/j.indcrop.2016.07.047.

GAMELAS, J. A. F.; PEDROSA, J.; LOURENÇO, A. F.; FERREIRA, P. J. Surface properties of distinct nanofibrillated celluloses assessed by inverse gas chromatography. **Colloids and Surfaces A: Physicochemical and Engineering Aspects**, vol. 469, p. 36–41, 2015.

GAZZOTTI, S.; RAMPAZZO, R.; HAKKARAINEN, M.; BUSSINI, D.; ORTENZI, M. A.; FARINA, H.; LESMA, G.; SILVANI, A. Cellulose nanofibrils as reinforcing agents for PLA-based nanocomposites: An in situ approach. **Composites Science and Technology**, vol. 171, no. October 2018, p. 94–102, 2019. <https://doi.org/10.1016/j.compscitech.2018.12.015>.

GEORGE, J.; RAMANA, K. V.; BAWA, A. S.; SIDDARAMAIAH. Bacterial cellulose nanocrystals exhibiting high thermal stability and their polymer nanocomposites. **International Journal of Biological Macromolecules**, vol. 48, no. 1, p. 50–57, 2011. DOI 10.1016/j.ijbiomac.2010.09.013.

HAN, X.; BI, R.; KHATRI, V.; OGUZLU, H.; TAKADA, M.; JIANG, J.; JIANG, F.; BAO, J.; SADDLER, J. N. Use of Endoglucanase and Accessory Enzymes to Facilitate Mechanical Pulp Nanofibrillation. **ACS Sustainable Chemistry and Engineering**, 2021. DOI 10.1021/acssuschemeng.0c08588.

HAN, X.; BI, R.; OGUZLU, H.; TAKADA, M.; JIANG, J.; JIANG, F.; BAO, J.; SADDLER, J. N. Potential to Produce Sugars and Lignin-Containing Cellulose Nanofibrils from Enzymatically Hydrolyzed Chemi-Thermomechanical Pulps. **ACS Sustainable Chemistry and Engineering**, 2020. DOI 10.1021/acssuschemeng.0c05183.

HASSAN, M. L.; BRAS, J.; HASSAN, E. A.; SILARD, C.; MAURET, E. Enzyme-assisted isolation of microfibrillated cellulose from date palm fruit stalks. **Industrial Crops and Products**, vol. 55, p. 102–108, 2014. DOI 10.1016/j.indcrop.2014.01.055.

HASSAN, M. L.; HASSAN, E. A.; OKSMAN, K. N. Effect of pretreatment of bagasse fibers on the properties of chitosan/microfibrillated cellulose nanocomposites. **Journal of Materials Science**, vol. 46, no. 6, p. 1732–1740, 2011. <https://doi.org/10.1007/s10853-010-4992-4>.

HAYASHI, N.; KONDO, T.; ISHIHARA, M. Enzymatically produced nano-ordered short elements containing cellulose I-beta crystalline domains. **CARBOHYDRATE POLYMERS**, vol. 61, no. 2, p. 191–197, 2005. <https://doi.org/10.1016/j.carbpol.2005.04.018>.

HENRIKSSON, M.; HENRIKSSON, G.; BERGLUND, L. A.; LINDSTRÖM, T. An environmentally friendly method for enzyme-assisted preparation of microfibrillated cellulose (MFC) nanofibers. **European Polymer Journal**, vol. 43, no. 8, p. 3434–3441, 2007.

HIDENO, A.; ABE, K.; UCHIMURA, H.; YANO, H. Preparation by combined enzymatic and mechanical treatment and characterization of nanofibrillated cotton fibers. **Cellulose**, vol. 23, no. 6, p. 3639–3651, 2016.

HOLLAND, C.; PERZON, A.; CASSLAND, P. R. C. C.; JENSEN, J. P.; LANGEBECK, B.; SØRENSEN, O. B.; WHALE, E.; HEPWORTH, D.; PLAICE-INGLIS, R.; MOESTRUP, Ø.; ULVSKOV, P.; JØRGENSEN, B. Nanofibers Produced from Agro-Industrial Plant Waste Using Entirely Enzymatic Pretreatments. **Biomacromolecules**, vol. 20, no. 1, p. 443–453, 2019. DOI 10.1021/acs.biomac.8b01435.

HU, J.; TIAN, D.; RENNECKAR, S.; SADDLER, J. N. Enzyme mediated nanofibrillation of cellulose by the synergistic actions of an endoglucanase, lytic polysaccharide monooxygenase (LPMO) and xylanase. **Scientific reports**, vol. 8, no. 1, p. 1–8, 2018. .

JANARDHANAN, S.; SAIN, M. Bio-Treatment of Natural Fibers in Isolation of Cellulose Nanofibres: Impact of Pre-Refining of Fibers on Bio-Treatment Efficiency and Nanofiber Yield. **Journal of Polymers and the Environment**, vol. 19, no. 3, p. 615–621, 2011. <https://doi.org/10.1007/s10924-011-0312-6>.

JANG, J. H. J.-H.; HAYASHI, N.; HAN, S. Y. S.-Y.; PARK, C.-W. C. W.; FEBRIANTO, F.; LEE, S.-H. S. H.; KIM, N. H. N.-H. Changes in the dimensions of lignocellulose nanofibrils with different lignin contents by enzymatic hydrolysis. **Polymers**, vol. 12, no. 10, 2020. DOI 10.3390/POLYM12102201.

JAUŠOVEC, D.; VOGRINČIČ, R.; KOKOL, V. Introduction of aldehyde vs. carboxylic groups to cellulose nanofibers using laccase/TEMPO mediated oxidation. **Carbohydrate polymers**, vol. 116, p. 74–85, 2015.

JIANG, J.; CHEN, H.; LIU, L.; YU, J.; FAN, Y.; SAITO, T.; ISOGAI, A. Influence of chemical and enzymatic TEMPO-mediated oxidation on chemical structure and nanofibrillation of lignocellulose. **ACS Sustainable Chemistry & Engineering**, vol. 8, no. 37, p. 14198–14206, 2020. <https://doi.org/10.1021/acssuschemeng.0c05291>.

JIANG, J.; CHEN, H.; YU, J.; LIU, L.; FAN, Y.; SAITO, T.; ISOGAI, A. Rate-Limited Reaction in TEMPO/Laccase/O₂ Oxidation of Cellulose. **Macromolecular Rapid Communications**, vol. 42, no. 3, p. 2000501, 2021.

JO, H. M.; LEE, J. Y.; KIM, S. H.; LEE, Y. H. Effect of Nanofibrillated Cellulose Made from Enzyme-pretreated Bamboo Pulp on Paper Strength. **BIORESOURCES**, vol. 16, no. 1, p. 964–978, 2021. <https://doi.org/10.15376/biores.16.1.964-978>.

JUÁREZ-LUNA, G. N.; FAVELA-TORRES, E.; QUEVEDO, I. R.; BATINA, N. Enzymatically assisted isolation of high-quality cellulose nanoparticles from water hyacinth stems. **Carbohydrate Polymers**, 2019. DOI 10.1016/j.carbpol.2019.05.058.

KARNAOURI, A.; JALVO, B.; MORITZ, P.; MATSAKAS, L.; ROVA, U.; HÖFFT, O.; SOURKOUNI, G.; MAUS-FRIEDRICH, W.; MATHEW, A. P.; CHRISTAKOPOULOS, P. Lytic Polysaccharide Monooxygenase-Assisted Preparation of Oxidized-Cellulose Nanocrystals with a High Carboxyl Content from the Tunic of Marine Invertebrate *Ciona intestinalis*. **ACS Sustainable Chemistry and Engineering**, 2020. DOI 10.1021/acssuschemeng.0c05036.

KIM, K. J.; LEE, J. M.; AHN, E. B.; EOM, T. J. Effect of enzyme beating on grinding method for microfibrillated cellulose preparation as a paper strength enhancer. **Cellulose**, vol. 24, no. 8, p. 3503–3511, 2017. <https://doi.org/10.1007/s10570-017-1368-9>.

KO, C.-H.; YANG, B.-Y.; LIN, L.-D.; CHANG, F.-C.; CHEN, W.-H. Impact of pretreatment methods on production of bioethanol and nanocrystalline cellulose. **Journal of Cleaner Production**, 2020. DOI 10.1016/j.jclepro.2019.119914.

KOSKELA, S.; WANG, S.; XU, D.; YANG, X.; LI, K.; BERGLUND, L. A.; MCKEE, L. S.; BULONE, V.; ZHOU, Q. Lytic polysaccharide monooxygenase (LPMO) mediated production of ultra-fine cellulose nanofibres from delignified softwood fibres. **Green Chemistry**, vol. 21, no. 21, p. 5924–5933, 2019. <https://doi.org/10.1039/c9gc02808k>.

KUMARI, P.; PATHAK, G.; GUPTA, R.; SHARMA, D.; MEENA, A. Cellulose nanofibers from lignocellulosic biomass of lemongrass using enzymatic hydrolysis: characterization and cytotoxicity assessment. **DARU, Journal of Pharmaceutical Sciences**, 2019. DOI 10.1007/s40199-019-00303-1.

LAADILA, M. A.; SURESH, G.; ROUISSI, T.; KUMAR, P.; BRAR, S. K.; CHEIKH, R. Ben; ABOKITSE, K.; GALVEZ-COLTIER, R.; JACOB, C. Biocomposite fabrication from enzymatically treated nanocellulosic fibers and recycled polylactic acid. **Energies**, vol. 13, no. 4, 2020. <https://doi.org/10.3390/en13041003>.

LI, L.; ZHUANG, J.; ZOU, H.; PANG, J.; YU, S. Partition usage of cellulose by coupling approach of supercritical carbon dioxide and cellulase to reducing sugar and nanocellulose. **Carbohydrate Polymers**, 2020. DOI 10.1016/j.carbpol.2019.115533.

LI, X.; WANG, N.; ZHANG, X.; CHANG, H.; WANG, Y.; ZHANG, Z. Optical haze regulation of cellulose nanopaper via morphological tailoring and nano-hybridization of cellulose nanoparticles. **Cellulose**, 2020. DOI 10.1007/s10570-019-02876-1.

LIU, P.; BORRELL, P. F.; BOŽIČ, M.; KOKOL, V.; OKSMAN, K.; MATHEW, A. P. Nanocelluloses and their phosphorylated derivatives for selective adsorption of Ag⁺, Cu²⁺ and Fe³⁺ from industrial effluents. **Journal of Hazardous Materials**, vol. 294, p. 177–185, 2015. <https://doi.org/10.1016/j.jhazmat.2015.04.001>.

LIU, X.; JIANG, Y.; QIN, C.; YANG, S.; SONG, X.; WANG, S.; LI, K. Enzyme-assisted mechanical grinding for cellulose nanofibers from bagasse: energy consumption and nanofiber characteristics. **Cellulose**, 2018. DOI 10.1007/s10570-018-2071-1.

LIU, Xiuyu; JIANG, Y.; SONG, X.; QIN, C.; WANG, S.; LI, K. A bio-mechanical process for cellulose nanofiber production – Towards a greener and energy conservation solution. **Carbohydrate Polymers**, vol. 208, no. November 2018, p. 191–199, 2019. DOI 10.1016/j.carbpol.2018.12.071.

LIU, Xiuyu; JIANG, Y.; WANG, L.; SONG, X.; QIN, C.; WANG, S. Tuning of size and properties of cellulose nanofibers isolated from sugarcane bagasse by endoglucanase-assisted mechanical grinding. **Industrial Crops and Products**, vol. 146, no. July 2019, p. 112201, 2020. DOI 10.1016/j.indcrop.2020.112201.

LIU, Y.; YU, Y.; WANG, Q.; XU, J.; FAN, X.; WANG, P.; YUAN, J. Biological–chemical modification of cellulose nanocrystal to prepare highly compatible chitosan-based nanocomposites. **Cellulose**, vol. 26, no. 9, p. 5267–5279, 2019. DOI 10.1007/s10570-019-02486-x.

LONG, L.; TIAN, D.; HU, J.; WANG, F.; SADDLER, J. A xylanase-aided enzymatic

pretreatment facilitates cellulose nanofibrillation. **Bioresource technology**, vol. 243, p. 898–904, 2017.

LOURENÇO, A F.; GAMELAS, J. A. F.; SARMENTO, P.; FERREIRA, P. J. T. Enzymatic nanocellulose in papermaking – The key role as filler flocculant and strengthening agent. **Carbohydrate Polymers**, 2019. DOI 10.1016/j.carbpol.2019.115200.

LOURENÇO, Ana F.; GAMELAS, J. A. F. J. A. F. F.; SARMENTO, P.; FERREIRA, P. J. T. T.; LOURENÇO, A. F.; GAMELAS, J. A. F. J. A. F. F.; SARMENTO, P.; FERREIRA, P. J. T. T.; LOURENÇO, A. F.; GAMELAS, J. A. F. J. A. F. F.; SARMENTO, P.; FERREIRA, P. J. T. T. A comprehensive study on nanocelluloses in papermaking: the influence of common additives on filler retention and paper strength. **Cellulose**, vol. 27, no. 9, p. 5297–5309, Jun. 2020. DOI 10.1007/s10570-020-03105-w.

LOURENÇO, Ana F.; GAMELAS, J. A. F.; SARMENTO, P.; FERREIRA, P. J. T. Cellulose micro and nanofibrils as coating agent for improved printability in office papers. **Cellulose**, vol. 27, no. 10, p. 6001–6010, 2020. <https://doi.org/10.1007/s10570-020-03184-9>.

LUZI, F.; FORTUNATI, E.; PUGLIA, D.; LAVORGNA, M.; SANTULLI, C.; KENNY, J. M.; TORRE, L. Optimized extraction of cellulose nanocrystals from pristine and carded hemp fibres. **Industrial Crops and Products**, 2014. DOI 10.1016/j.indcrop.2014.03.006.

LUZI, F.; PUGLIA, D.; SARASINI, F.; TIRILLÒ, J.; MAFFEI, G.; ZUORRO, A.; LAVECCHIA, R.; KENNY, J. M.; TORRE, L. Valorization and extraction of cellulose nanocrystals from North African grass: *Ampelodesmos mauritanicus* (Diss). **Carbohydrate Polymers**, 2019. DOI 10.1016/j.carbpol.2019.01.048.

MA, L.; ZHANG, Y.; CAO, J.; YAO, J. Preparation of Unmodified Cellulose Nanocrystals from *Phyllostachys heterocycla* and their Biocompatibility Evaluation. **Bioresources**, vol. 9, no. 1, p. 210–217, 2014.

MAQSOOD, H. S.; BAHETI, V.; WIENER, J.; MILITKY, J. Reinforcement of enzyme hydrolyzed longer jute microcrystals in polylactic acid. **Polymer Composites**, vol. 39, no. 4, p. 1089–1097, 2018. <https://doi.org/10.1002/pc.24036>.

MARIÑO, M.; LOPES DA SILVA, L.; DURÁN, N.; TASIC, L. Enhanced materials from nature: nanocellulose from citrus waste. **Molecules**, vol. 20, no. 4, p. 5908–5923, 2015.

MARTELLI-TOSI, M.; MASSON, M. M.; SILVA, N. C.; ESPOSTO, B. S.; BARROS, T. T.; ASSIS, O. B. G.; TAPIA-BLÁCIDO, D. R. Soybean straw nanocellulose produced by enzymatic or acid treatment as a reinforcing filler in soy protein isolate films. **Carbohydrate Polymers**, 2018. DOI 10.1016/j.carbpol.2018.06.053.

MARTELLI-TOSI, Milena; TORRICILLAS, M. da S.; MARTINS, M. A.; DE ASSIS, O. B.; TAPIA-BLACIDO, D. R. Using Commercial Enzymes to Produce Cellulose Nanofibers from Soybean Straw. **Journal of Nanomaterials**, vol. 2016, 2016. <https://doi.org/10.1155/2016/8106814>.

MEESUPHONG, R.; YINGKAMHAENG, N.; NIMCHUA, T.; PINMANEE, P.;

MUSSATTO, S. I.; LI, B.; SUKYAI, P. Xylanase pretreatment of energy cane enables facile cellulose nanocrystal isolation. **Cellulose**, vol. 28, no. 2, p. 799–812, 2021. .

MOHARRAMI, P.; MOTAMEDI, E. Application of cellulose nanocrystals prepared from agricultural wastes for synthesis of starch-based hydrogel nanocomposites: Efficient and selective nanoadsorbent for removal of cationic dyes from water. **Bioresource Technology**, vol. 313, no. April, p. 123661, 2020. DOI 10.1016/j.biortech.2020.123661.

MOREAU, C.; TAPIN-LINGUA, S.; GRISEL, S.; GIMBERT, I.; LE GALL, S.; MEYER, V.; PETIT-CONIL, M.; BERRIN, J.-G.; CATHALA, B.; VILLARES, A. Lytic polysaccharide monooxygenases (LPMOs) facilitate cellulose nanofibrils production. **BIOTECHNOLOGY FOR BIOFUELS**, vol. 12, Jun. 2019. <https://doi.org/10.1186/s13068-019-1501-0>.

NARKPIBAN, K.; SAKDARONNARONG, C.; NIMCHUA, T.; PINMANEE, P.; THONGKRED, P.; POONSAWAT, T. The effect of mechano-enzymatic treatment on the characteristics of cellulose nanofiber obtained from kenaf (*Hibiscus cannabinus* L.) bark. **BioResources**, 2019. DOI 10.15376/biores.14.1.99-119.

NECHYPORCHUK, O.; BELGACEM, M. N.; PIGNON, F. Rheological properties of micro-/nanofibrillated cellulose suspensions: wall-slip and shear banding phenomena. **Carbohydrate polymers**, vol. 112, p. 432–439, 2014.

NECHYPORCHUK, O.; PIGNON, F.; BELGACEM, M. N. Morphological properties of nanofibrillated cellulose produced using wet grinding as an ultimate fibrillation process. **Journal of Materials Science**, vol. 50, no. 2, p. 531–541, Jan. 2015. <https://doi.org/10.1007/s10853-014-8609-1>.

NIE, S.; ZHANG, C.; ZHANG, Q.; ZHANG, K.; ZHANG, Y.; TAO, P.; WANG, S. Enzymatic and cold alkaline pretreatments of sugarcane bagasse pulp to produce cellulose nanofibrils using a mechanical method. **Industrial Crops and Products**, vol. 124, no. July, p. 435–441, 2018. DOI 10.1016/j.indcrop.2018.08.033.

PAAKKO, M.; ANKERFORS, M.; KOSONEN, H.; NYKANEN, A.; AHOLA, S.; OSTERBERG, M.; RUOKOLAINEN, J.; LAINE, J.; LARSSON, P. T.; IKKALA, O.; LINDSTROM, T.; PÄÄKKÖ, M.; ANKERFORS, M.; KOSONEN, H.; NYKÄNEN, A.; AHOLA, S.; ÖSTERBERG, M.; RUOKOLAINEN, J.; LAINE, J.; ... IKKALA, O. Enzymatic hydrolysis combined with mechanical shearing and high-pressure homogenization for nanoscale cellulose fibrils and strong gels. **Biomacromolecules**, 1155 16TH ST, NW, WASHINGTON, DC 20036 USA, vol. 8, no. 6, p. 1934–1941, Jun. 2007. DOI 10.1021/bm061215p.

PÄÄKKÖ, M.; VAPAAVUORI, J.; SILVENNOINEN, R.; KOSONEN, H.; ANKERFORS, M.; LINDSTRÖM, T.; BERGLUND, L. A.; IKKALA, O. Long and entangled native cellulose i nanofibers allow flexible aerogels and hierarchically porous templates for functionalities. **Soft Matter**, vol. 4, no. 12, p. 2492–2499, 2008. <https://doi.org/10.1039/b810371b>.

PENG, J.; ELLINGHAM, T.; SABO, R.; CLEMONS, C. M.; TURNG, L.-S. Oriented polyvinyl alcohol films using short cellulose nanofibrils as a reinforcement. **Journal of Applied Polymer Science**, 2015. DOI 10.1002/app.42283.

PENG, J.; ELLINGHAM, T.; SABO, R.; TURNG, L.-S.; CLEMONS, C. M. Short cellulose nanofibrils as reinforcement in polyvinyl alcohol fiber. **Cellulose**, 2014. DOI 10.1007/s10570-014-0411-3.

PERE, J.; TAMMELIN, T.; NIEMI, P.; LILLE, M.; VIRTANEN, T.; PENTTILÄ, P. A.; AHVENAINEN, P.; GRÖNQVIST, S. Production of high solid nanocellulose by enzyme-aided fibrillation coupled with mild mechanical treatment. **ACS Sustainable Chemistry & Engineering**, vol. 8, no. 51, p. 18853–18863, 2020. .

PEREIRA, B.; ARANTES, V. Production of cellulose nanocrystals integrated into a biochemical sugar platform process via enzymatic hydrolysis at high solid loading. **Industrial Crops and Products**, 2020. DOI 10.1016/j.indcrop.2020.112377.

PERIĆ, M.; PUTZ, R.; PAULIK, C. 3D-printed pla filaments reinforced with nanofibrillated cellulose. **Journal of Renewable Materials**, 2020. DOI 10.32604/jrm.2020.09284. Available at: <https://www.scopus.com/inward/record.uri?eid=2-s2.0-85085878372&doi=10.32604%2Fjrm.2020.09284&partnerID=40&md5=c07392fa051a31881978bf063332df36>.

PERZON, A.; JØRGENSEN, B.; ULVSKOV, P. Sustainable production of cellulose nanofiber gels and paper from sugar beet waste using enzymatic pre-treatment. **Carbohydrate polymers**, vol. 230, p. 115581, 2020. .

PICCINNO, F; HISCHIER, R.; SEEGER, S.; SOM, C. Predicting the environmental impact of a future nanocellulose production at industrial scale: Application of the life cycle assessment scale-up framework. **Journal of Cleaner Production**, 2018. DOI 10.1016/j.jclepro.2017.10.226.

PICCINNO, Fabiano; HISCHIER, R.; SEEGER, S.; SOM, C. Eco-efficient process improvement at the early development stage: identifying environmental and economic process hotspots for synergetic improvement potential. **Environmental science & technology**, vol. 52, no. 10, p. 5959–5967, 2018.

PICCINNO, Fabiano; HISCHIER, R.; SEEGER, S.; SOM, C. Life cycle assessment of a new technology to extract, functionalize and orient cellulose nanofibers from food waste. **ACS Sustainable Chemistry and Engineering**, vol. 3, no. 6, p. 1047–1055, 2015. DOI 10.1021/acssuschemeng.5b00209.

PYLKKÄNEN, R.; MOHAMMADI, P.; AROLA, S.; DE RUIJTER, J. C.; SUNAGAWA, N.; IGARASHI, K.; PENTTILÄ, M. In Vitro Synthesis and Self-Assembly of Cellulose II Nanofibrils Catalyzed by the Reverse Reaction of *Clostridium thermocellum* Cellodextrin Phosphorylase. **Biomacromolecules**, vol. 21, no. 10, p. 4355–4364, 2020. <https://doi.org/10.1021/acs.biomac.0c01162>.

QIAN, M.; LEI, H.; VILLOTA, E.; ZHAO, Y.; WANG, C.; HUO, E.; ZHANG, Q.; MATEO, W.; LIN, X. High yield production of nanocrystalline cellulose by microwave-assisted dilute-acid pretreatment combined with enzymatic hydrolysis. **Chemical Engineering and Processing - Process Intensification**, vol. 160, no. December 2020, p. 108292, 2021. DOI 10.1016/j.cep.2020.108292.

QING, Y.; SABO, R.; ZHU, J. Y.; AGARWAL, U.; CAI, Z.; WU, Y. A comparative

study of cellulose nanofibrils disintegrated via multiple processing approaches. **Carbohydrate Polymers**, vol. 97, no. 1, p. 226–234, 2013. DOI 10.1016/j.carbpol.2013.04.086.

REID, M. S.; KARLSSON, M.; ABITBOL, T. Fluorescently labeled cellulose nanofibrils for detection and loss analysis. **Carbohydrate Polymers**, vol. 250, p. 116943, 2020.

REN, H.; SHEN, J.; PEI, J.; WANG, Z.; PENG, Z.; FU, S.; ZHENG, Y. Characteristic microcrystalline cellulose extracted by combined acid and enzyme hydrolysis of sweet sorghum. **Cellulose**, 2019. DOI 10.1007/s10570-019-02712-6.

RIBEIRO, R. S. A.; BOJORGE, N.; PEREIRA JR., N. Statistical analysis of the crystallinity index of nanocellulose produced from Kraft pulp via controlled enzymatic hydrolysis. **Biotechnology and Applied Biochemistry**, 2020. DOI 10.1002/bab.1873.

ROL, F.; KARAKASHOV, B.; NECHYPORCHUK, O.; TERRIEN, M.; MEYER, V.; DUFRESNE, A.; BELGACEM, M. N.; BRAS, J. Pilot-Scale Twin Screw Extrusion and Chemical Pretreatment as an Energy-Efficient Method for the Production of Nanofibrillated Cellulose at High Solid Content. **ACS Sustainable Chemistry and Engineering**, 2017. DOI 10.1021/acssuschemeng.7b00630.

ROSSI, B. R.; PELLEGRINI, V. O. A.; CORTEZ, A. A.; CHIROMITO, E. M. S.; CARVALHO, A. J. F.; PINTO, L. O.; REZENDE, C. A.; MASTELARO, V. R.; POLIKARPOV, I. Cellulose nanofibers production using a set of recombinant enzymes. **Carbohydrate Polymers**, vol. 256, Mar. 2021. <https://doi.org/10.1016/j.carbpol.2020.117510>.

ROVERA, C.; FIORI, F.; TRABATTONI, S.; ROMANO, D.; FARRIS, S. Enzymatic hydrolysis of bacterial cellulose for the production of nanocrystals for the food packaging industry. **Nanomaterials**, 2020. DOI 10.3390/nano10040735.

ROVERA, C.; GHAANI, M.; SANTO, N.; TRABATTONI, S.; OLSSON, R. T.; ROMANO, D.; FARRIS, S. Enzymatic Hydrolysis in the Green Production of Bacterial Cellulose Nanocrystals. **ACS Sustainable Chemistry and Engineering**, 2018. DOI 10.1021/acssuschemeng.8b00600.

SAASTAMOINEN, P.; MATTINEN, M. L.; HIPPI, U.; NOUSIAINEN, P.; SIPILÄ, J.; LILLE, M.; SUURNÄKKI, A.; PERE, J. Laccase aided modification of nanofibrillated cellulose with dodecyl gallate. **BioResources**, vol. 7, no. 4, p. 5749–5770, 2012. <https://doi.org/10.15376/biores.7.4.5749-5770>.

SACUI, I. A.; NIEUWENDAAL, R. C.; BURNETT, D. J.; STRANICK, S. J.; JORFI, M.; WEDER, C.; FOSTER, E. J.; OLSSON, R. T.; GILMAN, J. W. Comparison of the properties of cellulose nanocrystals and cellulose nanofibrils isolated from bacteria, tunicate, and wood processed using acid, enzymatic, mechanical, and oxidative methods. **ACS Applied Materials and Interfaces**, vol. 6, no. 9, p. 6127–6138, 2014. <https://doi.org/10.1021/am500359f>.

SAELEE, K.; YINGKAMHAENG, N.; NIMCHUA, T.; SUKYAI, P. An environmentally friendly xylanase-assisted pretreatment for cellulose nanofibrils isolation from sugarcane bagasse by high-pressure homogenization. **Industrial Crops and Products**, 2016. DOI 10.1016/j.indcrop.2015.11.064.

SANTUCCI, B. S.; BRAS, J.; BELGACEM, M. N.; CURVELO, A. A. D. S.; PIMENTA, M. T. B. Evaluation of the effects of chemical composition and refining treatments on the properties of nanofibrillated cellulose films from sugarcane bagasse. **Industrial Crops and Products**, 2016. DOI 10.1016/j.indcrop.2016.07.017.

SATYAMURTHY, P; VIGNESHWARAN, N. A novel process for synthesis of spherical nanocellulose by controlled hydrolysis of microcrystalline cellulose using anaerobic microbial consortium. **Enzyme and microbial technology**, vol. 52, no. 1, p. 20–25, 2013.

SATYAMURTHY, Prasad; JAIN, P.; BALASUBRAMANYA, R. H.; VIGNESHWARAN, N. Preparation and characterization of cellulose nanowhiskers from cotton fibres by controlled microbial hydrolysis. **Carbohydrate Polymers**, vol. 83, no. 1, p. 122–129, 2011. .

SATYAMURTHY, Prasad; NADANATHANGAM, V. Nanocellulose as functional filler in starch/polyvinyl alcohol film for preparation of urea biosensor. **Current Science**, vol. 114, no. 4, p. 897–901, 2018. <https://doi.org/10.18520/cs/v114/i04/897-901>.

SERIZAWA, T.; KATO, M.; OKURA, H.; SAWADA, T.; WADA, M. Hydrolytic activities of artificial nanocellulose synthesized via phosphorylase-catalyzed enzymatic reactions. **Polymer Journal**, vol. 48, no. 4, p. 539–544, 2016. <https://doi.org/10.1038/pj.2015.125>.

SIDDIQUI, N.; MILLS, R. H.; GARDNER, D. J.; BOUSFIELD, D. Production and Characterization of Cellulose Nanofibers from Wood Pulp. **Journal of Adhesion Science and Technology**, vol. 25, no. 6–7, SI, p. 709–721, 2011. <https://doi.org/10.1163/016942410X525975>.

SIQUEIRA, G. A.; DIAS, I. K. R.; ARANTES, V. Exploring the action of endoglucanases on bleached eucalyptus kraft pulp as potential catalyst for isolation of cellulose nanocrystals. **International journal of biological macromolecules**, vol. 133, p. 1249–1259, 2019. .

SIQUEIRA, G.; TAPIN-LINGUA, S.; BRAS, J.; DA SILVA PEREZ, D.; DUFRESNE, A. Mechanical properties of natural rubber nanocomposites reinforced with cellulosic nanoparticles obtained from combined mechanical shearing, and enzymatic and acid hydrolysis of sisal fibers. **Cellulose**, 2011. DOI 10.1007/s10570-010-9463-1.

SIQUEIRA, G.; TAPIN-LINGUA, S.; BRAS, J.; DA SILVA PEREZ, D.; DUFRESNE, A. Morphological investigation of nanoparticles obtained from combined mechanical shearing, and enzymatic and acid hydrolysis of sisal fibers. **Cellulose**, 2010. DOI 10.1007/s10570-010-9449-z.

SOBRAL TEIXEIRA, R. S.; DA SILVA, A. S.; JANG, J.-H.; KIM, H.-W.; ISHIKAWA, K.; ENDO, T.; LEE, S.-H.; BON, E. P. S. Combining biomass wet disk milling and endoglucanase/beta-glucosidase hydrolysis for the production of cellulose nanocrystals. **Carbohydrate Polymers**, vol. 128, p. 75–81, 2015. <https://doi.org/10.1016/j.carbpol.2015.03.087>.

SONG, Q.; WINTER, W. T.; BUJANOVIC, B. M.; AMIDON, T. E. Nanofibrillated Cellulose (NFC): A High-Value Co-Product that Improves the Economics of Cellulosic

Ethanol Production. **Energies**, vol. 7, no. 2, p. 607–618, 2014. <https://doi.org/10.3390/en7020607>.

SQUINCA, P.; BILATTO, S.; BADINO, A. C.; FARINAS, C. S. Nanocellulose Production in Future Biorefineries: An Integrated Approach Using Tailor-Made Enzymes. **ACS Sustainable Chemistry and Engineering**, vol. 8, no. 5, p. 2277–2286, 2020. <https://doi.org/10.1021/acssuschemeng.9b06790>.

SRI APRILIA, N. A.; ASNIZA, M.; OWOLABI, F. A. T.; RIZAL, S.; SYAKIR, M. I.; PARIDAH, M. T.; UTHAYA KUMAR, U. S.; NASRULLAH, R. C. L.; HAAFIZ, M. K.; ABDUL KHALIL, H. P. S.; APRILIA, N. A. S.; ASNIZA, M.; OWOLABI, F. A. T.; RIZAL, S.; SYAKIR, M. I.; PARIDAH, M. T.; KUMAR, U. S. U.; NASRULLAH, R. C. L.; HAAFIZ, M. K.; KHALIL, H. P. S. A. Role of dispersion time on the properties of enzymatic-treated bamboo cellulose nanofibers. **Materials Research Express**, vol. 5, no. 10, 2018. DOI 10.1088/2053-1591/aadaca.

SRI APRILIA, N. A.; HOSSAIN, M. S.; MUSTAPHA, A.; SITI SUHAILY, S.; NIK NORULIANI, N. A.; PENG, L. C.; MOHD OMAR, A. K.; ABDUL KHALIL, H. P. S.; SUHAILY, S. S.; NIK NORULIANI, N. A.; PENG, L. C.; MOHD OMAR, A. K.; ABDUL KHALIL, H. P. S. Optimizing the isolation of microfibrillated bamboo in high pressure enzymatic hydrolysis. **BioResources**, vol. 10, no. 3, p. 5293–5304, 2015. DOI 10.15376/biores.10.3.5305-5316.

STEVANIC, J. S.; MIKKONEN, K. S.; XU, C.; TENKANEN, M.; BERGLUND, L.; SALMEN, L. Wood cell wall mimicking for composite films of spruce nanofibrillated cellulose with spruce galactoglucomannan and arabinoglucuronoxylan. **Journal of Materials Science**, vol. 49, no. 14, p. 5043–5055, Jul. 2014. <https://doi.org/10.1007/s10853-014-8210-7>.

SVAGAN, A. J.; SAMIR, M. A. S. A.; BERGLUND, L. A. Biomimetic foams of high mechanical performance based on nanostructured cell walls reinforced by native cellulose nanofibrils. **Advanced Materials**, 2008. DOI 10.1002/adma.200701215.

TANG, Y.; SHEN, X.; ZHANG, J.; GUO, D.; KONG, F.; ZHANG, N. Extraction of cellulose nano-crystals from old corrugated container fiber using phosphoric acid and enzymatic hydrolysis followed by sonication. **Carbohydrate Polymers**, 2015. DOI 10.1016/j.carbpol.2015.02.063.

TAO, P.; WU, Z.; XING, C.; ZHANG, Q.; WEI, Z.; NIE, S. Effect of enzymatic treatment on the thermal stability of cellulose nanofibrils. **Cellulose**, 2019. DOI 10.1007/s10570-019-02634-3.

TAO, P.; ZHANG, Y.; WU, Z.; LIAO, X.; NIE, S. Enzymatic pretreatment for cellulose nanofibrils isolation from bagasse pulp: Transition of cellulose crystal structure. **Carbohydrate Polymers**, vol. 214, no. February, p. 1–7, 2019. DOI 10.1016/j.carbpol.2019.03.012.

TARRES, Q.; ANGELS PELACH, M.; ALCALA, M.; DELGADO-AGUILAR, M. Cardboard boxes as raw material for high-performance papers through the implementation of alternative technologies: More than closing the loop. **JOURNAL OF INDUSTRIAL AND ENGINEERING CHEMISTRY**, vol. 54, p. 52–58, 2017.

<https://doi.org/10.1016/j.jiec.2017.05.016>.

TARRÉS, Q; DELGADO-AGUILAR, M.; PÈLACH, M. A.; GONZÁLEZ, I.; BOUFI, S.; MUTJÉ, P. Remarkable increase of paper strength by combining enzymatic cellulose nanofibers in bulk and TEMPO-oxidized nanofibers as coating. **Cellulose**, 2016. DOI 10.1007/s10570-016-1073-0.

TARRÉS, Q; SAGUER, E.; PÈLACH, M. A.; ALCALÀ, M.; DELGADO-AGUILAR, M.; MUTJÉ, P. The feasibility of incorporating cellulose micro/nanofibers in papermaking processes: the relevance of enzymatic hydrolysis. **Cellulose**, 2016. DOI 10.1007/s10570-016-0889-y.

TARRÉS, Quim; BOUFI, S.; MUTJÉ, P.; DELGADO-AGUILAR, M.; TARRÉS, Q.; BOUFI, S.; MUTJE, P.; DELGADO-AGUILAR, M.; TARRÉS, Q.; BOUFI, S.; MUTJÉ, P.; DELGADO-AGUILAR, M. Enzymatically hydrolyzed and TEMPO-oxidized cellulose nanofibers for the production of nanopapers: morphological, optical, thermal and mechanical properties. **Cellulose**, vol. 24, no. 9, p. 3943–3954, 2017. DOI 10.1007/s10570-017-1394-7.

TARRÉS, Quim; OLIVER-ORTEGA, H.; ALCALÀ, M.; MERAYO, N.; BALEA, A.; BLANCO, Á.; MUTJÉ, P.; DELGADO-AGUILAR, M. Combined effect of sodium carboxymethyl cellulose, cellulose nanofibers and drainage aids in recycled paper production process. **Carbohydrate Polymers**, vol. 183, no. November 2017, p. 201–206, 2018. DOI 10.1016/j.carbpol.2017.12.027.

TARRÉS, Quim; OLIVER-ORTEGA, H.; LLOP, M.; PÈLACH, M. À.; DELGADO-AGUILAR, M.; MUTJÉ, P. Effective and simple methodology to produce nanocellulose-based aerogels for selective oil removal. **Cellulose**, vol. 23, no. 5, p. 3077–3088, 2016. <https://doi.org/10.1007/s10570-016-1017-8>.

TIAN, D.; ZHONG, N.; LEUNG, J.; SHEN, F.; HU, J.; SADDLER, J. N. Potential of Xylanases to Reduce the Viscosity of Micro/Nanofibrillated Bleached Kraft Pulp. **ACS Applied Bio Materials**, 2020. DOI 10.1021/acsabm.0c00041.

TIAN, X.; LU, P.; SONG, X.; NIE, S.; LIU, Y.; LIU, M.; WANG, Z. Enzyme-assisted mechanical production of microfibrillated cellulose from Northern Bleached Softwood Kraft pulp. **Cellulose**, vol. 24, no. 9, p. 3929–3942, 2017. <https://doi.org/10.1007/s10570-017-1382-y>.

TIBOLLA, H.; PELISSARI, F. M.; MARTINS, J. T.; LANZONI, E. M.; VICENTE, A. A.; MENEGALLI, F. C.; CUNHA, R. L. Banana starch nanocomposite with cellulose nanofibers isolated from banana peel by enzymatic treatment: In vitro cytotoxicity assessment. **Carbohydrate Polymers**, vol. 207, no. May 2018, p. 169–179, 2019. DOI 10.1016/j.carbpol.2018.11.079.

TIBOLLA, Heloisa; PELISSARI, F. M.; MENEGALLI, F. C. Cellulose nanofibers produced from banana peel by chemical and enzymatic treatment. **LWT - Food Science and Technology**, vol. 59, no. 2P2, p. 1311–1318, 2014. DOI 10.1016/j.lwt.2014.04.011.

TIBOLLA, Heloisa; PELISSARI, F. M.; RODRIGUES, M. I.; MENEGALLI, F. C. Cellulose nanofibers produced from banana peel by enzymatic treatment: Study of process conditions. **Industrial Crops and Products**, vol. 95, p. 664–674, 2017. DOI

10.1016/j.indcrop.2016.11.035.

TONG, X.; SHEN, W.; CHEN, X.; JIA, M.; ROUX, J.-C. Preparation and mechanism analysis of morphology-controlled cellulose nanocrystals via compound enzymatic hydrolysis of eucalyptus pulp. **Journal of Applied Polymer Science**, 2020. DOI 10.1002/app.48407.

TONOLI, G. H. D.; HOLTMAN, K. M.; GLENN, G.; FONSECA, A. S.; WOOD, D.; WILLIAMS, T.; SA, V. A.; TORRES, L.; KLAMCZYNSKI, A.; ORTS, W. J. Properties of cellulose micro/nanofibers obtained from eucalyptus pulp fiber treated with anaerobic digestate and high shear mixing. **Cellulose**, vol. 23, no. 2, p. 1239–1256, 2016. <https://doi.org/10.1007/s10570-016-0890-5>.

TSUKAMOTO, J.; DURÁN, N.; TASIC, L. Nanocellulose and bioethanol production from orange waste using isolated microorganisms. **Journal of the Brazilian Chemical Society**, vol. 24, no. 9, p. 1537–1543, 2013. .

VALENZUELA, S. V.; VALLS, C.; SCHINK, V.; SÁNCHEZ, D.; RONCERO, M. B.; DIAZ, P.; MARTÍNEZ, J.; PASTOR, F. I. J.; SANCHEZ, D.; BLANCA RONCERO, M.; DIAZ, P.; MARTINEZ, J.; JAVIER PASTOR, F. I. Differential activity of lytic polysaccharide monooxygenases on celluloses of different crystallinity. Effectiveness in the sustainable production of cellulose nanofibrils. **Carbohydrate Polymers**, vol. 207, no. July 2018, p. 59–67, Mar. 2019. <https://doi.org/10.1016/j.carbpol.2018.11.076>.

VALLS, C.; JAVIER PASTOR, F. I.; BLANCA RONCERO, M.; VIDAL, T.; DIAZ, P.; MARTÍNEZ, J.; VALENZUELA, S. V. Assessing the enzymatic effects of cellulases and LPMO in improving mechanical fibrillation of cotton linters. **Biotechnology for Biofuels**, vol. 12, p. 1–14, 2019. DOI 10.1186/s13068-019-1502-z.

VANHATALO, K.; LUNDIN, T.; KOSKIMÄKI, A.; LILLANDT, M.; DAHL, O. Microcrystalline cellulose property–structure effects in high-pressure fluidization: microfibril characteristics. **Journal of Materials Science**, vol. 51, no. 12, p. 6019–6034, 2016. <https://doi.org/10.1007/s10853-016-9907-6>.

WANG, J.; CHAE, M.; BEYENE, D.; SAUVAGEAU, D.; BRESSLER, D. C. Co-production of ethanol and cellulose nanocrystals through self-cycling fermentation of wood pulp hydrolysate. **Bioresour Technol**, 2021. DOI 10.1016/j.biortech.2021.124969.

WANG, Q.; JI, C.; SUN, J.; ZHU, Q.; LIU, J. Structure and properties of polylactic acid biocomposite films reinforced with cellulose nanofibrils. **Molecules**, 2020. DOI 10.3390/molecules25143306.

WANG, Q.; JI, C.; SUN, L.; SUN, J.; LIU, J. Cellulose nanofibrils filled poly(lactic acid) biocomposite filament for FDM 3D printing. **Molecules**, 2020. DOI 10.3390/molecules25102319.

WANG, Qianqian; WEI, W.; CHANG, F.; SUN, J.; XIE, S.; ZHU, Q.; MICROFLUIDIZATION, H. P.; WANG, Q.; WEI, W.; CHANG, F.; SUN, J.; XIE, S. Controlling the Size and Film Strength of Individualized Cellulose Nanofibrils Prepared by Combined Enzymatic Pretreatment and High Pressure Microfluidization. **Bioresour**, vol. 11, no. 1, p. 2536–2547, 2016.

WANG, Shengdan; GAO, W.; CHEN, K.; XIANG, Z.; ZENG, J.; WANG, B.; XU, J. Deconstruction of cellulosic fibers to fibrils based on enzymatic pretreatment. **Bioresource Technology**, vol. 267, no. July, p. 426–430, Nov. 2018. DOI 10.1016/j.biortech.2018.07.067.

WANG, Si; WANG, X.; LIU, W.; ZHANG, L.; OUYANG, H.; HOU, Q.; FAN, K.; LI, J.; LIU, P.; LIU, X. Fabricating cellulose nanofibril from licorice residues and its cellulose composite incorporated with natural nanoparticles. **Carbohydrate Polymers**, vol. 229, no. August 2019, p. 115464, 2020. DOI 10.1016/j.carbpol.2019.115464.

WANG, W; MOZUCH, M. D.; SABO, R. C.; KERSTEN, P.; ZHU, J. Y.; JIN, Y. Production of cellulose nanofibrils from bleached eucalyptus fibers by hyperthermostable endoglucanase treatment and subsequent microfluidization. **Cellulose**, 2015. DOI 10.1007/s10570-014-0465-2.

WANG, Wangxia; MOZUCH, M. D.; SABO, R. C.; KERSTEN, P.; ZHU, J. Y.; JIN, Y. Endoglucanase post-milling treatment for producing cellulose nanofibers from bleached eucalyptus fibers by a supermasscolloider. **Cellulose**, vol. 23, no. 3, p. 1859–1870, 2016.

WANG, X.; ZENG, J.; GAO, W.; CHEN, K.; WANG, B.; XU, J. Endoglucanase recycling for disintegrating cellulosic fibers to fibrils. **Carbohydrate Polymers**, vol. 223, Nov. 2019. <https://doi.org/10.1016/j.carbpol.2019.115052>.

XIANG, Z.; GAO, W.; CHEN, L.; LAN, W.; ZHU, J. Y.; RUNGE, T. A comparison of cellulose nanofibrils produced from *Cladophora glomerata* algae and bleached eucalyptus pulp. **Cellulose**, 2016. DOI 10.1007/s10570-015-0840-7.

XU, J.-T.; CHEN, X.-Q. Preparation and characterization of spherical cellulose nanocrystals with high purity by the composite enzymolysis of pulp fibers. **Bioresource Technology**, 2019. DOI 10.1016/j.biortech.2019.121842.

XU, J.-T.; CHEN, X.-Q.; SHEN, W.-H.; LI, Z. Spherical vs rod-like cellulose nanocrystals from enzymolysis: A comparative study as reinforcing agents on polyvinyl alcohol. **Carbohydrate Polymers**, 2021. DOI 10.1016/j.carbpol.2020.117493.

XU, R.; DU, H.; WANG, H.; ZHANG, M.; WU, M.; LIU, C.; YU, G.; ZHANG, X.; SI, C.; CHOI, S.-E. Valorization of enzymatic hydrolysis residues from corncob into lignin-containing cellulose nanofibrils and lignin nanoparticles. **Frontiers in Bioengineering and Biotechnology**, vol. 9, p. 252, 2021.

XU, Yali; SALMI, J.; KLOSER, E.; PERRIN, F.; GROSSE, S.; DENAULT, J.; LAU, P. C. K. Feasibility of nanocrystalline cellulose production by endoglucanase treatment of natural bast fibers. **Industrial Crops and Products**, vol. 51, p. 381–384, Nov. 2013. <https://doi.org/10.1016/j.indcrop.2013.09.029>.

XU, Ying; YANG, S.; ZHAO, P.; WU, M.; SONG, X.; RAGAUSKAS, A. J. Effect of endoglucanase and high-pressure homogenization post-treatments on mechanically grinded cellulose nanofibrils and their film performance. **Carbohydrate Polymers**, vol. 253, no. August 2020, p. 117253, 2021. DOI 10.1016/j.carbpol.2020.117253.

YAN, J.; HU, J.; YANG, R.; ZHANG, Z.; ZHAO, W. Innovative Nanofibrillated

Cellulose from Rice Straw as Dietary Fiber for Enhanced Health Benefits Prepared by a Green and Scale Production Method. **Acs Sustainable Chemistry & Engineering**, vol. 6, no. 3, p. 3481–3492, Mar. 2018. <https://doi.org/10.1021/acssuschemeng.7b03765>.

YANG, T.; LI, X.; GUO, Y.; PENG, S.; LIU, G.; ZHAO, J. Effect of endoglucanases from different glycoside hydrolase families on enzymatic preparation of cellulose nanocrystal. **Industrial Crops and Products**, 2020. DOI 10.1016/j.indcrop.2020.112755.

YANG, Tiantian; GUO, Y.; GAO, N.; LI, X.; ZHAO, J. Modification of a cellulase system by engineering *Penicillium oxalicum* to produce cellulose nanocrystal. **Carbohydrate Polymers**, vol. 234, no. September 2019, p. 115862, 2020. DOI 10.1016/j.carbpol.2020.115862.

YARBROUGH, J. M.; ZHANG, R.; MITTAL, A.; VANDER WALL, T.; BOMBLE, Y. J.; DECKER, S. R.; HIMMEL, M. E.; CIESIELSKI, P. N. Multifunctional cellulolytic enzymes outperform processive fungal cellulases for coproduction of nanocellulose and biofuels. **Acs Nano**, vol. 11, no. 3, p. 3101–3109, 2017. .

YASSIN, M. A.; GAD, A. A. M.; GHANEM, A. F.; ABDEL REHIM, M. H. Green synthesis of cellulose nanofibers using immobilized cellulase. **Carbohydrate Polymers**, vol. 205, no. June 2018, p. 255–260, 2019. DOI 10.1016/j.carbpol.2018.10.040.

YUAN, Z.; WEI, W.; WEN, Y. Improving the production of nanofibrillated cellulose from bamboo pulp by the combined cellulase and refining treatment. **Journal Of Chemical Technology and Biotechnology**, vol. 94, no. 7, p. 2178–2186, Jul. 2019. <https://doi.org/10.1002/jctb.5998>.

ZENG, J.; LIU, L.; LI, J.; DONG, J.; CHENG, Z. Properties of cellulose nanofibril produced from wet ball milling after enzymatic treatment vs. mechanical grinding of bleached softwood kraft fibers. **BioResources**, 2020. DOI 10.15376/biores.15.2.3809-3820.

ZHANG, C.; WU, M.; YANG, S.; SONG, X.; XU, Y. Combined mechanical grinding and enzyme post-treatment leading to increased yield and size uniformity of cellulose nanofibrils. **Cellulose**, vol. 27, no. 13, p. 7447–7461, 2020. DOI 10.1007/s10570-020-03335-y.

ZHANG, K.; ZHANG, Y.; YAN, D.; ZHANG, C.; NIE, S. Enzyme-assisted mechanical production of cellulose nanofibrils: thermal stability. **Cellulose**, 2018. DOI 10.1007/s10570-018-1928-7.

ZHANG, Q.; LU, Z.; SU, C.; FENG, Z.; WANG, H.; YU, J.; SU, W. High yielding, one-step mechano-enzymatic hydrolysis of cellulose to cellulose nanocrystals without bulk solvent. **Bioresource Technology**, vol. 331, 2021. DOI 10.1016/j.biortech.2021.125015.

ZHANG, Z.-J.; QIU, L.-X.; CHEN, Y.-Z.; LI, Z.-H.; SONG, H.-Y.; CHEN, Q.-W. Effect of Pulp Concentration during Cellulase Pretreatment on Microfibrillated Cellulose and Its Film Properties. **Bioresources**, vol. 11, no. 3, p. 6540–6551, 2016. <https://doi.org/10.15376/biores.11.3.6540-6551>.

ZHANG, Z.; WANG, X.; GAO, M.; ZHAO, Y.; CHEN, Y. Sustained release of an essential oil by a hybrid cellulose nanofiber foam system. **Cellulose**, 2020. DOI

10.1007/s10570-019-02957-1.

ZHANG, Zhengjian; ZHANG, Q.; CHEN, Y.; LI, Z. Poly(dimethyldiallylammonium chloride) (polyDADMAC) assisted cellulose pretreatment for microfibrillated cellulose (MFC) preparation and MFC analysis. **Holzforschung**, vol. 72, no. 7, p. 531–538, Jul. 2018. <https://doi.org/10.1515/hf-2017-0152>.

ZHAO, G.; WANG, F.; LANG, X.; HE, B.; LI, J.; LI, X. Facile one-pot fabrication of cellulose nanocrystals and enzymatic synthesis of its esterified derivative in mixed ionic liquids. **RSC Advances**, vol. 7, no. 43, p. 27017–27023, 2017. DOI 10.1039/c7ra02570j.

ZHAO, Y.; ZHANG, Y.; LINDSTRÖM, M. E.; LI, J. Tunicate cellulose nanocrystals: Preparation, neat films and nanocomposite films with glucomannans. **Carbohydrate Polymers**, 2015. DOI 10.1016/j.carbpol.2014.09.020.

ZHAO, Yadong; MOSER, C.; LINDSTRÖM, M. E.; HENRIKSSON, G.; LI, J. Cellulose Nanofibers from Softwood, Hardwood, and Tunicate: Preparation-Structure-Film Performance Interrelation. **ACS Applied Materials and Interfaces**, vol. 9, no. 15, p. 13508–13519, 2017. DOI 10.1021/acsami.7b01738.

ZHOU, H.; JOHN, F. S.; ZHU, J. Y. Xylanase pretreatment of wood fibers for producing cellulose nanofibrils: a comparison of different enzyme preparations. **Cellulose**, vol. 26, no. 1, p. 543–555, 2019.

ZHU, H.; HELANDER, M.; MOSER, C.; STÅHLKRANZ, A.; SÖDERBERG, D.; HENRIKSSON, G.; LINDSTRÖM, M. A Novel Nano Cellulose Preparation Method and Size Fraction by Cross Flow Ultra- Filtration. **Current Organic Chemistry**, vol. 16, no. 16, p. 1871–1875, 2012. <https://doi.org/10.2174/138527212802651197>.

ZHU, J. Y.; SABO, R.; LUO, X. Integrated production of nano-fibrillated cellulose and cellulosic biofuel (ethanol) by enzymatic fractionation of wood fibers. **Green Chemistry**, vol. 13, no. 5, p. 1339–1344, 2011. .

ZIELINSKA, D.; RYDZKOWSKI, T.; THAKUR, V. K.; BORYSIK, S. S.; ZIELIŃSKA, D.; RYDZKOWSKI, T.; THAKUR, V. K.; BORYSIK, S. S. Enzymatic engineering of nanometric cellulose for sustainable polypropylene nanocomposites. **Industrial Crops and Products**, vol. 161, no. December 2020, Mar. 2021. DOI 10.1016/j.indcrop.2020.113188.

ZIELIŃSKA, D.; SZENTNER, K.; WAŚKIEWICZ, A.; BORYSIK, S. Production of nanocellulose by enzymatic treatment for application in polymer composites. **Materials**, vol. 14, no. 9, p. 2124, 2021.

APPENDIX B

This appendix presents the publication rights and permissions acquired to use some figures and data in this thesis.

23/10/2021 15:55 Rightslink® by Copyright Clearance Center



Home
Help ▾
Email Support
Paula Squinca ▾



Nanocellulose toward Advanced Energy Storage Devices: Structure and Electrochemistry

Author: Chaoji Chen, Liangbing Hu

Publication: Accounts of Chemical Research

Publisher: American Chemical Society

Date: Dec 1, 2018

Copyright © 2018, American Chemical Society

PERMISSION/LICENSE IS GRANTED FOR YOUR ORDER AT NO CHARGE

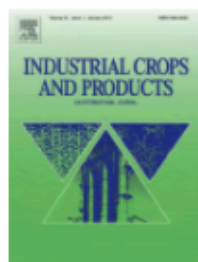
This type of permission/license, instead of the standard Terms and Conditions, is sent to you because no fee is being charged for your order. Please note the following:

- Permission is granted for your request in both print and electronic formats, and translations.
- If figures and/or tables were requested, they may be adapted or used in part.
- Please print this page for your records and send a copy of it to your publisher/graduate school.
- Appropriate credit for the requested material should be given as follows: "Reprinted (adapted) with permission from {COMPLETE REFERENCE CITATION}, Copyright {YEAR} American Chemical Society." Insert appropriate information in place of the capitalized words.
- One-time permission is granted only for the use specified in your RightsLink request. No additional uses are granted (such as derivative works or other editions). For any uses, please submit a new request.

If credit is given to another source for the material you requested from RightsLink, permission must be obtained from that source.

BACK
CLOSE WINDOW

© 2021 Copyright - All Rights Reserved | Copyright Clearance Center, Inc. | Privacy statement | Terms and Conditions
Comments? We would like to hear from you. E-mail us at customer-care@copyright.com



Thank you for your order!

Dear Paula Squinca,

Thank you for placing your order through Copyright Clearance Center's RightsLink® service.

Order Summary

Licensee: Paula Squinca
Order Date: Oct 23, 2021
Order Number: 5174920845164
Publication: Industrial Crops and Products
Title: Production of cellulose nanofibrils: A review of recent advances
Type of Use: reuse in a thesis/dissertation
Order Ref: 101120212
Order Total: 0.00 USD

View or print complete [details](#) of your order and the publisher's terms and conditions.

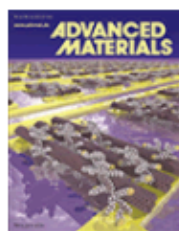
Sincerely,

Copyright Clearance Center

Tel: +1-855-239-3415 / +1-978-646-2777
customer care@copyright.com
<https://myaccount.copyright.com>



RightsLink®



Thank you for your order!

Dear Paula Squinca,

Thank you for placing your order through Copyright Clearance Center's RightsLink® service.

Order Summary

Licensee:	Paula Squinca
Order Date:	Oct 23, 2021
Order Number:	5174920522373
Publication:	Advanced Materials
Title:	Wood-Based Nanotechnologies toward Sustainability
Type of Use:	Dissertation/Thesis
Order Ref:	101120211
Order Total:	0.00 USD

View or print complete [details](#) of your order and the publisher's terms and conditions.

Sincerely,

Copyright Clearance Center

Tel: +1-855-239-3415 / +1-978-646-2777
customercare@copyright.com
<https://myaccount.copyright.com>



RightsLink®



Home



Help ▾



Email Support



Paula Squinca ▾

Nanocellulose Production in Future Biorefineries: An Integrated Approach Using Tailor-Made Enzymes



Author: Paula Squinca, Stanley Bilatto, Alberto C. Badino, et al

Publication: ACS Sustainable Chemistry & Engineering

Publisher: American Chemical Society

Date: Feb 1, 2020

Copyright © 2020, American Chemical Society

PERMISSION/LICENSE IS GRANTED FOR YOUR ORDER AT NO CHARGE

This type of permission/license, instead of the standard Terms and Conditions, is sent to you because no fee is being charged for your order. Please note the following:

- Permission is granted for your request in both print and electronic formats, and translations.
- If figures and/or tables were requested, they may be adapted or used in part.
- Please print this page for your records and send a copy of it to your publisher/graduate school.
- Appropriate credit for the requested material should be given as follows: "Reprinted (adapted) with permission from {COMPLETE REFERENCE CITATION}. Copyright {YEAR} American Chemical Society." Insert appropriate information in place of the capitalized words.
- One-time permission is granted only for the use specified in your RightsLink request. No additional uses are granted (such as derivative works or other editions). For any uses, please submit a new request.

If credit is given to another source for the material you requested from RightsLink, permission must be obtained from that source.

[BACK](#)

[CLOSE WINDOW](#)



Home



Help ▾



Email Support



Paula Squinca ▾



Multifunctional Ginger Nanofiber Hydrogels with Tunable Absorption: The Potential for Advanced Wound Dressing Applications

Author: Paula Squinca, Linn Berglund, Kristina Hanna, et al

Publication: Biomacromolecules

Publisher: American Chemical Society

Date: Aug 1, 2021

Copyright © 2021, American Chemical Society

PERMISSION/LICENSE IS GRANTED FOR YOUR ORDER AT NO CHARGE

This type of permission/license, instead of the standard Terms and Conditions, is sent to you because no fee is being charged for your order. Please note the following:

- Permission is granted for your request in both print and electronic formats, and translations.
- If figures and/or tables were requested, they may be adapted or used in part.
- Please print this page for your records and send a copy of it to your publisher/graduate school.
- Appropriate credit for the requested material should be given as follows: "Reprinted (adapted) with permission from (COMPLETE REFERENCE CITATION). Copyright (YEAR) American Chemical Society." Insert appropriate information in place of the capitalized words.
- One-time permission is granted only for the use specified in your RightsLink request. No additional uses are granted (such as derivative works or other editions). For any uses, please submit a new request.

If credit is given to another source for the material you requested from RightsLink, permission must be obtained from that source.

[BACK](#)

[CLOSE WINDOW](#)